AD-A049 161 VIRGINIA INST OF MARINE SCIENCE GLOUCESTER POINT F/G 8/6
RECENT HISTORY AND RESPONSE CHARACTERISTICS OF WACHAPREAGUE INL--ETC(U)
MAY 77 R J BYRNE, J T DEALTERIS, J P SOVICH N00014-71-C-0334

UNCLASSIFIED NL

1 OF 3
AD A049161

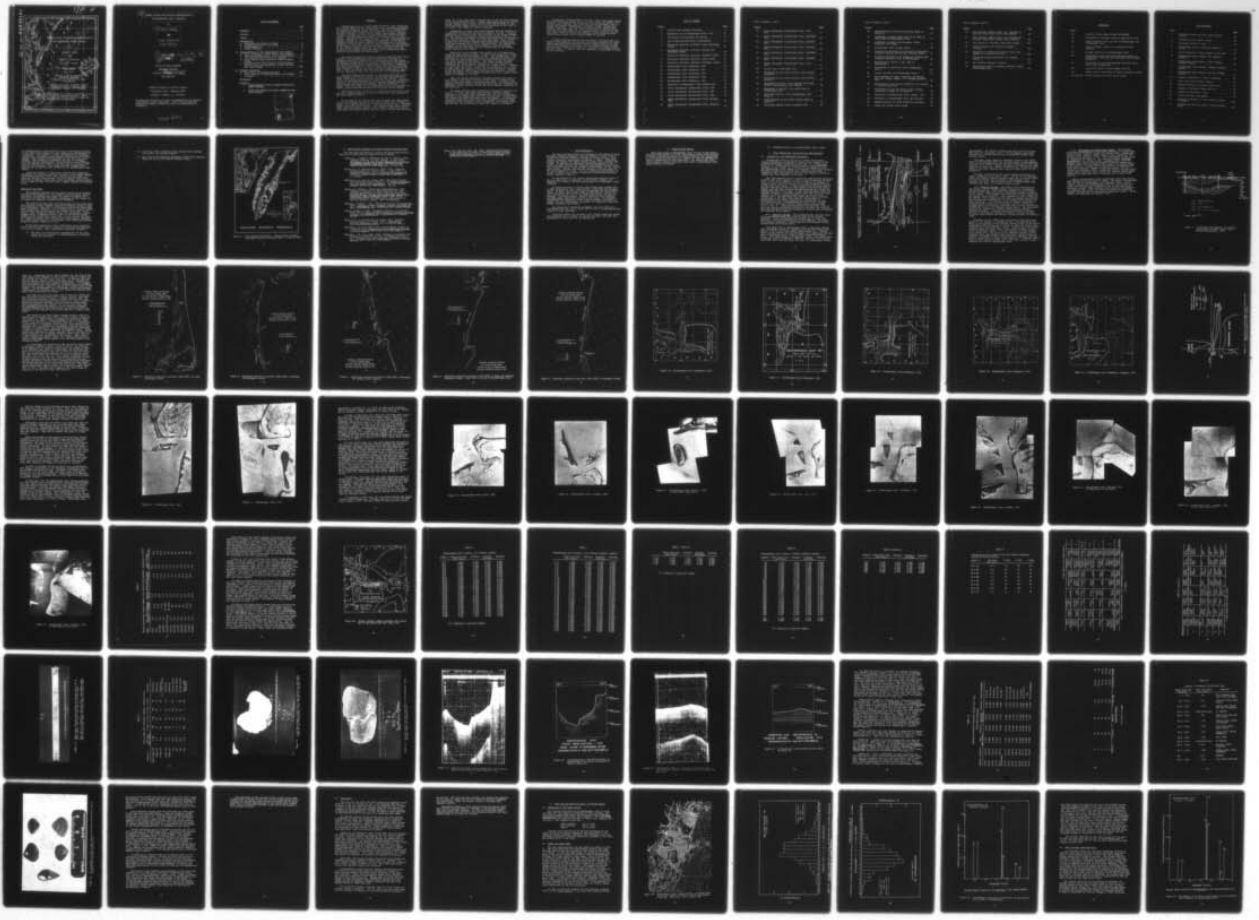

(12)

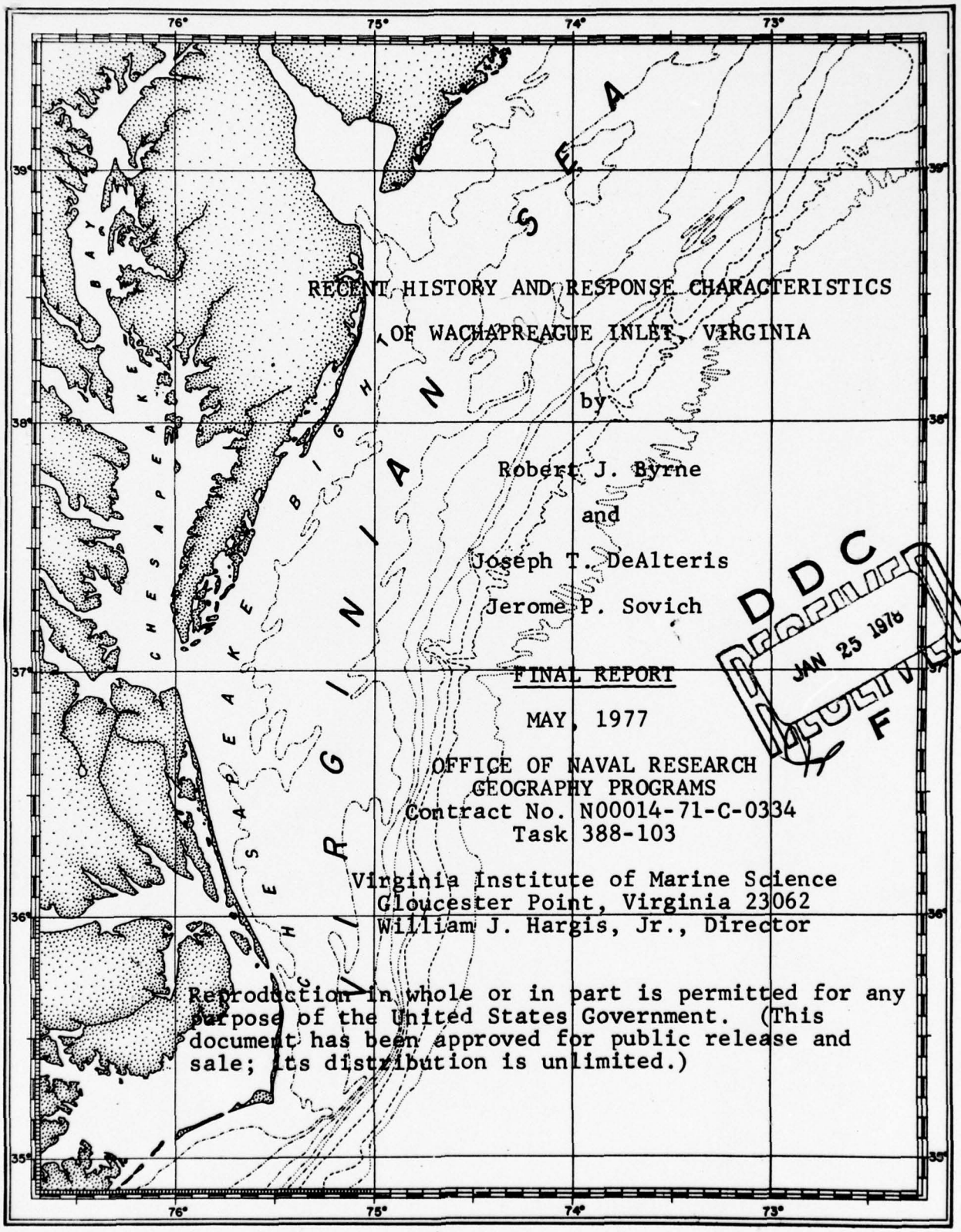

RECENT HISTORY AND RESPONSE CHARACTERISTICS OF WACHAPREAGUE INLET, VIRGINIA

by

Robert J. Byrne

and

Joseph T. DeAlteris

Jerome P. Sovich

FINAL REPORT

MAY, 1977

OFFICE OF NAVAL RESEARCH
GEOGRAPHY PROGRAMS
Contract No. N00014-71-C-0334
Task 388-103

Virginia Institute of Marine Science
Gloucester Point, Virginia 23062
William J. Hargis, Jr., Director

(6)

RECENT HISTORY AND RESPONSE CHARACTERISTICS OF WACHAPREAGUE INLET, VIRGINIA.

by

(10) Robert J./Byrne,

~~and~~

Joseph T./DeAlteris

Jerome P./Sovich

(9) FINAL REPORT. Apr 71 - Dec 74,

(11) May [redacted]77 (12) 196p.

OFFICE OF NAVAL RESEARCH

GEOGRAPHY PROGRAMS

Contract No. (15) N00014-71-C-0334

Task 388-103

Virginia Institute of Marine Science

Gloucester Point, Virginia 23062

William J. Hargis, Jr., Director

TABLE OF CONTENTS

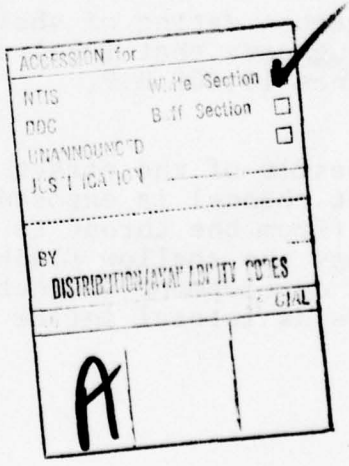

ABSTRACT

Wachapreague Inlet, a large downdrift offset inlet in the barrier island complex of the mid-Atlantic coast (Delmarva peninsula), was studied during the period 1971-1974. The inlet channel width is about 500 m and the throat cross-sectional is about 4,500 m^2. The inlet channel is about 3 km in length, approximately one-half of which is within the well-developed horseshoe shaped ebb delta complex. The maximum channel depth is 20 m which occurs at the throat. Elements of the study included: (1) the inlet morphometric history (120 years), (2) assessment of surficial and sub-bottom sediments within the inlet complex, (3) determination of the distribution of tidal flows within the inlet channel, (4) determination of the zone of influence of inlet hydraulic currents along the face of the updrift barrier island and (5) the determination of the response of the channel cross-sectional area to short-term variations in wave activity and tidal prisms.

The work of other investigators indicates that the basin-inlet complex of the Wachapreague system developed in relation to a drainage formed on a Pleistocene erosion surface and that during the Holocene transgression an extensive flood delta sand deposit of the ancestral inlet led to segmentation of the basin. Comparison of a series of bathymetric surveys between 1852 and 1972 indicate that appreciable sand is no longer advected to the interior of the inlet. Thus, it appears that the inlet has evolved from a condition of advection of sand into the interior to a bypassing mode.

The inlet channel has migrated to the south about 460 m (one inlet width) since 1852 and during the migration has deposited about 73,000 m^3/yr on the northern flank of the channel. In the course of southerly migration the offset has become more pronounced. The inlet has incised relatively firm cohesive lagoonal deposits which compose the bottom and southern side of the channel. It appears that the erosion of the thalweg has been due to abrasion by shells, gravel and sand shifting back and forth in the bedload.

Radiocarbon dating of shells recovered from a well driven near the inlet suggests that local uplift of about 92 m has occurred in the area since 19,000 B.P.

As a result of the offset nature of the inlet the north flank of the inlet channel is exposed to lateral inflow for a distance of about 1 km (from the throat to the base of the ebb delta). Ephemeral shoals occupy the shallow flank. Flow gaging during times of diminished shoal development indicate that as much as 35% of the flood prism enters as lateral inflow from the north. During ebb flow only

about 15% of the prism exits laterally due to the jet like structure of the channelized ebb flows. Drogue measurements along the updrift barrier island (Cedar Island) indicate that the influence of the flood hydraulic regime extends 3 or 4 inlet widths to the north of the inlet. This effect is absent during ebb.

Examination of basin tide records showed that the duration of rising water exceeds that of falling stages by 0.45 hr. Likewise examination of records of the tidal currents at the throat indicate that the duration of flooding currents exceed that of ebb by 0.35 hr. The duration difference is attributed principally to generation of M_4 and M_6 overtides within the inlet and basin. Thus, on the average the ebb current strength must exceed that of flood since equal water volumes must exit in a shorter time. The spatial distribution of ebb and flood flows augment the current strength asymmetry as the ebb flows are more concentrated in the central deeper portion of the channel.

Repetitive cross-sectional area surveys over 10 range lines along the inlet channel length ($\sim$ 1,500 m) were conducted 46 times during the thirteen month period of Aug., 1971 through Sept., 1972. Virtually all of the cross-sectional area modulations occurred as the result of sand accumulation on the north side of the channel over which lateral inflow occurs. The largest single filling episode at the throat section resulted in an area reduction of 7.2% which was in response to passage of a tropical storm. However, at some ranges there was a longer term area reduction due to sand cascading into the channel at the base of the ebb delta. Addition of the incremental sand volumes deposited and removed by currents within the segment of the channel surveyed over the 13 month period total to a minimum of $2 \times 10^6 m^3$.

There was general qualitative agreement between the sense of area change in the throat section and the sense of change in the ratio of ebb tidal power to incident wave power. It appears that agreement between channel response and the power ratio reflects the importance of wave activity on the ebb delta complex, regardless of wave direction.

The large sediment volume modulations observed during the surveys ($> 2 \times 10^6 m^3$) and other observations of sediment volume modulation on flanking shoals suggests that the area modulations observed in the channel were due, for the most part, to sand transfers between the ebb delta complex and the channel. An internally consistent qualitative model for such a sediment flow loop which incorporates the influence of wave refraction, the regional tidal flow and the flow distribution within the channel is presented.

An analysis of Wachapreague tides for a three year period showed mean tide levels are lowest in Jan. and Feb. while the highest occur in Sept., Oct. and Nov. The importance of this phenomena, due to steric and pressure differences, in complex storage systems with marshes is evident. Calculations show that an Oct. spring tidal prism is 18% larger than Jan. Thus, the period of enhanced prisms coincides with the advent of the northeast storm season on the east U.S. coast. Were it not for the enhanced prisms occurring simultaneously more severe inlet shoaling might be expected.

A remote sensing technique was developed to determine the tidal prism of the system for any incident tide range and mean tide level. Using sequential Black and White infrared imagery from low to high tide it was possible to delineate the relationship between flooded area and tide elevation and thence to calculate the storage function for the system. It appears that the technique is applicable to inlet basins in general.

LIST OF FIGURES

List of Figures, Cont'd.

List of Figures, Cont'd.

List of Figures, Cont'd.

APPENDICES

LIST OF TABLES

APPENDICES

Table

I. INTRODUCTION

A. Background and Purpose of the Study

The subject of the hydraulic and sedimentologic characteristics of tidal inlet-lagoon systems has received a great deal of previous investigation. Lucke (1934, a, b) emphasized the importance of the formation of the flood delta complex as a keystone to the evolution of lagoon deposits and morphology. Moreover, Lucke advanced qualitative hypotheses for the orderly evolution of tidal lagoon deposits for several sets of inlet circumstances. He did not however couple the hydraulic characteristics of the combined inlet-lagoon system to examine the stability characteristics of the inlet itself. Of all the aspects of inlet-lagoon behavior the question of the entrance stability has received the most recent attention. Observation of historical maps show that inlet entrances may migrate laterally as well as experience widely varying depths and widths through time or to close entirely due to choking from sands in the littoral drift system.

During the past several decades considerable attention has been focused on the interesting empirical results of O'Brien (1931, also 1969) which demonstrated a power low relationship between the basin tidal prism and the cross-sectional area of the throat of the inlet channel (a more recent compilation of an expanded data base is given by Jarrett (1976)). Since the cases representing the data set are based upon random survey times for inlet area or prism the relationship has become accepted as being representative of an "equilibrium" correlation. Given the randomness of the input information the correlation does not represent information on stability per se but rather an intriguing statement of an "equation of state", albeit empirical.

One of the first attempts to eludidate inlet hydraulics was that of Brown (1928), who presented an analysis based upon the geometric characteristics of the inlet and lagoon for the condition of a uniformly rising or falling basin water level. This classic work was extended by Keulegan (1967) to include the effect of non-sinusoidal tidal variation in the lagoon. As a result of his analysis he obtained a dimensionless parameter, the coefficient of repletion, which may be interpreted as a measure of the efficiency of the system toward filling the lagoon system to its full potential tidal prism. The analysis of Brown and Keulegan, although not dealing specifically with inlet stability, do provide a method for calculating the hydraulic characteristics of the inlet given specified inlet and lagoon characteristics and the ocean tide range. The question of channel cross-sectional area stability was explicitly examined by Escoffier (1940) who considered the influence of reduced

or enlarged channel cross-sectional area on the maximum velocity in the channel and whether the area change would consequently be accentuated. More recently, O'Brien and Dean (1972) presented a method for calculating inlet entrance stability due to closure tendency from transport and deposition of sand into the inlet channel. Their analysis incorporates the work of Keulegan, Escoffier and the "equilibrium" cross-sectional area of O'Brien so as to indicate the capability of the inlet to transport sand from its cross-section. They assume that the changed cross-section area is geometrically similar to the "equilibrium" cross section.

While all workers in tidal inlet stability have implicitly recognized that entrance stability represents some balance between the scouring capacity of the inlet currents and the amount of material carried to the entrance from the littoral drift system Bruun and co-workers (1960, 1967, 1974) explicitly consider stability in terms of ratio of tidal prism to gross quantity of littoral drift.

Purpose of the Study

The principal objective of the present study was to document the short-term response of inlet channel cross-sectional area to variations in incoming wave energy and tidal prism which arise from storm activity and fortnightly variations in tide range, and to relate the response to these process variables.

The impetus for the study was derived from the fact that while many previous studies examined long-term historical trends in channel configuration there was no information available on short-term channel response. Obviously, the interpretation of cross-sectional area surveys taken decades apart are tenuous unless they can be placed in the context of expected short-term variability. Wachapreague Inlet, a downdrift off-set inlet in the barrier island complex of the mid-Atlantic coast (Fig. 1) was selected for study as it posses a single, well defined tidal basin system. Moreover, its offset nature appeared to be typical of the many offset inlets along the Atlantic coast of the U.S.

As the study progressed several subordinate study objectives were identified which would be required to elucidate the behavior of the inlet complex. These subordinate objectives included:

a.) The study of the historical configuration of the inlet region and the geologic or sedimentological constraints acting on the system.

b.) The study of the character of the current flow distribution within the entrance channel.

c.) The study of the hydraulic influence of the inlet currents along the face of the updrift barrier island.

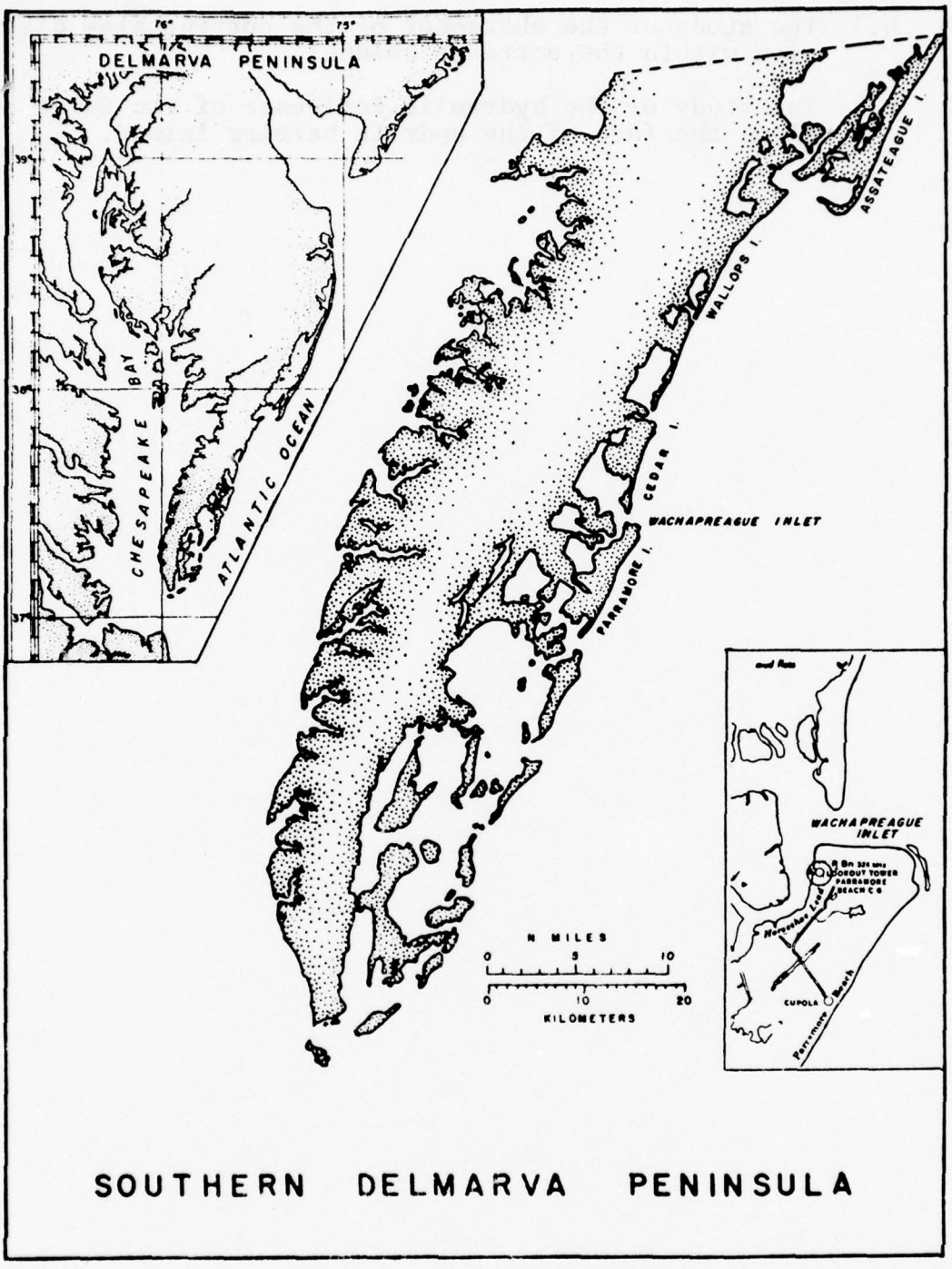

Figure 1. Lower Delmarva Peninsula. Extreme upper is lower Assateague Island and Fishing Point, a recurved spit.

B. Publications, Reports and Theses Derived from the Study

The following publications, reports and theses were derived wholly or in part from the support of this contract.

Byrne, R.J., Joseph T. DeAlteris and Paul A. Bullock, 1974, "Channel Stability in Tidal Inlets: A Case Study", Proceedings of the 14th Coastal Engineering Conference, Copenhagen, Denmark, June 1974, Published by the American Society of Civil Engineers, p. 1585-1604.

Byrne, R.J., P. Bullock and D.G. Tyler, 1975, "Response Characteristics of a Tidal Inlet: A Case Study", in Estuarine Research, Vol. II; Geology and Engineering, (ed. L.E. Cronin) Academic Press, Inc., New York, p. 201-216.

DeAlteris, J.T. and R.J. Byrne, 1975, "The Recent History of Wachapreague Inlet, Virginia", in Estuarine Research, Vol. II; Geology and Engineering, (ed. L.E. Cronin) Academic Press, Inc., New York, p. 167-182.

Mehta, A.J., Robert J. Byrne and Joseph DeAlteris, 1975, "Hydraulic Constants of Tidal Entrances III: Bed Friction Measurements at John's Pass and Blend Pass" UFL/COEL/TR-026, Coastal and Oceanographic Engineering Laboratory, Univ. of Florida, March, 1975, 86 pp. (also published in the 15th Coastal Engineering Conference, Honolulu, Hawaii, 1976, in printing).

DeAlteris, Joseph T., 1973, "The Recent History of Wachapreague Inlet", School of Marine Science, College of William and Mary, Williamsburg, Va., unpublished M.S. Thesis, 86 pp.

Sovich, Jerome P., 1974, "Nearshore Influence of a Natural Tidal Inlet", School of Marine Science, College of William and Mary, Williamsburg, Va., unpublished M.S. Thesis, 108 pp.

Byrne, R.J., P. Bullock and D.G. Tyler, 1973, "Response Characteristics of a Tidal Inlet", Transactions American Geophysical Union, Vol. 54, No. 4, (abs.).

DeAlteris, J.T., R.J. Byrne, 1973, "A Geological Control of a Natural Inlet" Geological Society of America Meetings of the NE Section, Vol. 5, No. 2, p. 155, (abs.).

DeAlteris, J.T., R.J. Byrne, 1975, "Evidence of Possible Late Quarternary Uplife in the Area of Wachapreague Inlet, Va.", Geological Society of America, Meetings of the NE Section, Vol. 7, No. 1, p. 44, (abs.).

Byrne, R.J. and J.D. Boon, III, 1976, "Speculative Hypothesis on the Evolution of Barrier Island-Inlet-Lagoon Systems", Joint NE-SE Geological Society of America Meetings, Vol. 8, No. 2, p. 159, (abs.).

C. Acknowledgements

The work described herein was supported by the Office of Naval Research, Geography Programs, Contract N00014-71-C-0334, Task No. NR 388-103, with the Virginia Institute of Marine Science. The contract principal investigator was Robert J. Byrne. Additional support was derived from NASA, Wallops Island, under Contract NAS-6-1902. In addition to substantial aerial photography of the study area NASA provided the sequential photography (Mission W226) for the determination of the storage characteristics of the interior basin system. Finally NASA Wallops provided a tracking radar for the 1972 bathymetric survey. We also acknowledge the generous use of the I^2S Digicol for imagery analysis at NASA-Langley Research Center, Hampton, Virginia.

We are grateful to the Coastal Engineering Research Center of the U.S. Army Corps of Engineers, Fort Belvoir, Virginia for supplying to us daily surf wave observations for Assateague Island, Virginia.

To achieve success in arduous field observation program such as that conducted in this study requires a dedicated and diligent staff. We therefore very gratefully acknowledge the extraordinary efforts of Mssrs. David Tyler, Paul Bullock and Ray O'Quinn who were responsible for much of the field observations and data preparation. In addition Mssrs. Michael Carron and Gary Anderson provided highly appreciated support in the field. We gratefully acknowledge the assistance of Mr. Michael Castagna, Scientist in Charge, V.I.M.S. Wachapreague Laboratory for thoughtful logistical support throughout the project.

The authors have benefited throughout the study from many discussions with Dr. John D. Boon, III, V.I.M.S., concerning various aspects of tidal phenomena.

Particular thanks are extended to Ms. Cynthia Diggs for typing the manuscript and to members of the Art and Photo Lab staff for preparation of materials for the publication.

D. Format of the Report

Since this study of Wachapreague Inlet focuses on the several important characteristics of the inlet-lagoon system which describe or explain its history and/or its present behavior the characteristics are presented sequentially in Chapter II with the methods and results incorporated in each subsection. The authors felt this would provide a clearer exposition than would a presentation which lumped methods and results.

II. CHARACTERISTICS OF THE WACHAPREAGUE INLET SYSTEM

A. Inlet Morphology, Recent History and Sediments

A1. Introduction and background discussion.

Wachapreague Inlet is typical of several inlets with a similar bathymetric configuration along a 60 km expanse of the southeastern Delmarva Peninusla coast (Fig. 1). Wachapreague Inlet is an "offset coastal inlet" similar to those described by Hayes, et al. (1970); it is offset to the downdrift side. The "Wachapreague Inlet Complex" is composed of the inlet channel, Parramore Island to the south, Cedar Island to the north, a crescentric ebb tidal delta to the east and finally a system of lagoons and tidal channels to the west.

Most investigators in the engineering sciences have generally assumed tidal inlet channels to incise a bed of material of sand size. It is then assumed to be free to migrate in response to littoral drift, and to scour and fill as the flushing capability of the tidal flow varies. Little consideration has been paid to the fact that many inlets on sandy coasts incise barrier island chains, and that many of these transgressive barrier islands are nothing more than thin veneers of sand overlying marsh peats and lagoonal sediments. One might suspect then that the tidal inlet channels in these instances would incise not only sand but cohesive muds, and that these muds might exert some noticeable constraints on the tidal inlet system. The geometry of Wachapreague Inlet channel suggests such constraints in that the south flank has a maximum measured slope of 45° (average slope of 30°) while the northern flank has an average slope of 3.5° (Fig. 2). These characteristics motivated the study to trace the recent morphometric history of the inlet and to determine what geological and sedimentological controls have influenced its stability and evolution.

A1.1 Regional Setting. Four geomorphically distinct zones can be recognized along the Atlantic coast of the Delmarva Peninsula. From Cape Henlopen in Delaware Bay to Ocean City, Maryland, a barrier beach impinges on the mainland. Bay mouth bars separate estuaries or bays associated with drowned fluvial systems from the Atlantic Ocean.

From Ocean City to Chincoteague Inlet a continuous barrier spit, Assateague Island, is separated from the Pleistocene mainland by a 10 to 13 km wide lagoon, Chincoteague Bay. Fishing Point, on the southern end of Assateague, is a pronounced recurved spit of relatively recent origin pointed toward Chincoteague Inlet. From Chincoteague to Wachapreague inlets, the broken chain of barrier islands in markedly indented. Harrison (1971) speculated that this reentrant marks the path of a paleochannel across

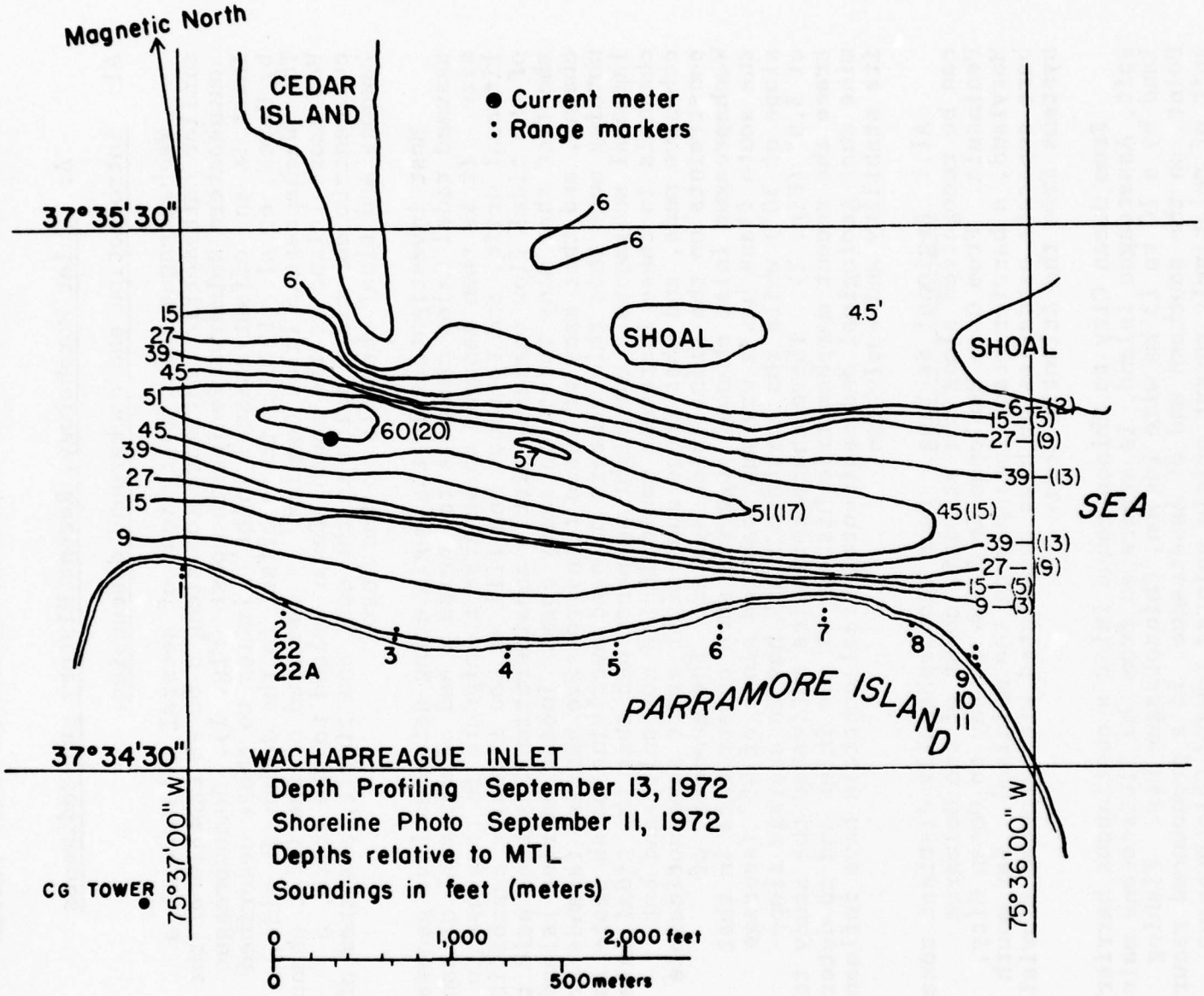

Figure 2. Wachapreague Inlet channel. Note shelf on south and asymmetry of channel cross-section. Numbers on south shoreline are survey range line positions, 1 through 11.

the Delmarva. The barrier islands along this section of coast have very low topographic relief, and the lagoons separating the barriers from the mainland are considerably smaller than adjacent areas.

The final sector begins at Parramore Island on the south flank of Wachapreague Inlet and continues south to Cape Charles. This sector is characterized by strongly offset inlets with deep channels (20 to 25 m). Between the barrier islands and the mainland lies a tidal flat complex of shallow bays, intertidal flats, marshes, and tidal channels that varies in width from 7 to 15 kilometers.

No major streams drain the eastern Delmarva Peninsula to supply sediments to the modern coast. Erosion of the headlands along the northern Delmarva provides sands for the beaches there and for the barrier spit extending to Chincoteague Inlet. In contrast, the thin, narrow beaches south of Chincoteague Inlet indicate that there is a limited supply of sand.

A1 2 Regional Geology. The Eastern Shore Peninsula has low relief (< 20 m) and the surface deposits are of Holocene and Pleistocene age. The Pleistocene geology of the Virginia section of the Delmarva has been extensively studied by Sinnott, et al. (1961). Four terraces were identified on the mainland of the Eastern Shore Peninsula. From youngest to oldest, there are the Chowan, Dismal Swamp, Princess Anne, Pre-Chowan and Wicomico. The terraces are considered to be the emerged upper surfaces of these formations. The Columbia group of terrace formations of Pleistocene Age consist of a succession of thin, very gently sloping marine and estuarine formations that overlie the Tertiary sedimentary rocks of the Virginia Coastal Plain. The Pleistocene deposits are underlain by seaward dipping Miocene deposits (Chesapeake Group). Scattered well-log information indicates the top of the Miocene (Yorktown Formation) is found at about 25 meters depth beneath the barrier islands (Sinnott and Tibbitts, 1968).

Harrison, et al. (1965) have postulated a late Pleistocene uplift of the entrance to Chesapeake Bay. This hypothesis was based on the expected versus observed thalweg depths of the buried Susquehanna River Valley and C^{14} dating of peats and shells overlying the Pleistocene-Miocene contact. Harrison also encountered elevated peats and oyster shell on Hog Island, located to the south of Parramore Island. From the totality of their evidence it is argued that, "the crust in the immediate vicinity of the Virginia capes, and probably along the entire Atlantic Coast of Virginia to somewhat north of Hog Island has undergone some 160 feet of uplift since at least 15,000 years B.P." Evidence offered later in this chapter confirms that uplift has occurred in the immediate vicinity of Wachapreague Inlet.

A1.3 Development of Wachapreague Lagoon. The Holocene-Pleistocene stratigraphy of the basin influenced by Wachapreague Inlet has been studied by Newman and Rusnak (1965), Newman and Munsart (1967), DeVries (1970), Kemerer (1972), Harrison, 1971 and Morton and Donaldson (1973). The stratigraphy of the system is illustrated in Figure 3. The surficial marshes (Spartina alternaflora) are relatively thin, averaging about 1.5 m in thickness and, based upon palynological evidence, Newman and Munsart reason that the rhizome layer began to accumulate after 1,500 years B.P. Beneath the rhizome horizon are lagoonal and flood delta deposits, ranging in thickness from 1.5 to 15 m (Morton and Donaldson, 1973). Newman and Munsart obtained radiocarbon dates from basal peats beneath the lagoonal facies which indicate the lagoon had been in existence for at least 5,000 years B.P.

Morton and Donaldson (1973) established three lines of jet wash borings across the interior basin. The center line extended from the Town of Wachapreague to Wachapreague Inlet. These authors conclude that Wachapreague Inlet is a site which coincides with drainage from topographic lows of the Pleistocene erosional surface. Their evidence also indicates the existence of extensive flood delta sand deposits between the overlying lagoonal deposits and the underlying Pleistocene contact. These results are summarized in Figures 3 and 4.

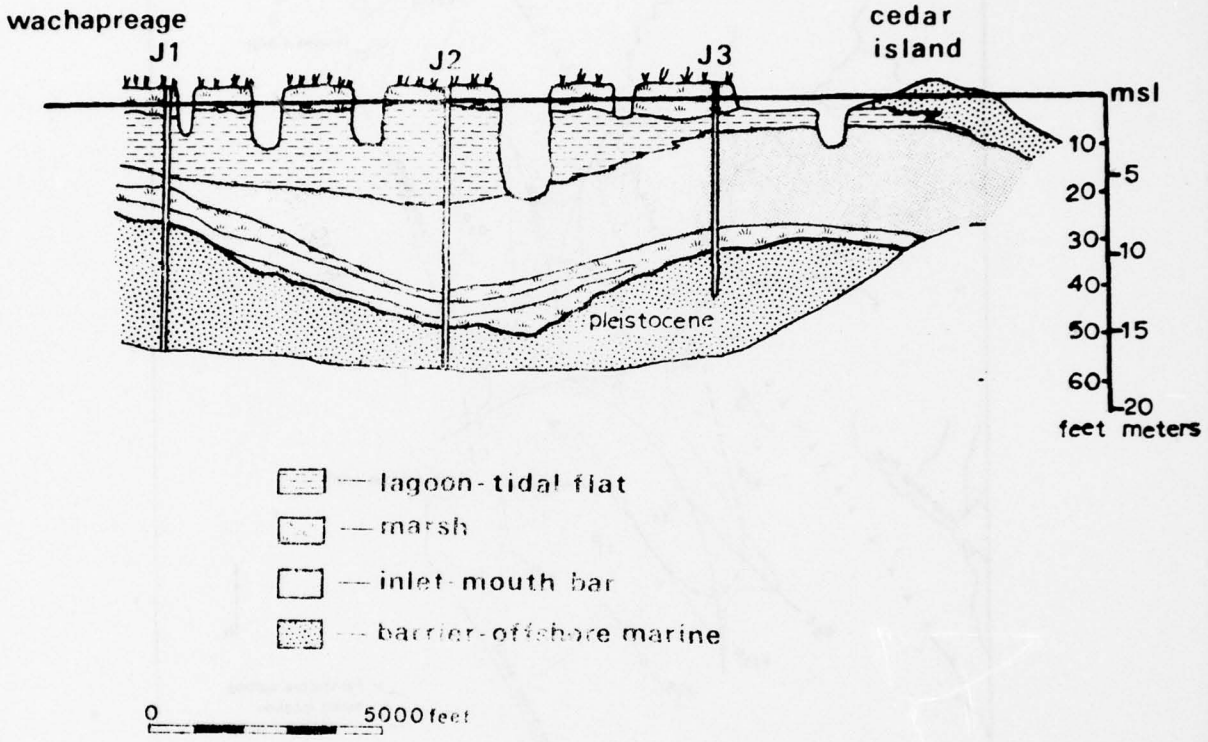

Figure 3. Interpreted stratigraphic dip section, Wachapreague to Cedar Island (after Morton and Donaldson, 1973).

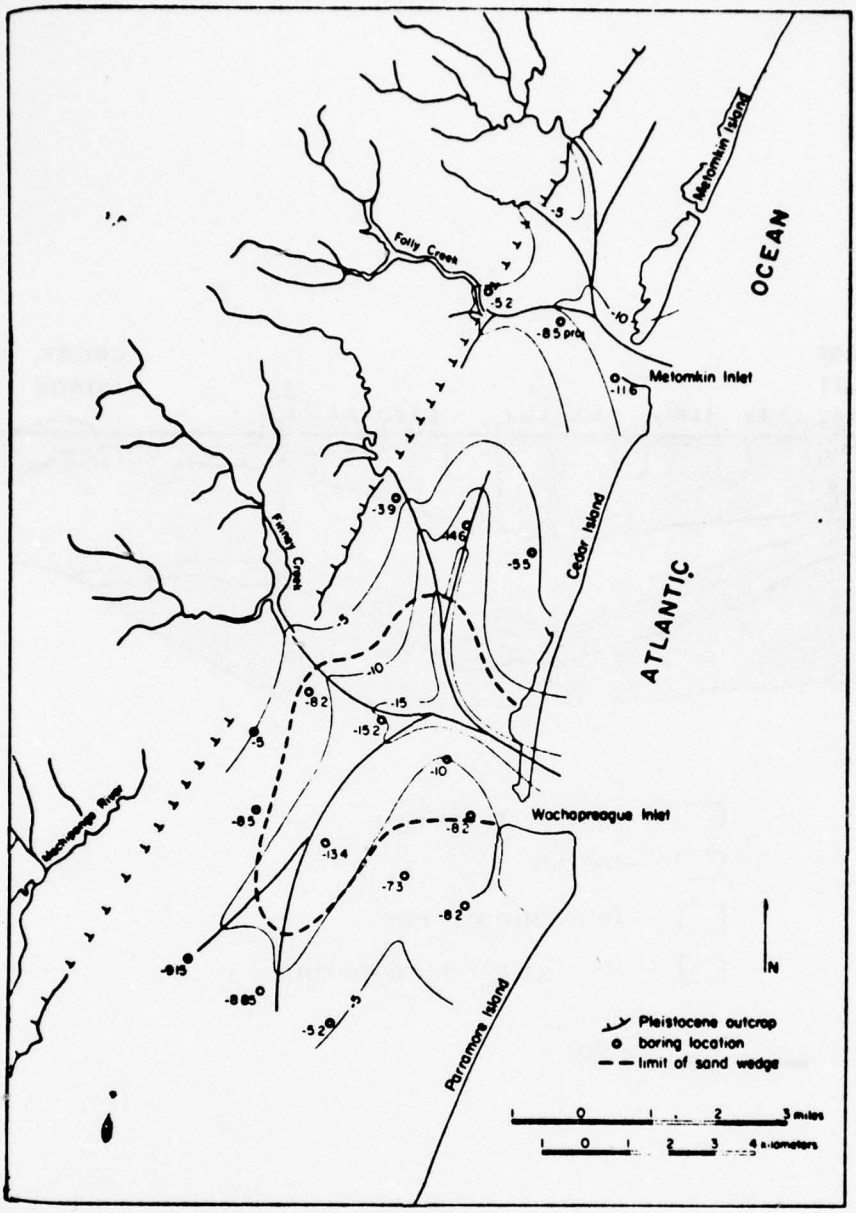

Figure 4. Map of the Holocene-Pleistocene unconformity showing the position of present-day drainage and tidal inlets in relation to Pleistocene drainage. Depths are in meters below mean sea level. (From Morton and Donaldson, 1973.)

A2. Recent History of the inlet and shoreline; surficial and substrate sediments.

A2.1 Recent Erosion History of the Barrier Islands. Inspection of regional wave refraction patterns (Goldsmith, et al., 1974) and wave climate information (Saville, 1954) indicates that the principal supply of littoral drift to Wachapreague Inlet is derived from erosion of the barrier islands to the north (see Figure 1). These islands from Wallops thru Cedar Islands, have beaches with small sand volumes; that is, the beaches are a sand veneer covering eroding marsh facies. It is not uncommon after severe storms to find exposed marsh deposits at foreshore positions.

The shoreline positions between the years 1852-1962 for the islands to the north of Wachapreague are shown in Figures 5 thru 9 which maybe keyed to Figure 1. The lower end of Assateague Island is a recurved spit, Fishing Point, which formed since 1852. The U.S. Corps of Engineers estimated that .46 x $10^6 m^3/yr$ of sand drifts to the south along northern Assateague Island and that, based on the accumulation in the spit, about 0.3 x $10^6 m^3/yr$ is trapped at the southern terminus of the island. A reasonable estimate for material bypassing Chincoteague Inlet from the north is then (.46 - 0.3) x $10^6 m^3/yr$ or 0.16 x $10^6 m^3/yr$.

The long term (110 yr) average erosion rate within the island sequence from Wallops Island to Cedar Island increases to the south; Wallops Island erosion rate was calculated at 2.3 m/yr while Cedar Island was 4.8 m/yr. A rough estimate of the mean annual littoral drift rate may be made if an assumption is accepted as to the percentage of sand in the eroding marsh face. Measurement of area lost in the island chain due to shoreline shift indicates 160,000 m^2/yr has been eroded. Using the U.S. Corps of Engineers rule of thumb that 1/sq. ft. of area loss equals 1/cu. ft. of sand volume loss the eroded area converts to 1.32 x $10^6 m^3$ of material per year. Assuming only 25% of the eroding marsh is of sand size material this reduces the maximum sand available for transport to .33 x $10^6 m^3/yr$.

Given the embodied assumptions a reasonable estimate for maximum southerly drift is 0.5 x $10^6 m^3/yr$. It should be emphasized that this figure is based on data averaged over a 110 year period.

A2.2 Historical Changes in the Inlet Configuration. United States Coast and Geodetic Survey Hydrographic Survey Sheets for 1852, 1871, 1911, and 1934 (Figs. 10, 11, 12, 13) were compiled and contoured at 0.913 m (3 ft.) intervals. It is worthwhile to note that the 1871 and 1934 surveys followed severe storms, and that this may explain the abbreviated south end of Cedar Island apparent in the 1934 survey. A new bathymetric survey of the entire Wachapreague Inlet system was made by the authors in 1972

(Fig. 14). Comparison of the charts showed that the axis of the inlet channel has migrated to the south at a rate of 1 meter per year during the last 120 years (Fig. 15). In addition the channel has rotated slightly counter-clockwise from a southeastern axial orientation to a more easterly orientation. In its migration the channel flow has eroded the northern flank of Parramore Island while leaving a wedge of sand on the northern flank of the channel. The northeastern face of Parramore Island has accreted seaward while the southern end of Cedar Island has migrated landward, thus accentuating the offset.

The long term cross-sectional area of the inlet throat has been relatively stable since 1871 at about 4,200 m^2 (less than 15% variation from mean); however, between 1852 and 1871, the cross-sectional area increased from 1,845 m to 4,473 m^2 (Table 1). Historical evidence indicates that the interior marsh-lagoon system configuration has changed very little since 1852, thus the potential tidal prism appears to have remained unchanged. There is insufficient tide information for the 1850 period to determine if the reduced cross-section admitted a smaller tidal prism.

The length of the inlet throat channel (based on the 12 m contour) has increased from 1,600 m in 1852 to about 3,000 m in 1972 (Table 2), significantly increasing the frictional characteristics of the inlet. Various hydraulic radii of the inlet throat cross-sections were calculated based on 1) an unmodified cross-section, 2) a modified cross-section (long shallow tails removed), and 3) a modified and normalized cross-sectional area (expanded to uniform area, yet maintaining geometric similarity in order to allow a valid comparison of hydraulic radii). These results are tabulated in Table 3 and the trend is similar for all three techniques, an increasing hydraulic radius until the turn of the century, then decreasing to the present. Thus, with a steadily increasing channel length, and a decreasing hydraulic radius, Wachapreague Inlet appears to be evolving toward a less efficient channel.

To investigate the possibility that the entire inlet complex is serving as either a source or sink of sand to the littoral drift moving down the barrier island coast, the volume of sand, to an arbitrary base level 21 m below MLW, was calculated for each of the survey charts from 1852 to 1972 (no data for 1871). This was accomplished by dividing each of the contoured charts for 1852, 1911, 1934, and 1972 into a matrix of smaller areas denoted by 1A, 2A, 1B, 2B, etc. The volume of material in each of these smaller areas was determined by measuring the area between individual contours with a Compensating Polar Planimeter, and multiplying this by the difference between the mean depth of the two contours and 21 meters, the base depth. Then each of these volumes were summed to the total volume of smaller areas (1A, 1B, etc.), and these were summed to the total volume of material in the system at that time (Table 4).

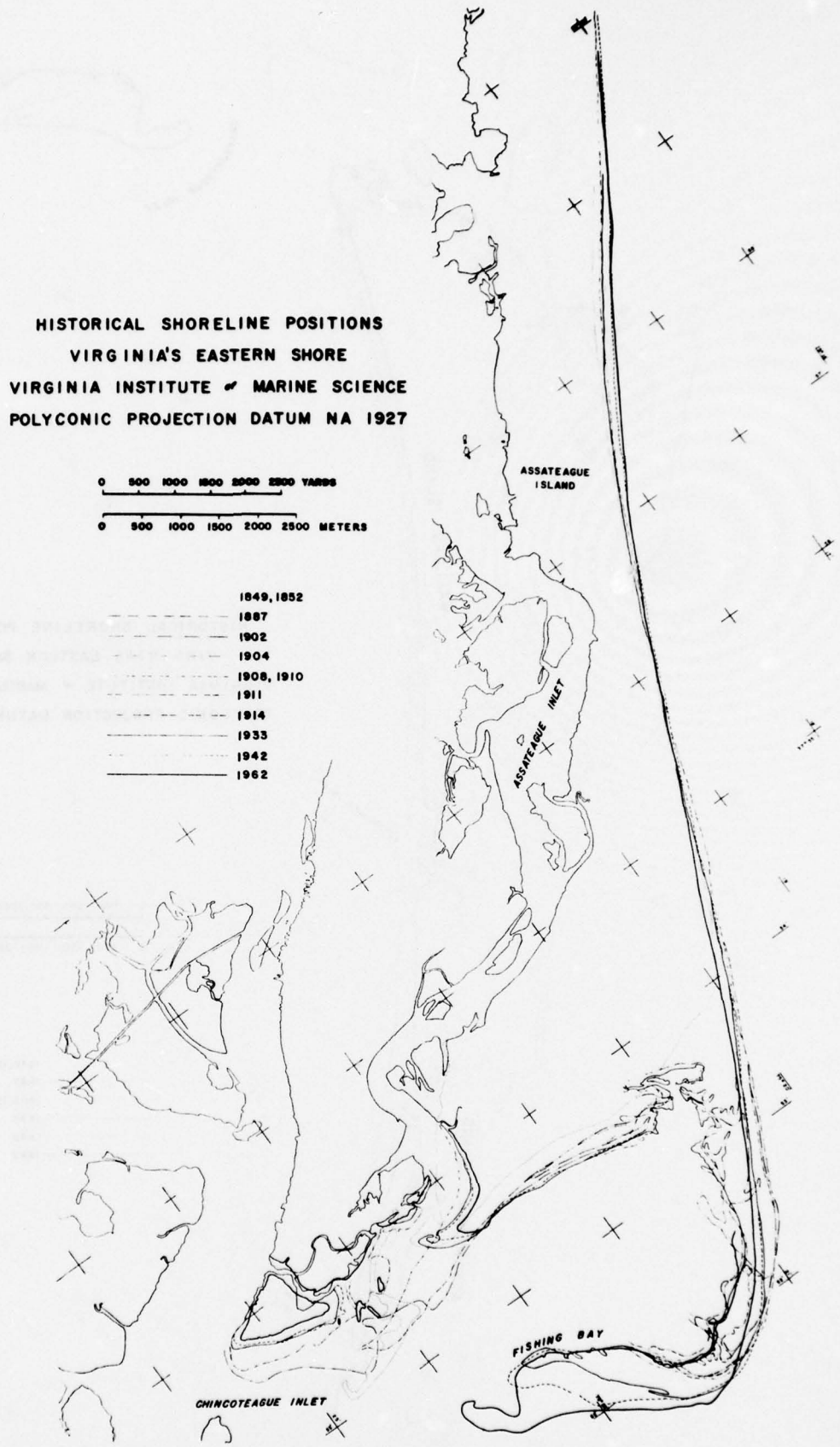

Figure 5. Historical shoreline positions (1852-1962) of lower Assateague Island.

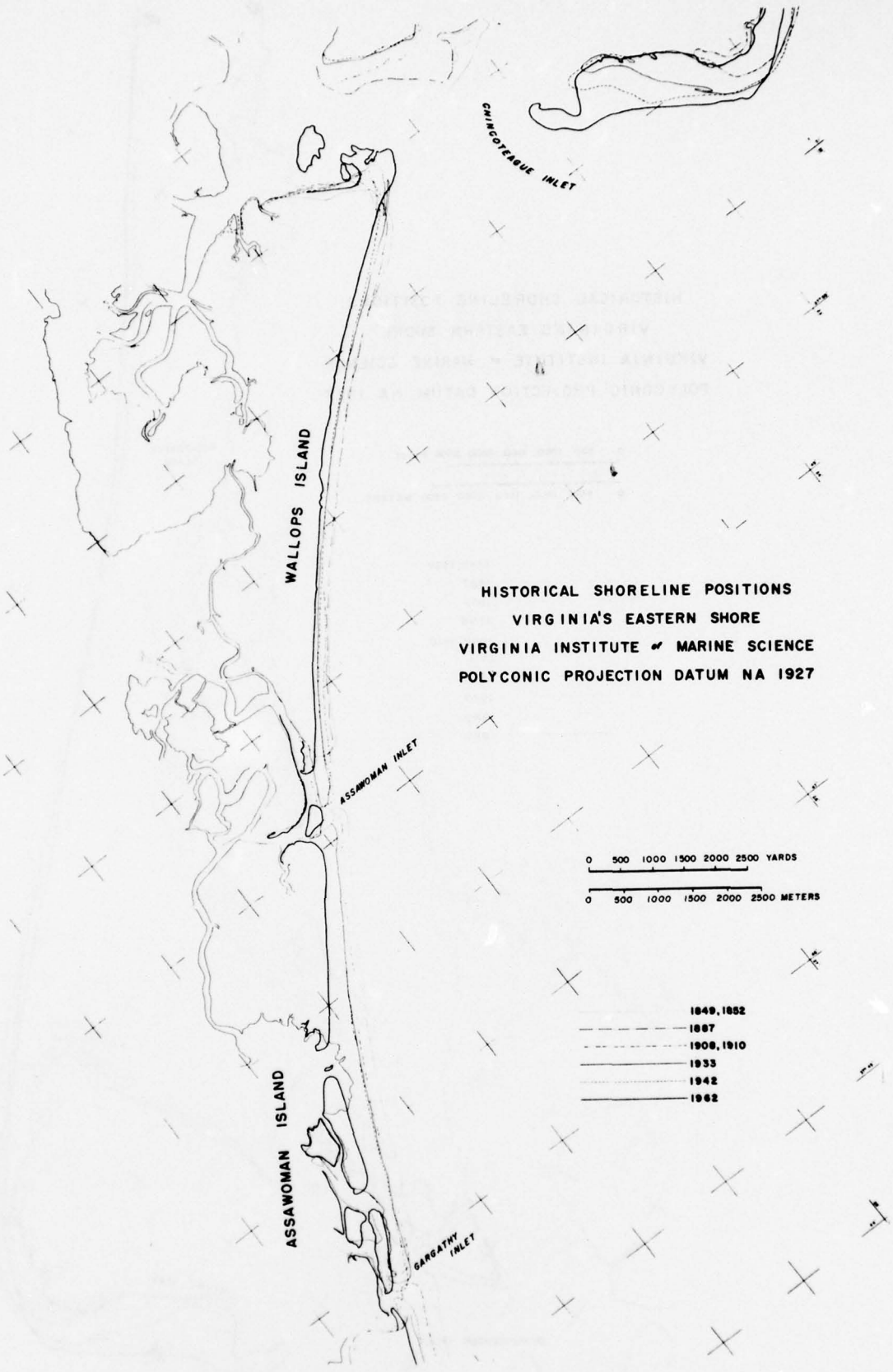

Figure 6. Historical shoreline positions (1852-1962) of Wallops and Assawoman Islands.

Figure 7. Historical shoreline positions (1852-1962) of Metomkin and northern Cedar Islands.

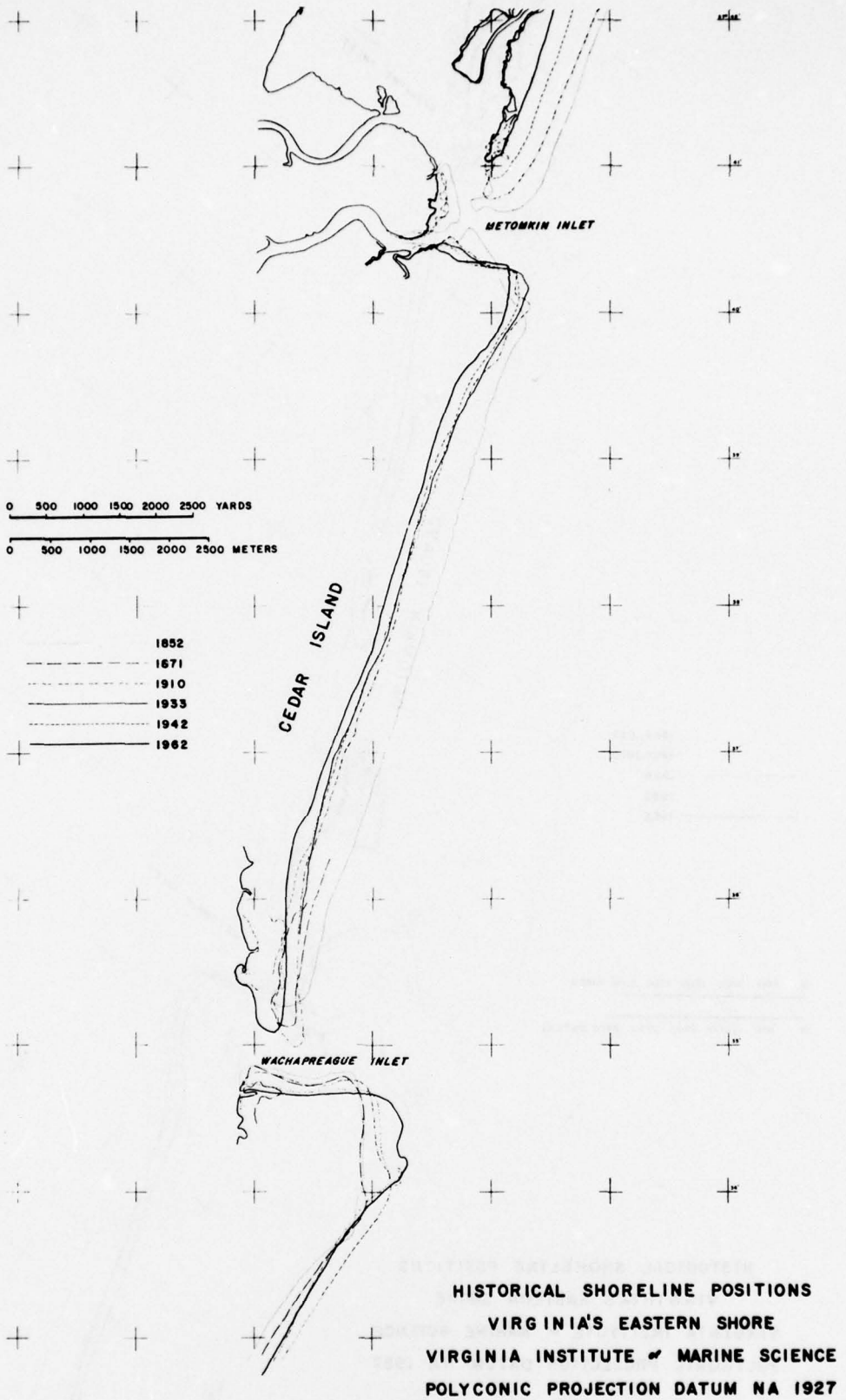

Figure 8. Historical shoreline positions (1852-1962) of Cedar and northern Parramore Islands. Note shift to south of Wachapreague Inlet.

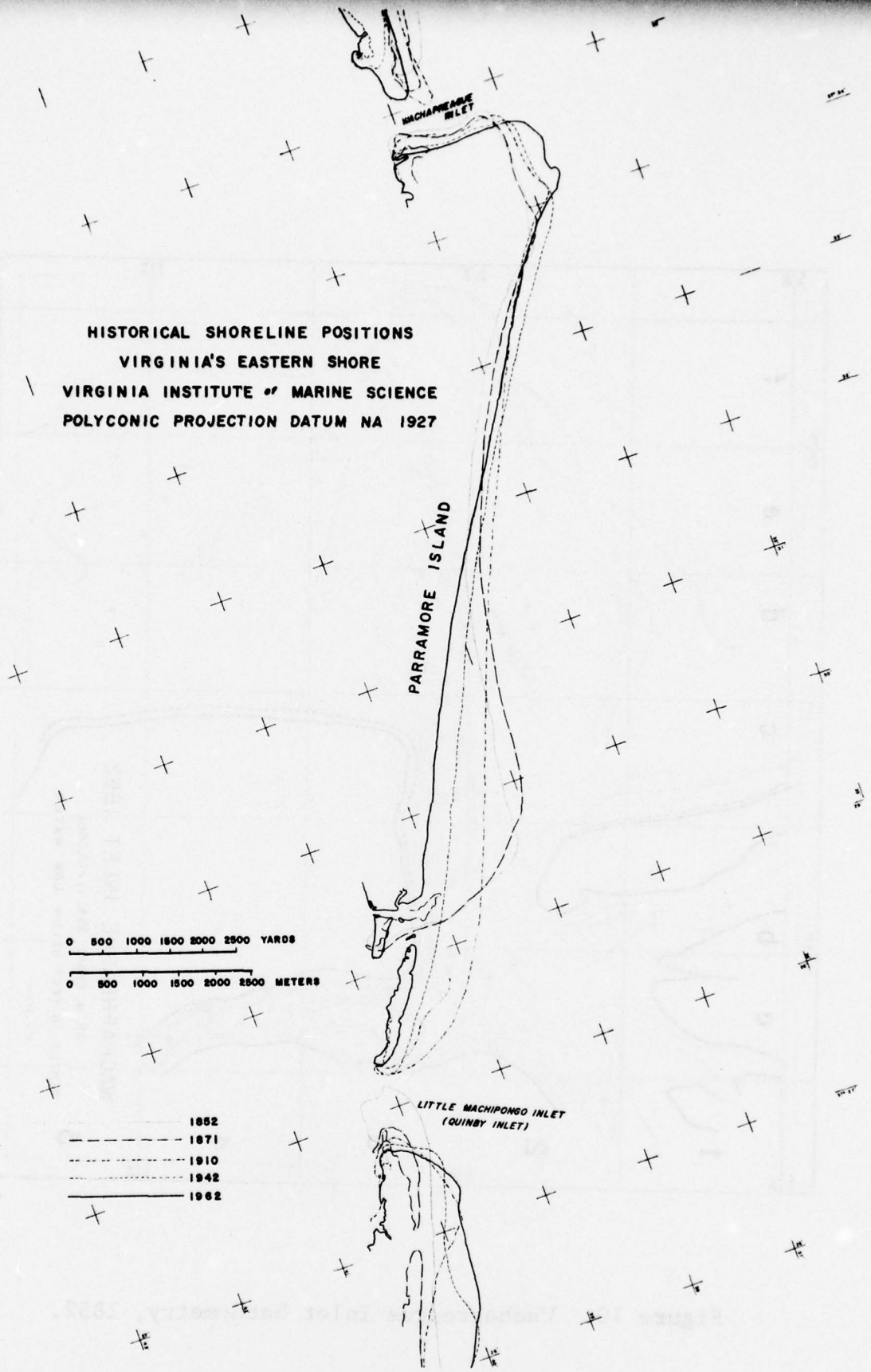

Figure 9. Historical shoreline positions (1852-1962) of Parramore Island.

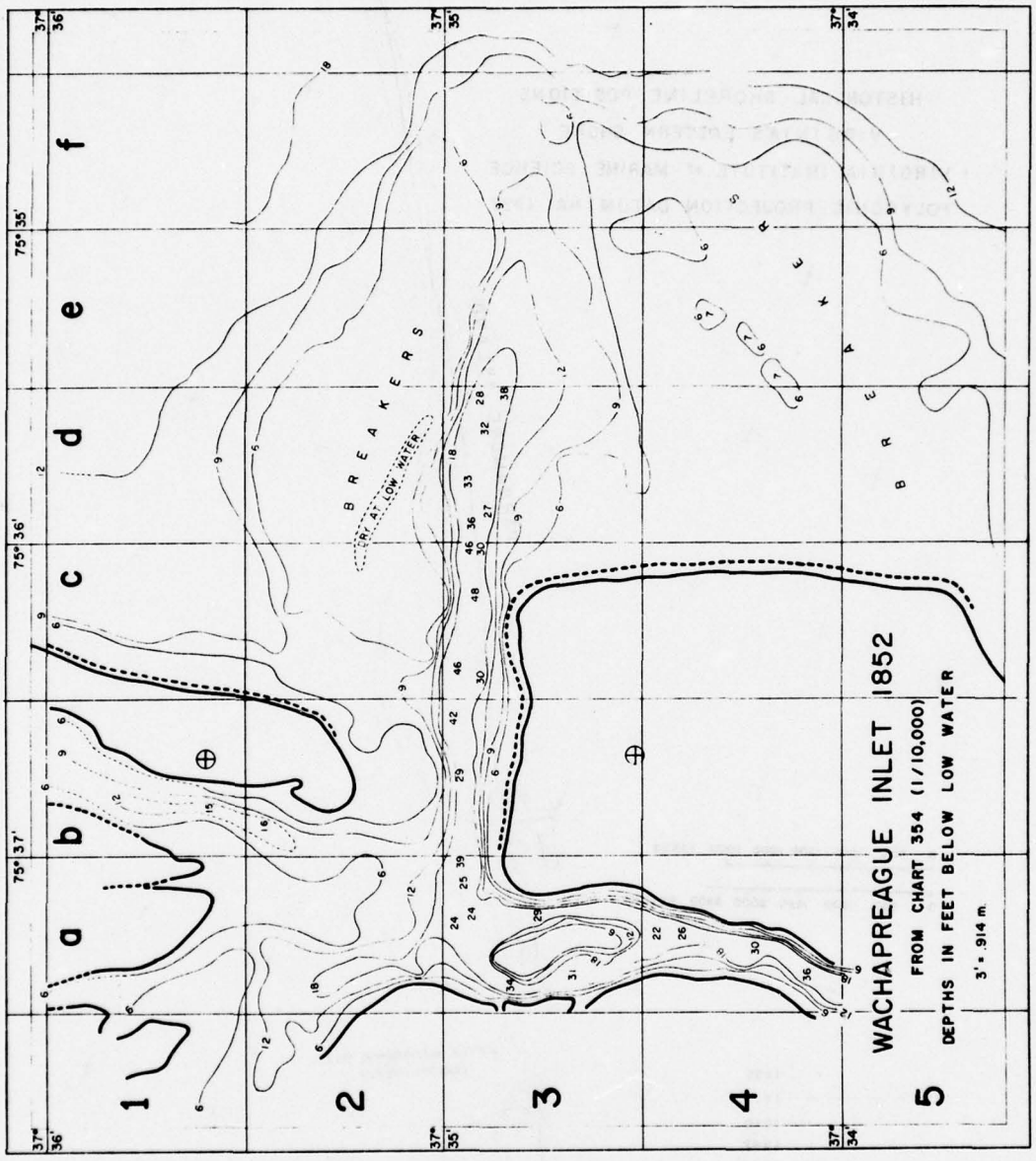

Figure 10. Wachapreague Inlet bathymetry, 1852.

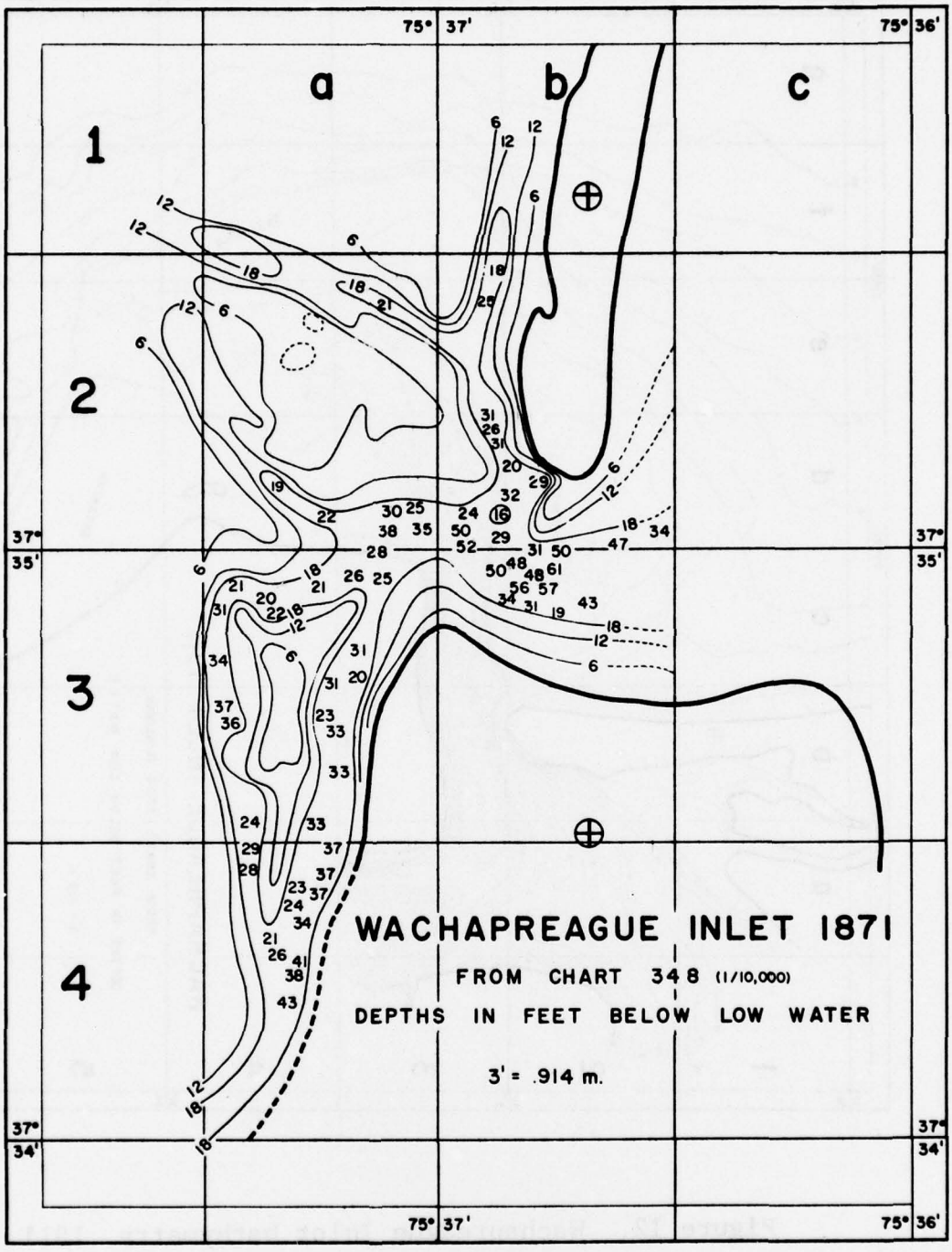

Figure 11. Wachapreague Inlet bathymetry, 1871.

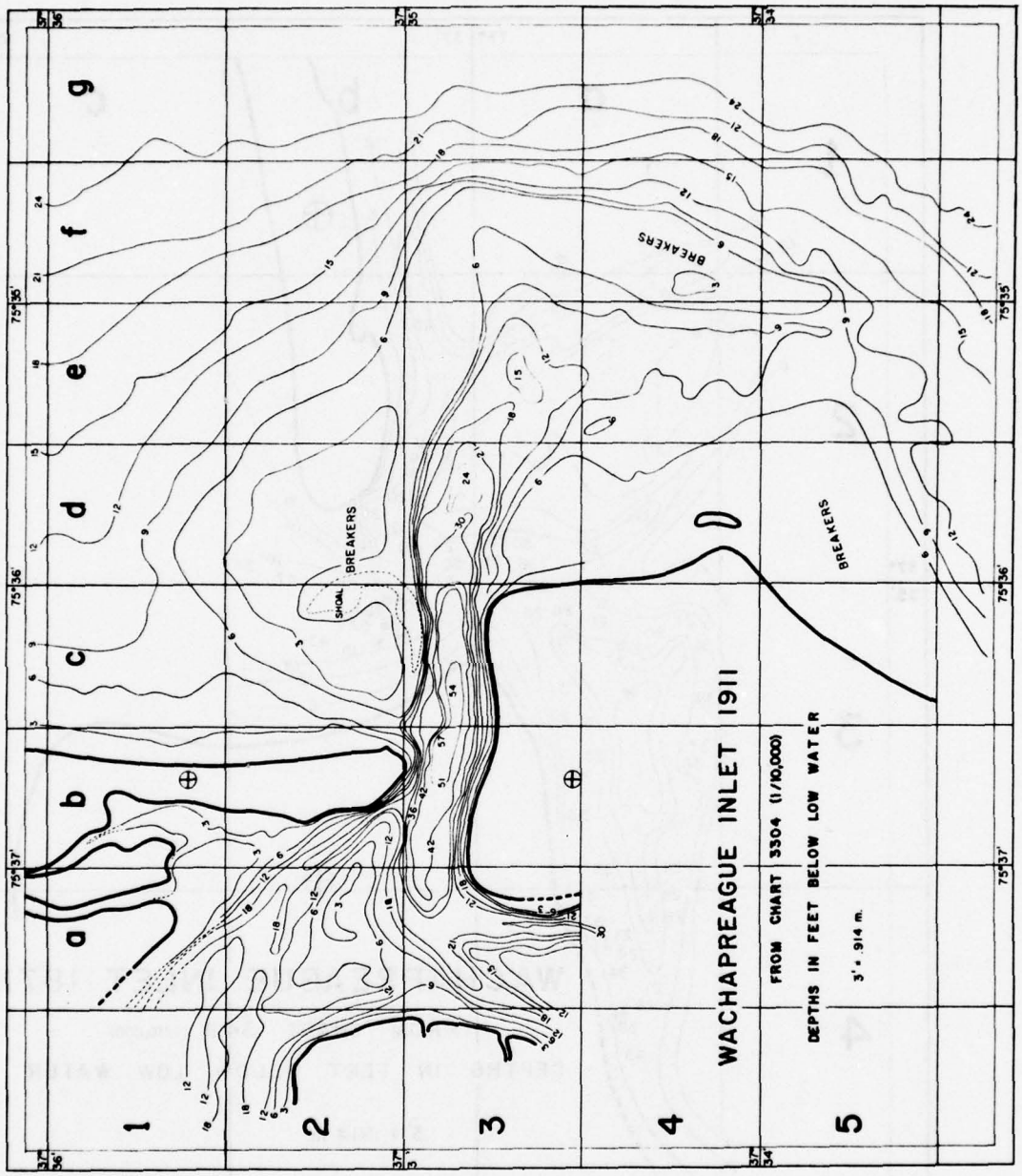

Figure 12. Wachapreague Inlet bathymetry, 1911.

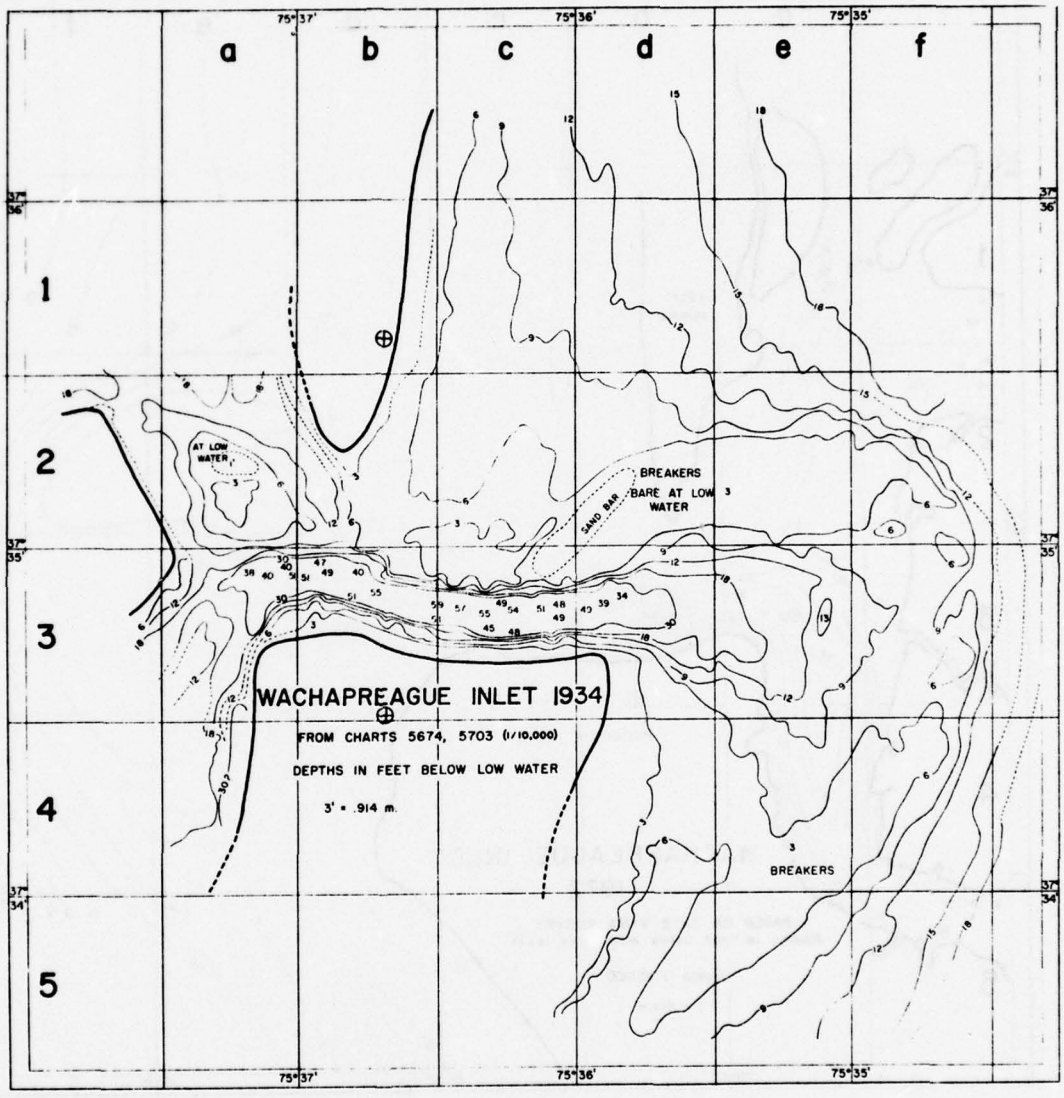

Figure 13. Wachapreague Inlet bathymetry, 1934.

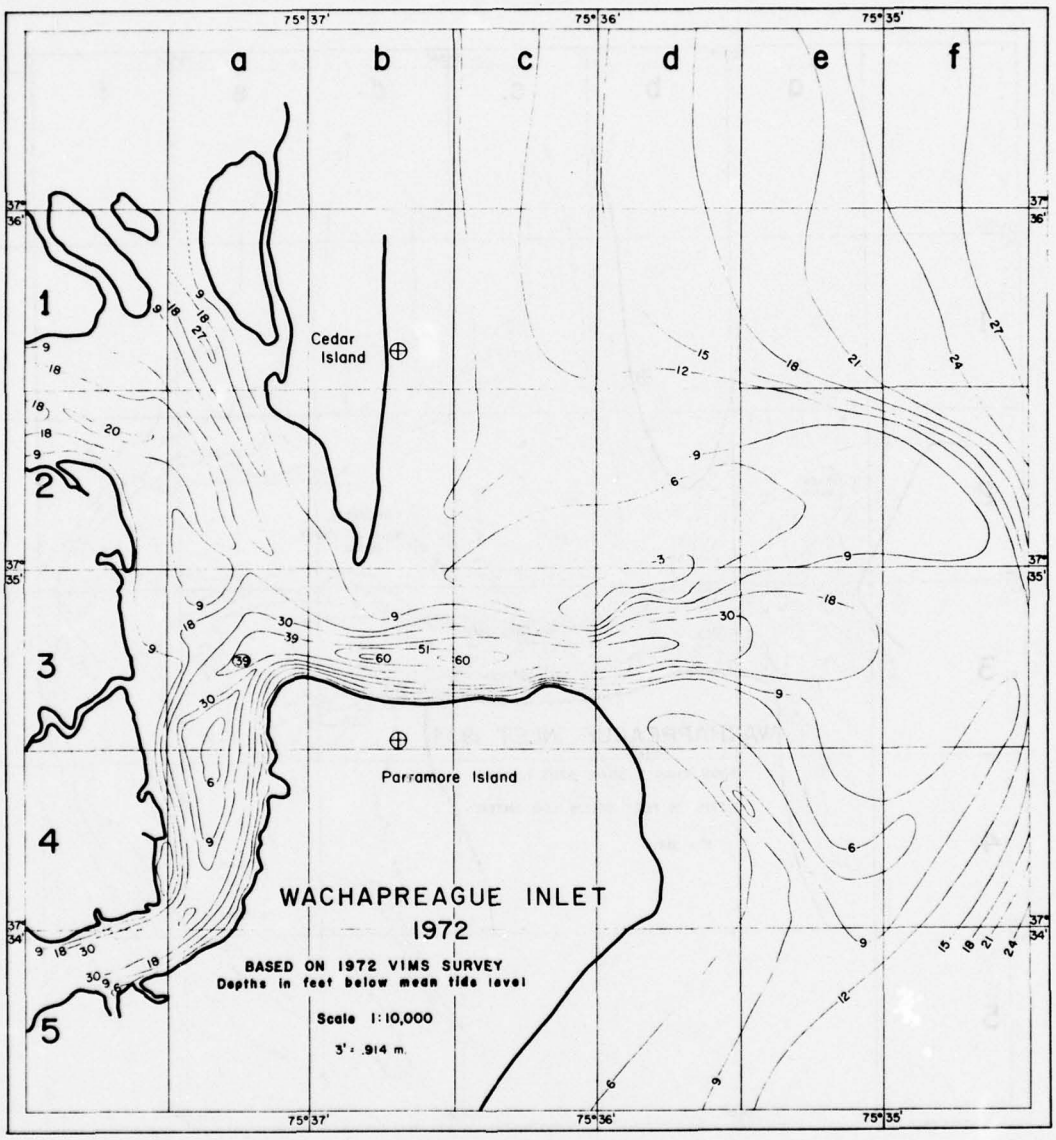

Figure 14. Wachapreague Inlet bathymetry, December, 1972.

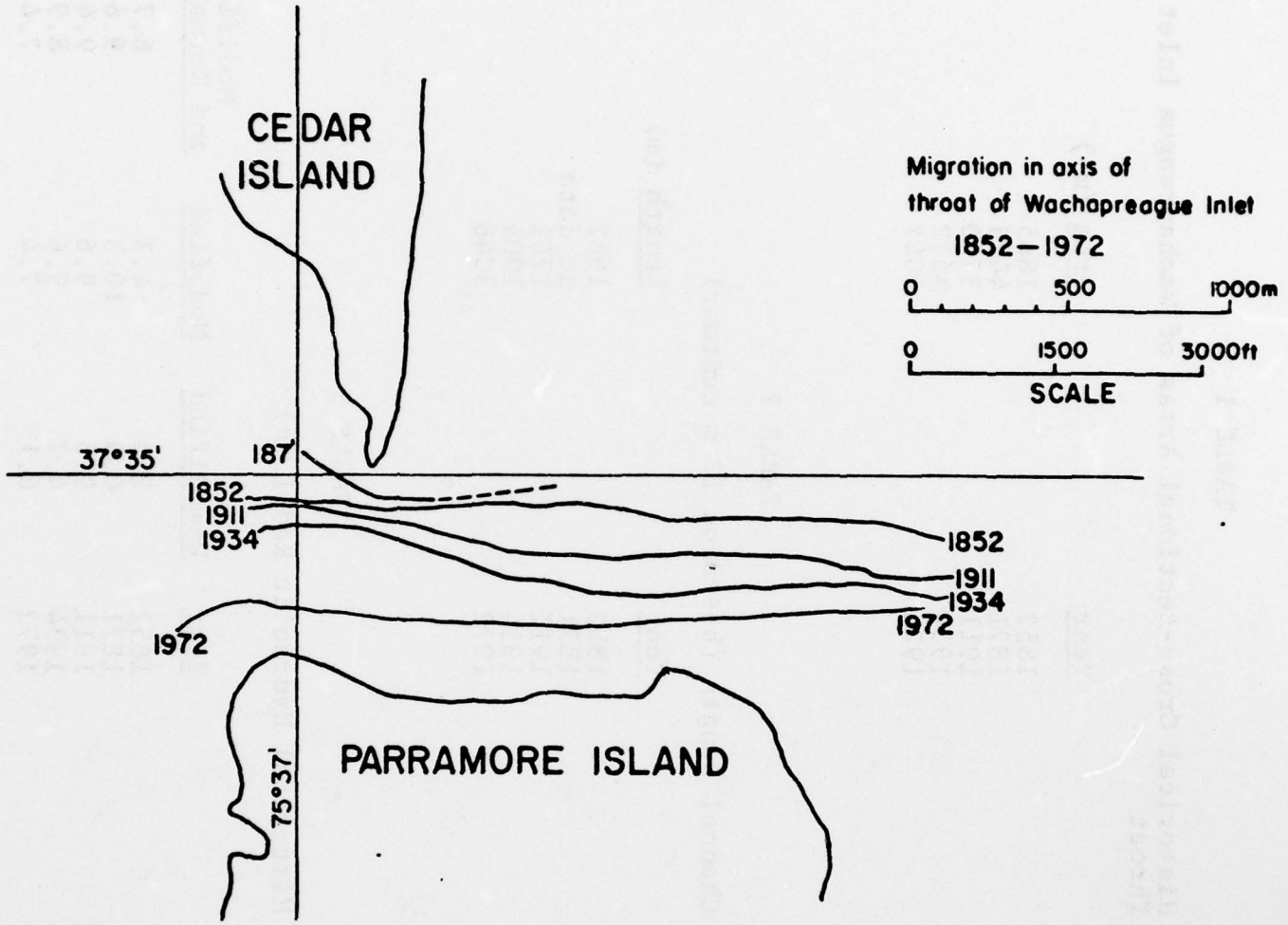

Figure 15. Migration of Wachapreague Inlet channel axis (shoreline based on 1962 survey).

TABLE 1

Historical Cross-sectional Areas of Wachapreague Inlet Throat

Year	Area (m^2)
1852	1845
1871	4473
1911	3760
1934	4572
1972	4047

TABLE 2

Channel Length (based on 12 m contour)

Year	Length (m)
1852	1662
1871	no data
1911	1701
1934	1909
1972	3046

TABLE 3

Historical Hydraulic Radii (m)

Year	Unmodified	Modified	Modified and Normalized
1852	2.5	4.3	6.7
1871	6.9	10.3	9.6
1911	9.6	9.6	9.4
1934	4.7	9.6	8.9
1972	6.1	7.4	7.4

TABLE 4

Wachapreague Inlet Complex, historical changes in the volume of material present. (Base depth 21 meters below MTL, expressed in millions of cubic meters).

Region	1852	1911	1934	1972
(1A)	14.6	14.3	No data	13.9
1B	14.1	14.7	14.9	14.6
1C	13.1	13.1	12.9	12.5
1D	12.0	12.3	11.9	11.6
1E	11.6	11.3	10.8	10.8
2A	12.6	12.7	12.3	11.1
2B	13.8	14.1	13.7	14.3
2C	13.6	13.9	13.3	13.2
2D	13.9	14.0	13.8	13.4
2E	13.3	12.9	13.2	12.9
2F	11.6	11.1	12.7	12.2
3A	12.3	11.3	12.1	10.8
3B	14.1	12.1	12.6	12.0
3C	13.5	11.8	12.5	11.8
3D	11.9	11.5	11.5	11.8
3E	12.3	12.3	12.0	11.4
3F	12.9	13.0	13.0	12.7
(4A)	13.7	No data	No data	11.8
4B	15.1	15.1	15.1	15.1
4C	13.9	15.1	15.0	15.1
4D	13.9	13.9	14.0	14.3
4E	13.3	12.6	13.5	13.3
4F	12.7	12.6	12.5	12.3
5D	13.7	13.5	13.2	13.2
5E	13.1	12.7	12.7	12.5
Total material at time of survey, less regions 1A and 4A	302.3	297.6	299.2	292.9

The net change in total material gained or lost during the 120 years was a loss of about $9 \times 10^6 m^3$. Most of the change was due to the southerly shift of the channel axis and channel deepening. It is of greater interest to ask how much sand has been stored on the north flank of the channel as the channel migrated to the south. Comparison of the 1852 and 1972 maps indicates approximately $8.7 \times 10^6 m^3$ of sand has been stored, which when considered on an annual basis amounts to about 73,000 m^3/yr.

Comparison of the maps and Table 4 also indicates that the interior shoals (quadrants 2a and 3a of the maps) have diminished since 1934. The channel depths of the interior feeder channels have not changed appreciably in depth; thus, it appears that the material on the interior shoals has left the system via the inlet channel. This will be further discussed in a later section.

Short term changes in the geometry of the barrier islands flanking the inlet and of the lateral ramp margin shoals were studied during the period from 1949 to 1973 by using aerial photography. The areas of the variable portions of the barrier islands, and the shoals were measured on maps drawn from the aerial photographs. No corrections were made for tide stage or distortions in the photographs. To test the error of not correcting for photograph distortions, an area measured from a 1971 uncorrected map was compared with the measured area from a distortion (by means of a Kelsh Plotter) corrected map (Penney, personal communication, 1973). There was less than 5% error. Based on the U.S. Army Corps of Engineers thumb rule that "one square foot of beach is equivalent to one cubic yard of sand" (U.S. Army Corps of Engineers, 1966), the areas of beach or shoal were converted to volumes of sand lost or accreted.

In order to estimate the errors due to not correcting for tide stage, a measurement of the shoreline encompassing each of the planimetered areas was made. Assuming a 10° beach slope, and a 3 ft. (.91 m) tidal range, the area of beach covered or exposed by the tide was calculated. These areas were converted to volumes, and these volumes were all less than 5% of the total calculated volumes.

In 1949 (Fig. 16), the Wachapreague Inlet system consisted of a main channel and an apparently well developed north channel. Note the large accretional sand wedge on the northeast face of Parramore Island, and that the lateral ramp margin shoals were well developed. A 1957 photograph (Fig. 17) shows the inlet complex at a critical time in its life history; note the breakthrough inlet on Cedar Island. More significantly, note the wedges of sand on the northeast face of Parramore Island, and on the south tip of Cedar Island. These accretional features represent $3.3 \times 10^6 m^3$ and $2.4 \times 10^6 m^3$ of sand, respectively; while the north shoal represents $1.5 \times 10^6 m^3$ of sand. Since 1949, this

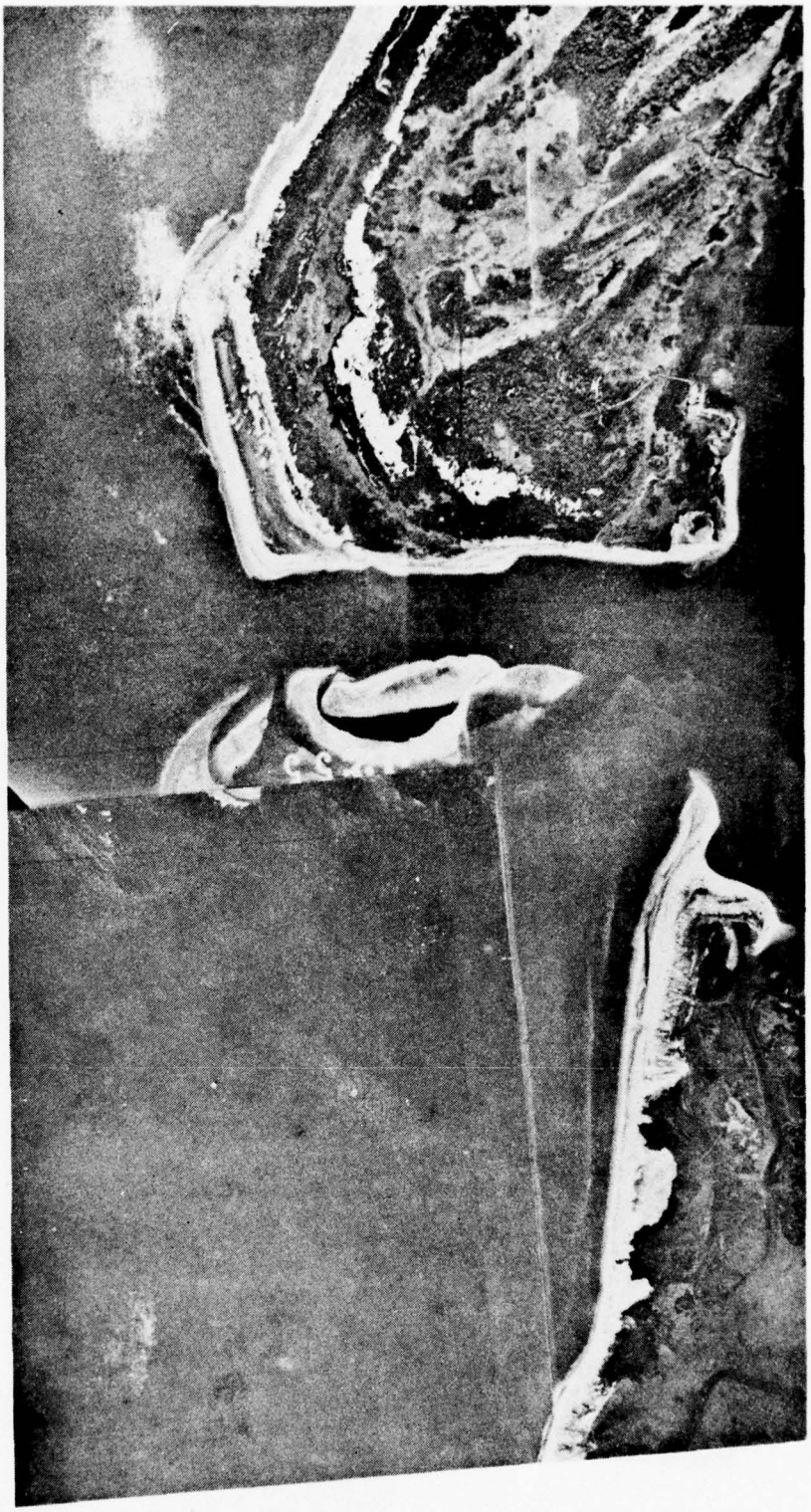

Figure 16. Wachapreague Inlet, 1949.

Figure 17. Wachapreague Inlet, 1957.

represents an increase of 1.3 x $10^6 m^3$ of sand on the northeast face of Parramore Island, a decrease of 0.9 x $10^6 m^3$ on the shoals, and an increase on Cedar Island of 2.5 x $10^6 m^3$ of sand.

In April of 1962 (Fig. 18), after the "Ash Wednesday" storm, the shoal had disappeared below the water line, a loss of 1.5 x $10^6 m^3$ of sand. The southeast tip of Cedar Island, although elongated, has lost 0.6 x $10^6 m^3$ of sand and the northern face of Parramore Island gained about 0.5 x $10^6 m^3$ to a total volume of 3.8 x $10^6 m^3$. Note also that the north shoreline of Parramore Island was straight. In 1966 (Fig. 19) the northeast face of Parramore Island had retrograded back to the base line, a loss of 3.8 x $10^6 m^3$ of sand. A shoal had developed, where in 1962 there was nothing, to a volume of 1.9 x $10^6 m^3$; and the south tip of Cedar Island had accreted eastward slightly (0.1 x $10^6 m^3$). In February of 1970 (Fig. 20) the north shoal had accreted another 1.0 x $10^6 m^3$ of sand to a total of 2.9 x $10^6 m^3$, while Cedar Island had lost 0.1 x $10^6 m^3$.

In June of 1971 (Fig. 21), the north shoal had decreased in size by 1.4 x $10^6 m^3$, while Cedar Island, narrowed and lengthened, had remained unchanged, and Parramore Island had remained unchanged since the 1966 photograph. But, note that the north lateral ramp margin shoals consisted of two shoals, not one as in February, 1970. Also note the presence of a concavity of the north shoreline of Parramore Island. This is due to diffraction of waves approaching from the northeast sector and then passing through the channel between Cedar Island and the north shoals. In September, 1971 (Fig. 22), the system was virtually unchanged since June, 1971, with the exception that the shoals have decreased by 0.3 x $10^6 m^3$ of sand. Note the interesting configuration of the eastern section of the north shore of Parramore Island. It appears that a small wedge of sand is building out on a submerged shelf, due to the protection afforded by the shoal, from waves approaching from the north. Again in November of 1971 (Fig. 23), there had been very little change in the system.

By February, 1972 (Fig. 24), the inlet system had begun to change again. The north lateral ramp margin shoal had decreased in size by 0.7 x $10^6 m^3$. The configuration of the northeast face of Parramore Island had changed, but the total sand present had not changed. The sand had simply been redistributed. This probably can be related to the disappearance of the most seaward shoal of the two shoals that existed in 1971. Note also the calving or apparent slumping of the sand on that sand wedge that has been accreting on the easterly portion of the north flank of Parramore Island.

By September of 1972 (Fig. 25), the north lateral ramp margin shoals totally disappeared, a further loss of 0.5 x $10^6 m^3$ of sand since February, 1972. The small wedge of sand that had existed

Figure 18. Wachapreague Inlet, April, 1962.

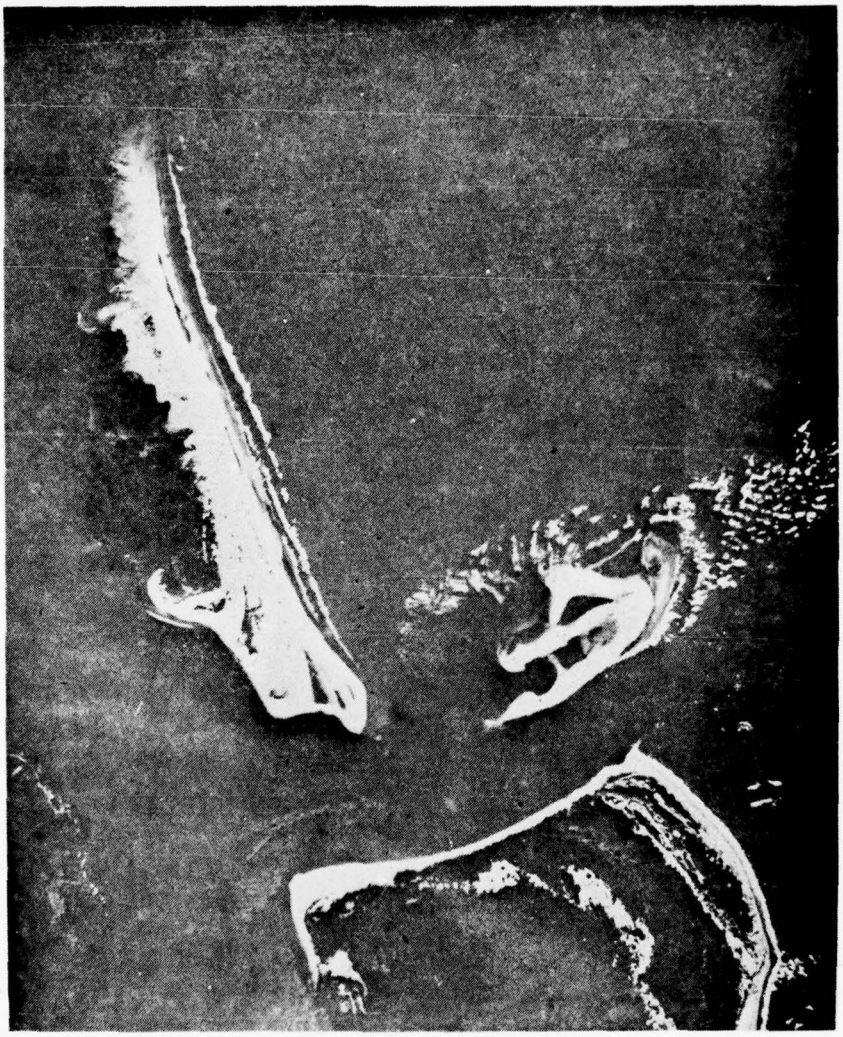

Figure 19. Wachapreague Inlet, October, 1966.

Figure 20. Wachapreague Inlet, February, 1970, (2 hours after high water).

Figure 21. Wachapreague Inlet, June, 1971.

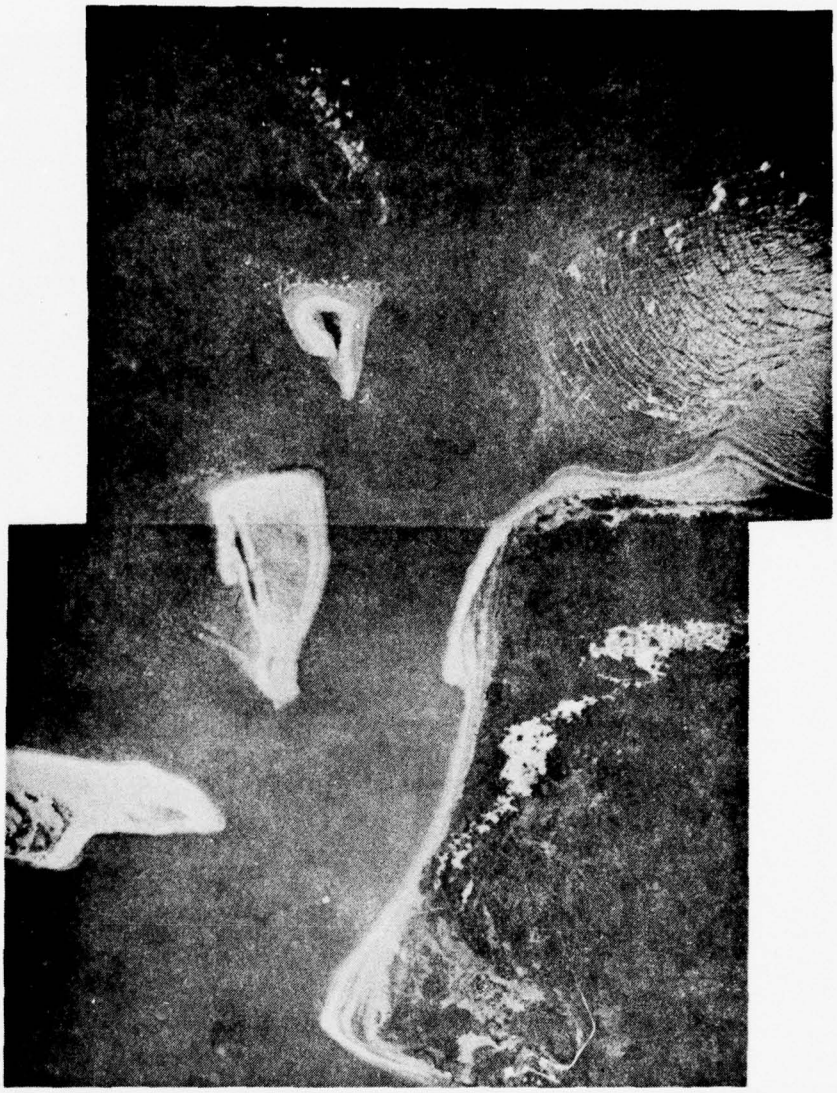

Figure 22. Wachapreague Inlet, September, 1971.

Figure 23. Wachapreague Inlet, November, 1971.

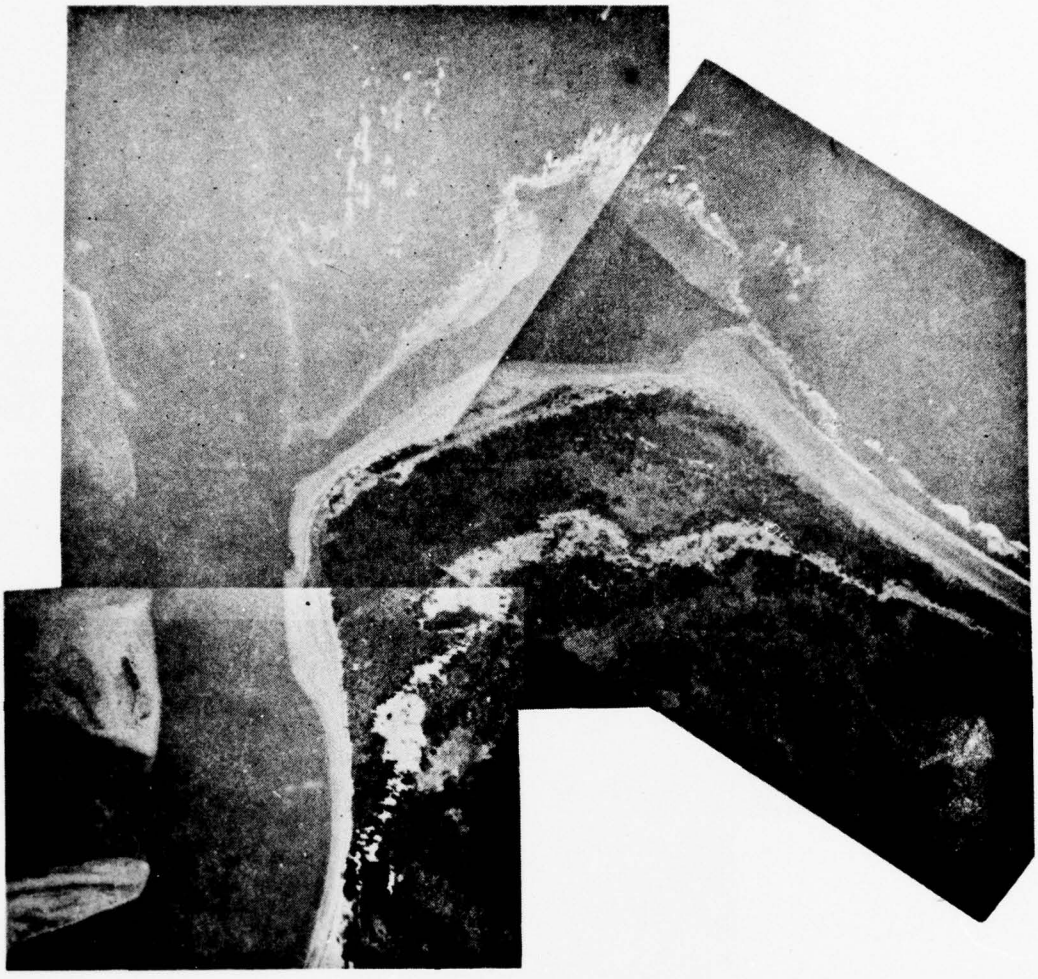

Figure 24. Wachapreague Inlet, February, 1972, (2 hours prior to low water).

Figure 25. Wachapreague Inlet, September, 1972, (1 hour after high water).

on the easterly portion of the north flank of Parramore Island disappeared, probably because of the loss of the protection afforded by the shoals. With the loss of that northeast sand wedge, the apparent concavity in the north face of Parramore Island was reduced.

By November of 1972 (Fig. 26), another north shoal had emerged with a volume of $0.4 \times 10^6 m^3$ of sand. But more significantly, another sand wedge developed on the northeast flank of Parramore Island, similar to the one that existed in 1949, 1957, and 1962 photographs. This feature represents an accretion of $1.9 \times 10^6 m^3$ of sand in only two months time.

By July of 1973 (Fig. 27), the new north shoal had accreted another $0.5 \times 10^6 m^3$ sand to a total volume of $0.9 \times 10^6 m^3$; while the northeast face of Parramore Island had lost $0.1 \times 10^6 m^3$ of sand.

The results of this twenty-four year survey of available aerial photography are summarized in Table 5. During the period from February, 1970, to September, 1972, a shoal of $2.9 \times 10^6 m^3$ of sand disappeared. Yet by July, 1973, another shoal reappeared with a volume of $0.9 \times 10^6 m^3$; and an accretion of $1.9 \times 10^6 m^3$ occurred on the northeast face of Parramore Island. In the light of the previous discussion on estimated drift rates, changes of this magnitude cannot be reasonably related to fluctuations in littoral drift; they are more likely due to cyclic short-term changes on the ebb tidal delta. For example, a 1 m change in the depth over the area of the ebb tidal delta ($4 \times 10^6 m^2$) will yield a volume change of $4 \times 10^6 m^3$.

A2.3 Surficial Sediment Distribution of Wachapreague Inlet Complex. The mobile sediment distribution was investigated with respect to both spatial variations over the entire inlet complex and temporal variation in the inlet throat channel. Sediment samples were gathered by a mini-Van Veen grab sampler, along planned transects. Sample sites were determined by shooting azimuths on fixed known locations or by shooting adjacent angle pairs with a sextant; later these were plotted on the 1972 bathymetry chart. In addition to the samples, observations were made by divers in all those areas of the inlet complex that were of particular interest.

All samples were initially described as to contents (shell, sand, mud, etc.). Sand fraction characteristics were determined by sieving on ¼ PHI screens and fine grained samples were analyzed by the pipette method described in Ward (1968), samples were taken at the 4Ø, 5Ø, 6Ø, and 8Ø intervals. The standard graphic textural parameters were computed for the samples. The equations for the analysis are based on those published by Folk, et al. (1957).

Figure 27. Wachapreague Inlet, July, 1973.

Figure 26. Wachapreague Inlet, November, 1972, (1 hour prior to low water).

TABLE 5

Recent historical volume changes from aerial photography, expressed in $10^6 m^3$.

Date	N.E. Face Parramore		Lateral Ramp Margin Shoal		Cedar Island	
	total	change	total	change	total	change
1949	2.0		2.4		0.0	
		+1.3		-0.9		+2.5
1957	3.3		1.5		2.5	
		+0.5		-1.5		-0.6
04/1962	3.8		0.0		1.9	
		-3.8		+1.9		+0.1
10/1966	0.0		1.9		2.0	
		No Data		+1.0		-0.1
02/1970	No Data		2.9		1.9	
		No Data		-1.4		NC
06/1971	0.0		1.5		1.9	
		NC		-0.3		NC
09/1971	0.0		1.2		1.9	
		NC		NC		NC
11/1971	0.0		1.2		1.9	
		NC		-0.7		NC
02/1972	0.0		0.5		1.9	
		NC		-0.5		NC
09/1972	0.0		0.0		1.9	
		+1.9		+0.4		NC
11/1972	1.9		0.4		1.9	
		-0.1		+0.5		NC
07/1973	1.8		0.9		1.9	

The results of the spatial sediment distribution survey are summarized in Figure 28. The sediments varied from a veneer of very coarse sediments, composed of shell debris, cobbles, and gravels overlying a stiff, cohesive, sandy clay substrate in the deep inlet throat channel, to well sorted, medium to fine sand surrounding the inlet throat to a very fine silty sand both inside and outside the immediate area of the inlet channel. The sediment distribution appears to correlate well with the various depositional environments. That is, coarser sediments are localized in the higher energy areas and the finer sediments are restricted to the low energy areas.

Tables 6, 7, 8, and 9 tabulate the results of the various surveys of the ebb tidal delta, the inlet throat, and the interior lagoons and tidal channels. Several very interesting points came to light as a result of the survey. The apparent flood tidal deltas or bathymetric highs are in fact relative topographic highs of lagoonal sediments, overlain by a thin veneer of fine sand. Secondly, the north flank of Parramore Island, on the steep wall adjacent to the inlet, is an exposure of very firm lagoonal deposits. And finally, that there appears to be a swath of fine sand ($>2.0\,\phi$, $<2.5\,\phi$) that intersects the coarser sediments in the inlet axial channel.

In order to discern temporal variations of the sediments in the inlet channel, the bottom sediment distribution was sampled fortnightly for a period of three months at various high and low slack waters. Sample stations were located at the deepest part of each of eleven transects (Fig. 2) that cross the throat of the inlet. The loose sediments recovered from the bottom included medium and coarse grain sands, gravels, boulders (up to 6 inches in diameter), shell debris of various sizes and shapes, and rounded chunks of hard mud. These mud chunks proved to be identical to the substrate material along the south flank and bottom of the inlet throat. The results of these surveys are tabulated in Table 10.

No obvious resorting pattern between high and low slack was observed during the sampling period. In the deepest parts of the inlet throat, below 15 meters, the loose bottom sediment usually consisted of gravels and large shell debris (Mercenaria sp. and Crassostera sp.). Toward the eastern and western extremities of the throat channel, at depths ranging between 12 and 15 meters, the mobile bottom sediments usually varied between coarse sand and smaller shell fragments. The bottom sediment distribution did reflect measured fluctuations in the cross-sectional area of the inlet's throat during the sample period. That is, during the last week in May, 1972, and the first two weeks in June, 1972, appreciable amounts of sand were recovered from most of the transects across the gorge, perhaps indicating a choking or filling in of the throat. Later, this was correlated with

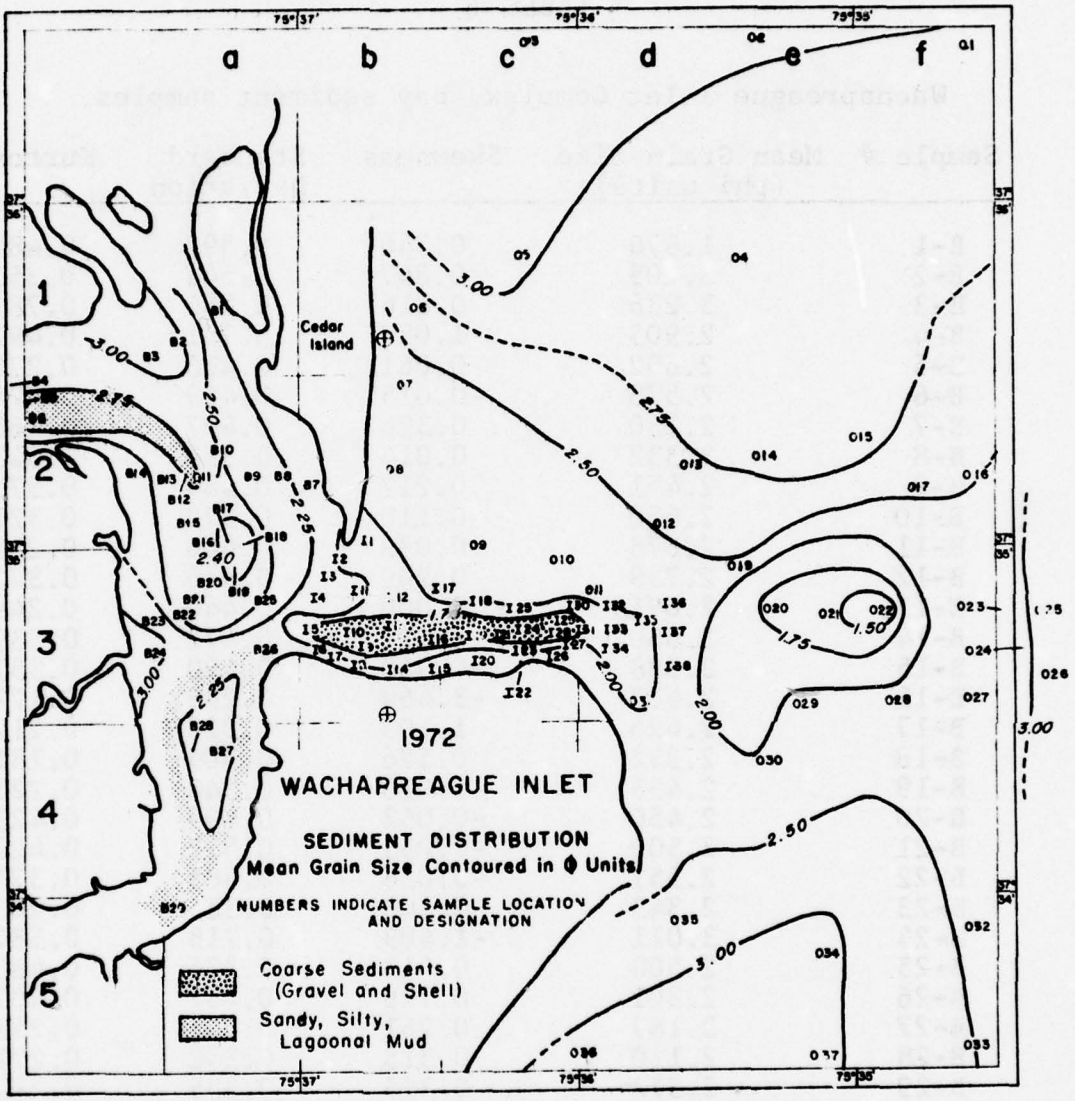

Figure 28. Surface sediment sample locations and contour map of mean grain size (ϕ), July, 1972.

TABLE 6

Wachapreague Inlet Complex, bay sediment samples.

Sample #	Mean Grain Size (phi units)	Skewness	Standard Deviation	Kurtosis
B-1	1.876	0.746	0.592	0.482
B-2	3.105	0.847	0.544	0.352
B-3	3.236	0.816	0.585	0.781
B-4	2.905	1.038	0.701	0.491
B-5	2.692	0.061	0.436	0.274
B-6	2.578	-0.015	0.429	0.270
B-7	2.130	0.326	0.497	0.466
B-8	2.332	0.014	0.555	0.543
B-9	2.451	0.217	0.489	0.375
B-10	2.650	0.110	0.372	0.321
B-11	2.678	0.039	0.406	0.232
B-12	2.758	0.209	0.516	0.372
B-13	2.621	0.000	0.440	0.249
B-14	2.680	-0.012	0.472	0.337
B-15	2.588	-0.010	0.490	0.357
B-16	2.407	-3.469	0.289	0.172
B-17	2.426	1.105	0.328	0.212
B-18	2.332	0.526	0.304	0.181
B-19	2.458	-1.016	0.348	0.228
B-20	2.450	-0.063	0.499	0.423
B-21	2.500	-0.033	0.522	0.428
B-22	2.551	-0.036	0.485	0.377
B-23	2.343	-0.103	0.335	0.206
B-24	3.011	-1.409	0.718	0.584
B-25	2.500	0.015	0.376	0.489
B-26	2.301	0.129	0.457	0.407
B-27	2.187	0.261	0.381	0.258
B-28	2.110	0.315	0.352	0.271
B-29	2.372	0.355	0.335	0.222
B-29'	2.392	0.242	0.438	0.358

*(') indicates a replicate sample.

TABLE 7

Wachapreague Inlet Complex, inlet channel sediment samples.

	Mean Grain Size (phi units)	Skewness	Standard Deviation	Kurtosis
I 1	1.964	-0.785	0.448	0.333
I 2	1.994	-0.468	0.371	0.229
I 3	2.004	-0.321	0.343	0.267
I 4	2.341	0.228	0.372	0.252
I 5	1.604	0.031	0.363	0.269
I 6	2.071	1.351	0.427	0.261
I 7	2.101	0.634	0.372	0.321
I 8	1.790	-0.042	0.455	0.355
I 9	1.681	1.270	0.593	0.624
I 10	1.344	0.252	0.393	0.277
I 11	2.027	0.334	0.427	0.364
I 12	1.869	0.230	0.496	0.430
I 13	1.763	0.454	0.502	0.456
I 14	1.937	1.261	0.398	0.256
I 15	2.179	0.030	0.354	0.227
I 16	1.727	0.388	0.255	0.114
I 17	2.173	-0.479	0.384	0.284
I 18	2.099	-0.001	0.364	0.240
I 19	2.117	-0.030	0.392	0.297
I 20	2.105	0.494	0.321	0.206
I 21	1.773	1.191	0.587	0.636
I 22	2.000	1.346	0.426	0.437
I 23	2.046	1.163	0.337	0.212
I 24	1.554	1.177	0.516	0.648
I 25	1.987	0.170	0.363	0.219
I 26	2.130	-0.303	0.357	0.221
I 27	2.031	0.216	0.434	0.231
I 28	1.423	0.236	0.516	0.527
I 29	1.514	-3.028	0.575	0.644
I 30	1.894	-0.012	0.538	0.554
I 31	1.534	-0.559	0.326	0.223
I 32	2.029	0.209	0.489	0.377
I 33	2.096	0.176	0.432	0.261
I 34	2.033	-2.755	0.295	0.159
I 35	2.015	-0.226	0.400	0.331
I 36	2.373	0.226	0.441	0.361
I 37	2.360	2.154	0.355	0.252
I 38	2.313	-1.103	0.304	0.186

TABLE 7 (Cont'd.)

	Mean Grain Size (phi units)	Skewness	Standard Deviation	Kurtosis
I 24'	1.773	1.191	0.582	0.636
I 28'	1.615	0.329	0.627	0.783
I 30'	1.879	0.109	1.135	0.482
I 35'	2.090	-0.047	0.428	0.341

*(') indicates a replicate sample.

TABLE 8

Wachapreague Inlet Complex, offshore sediment samples.

Sample #	Mean Grain Size (phi units)	Skewness	Standard Deviation	Kurtosis
01	2.971	0.837	0.703	0.658
02	3.048	0.921	0.713	1.158
03	3.554	0.434	0.514	0.593
04	2.751	-2.464	0.508	0.452
05	3.302	-2.765	0.560	0.751
06	2.697	0.053	0.506	0.350
07	2.434	0.347	0.327	0.200
08	2.396	0.388	0.342	0.240
09	2.427	-1.599	0.337	0.226
010	2.360	2.154	0.355	0.252
011	2.058	-0.171	0.373	0.242
012	2.529	-0.719	0.311	0.173
013	2.685	0.060	0.476	0.321
014	2.992	1.033	0.612	0.402
015	2.987	1.008	0.609	0.385
016	2.571	0.137	0.526	0.326
017	2.610	0.527	0.875	0.683
019	2.10	0.174	0.362	0.234
020	1.739	0.222	0.422	0.327
021	1.617	0.522	0.442	0.372
022	1.415	-0.293	0.424	0.224
023	2.332	-0.055	0.433	0.374
024	2.948	1.502	0.739	1.207
025	3.565	0.425	0.586	0.782
026	3.536	0.434	0.578	0.787
027	2.202	0.317	0.433	0.365
028	2.048	0.228	0.944	1.659
029	2.058	-0.581	0.455	0.311
030	2.03	-0.413	0.379	0.427
011'	2.146	0.234	0.341	0.228
026'	3.449	0.535	0.633	0.898

*(') indicates a replicate sample.

TABLE 8 (Cont'd.)

Sample #	Mean Grain Size (phi units)	Skewness	Standard Deviation	Kurtosis
032	2.424	0.032	0.590	0.758
033	2.440	-0.004	0.593	0.794
034	3.046	5.264	0.716	0.918
035	2.772	-0.824	0.512	0.462
036	3.109	0.169	0.754	1.286
037	3.085	-1.870	0.704	0.922

TABLE 9

Wachapreague Inlet Complex, bay mud sediment analysis, results of pipet analysis.

Sample #	50% Mean (phi units)	% Sand	% Silt	% Clay
TB 1 #5	4.2	44	40	16
TB 2 #5	3.9	51	37	12
TB 9 #4	5.0	26	51	23
TB 1 #6	4.2	42	41	17
TB 1 #4	5.8	18	56	26
TB 1 #3	6.0	17	50	33
TB 2 #6	< 4.0	61	30	9
TB 2 #7	4.4	42	42	16

TABLE 10

Temporal variations Wachapreague Inlet throat sediments, 1972.

Transect	High Water 4 May	High Water 18 May	High Water 2 June	High Water 13 June	High Water 27 June	High Water 14 July	Low Water 26 July	Low Water 10 August
1	hard dark green clay, sand 1.49ϕ	small shell frags. sand 1.68ϕ	sand 1.94ϕ	mud, sand, shell	sand 1.72ϕ	sand, mud chunks	sand	shells, gravels, large shells
2	clay, mud, sand, gravel, 1.76ϕ	sand, shells, gravels	sand 1.68ϕ	sand	shell, sand, mud, gravel	no sample	no sample	no sample
2-2	mud, sand, gravel, 1.38ϕ	shells, gravels, clay smear on sample	sand	sand, shell	no sample	mud chunks	shells, sand, gravels	no sample
2-2-A	no sample	large shells, gravels	sand, gravel	no sample	no sample	no sample	no sample	no sample
3	firm green clay mud	large shells, gravels	sand, large shell frags.	large shell, sand	hard mud	mud, gravel, shells	large shells	shells, sand, small shell
4	no sample	shells, sand, gravels	sand, shells	no sample	shells	shells, mud, gravels	large shells	shells, mud, sand

* mean grain size in PHI units

TABLE 10 (Cont'd.)

Transect	High Water 4 May	High Water 18 May	High Water 2 June	High Water 13 June	High Water 27 June	High Water 14 July	Low Water 26 July	Low Water 10 August
5	large shell debris, green clay, mud	large shell debris	large shells	sand, mud	shells	shells, mud chunks	shells, mud, sand	shells, sand, gravel
6	no sample	large shell debris	shell, sand 1.61ϕ	large shell on hard mud	hard mud	shells, mud chunks	mud	sand, mud
7	large shell frags.	shells, sand	shells, sand	shells, sand	shells, sand, mud	mud chunks	shells, sand, mud	shells, mud
8	large shell frags.	clean sand	sand 1.75ϕ	sand, shells	shells, sand, mud	shells, mud chunks	large shells	shells, sand
9	sand 1.29ϕ	no sample	sand	shells, sand	sand	sand	sand, shell, gravel	shells, sand

* mean grain size in PHI units

an overall decrease in the cross-sectional areas of the transects across the inlet throat (over a 15% decrease at one transect). In mid-July, 1972, principally mud clumps (rounded chunks of lagoonal mud) were recovered at almost all sample stations in the inlet. This indicated relative erosion in the inlet which later was verified by a significant overall increase in the cross-sectional areas.

Verification of the migration of shell debris was accomplished by direct visual observation by divers on the bottom shortly after a slack water work dive. These shifting coarse sediments appear to be abrading into the hard bottom substrate, as evidenced by pot holes observed in the bottom.

A2.4 Substrate Sediments. The character of substrate sediments in the inlet complex was studied from data from samples, cores, and observations taken while scuba diving, a well recently drilled on Parramore Island, and sub-bottom profiles made across the inlet throat and in Horseshoe Lead, landward of Parramore Island. The first indication that Wachapreague Inlet was different than the typical sandy trough described for inlets on sandy coasts came as a result of the mobile sediment distribution survey. Further observations, cores and samples made by divers along the inlet bottom and south flank confirmed that underlying the coarse sediments on the deep inlet bottom was a stiff, silty clay substrate, with interspersed layers of gravels and coarse sands (Figs. 29 and 30). Samples taken from the south wall of the inlet (6-9 m below MTL) showed it to be composed of lagoonal deposits with a mean grain size of 4.8 ϕ (Table 11 and Fig. 31). The "bottom debris samples" taken from 12.2 m listed in Table 11 and shown in Figure 32 had a mean grain size of about 8Ø.

Substrate characteristics were further elucidated by sub-bottom profiling across the inlet throat (Fig. 33) and the interpretation is shown in Figure 34. Note the horizontal reflectors below 20 m; these underlie both the sedimentary deposits to the north and to the south. The sloped reflectors on the north side between 20 and 15 m represent the recent sand deposits of the south tip of Cedar Island as it extends southward. On the south side of the inlet, the reflectors are parallel and horizontal from below 20 m to a depth of 15 m; but note the two strong reflectors between 15 and 16 m. Between 15 and 11 m on the south flank, the reflectors are again inclined toward the bottom, indicating either recent sand deposits or the deposits along the flank of an older channel. From 11 to 6 m the reflectors are again parallel and horizontal. Sub-bottom profiles across Horseshoe Lead (Fig. 35) and the interpretation (Fig. 36) show the recurrence of the pair of strong reflectors between 15 and 16 meters.

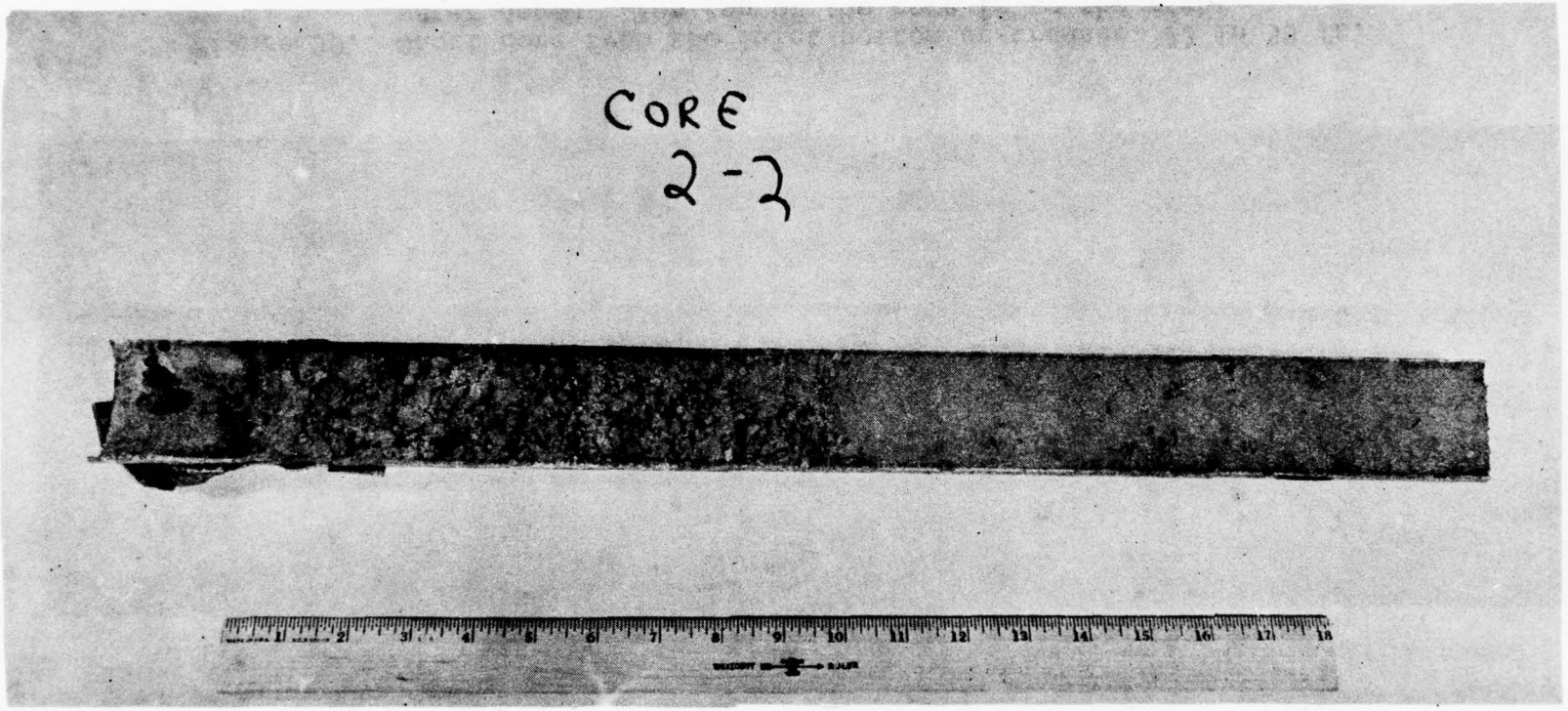

Figure 29. Short core from the inlet bottom at transect #2-2 in 62 ft. water depth. The top of the core is to the left.

Note the layer of gravels, sand and silt, over a very stiff sandy clay.

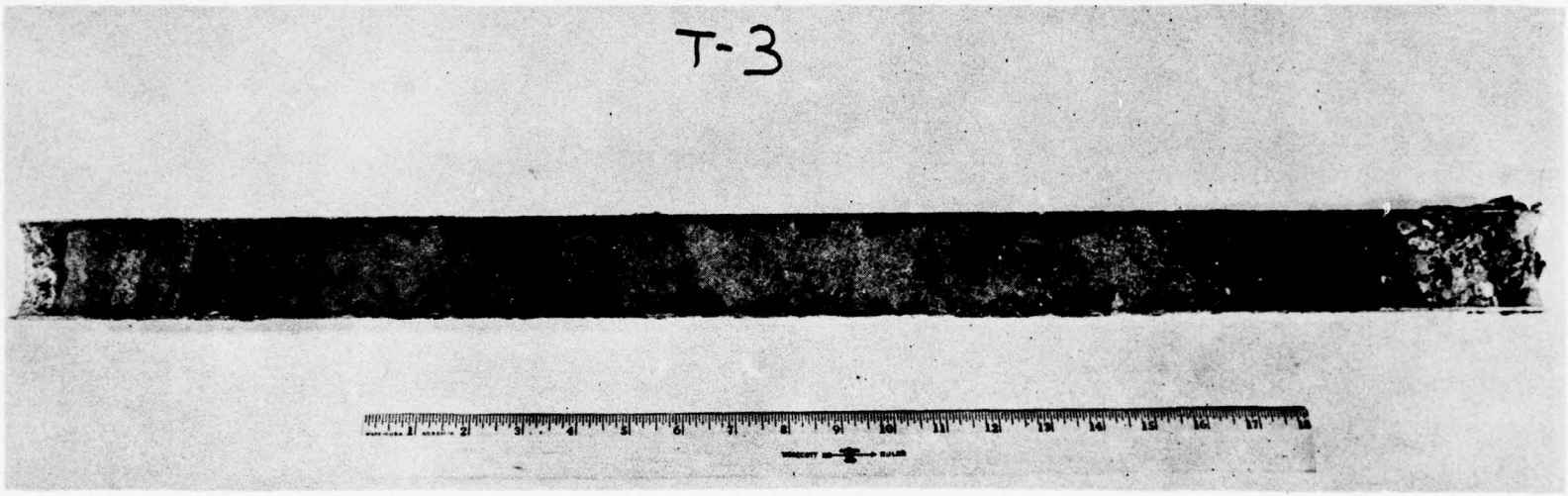

Figure 30. Short core from the inlet bottom at transect #3 in 58 ft. water depth. The top of the core is to the right.

Note the 4" of gravels, sand and silt, over medium sands, then interspersed layers of stiff sandy, and silty clays.

TABLE 11

Inlet south wall sediment samples, transect #2-2.

Sample #	50% Mean (phi units)	% Sand	% Silt	% Clay	% H_2O	Comments
Shelf Edge 18'	5.4Ø	28%	54%	18%	13	Substrate
Slope 20'	4.7	31	49	20	13	Substrate
Slope 20'	4.5	34	62	4	28	Substrate R.C. shell sample
Slope 28'	4.9	28	52	20	18	Substrate
Slope 33'	5.0	22	75	23	-	Substrate
40'	8.0	4	46	50	19	Bottom debris
40'	> 8.0	4	23	73	-	Bottom debris
40'	> 8.0	7	39	64	44	Bottom debris
40'	3.5	58	40	2	55	Local loose sediments

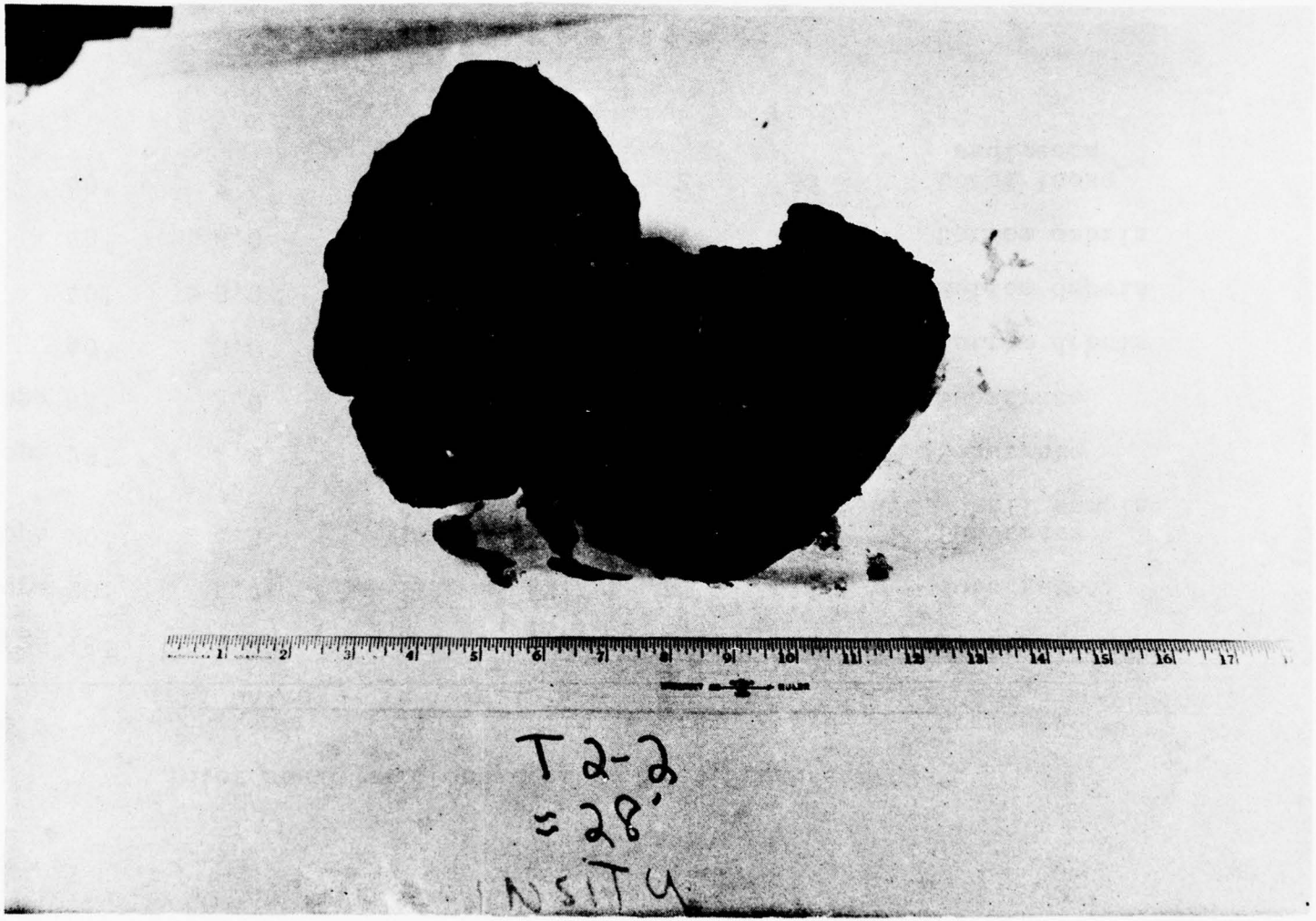

Figure 31. A sediment sample carved from a mud outcrop on the south flank of the Wachapreague Inlet channel at transect #2-2.

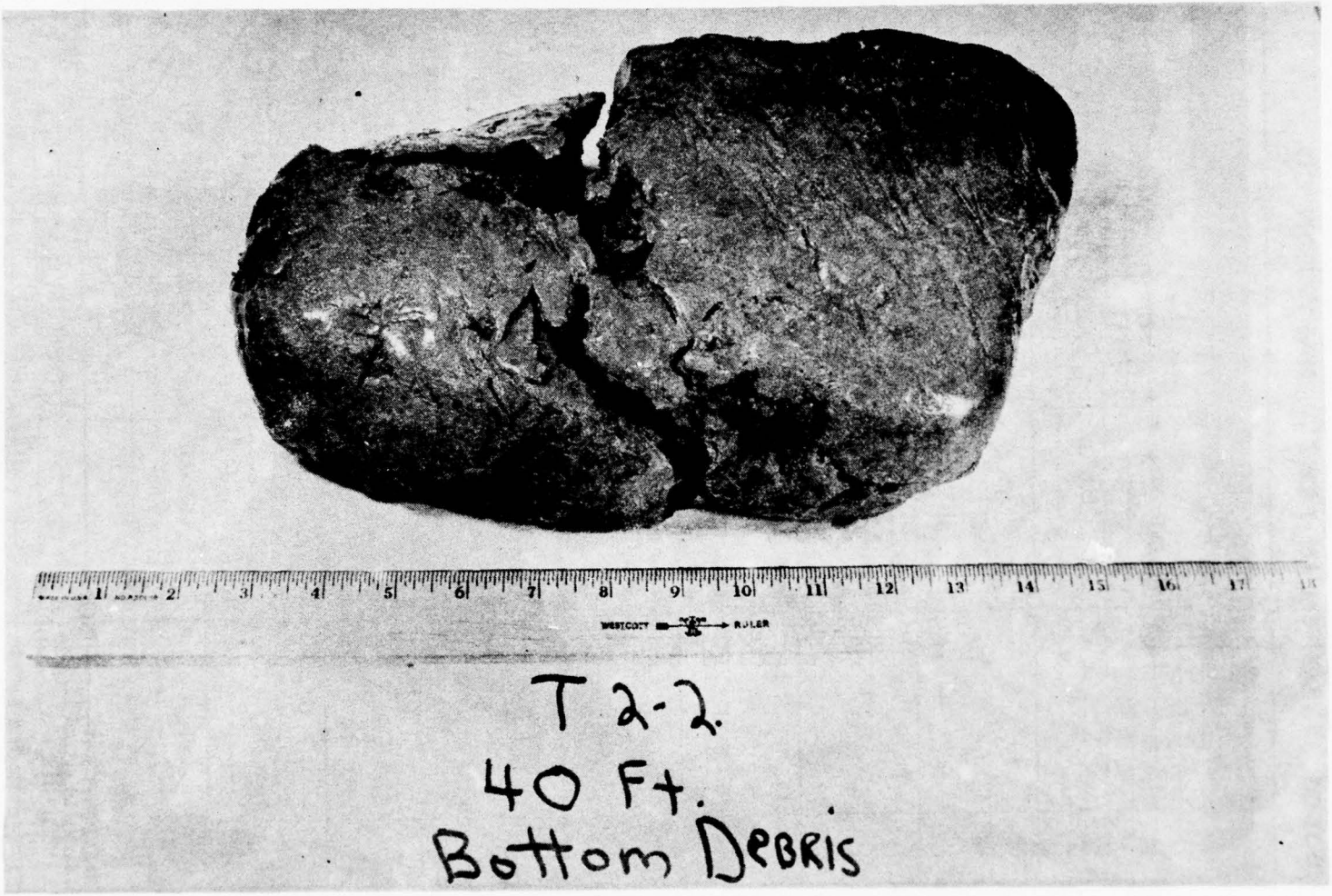

Figure 32. Mud ball taken from the south flank of Wachapreague Inlet, transect #2-2, at a depth of 40'.

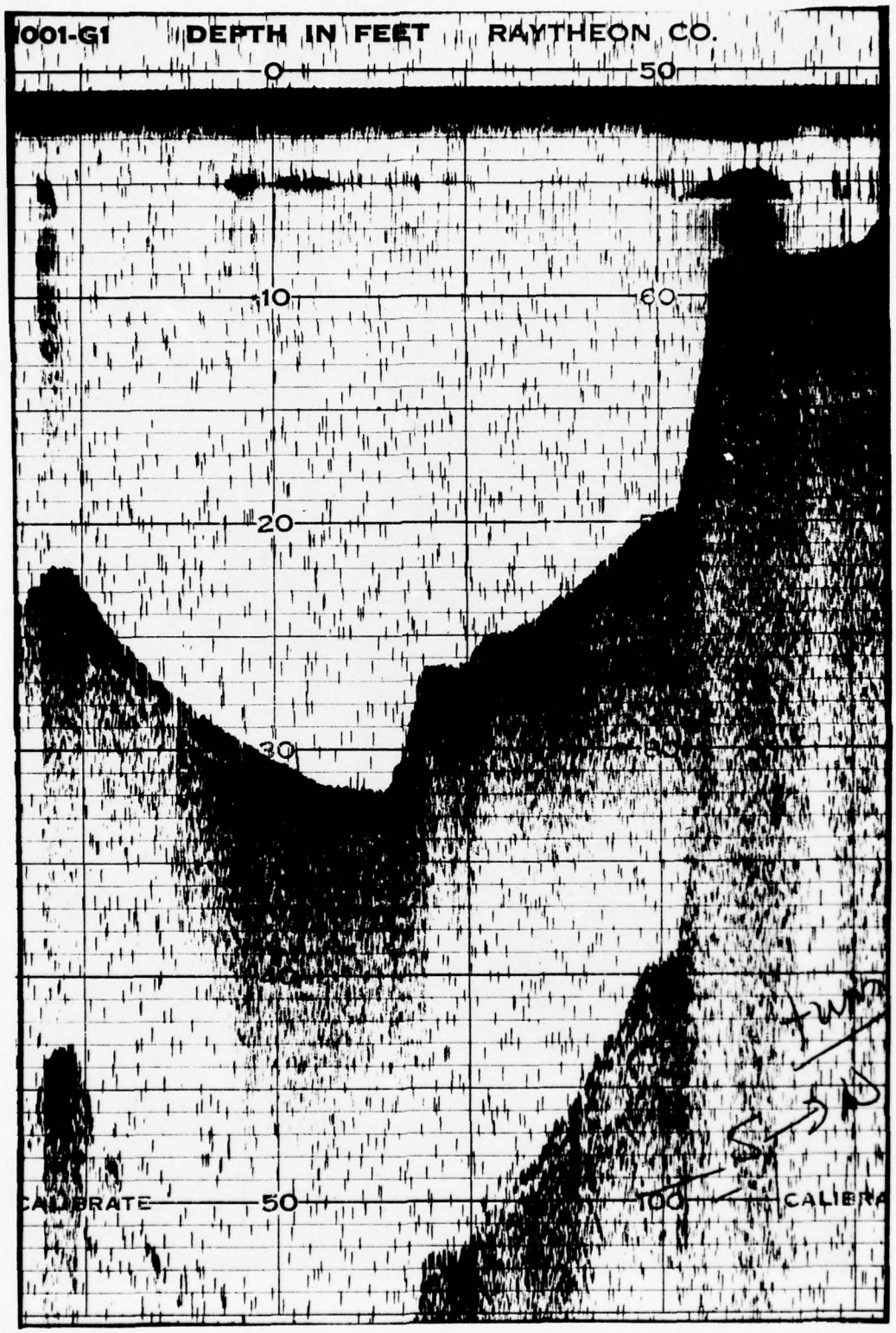

Figure 33. Sub-bottom profile across Wachapreague Inlet throat, Range 22 from north to south (north on left).

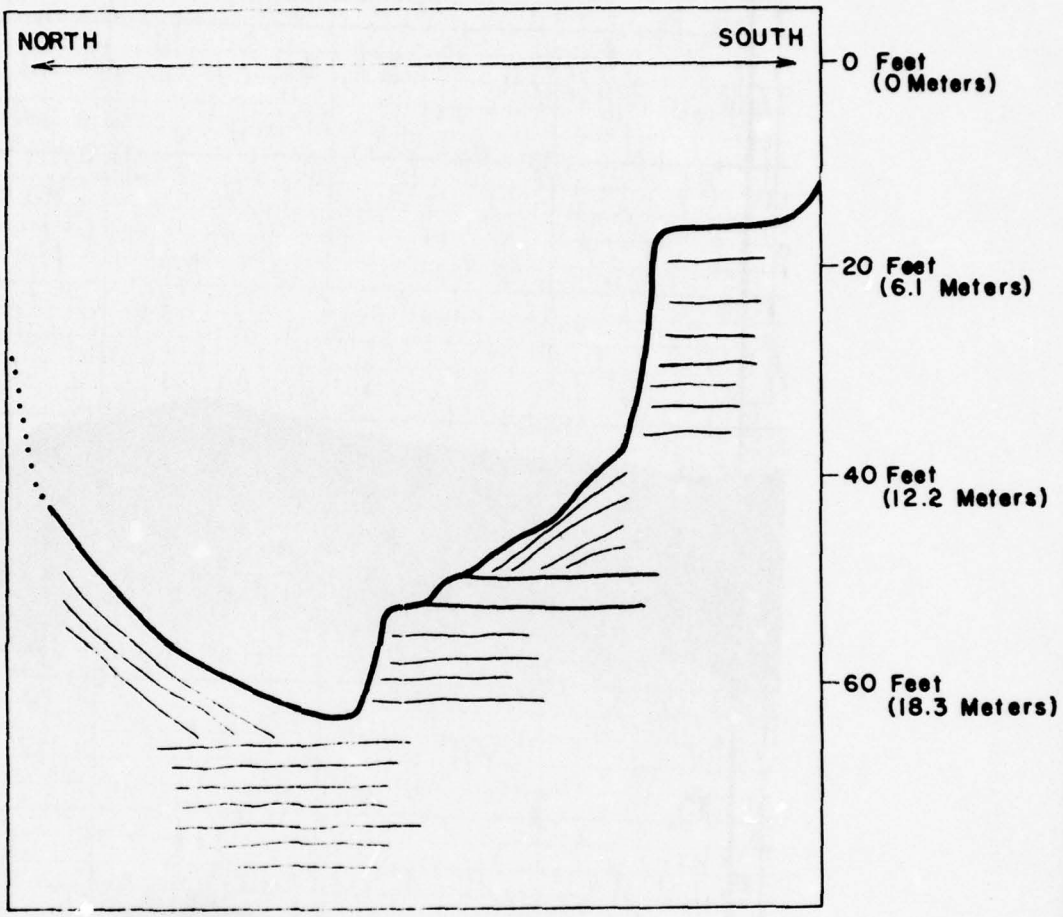

WACHAPREAGUE INLET
THROAT CROSS-SECTION - 1972
CEDAR ISLAND TO PARRAMORE ISLAND
INTERPRETATION OF SUB-BOTTOM PROFILE

Figure 34. Interpretation of sub-bottom profile of Wachapreague Inlet throat cross-section shown in Figure 33.

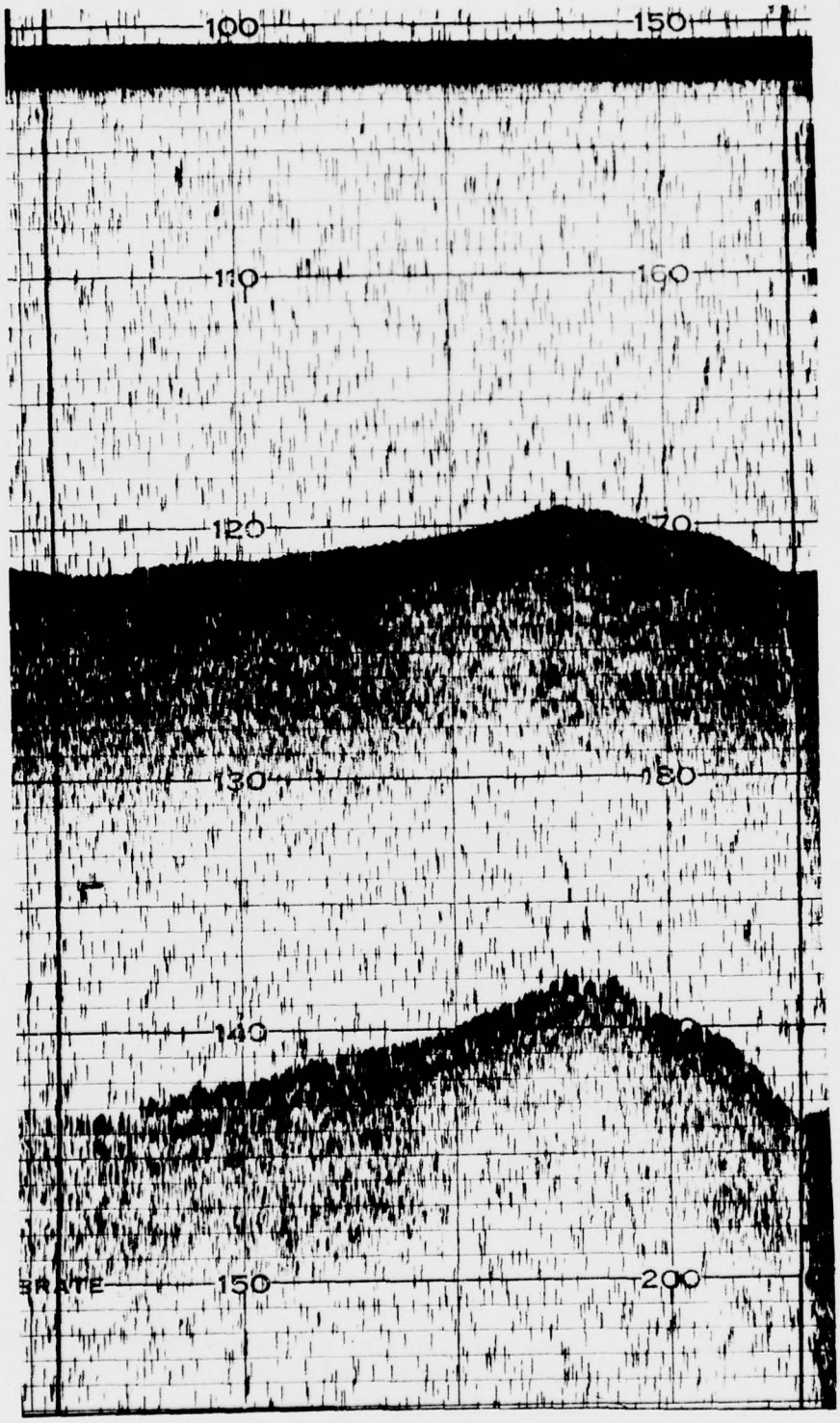

Figure 35. Sub-bottom profile in a portion of Horseshoe Lead, a tidal channel landward of Parramore Island (east is on the left).

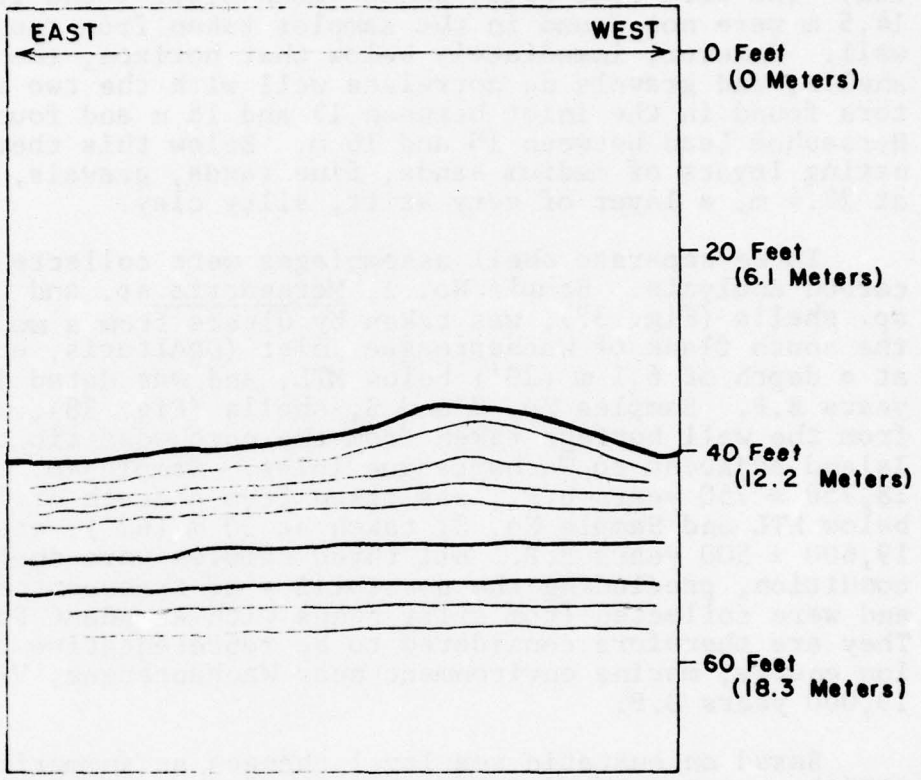

Figure 36. Interpretation of sub-bottom profile shown in Figure 35.

In order to be able to correlate the various reflectors with specific geologic strata, a well was drilled on Parramore Island and continuously split-spoon sampled to 22 m below MTL. Table 12 tabulates the sediment analysis of the well and a summary of this well log is in Table 13. There are some inconsistencies between the samples taken along the mud exposures on the north flank of Parramore Island in the inlet and the well log. The very fine silty sands (mean 3.5Ø) found from 9.0 m to 14.5 m were not found in the samples taken from the inlet south wall. However, immediately below that horizon, the coarse sands, shells, and gravels do correlate well with the two strong reflectors found in the inlet between 15 and 16 m and found also in Horseshoe Lead between 15 and 16 m. Below this there are alternating layers of medium sands, fine sands, gravels, and finally at 22.4 m, a layer of very stiff, silty clay.

Three separate shell assemblages were collected for radiocarbon analysis. Sample No. 1, Mercenaria sp. and Crassostrea sp. shells (Fig. 37), was taken by divers from a mud outcrop along the south flank of Wachapreague Inlet (DeAlteris, et al., 1973) at a depth of 6.1 m (20') below MTL, and was dated 3490 ± 125 years B.P. Samples No. 2 and 3, shells (Fig. 38), were recovered from the well borings taken from the northwest tip of Parramore Island adjacent to Wachapreague Inlet. Sample No. 2, dated 18,750 ± 750 years B.P., was taken from a depth of 15 m (46') below MTL and Sample No. 3, taken at 20 m (62'), was dated 19,600 ± 500 years B.P. All three samples were shells in mint condition, precluding the possibility of transport from afar, and were collected from silty sands with abundant Foraminifera. They are therefore considered to be representative of shallow, low energy, marine environment near Wachapreague, Virginia, 19,000 years B.P.

Based on eustatic sea level changes as summarized by Shepard (1963), sea level was lower than present sea level by 3 m (10') 3500 years B.P., 107 m (345') 18,750 years B.P., and 112 m (360') 19,600 years B.P. These data are summarized in Table 14.

Sample No. 1, taken 6.1 m below present MTL, was dated at 3490 years B.P., when sea level was estimated to be 3 m below present level. This Sample No. 1, an assemblage of Crassostrea sp. and Mercenaria sp. shells, was probably deposited in lagoonal mud sediments. Kraft (1971) found a similar assemblage of Crassostrea sp. shells in the growth position 10.7 m (35') below present MTL; these were radiocarbon dated 3430 years B.P.

Samples No. 2 and 3, assemblages on small gastropod and pelecypod shells, dated 18,750 and 19,600 years B.P., were taken from deposits presently only 15.0 (46') and 20.0 m (62') below MTL. However, eustatic sea level was 107 m (345') and 112 m (360') below present MTL 18,750 and 19,600 years B.P. In order to deposit marine sediments in the area of Wachapreague, Virginia

TABLE 12

Sediment analysis Parramore Island well log.

Sand Sieve Analysis

Sample #	(meters)	Mean (phi units)	Skewness	Standard Deviation	Kurtosis	Blows/of/Hammer
37-39	(11.6)	3.476	0.014	0.677	0.709	5-6-6-8
40-42	(12.5)	3.604	-0.457	0.454	0.439	5-10-11-12
42-44	(13.1)	3.300	0.662	0.673	0.815	9-8-10-10
47-49	(14.6)	3.464	-0.026	0.635	0.880	13-19-22-28
52-54 (Top Half)	(16.1)	1.712	0.589	1.124	1.489	Top Half
57-59	(17.7)	1.743	-0.158	0.893	1.753	14-15-52-40
59-61	(18.3)	2.525	-2.319	0.881	1.437	15-12-12-20
62-64	(18.9)	2.278	-9.249	1.136	2.016	12-10-5-4
65-67	(20.2)	1.983	0.281	1.112	2.172	10-7-8-3
67-69	(20.8)	1.885	0.039	0.996	1.967	9-9-8-22
70-72	(21.7)	2.876	0.036	1.048	1.495	6-11-12-35
72-74	(22.3)	1.830	0.118	1.010	1.862	Top
72-74	(22.3)	1.958	0.937	1.341	4.449	14-6-5-1(Middle)

TABLE 12 (Cont'd.)

Pipet Analysis

Sample #	(meters)	50% Mean ϕ	% Sand	% Silt	% Clay
17-19	(5.5)	5.8	12	81	7
20-22	(6.4)	4.4	38	58	4
25-27	(7.9)	4.9	23	73	4
54	(16.5)	5.8	12	85	3
74	(22.6)	5.3	18	79	3

TABLE 13

Summary of Parramore Island well log.

Depth Below MTL (meters)	Mean Grain Size (phi units)	Comments
0 - 8.9	5.0	firm lagoonal mud, shells and rhizomes
9.0 - 14.5	3.5	very fine silty sand, shells
14.6 - 15.3	1.71	medium sand, shells and shell fragments
15.4 - 15.7	transition zone	no samples
15.8 - 16.4	5.8	firm silty clay mud, small shell
16.5 - 17.4	1.74	medium sands, shells and gravels
17.5 - 19.0	2.40	clean fine sands, small shells
19.1 - 20.4	1.93	medium sand, shells fragments
20.5 - 20.9	2.87	fine sands
21.0 - 21.3	transition zone	no samples
21.4 - 21.6	-4.0	gravels, shell fragments
21.7 - 21.9	1.89	medium sands, shell fragments
22	-4.0	gravels
22.1 - 22.3	5.25	very stiff silty mud

TABLE 14

Summary of radiocarbon dates, present sample depths and hypothesized eustatic sea levels.

Sample No. and Material	Recovered Depth Below MTL	Radiocarbon Date Years B.P.	Eustatic Sea Level Lower than Present
#1, Shells	6.1 m (20')	3490 ± 125	3 m (10')
#2, Shells	15.0 m (46')	18,750 ± 750	107 m (345')
#3, Shells	20.0 m (62')	19,600 ± 500	112 m (360')

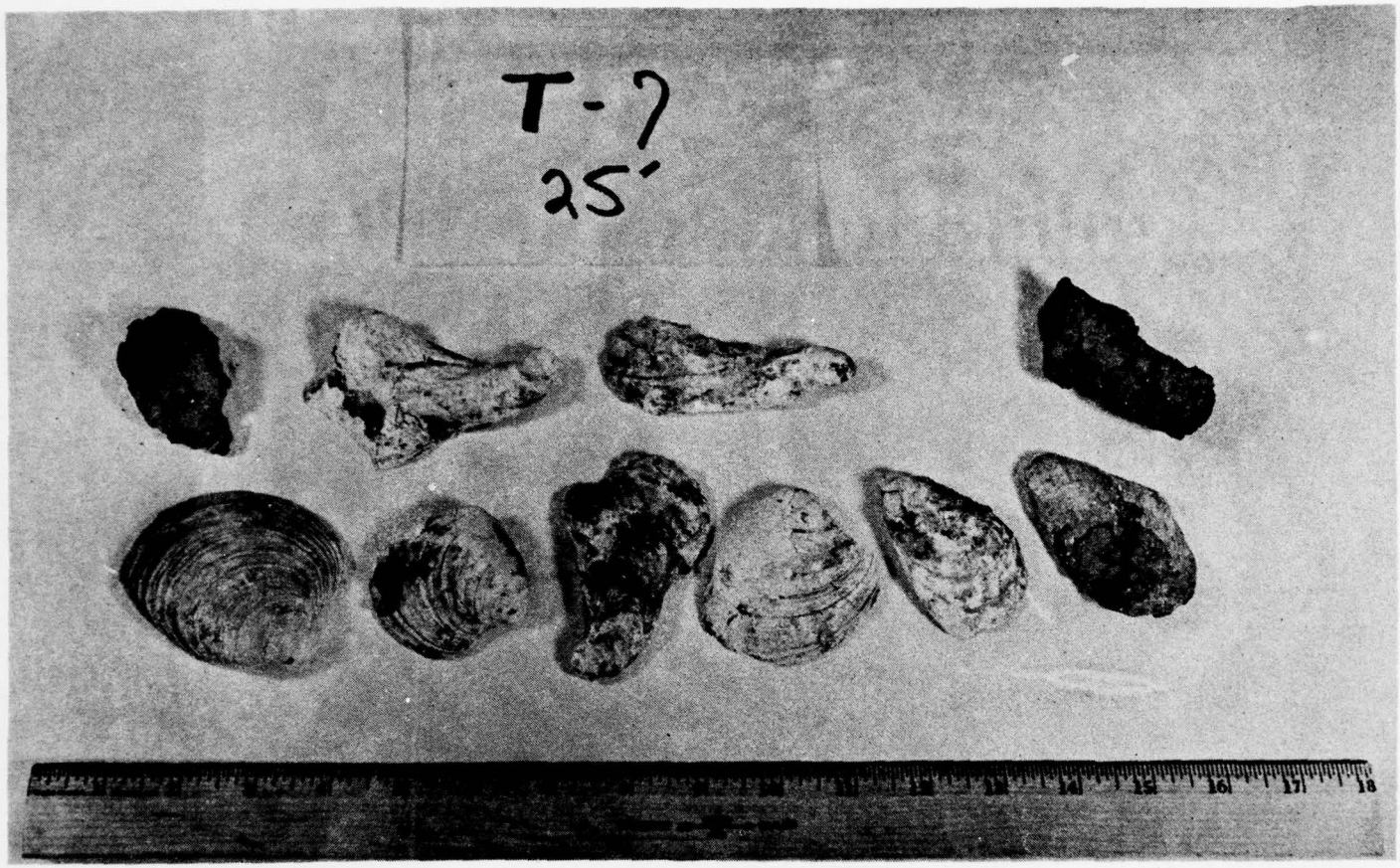

Figure 37. An assemblage of shells taken from a horizon 25 ft. (7.6 m) below M.T.L. along the south flank of the inlet channel at transect #7, similar to those taken at 20' (6.1 m) at transect #2-2, and dated at 3490 years B.P.

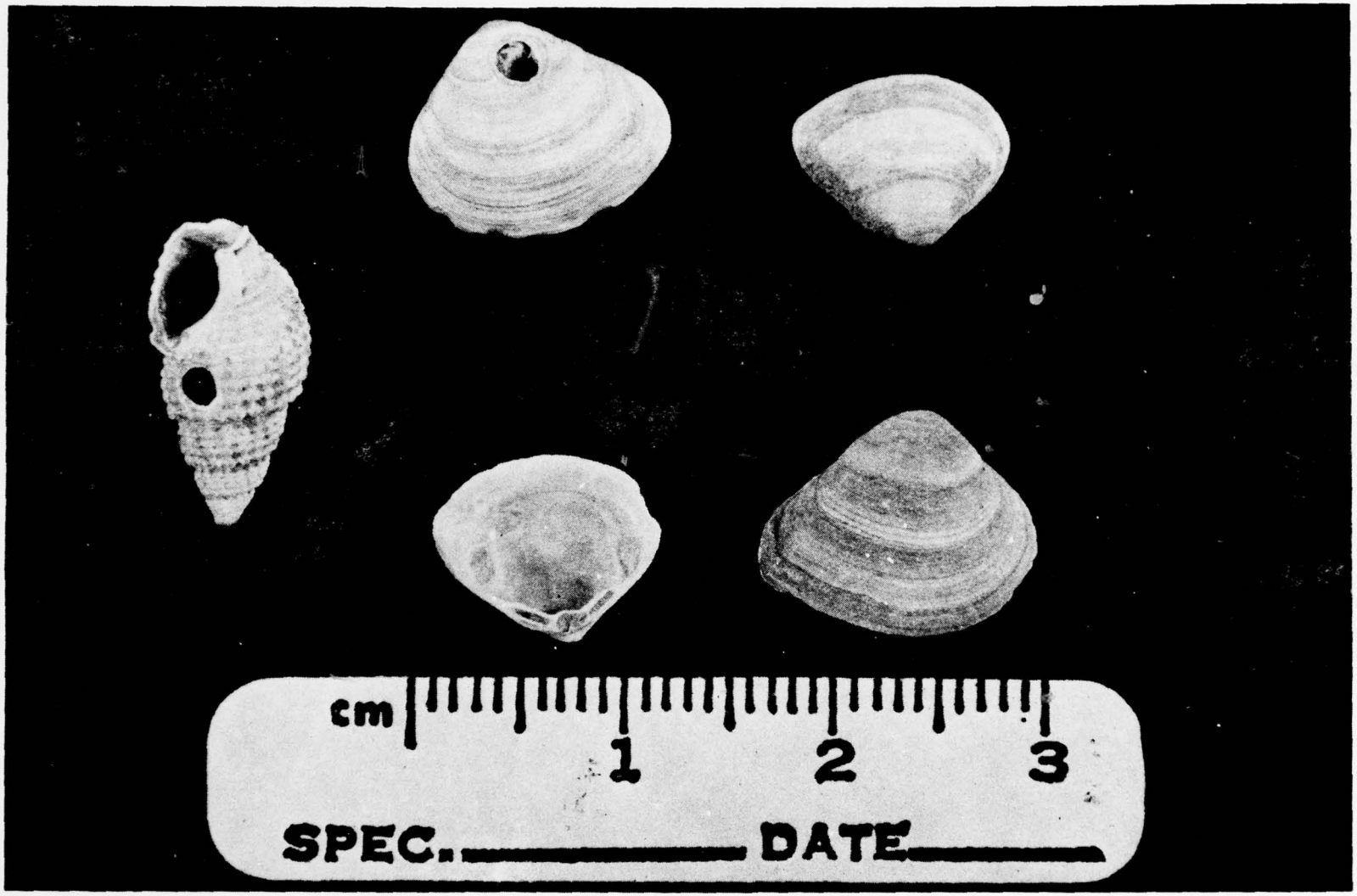

Figure 38. An assemblage of shells taken from the Parramore Island well log at horizons 15 m and 20 m below M.T.L.

the depositional surface must have been at least 92 m (310') lower than present. This implies that some time during the period from 18,750 years B.P. to 3,500 years B.P. the crystalline basement in the area of Wachapreague Inlet, Virginia, uplifted at least 92 m (310'). If the shells were not deposited at sea level, but at depths of 1, 2, or 3 m of water, the implied uplift would be even greater.

Late Quaternary uplifts have been described for other areas of the east coast of North America. Kaye and Barghoorn (1964) report 290' of crustal rise in Boston Harbor occurring between 14,000 and 6,000 years B.P. They theorized that the uplift was possible in response to deglaciation. Harrison, et al. (1965) suggested 170' crustal uplift in about the last 15,000 years in the area of Chesapeake Bay entrance. This conclusion was based on channel depths and expectable stream gradients by the thalweg of the buried Susquehanna River, as proposed by Hack (1957).

Several mechanisms can be postulated to account for the uplift in the area of Wachapreague Inlet. Woollard (1955) proposed an arcuate fracture in the underlying basement rocks running northwesterly through Virginia's Eastern Shore. The proposal was based on earthquake data, and the western side of this fracture, including lower Chesapeake Bay and up to Wachapreague Inlet would have been on the upthrown side of the fracture. Murray (1961) also suggests either faulting, simple uplift or a combination of both processes in the Norfolk-Fort Monroe uplift area. Taylor, et al. (1968) and Drake (1969) describe anomalies in the magnetic investigations of the eastern shore of Virginia, suggests a fault trending N. 30°W through Exmore with a structural throw of 400 m (1300').

In addition to evidence based on tectonic activity in the crystalline basement complex, evidence of uplift also exists in the overlying sedimentary rocks. Inspection of the west-east geologic sections across the eastern shore peninsula from Sinnott and Tibbetts (1969) show a gentle upwarping of the base of the Chesapeake Group of undifferentiated sediments of Miocene Age. This upwarping amounts to 122 m (400') in the area of Wachapreague, Virginia.

Variations in the textural characteristics of the beach zone sediments to the north and to the south of Wachapreague Inlet have recently been investigated (Ingram, 1975). Sands of greater size and lesser angularity were found north of Wachapreague Inlet when compared to the sands from the beaches to the south. A conclusion that may be drawn from this data is the difference in the sediment textural characteristics is due to the exposure of different geologic formations caused by differential warping or possibly a fault normal to the coastline, in the area of Wachapreague, Virginia.

The importance of the proposed uplift is that it may make a significant contribution not only to the understanding of the evolution of the present lower Delmarva Peninsula and in understanding the present geomorphology of the mid-Atlantic Coastal Plain, but also indicates possible recent active tectonism in this geologic province.

A3. Discussion.

Over the last 120 years the inlet channel has migrated to the south at a rate of 1 meter per year. The migration has been in response to the net littoral drift and the migration has occurred in spite of the fact that the southern flank of the channel is composed of fairly resistant cohesive sediments. In the process of migration approximately $8.7 \times 10^6 m^3$ of sand has been deposited on the northern flank in the form of an advancing sand wedge.

The barrier islands updrift of the inlet are sand starved. A reasonable estimate for southerly longshore drift, based upon updrift erosion rates and trapping characeristics at updrift inlets, is $0.5 \times 10^6 m^3/yr$. However, observed sand volume changes from aerial photographic evidence indicates temporal storage of up to $2 \times 10^6 m^3$ over a few months. These changes are attributed to adjustments in sand volumes on the ebb delta shield rather than sand drift input from adjacent islands.

Comparison of bathymetric maps between 1852 and 1972 indicate the interior feeded channels leading to the inlet have increased in depth. Thus it appears that sand was not, in recent times, taken into residency on the interior through the augmentation of flood delta features. In contrast the stratigraphic studies on the lagoon itself by other workers show that within the last 5,000 years large flood delta sand deposits were precursors of the segmentation into lagoonal compartments. Thus, it would appear that Wachapreague Inlet is a case wherein the hydraulic system changed from one favoring advection of sand into the interior with flood delta formation to one wherein sand bypassing at the channel and ebb delta dominates. This point will be discussed at a later time after the currents and nearshore circulation is discussed.

Since 1871, the cross-sectional area of the inlet throat has remained relatively constant at about 4,200 m^2. However, the inlet channel length (based in the 12 meter contour) has increased from 1,600 m in 1852 to 3,000 m in 1972. Since the turn of the century the hydraulic radius has decreased.

Investigation of the surficial sediment distributions indicate that the inlet channel floor is covered by a veneer of coarse grained gravels and shell debris overlying a firm silty clay substrate. These coarse materials appear to be abrading the resistant substrate as they migrate back and forth with each change in tidal flow direction. Examination of the short-term changes in bottom sediment characteristics demonstrated that during periods of temporary sediment choking of the inlet the channel bottom is lined with sand.

The collective evidence indicates that the inlet channel has limited freedom of movement: over the short term area reductions occur by movement of material on the north flank and filling of

the bottom. Over the long term, however, the channel has migrated to the south by erosion of the firm cohesive materials composing the south flank. Thus, the channel system is incising older lagoonal deposits.

Radiocarbon dating of shell material from the channel "wall" and from well borings within a kilometer of the channel indicate that local uplift has occurred. In order to bring these shell bearing horizons into conformity with accepted eustatic sea level curves uplift of 92 meters is required.

B. Tides and the Characteristics of Storage Basins

B1. Morphology of the basin system.

The storage basin serviced by Wachapreague Inlet is shown in Figure 39. The system is comprised of tidal channels, open bays with fringing tidal flats, and extensive areas of Spartina alternaflora marsh dissected by small channels. The main feeder channels from the inlet to the bays are quite deep, ranging from 6 to 10 m. The component areas are:

Tidal channels	$24.0 \times 10^6 m^2$
Bays and flats	$34.8 \times 10^6 m^2$
Marsh	$37.6 \times 10^6 m^2$

Although exact delineation of the area influenced by the inlet can not be specified, gaging of the tidal flows in the interior channels indicate relatively small leakage to and from the basins serviced by adjacent inlets via the Swash on the south and Teagles Ditch on the north.

B2. Ocean and basin tides.

The tide characteristics for the region are shown in Table 15. The inlet gates the full semi-diurnal oceanic tide range into the basin so the full potential tidal prism of the basin is realized. In fact the basin range, as reflected at the tide gage on the western fringe of the basin (Town of Wachapreague), is about 10% larger than the ocean range. This is likely due to inertial forces wherein the mass of water entering the deep inlet continues to flow in the same direction even though the surface slope has changed direction (King, 1974). Moreover, it should be noted that the durations of rising and falling tide stages within the basin are unequal. The comparison between duration differences for the ocean tide station of Wallops Island and that of Town of Wachapreague are shown in Figures 40 and 41. These observations for a one year period show the duration differences to be randomly distributed and that the basin experiences a duration asymmetry wherein the mean duration of rise is 0.45 hours longer than the fall duration (Byrne and Boon, 1976). It has been noted elsewhere (Shureman, 1958) that the M_4 tidal constituent is the leading contributor to long-term duration asymmetries in the vertical tides. A periodogram of the vertical tide in the basin system (Fig. 42) shows a significant contribution of the M_4 constituent.

In order to ascertain whether the same duration asymmetry exists in the tidal currents in the inlet the durations of ebb

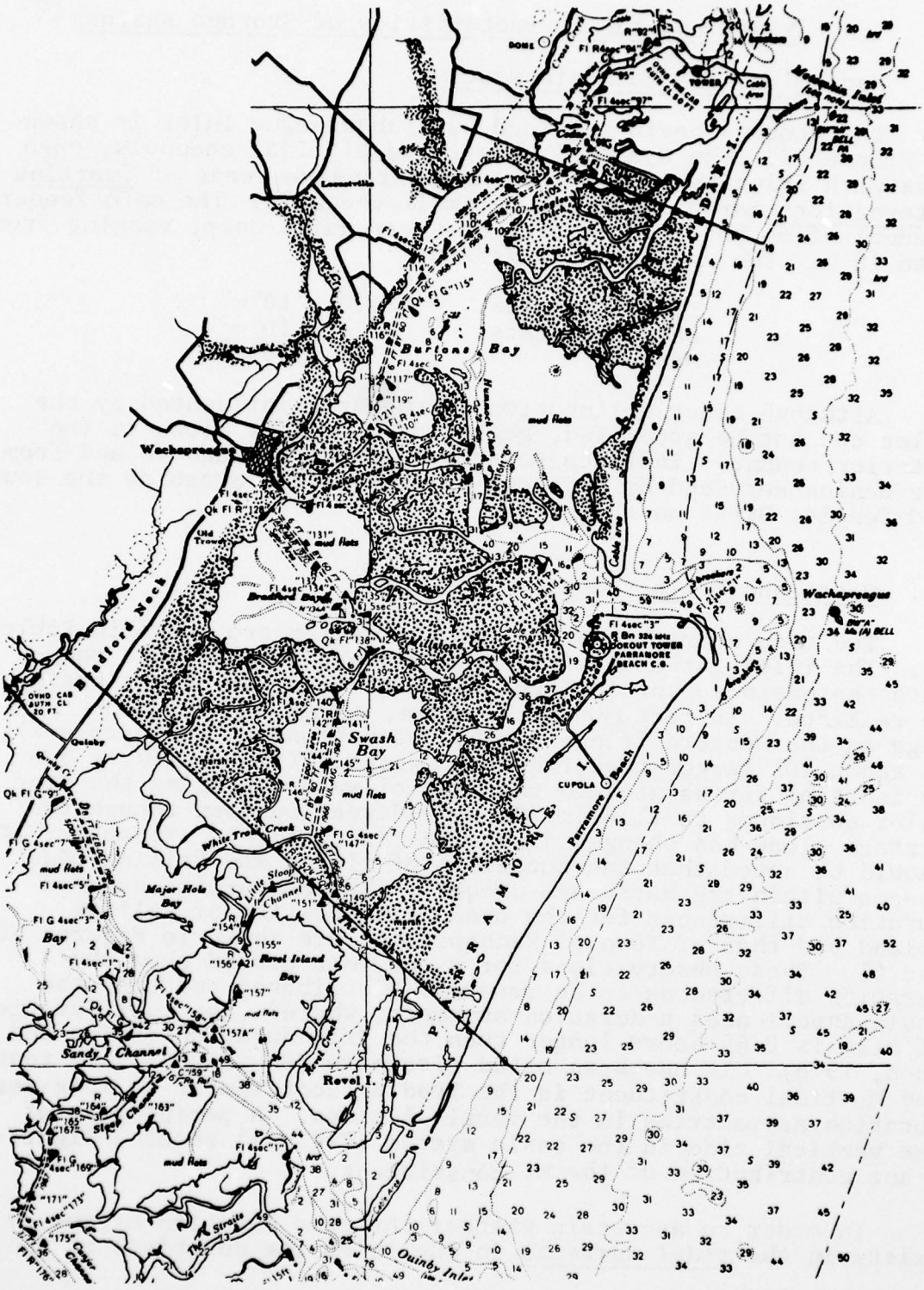

Figure 39. Wachapreague Inlet storage system. Stippled areas are marsh. Distance between latitude coordinates = 18.3 km. From U.S.C. & G.S. Chart 1221.

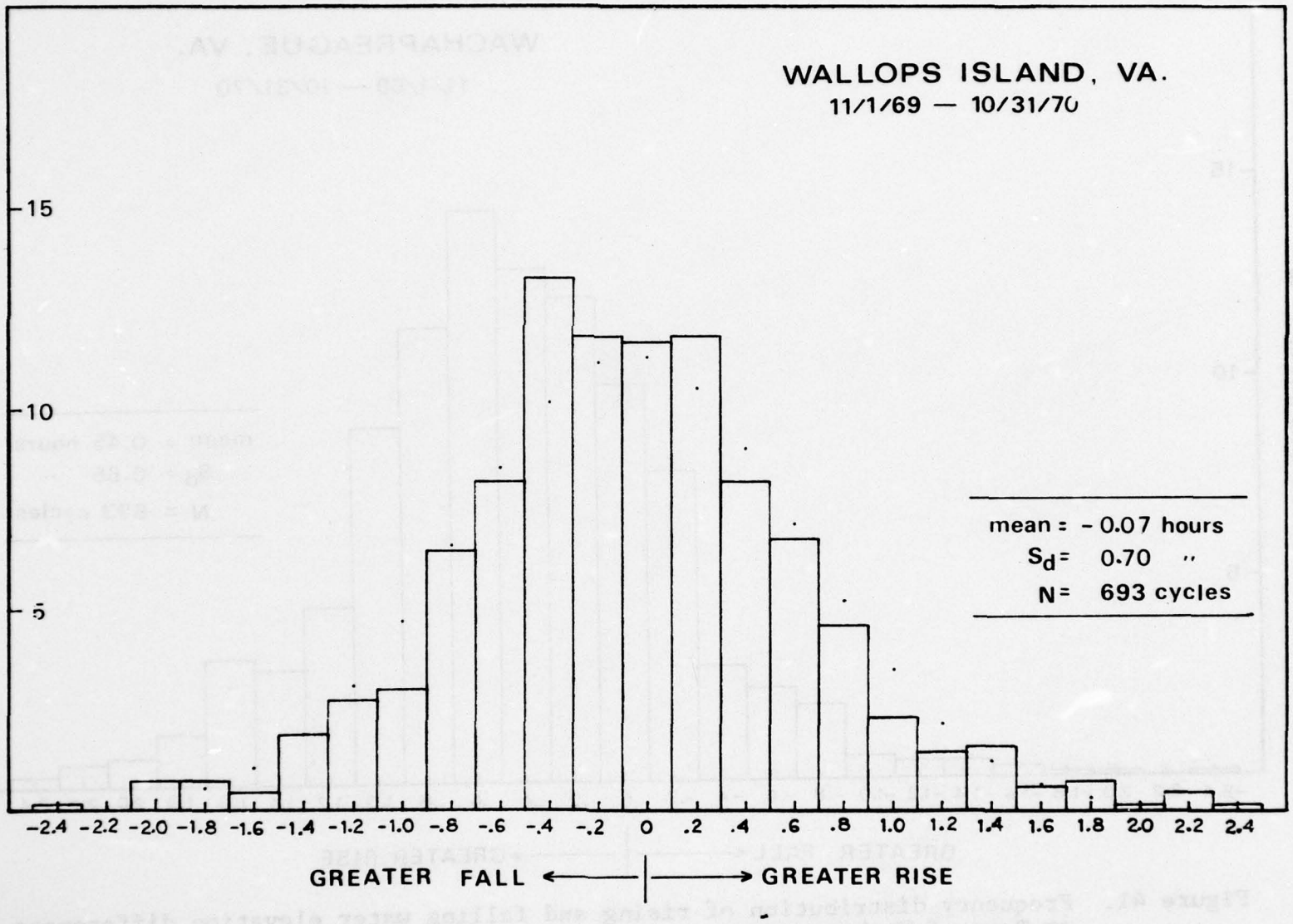

Figure 40. Frequency distribution of rising and falling water elevation differences at Wallops Island, an oceanic location.

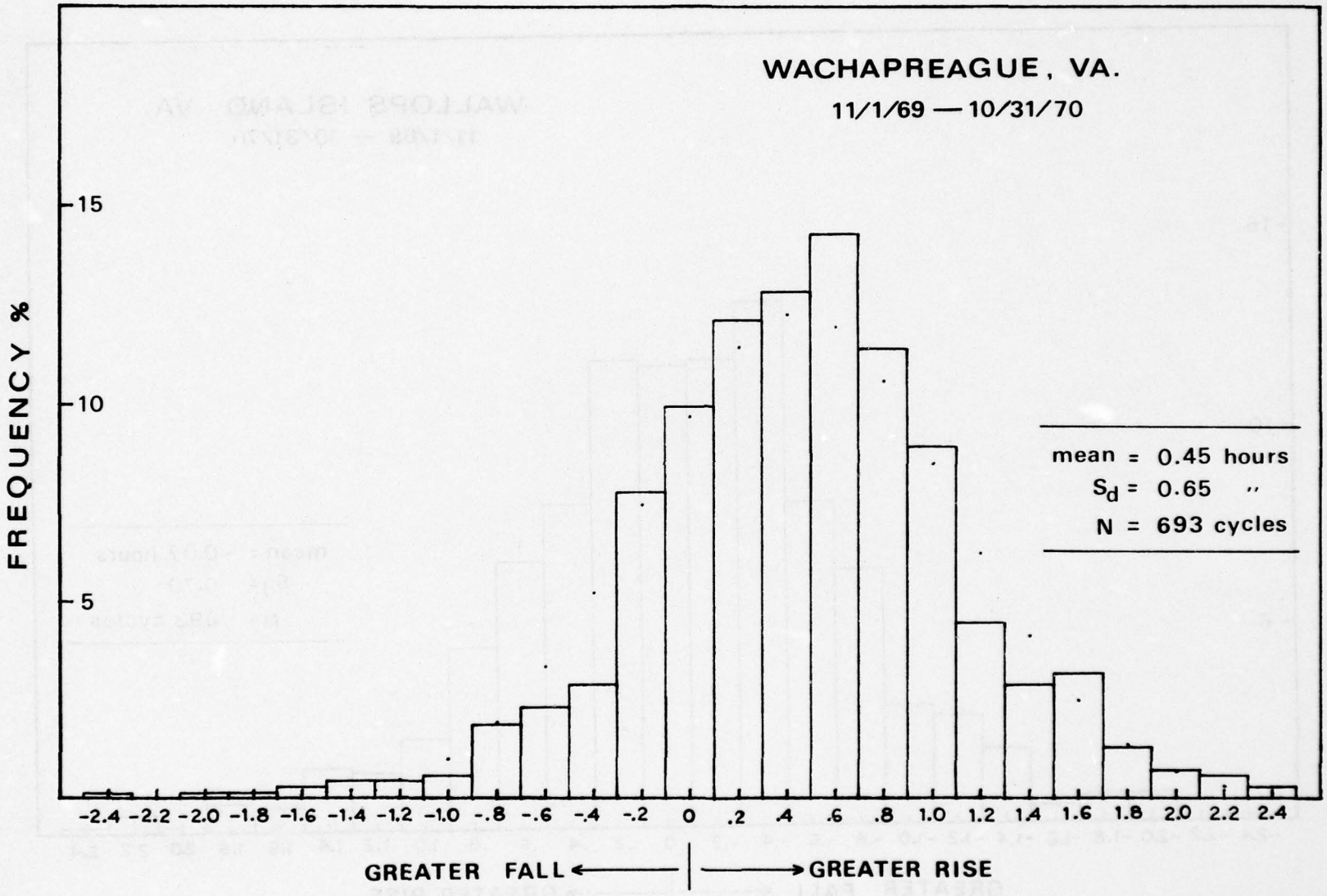

Figure 41. Frequency distribution of rising and falling water elevation differences at Town of Wachapreague.

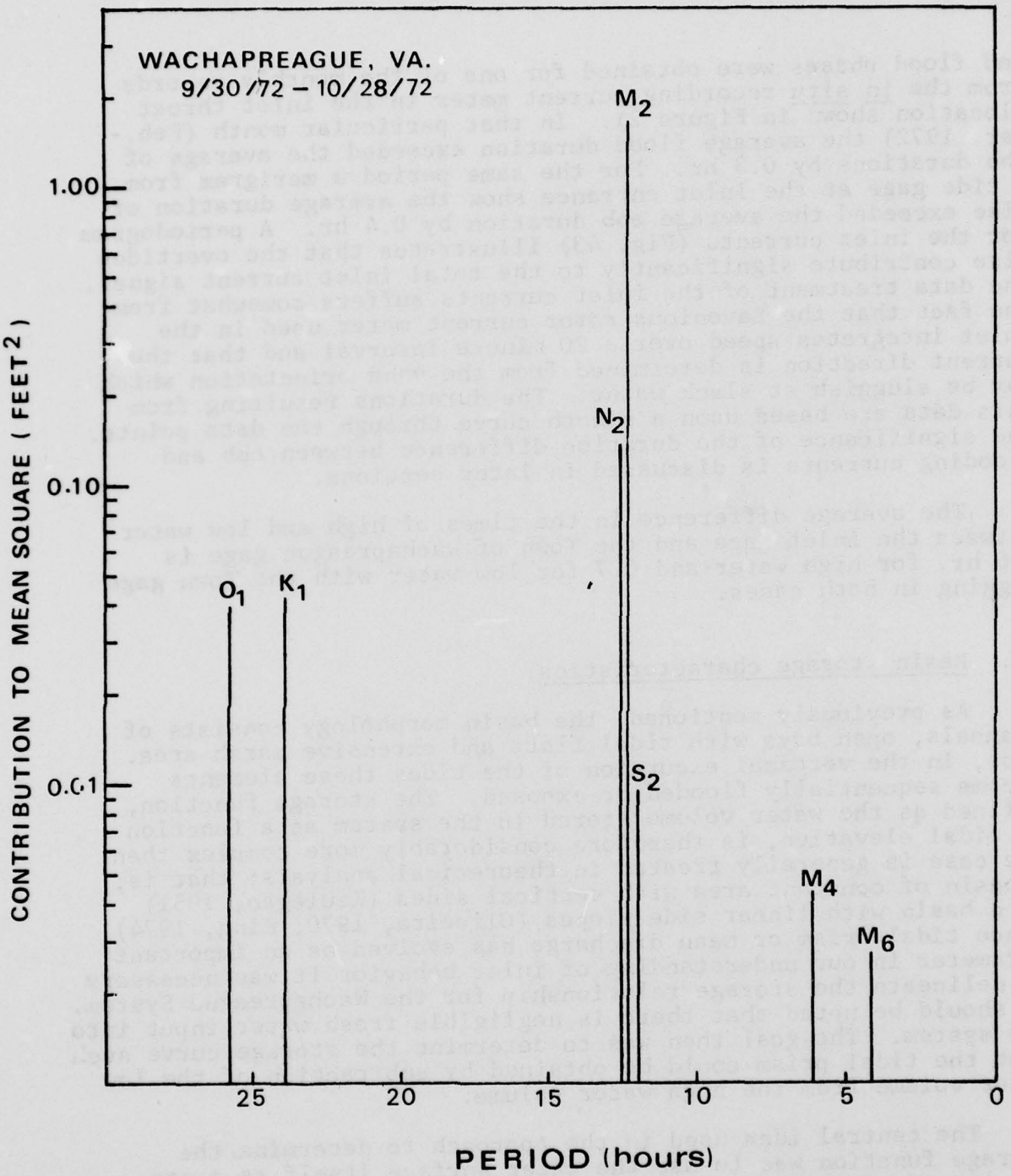

MAJOR CONSTITUENTS OF THE VERTICAL TIDE (29-DAY SERIES)

Figure 42. Periodogram of the major constituents of the vertical tide at Town of Wachapreague.

and flood phases were obtained for one of the monthly records from the in situ recording current meter in the inlet throat (location shown in Figure 2). In that particular month (Feb.-Mar. 1972) the average flood duration exceeded the average of ebb durations by 0.3 hr. For the same period a merigram from a tide gage at the inlet entrance show the average duration of rise exceeded the average ebb duration by 0.4 hr. A periodogram for the inlet currents (Fig. 43) illustrates that the overtides also contribute significantly to the total inlet current signal. The data treatment of the inlet currents suffers somewhat from the fact that the Savonious rotor current meter used in the inlet integrates speed over a 20 minute interval and that the current direction is determined from the vane orientation which may be sluggish at slack water. The durations resulting from this data are based upon a smooth curve through the data points. The significance of the duration difference between ebb and flooding currents is discussed in later sections.

The average difference in the times of high and low water between the inlet gage and the Town of Wachapreague gage is 0.6 hr. for high water and 0.7 for low water with the Town gage lagging in both cases.

B3. Basin storage characteristics.

As previously mentioned, the basin morphology consists of channels, open bays with tidal flats and extensive marsh area. Thus, in the vertical excursion of the tides these elements become sequentially flooded or exposed. The storage function, defined as the water volume stored in the system as a function of tidal elevation, is therefore considerably more complex than the case is generally treated in theoretical analysis; that is, a basin of constant area with vertical sides (Keulegan, 1951) or a basin with linear side slopes (Oliveira, 1970; King, 1974). Since tidal prism or mean discharge has evolved as an important parameter in our understanding of inlet behavior it was necessary to delineate the storage relationship for the Wachapreague System. It should be noted that there is negligible fresh water input into the system. The goal then was to determine the storage curve such that the tidal prism could be obtained by subtraction of the low water volume from the high water volume.

The central idea used in the approach to determine the storage function was to use the water surface itself as a contouring machine as the water surface rises over the variable topography during rising tide. This was achieved using sequential aerial photo coverage with black and white infrared film to enhance the contrast between flooded and exposed surfaces. In order to determine the vertical changes in tidal elevations

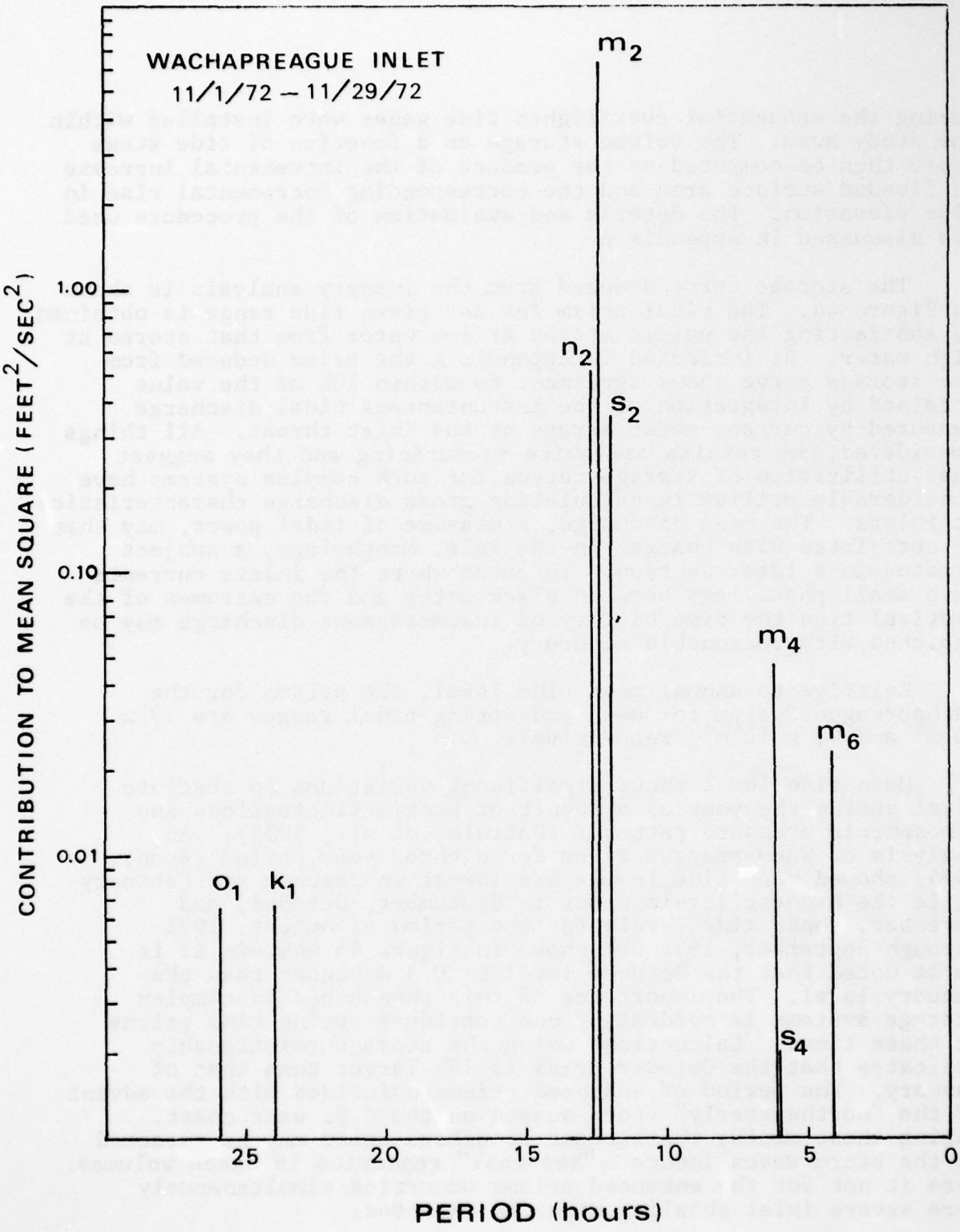

MAJOR CONSTITUENTS OF THE HORIZONTAL TIDE (29-DAY SERIES) E-W

Figure 43. Periodogram of the major constituents of the horizontal tide (currents) at Wachapreague Inlet.

AD-A049 161 VIRGINIA INST OF MARINE SCIENCE GLOUCESTER POINT F/G 8/6
RECENT HISTORY AND RESPONSE CHARACTERISTICS OF WACHAPREAGUE INL--ETC(U)
MAY 77 R J BYRNE, J T DEALTERIS, J P SOVICH N00014-71-C-0334

UNCLASSIFIED NL

2 OF 3
AD A049161

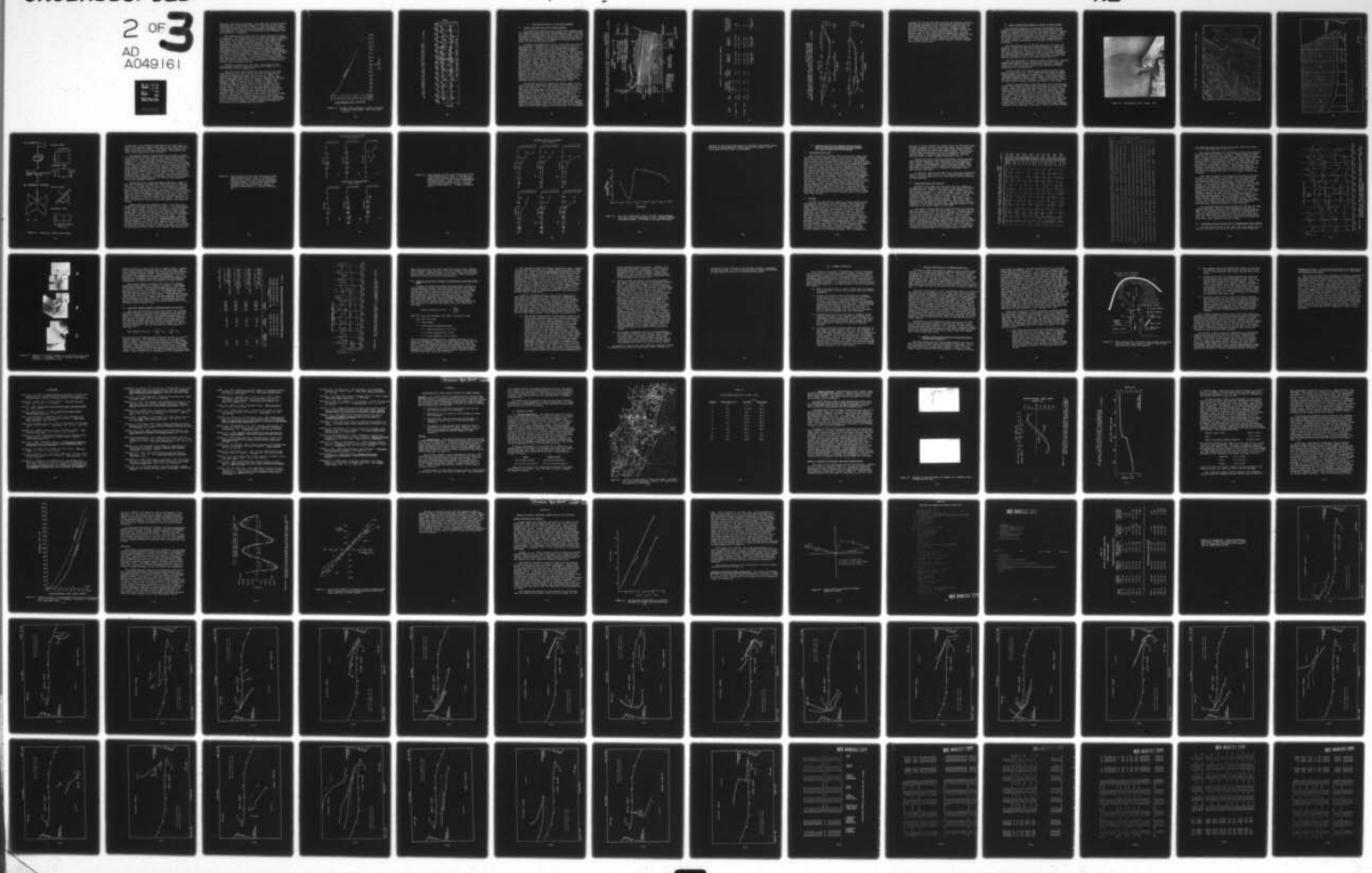

during the sequential overflights tide gages were installed within the study area. The volume storage as a function of tide stage could then be computed as the product of the incremental increase in flooded surface area and the corresponding incremental rise in tide elevation. The details and evaluation of the procedure used are discussed in Appendix A.

The storage curve deduced from the imagery analysis is shown in Figure 44. The tidal prism for any given tide range is obtained by subtracting the volume stored at low water from that stored at high water. As indicated in Appendix A the prism deduced from the storage curve shows agreement to within 10% of the value obtained by integration of the instantaneous tidal discharge measured by current meter arrays at the inlet throat. All things considered, the results are quite encouraging and they suggest that utilization of storage curves for such complex systems have considerable utility in calculating gross discharge characteristics at inlets. The mean discharge, a measure of tidal power, may then be correlated with charges in the inlet mrophology, a subject treated in a later section. In cases where the inlets currents have small phase lags between slack water and the extremes of the vertical tide the time history of instantaneous discharge may be depicted with reasonable accuracy.

Relative to annual mean tide level, the prisms for the Wachapreague System for mean and spring tidal ranges are 77 x $10^6 m^3$ and 91 x $10^6 m^3$, respectively.

Mean tide level shows significant variations in absolute level during the year as a result of steric fluctuations and atmospheric pressure patterns (Pattulo, et al., 1955). An analysis of Wachapreague tides for a three year period (Boon, 1974) showed mean tide levels are lowest in January and February while the highest levels occur in September, October, and November. Mean tide levels for the period of August, 1971 through September, 1972 are shown in Figure 45 wherein it is to be noted that the October level is 0.3 m higher than the January level. The importance of this phenomenon in complex storage systems is evident of one considers spring tide prisms at these times. Calcuations using the storage relationship indicates that the October prism is 18% larger than that of January. The period of enhanced prisms coincides with the advent of the "northeasterly" storm season on the U.S. east coast. During these months the largest longshore drift may be expected as the storm waves induce a "seasonal" reduction in beach volumes. Were it not for the enhanced prisms occurring simultaneously more severe inlet shoaling might be expected.

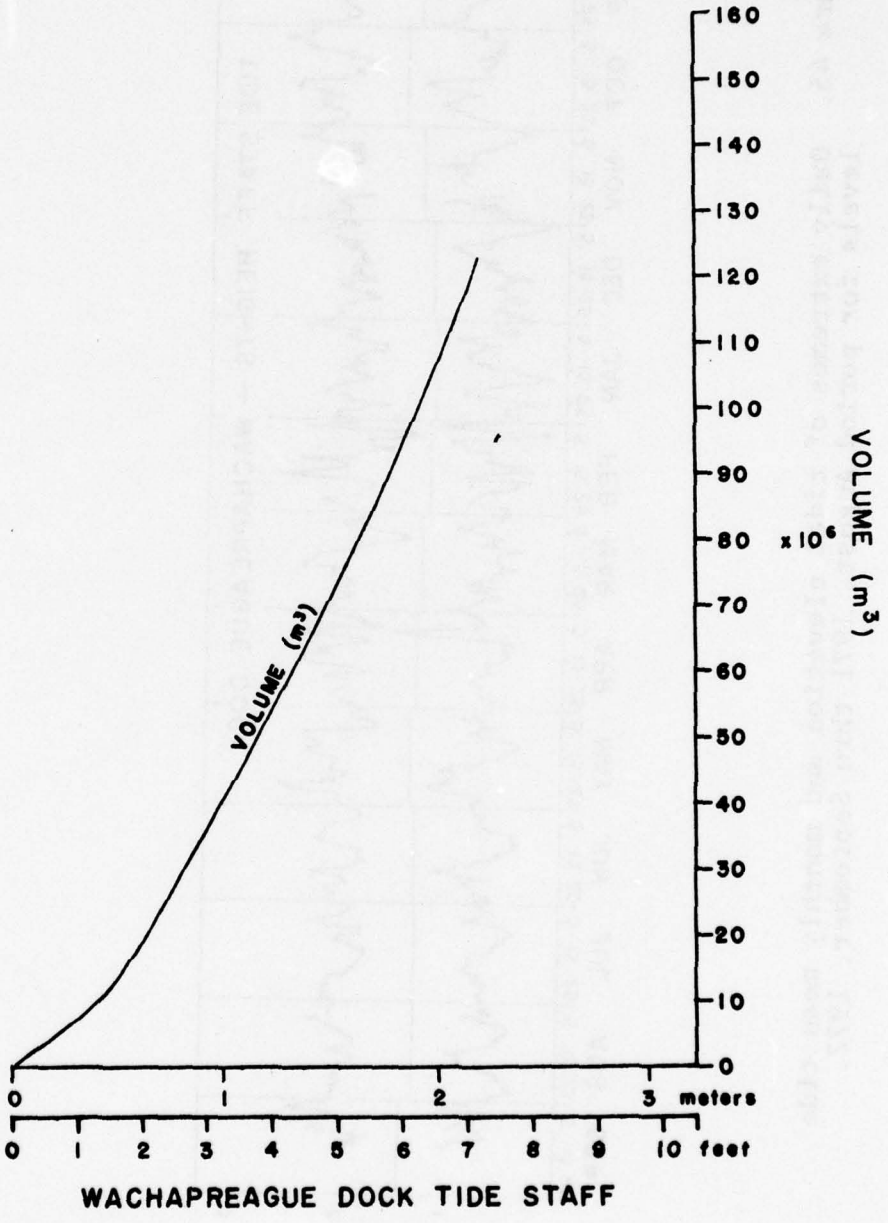

Figure 44. Storage volume relative to tidal elevations at town of Wachapreague. Mean tide level = 4.36 ft.

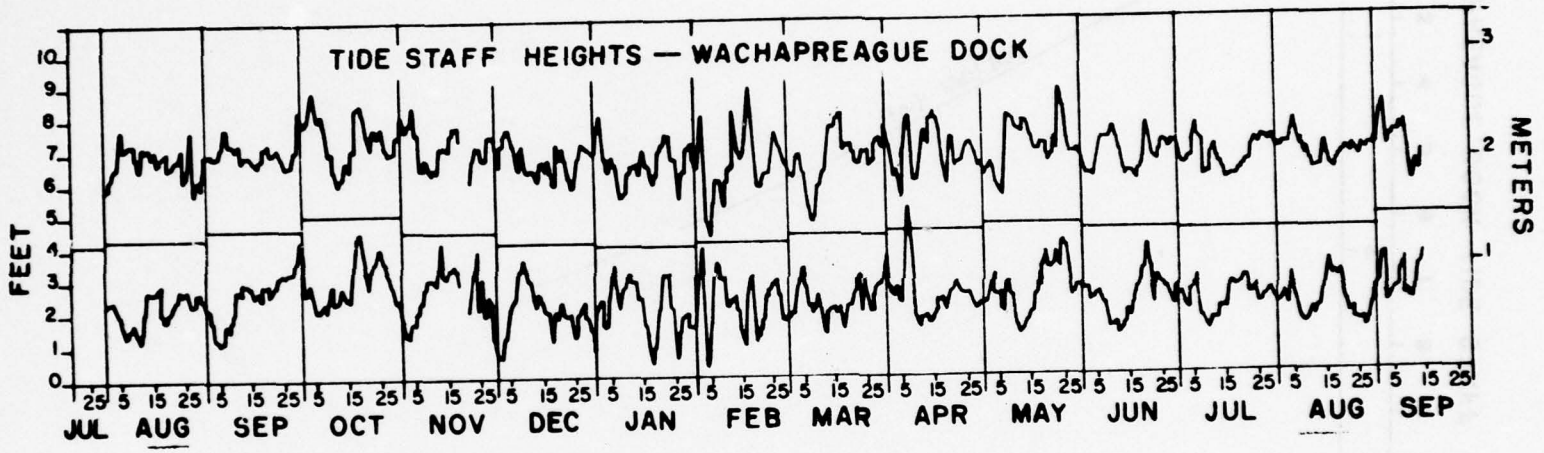

Figure 45. Daily extremes of tidal elevation and monthly mean tide levels for period August, 1971 thru September, 1972.

C. Flow Characteristics in the Inlet Channel

C1. Spatial distribution of the inlet currents.

The generalized pattern of flow at the inlet conforms with that expected wherein the flood flow behaves as a radial inflow to a point sink modified by the offset characteristic. The distribution of lateral inflow on the north side of the channel is controlled by the degree of development of the flanking shoals. During ebb flow conditions the channelized currents issue as a plane jet over the ebb delta system.

In order to determine the details of the flow distribution flow gaging was performed for a 26 hour period on 13 and 14 September 1972. Current meter measurements were obtained simultaneously at a transect across the throat of the channel (transect 22 in Fig. 46) and another at transect 8 which is the entrance point to the horseshoe shaped ebb delta. Six anchored buoys were arrayed across the throat transect and four more were positioned at the outer (#8) transect. During a measurement cycle the boat would secure to a buoy and a fast-response ducted current meter (Byrne and Boon, 1974) was lowered to the bottom on a weighted vane. The rotor revolution rate was monitored at the surface. Rather than reconstruct the velocity profile from discrete point measurements in the vertical the current meter was raised, by a powered capstan, to the surface at a constant rate of about 5 cm/sec thereby mechanically integrating for the mean velocity over the vertical profile In practice it was possible to repeat a measurement at each station every 30 to 40 minutes when four boats were used. Curves of discharge as a function of time were then calculated for each transect using small area partitions multiplied by the corresponding mean velocities taken from curves of transverse mean velocity constructed from the measured points (Troskolanski, 1960).

At the date of the flow gaging the lateral shoals on the north flank had dimenished to the extent of no exposure at low water (see Figure 25). The water depth at the crown of the shoal was about one meter. The lateral inflow and outflow was calculated by subtracting the prism passing transect 8 from that passing transect 22. The gross flow characteristics are shown in Table 15. It was found that lateral inflow was appreciable during flooding current when 30 to 40% of the incoming prism passed over the north flank. Lateral outflow during ebbing currents was appreciably smaller, as would be expected. At transect 8 the ebb flow distribution was strongly skewed with the higher speeds on the south side of the channel (Fig. 47) whereas during the flood currents the flow is slightly skewed with the higher speeds on the north side. At the throat

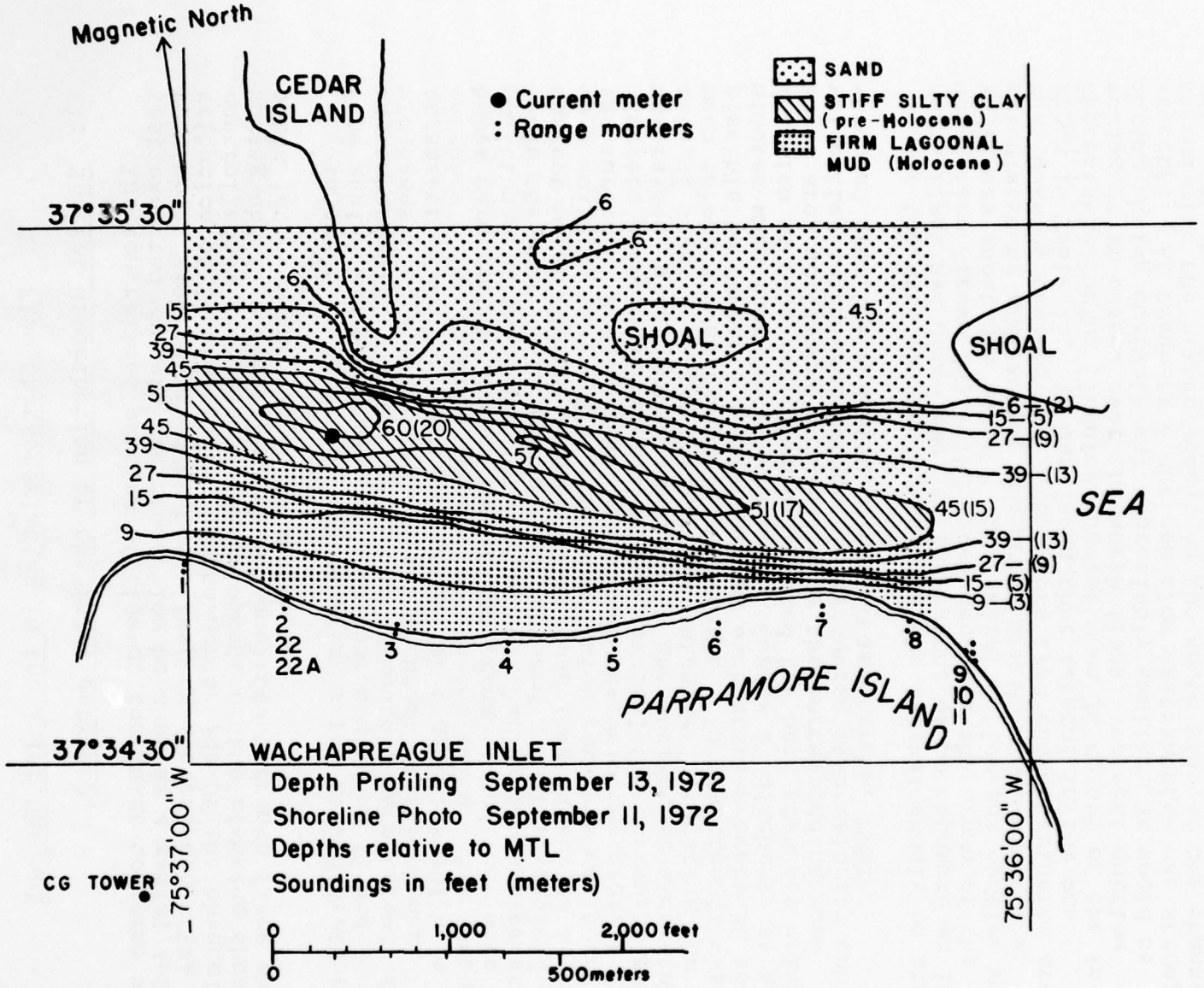

Figure 46. Wachapreague Inlet channel. Note shelf on south and asymmetry of channel cross-section. Numbers on south shoreline are survey range line positions, 1 through 11.

Table 15: Tidal Prism From Flow Gaging

Date	Tide	Tide Gage Staff Height (ft)		Tide Duration (hrs)	Prism at Range 22	Prism at Range 8	Lateral Inflow (% of prism at Range 22)
		high	low				
13 Sept. 1972	Ebb	6.4	3.2	5.9	63.18 X 10^6 m^3	52.38 X 10^6 m^3	17%
	Flood	5.7	3.2	6.1	47.56 X 10^6	27.54 X 10^6	42
14 Sept. 1972	Ebb	5.7	3.1	5.8	45.54 X 10^6	40.50 X 10^6	11
	Flood	6.1	3.1	7.1	61.02 X 10^6	41.22 X 10^6	32
					Section Area 4,409 m^2	Section Area 3,459 m^2	Section Area 950 m^2

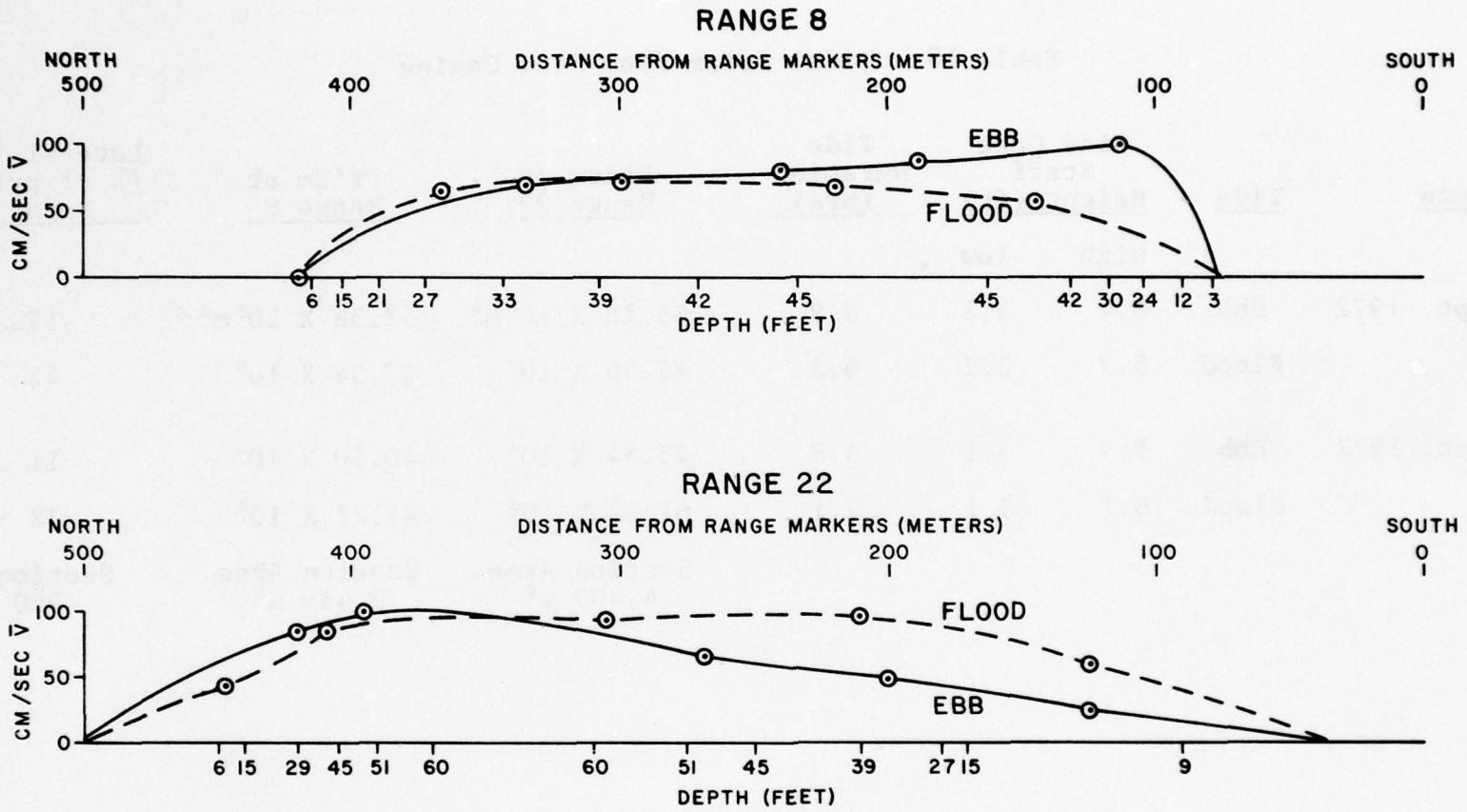

Figure 47. Distribution of ebb and flood vertically averaged maximum velocities across the channel at Ranges 8 and 22 (see Figure 46), 14 July 1972. See Table 16 for details on ebb and flood prism.

(transect 22) the ebb and flood currents are similarly distributed with the exception of the flow along the shallow shelf on the southern one-third of the section (see Figure 46 and note the shelf formed by the 15 ft. contour). During flooding currents about 10% of the prism passing the throat passes over the shelf (about 12% of the cross-sectional area). On ebb, however, only 4% of the prism passes through that flow area. The net effect is the enhancement the ebb current speeds in the deeper portion of the channel over those of flood currents. This factor plus the duration asymmetry noted earlier results in a condition where the ebb current induced transport exceeds that of the flood current.

D. Inlet Induced Tidal Motions in Front of Cedar Island

As previously discussed the degree of development of the ephemeral shoals flanking the north side of the inlet channel appears to regulate the distribution and magnitude of the lateral inflow and outflow of water into the main inlet channel. This observation leads quite naturally to the question as to how far up the face of Cedar Island the inlet exerts an influence on the tidal currents. In order to answer this question a series of current drogue measurements were excuted in 1973 (May to September).

The configuration of the flanking shoal and the south end of Cedar Island during the period of observation is shown in Figure 48. Figure 49 shows the regional bathymetry (1972 bathymetry for depths less than 30 ft.) wherein the well developed ebb delta is apparent. During the time of the field experiments the flanking shoal was moderately well developed with subaerial exposure extending from the base of the ebb delta to about one-half the distance to the tip of Cedar Island (Fig. 48).

The zone monitored by drogues is shown in Figure 50. Ranging targets were established at approximately 600 meter intervals along the backshore of Cedar Island which served as reference positions to fix the drogue position with horizontal sextant angles from the tracking boats.

Simple current cross drogues were constructed from canvas and iron pipe (Fig. 51). Their dimensions were large yet their design permitted folding and breakdown of the crosses to facilitate handling and storage in small boats. Floats consisted of styrofoam sandwiched between wooden plates with a bamboo staff and flag attached to aid tracking. A simple lanyard, the length of which could be varied, connected the float to the drogue.

Drogue runs were made on days when wind, wave, and sea conditions were unlikely to have major influence on the float-drogue system. Most runs were made with wind velocities less than 4.5 m/sec (10 miles per hour) and under calm sea conditions. Wind velocity and wave height data were collected during each drogue run. Drogues were deployed from a small boat at the beginning of a tidal cycle and their positions determined at half hour intervals. Usually three drogues and a surface float were deployed. Drogues or floats were recovered and recycled when they strayed out of the study area, entered the inlet, went aground, or drifted so far from shore that the fixed markers on Cedar Island could no longer be seen. It was hoped to obtain complete coverage of the area under investigation during different stages

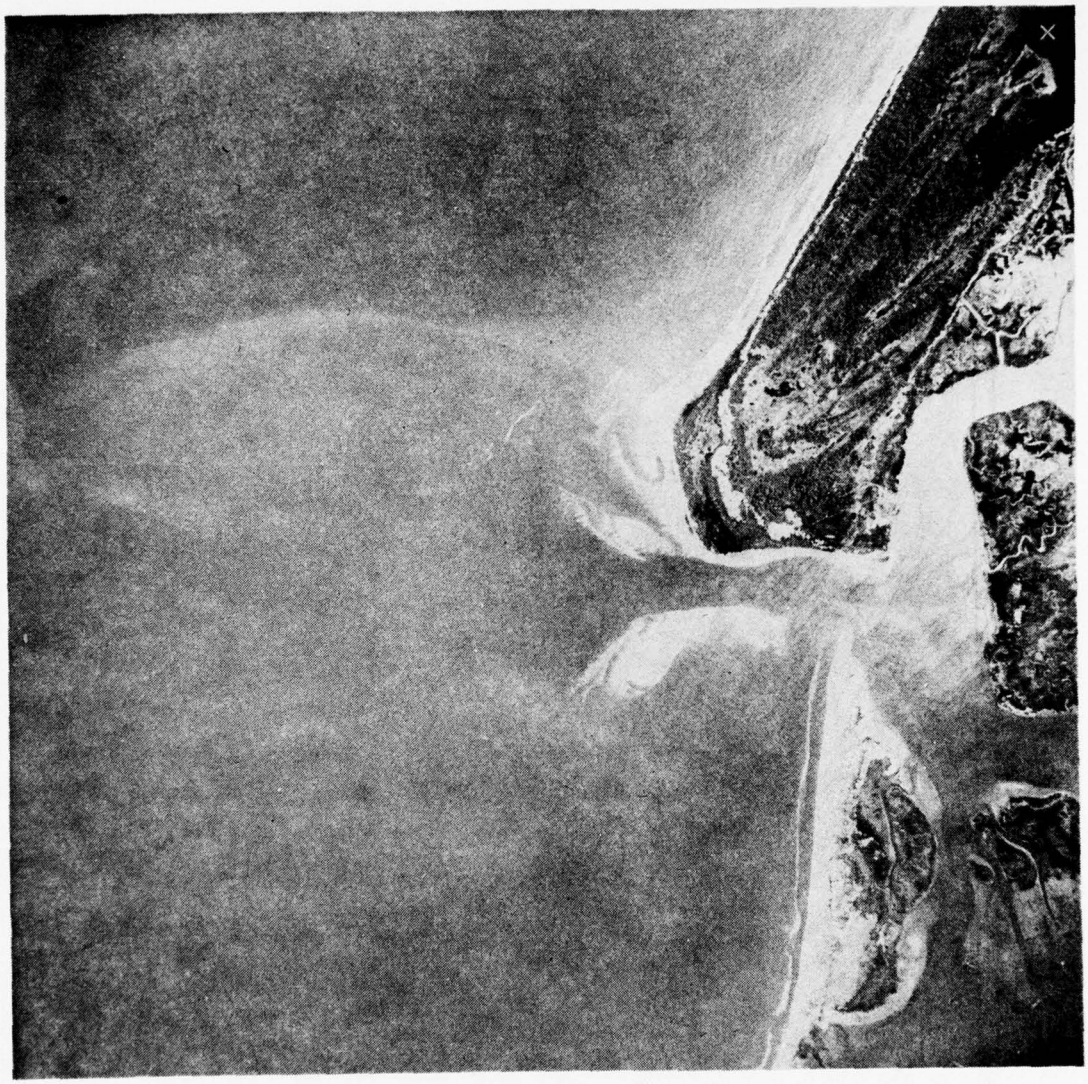

Figure 48. Wachapreague Inlet, August, 1973.

Figure 49. Bathymetry of Wachapreague Inlet and vicinity.

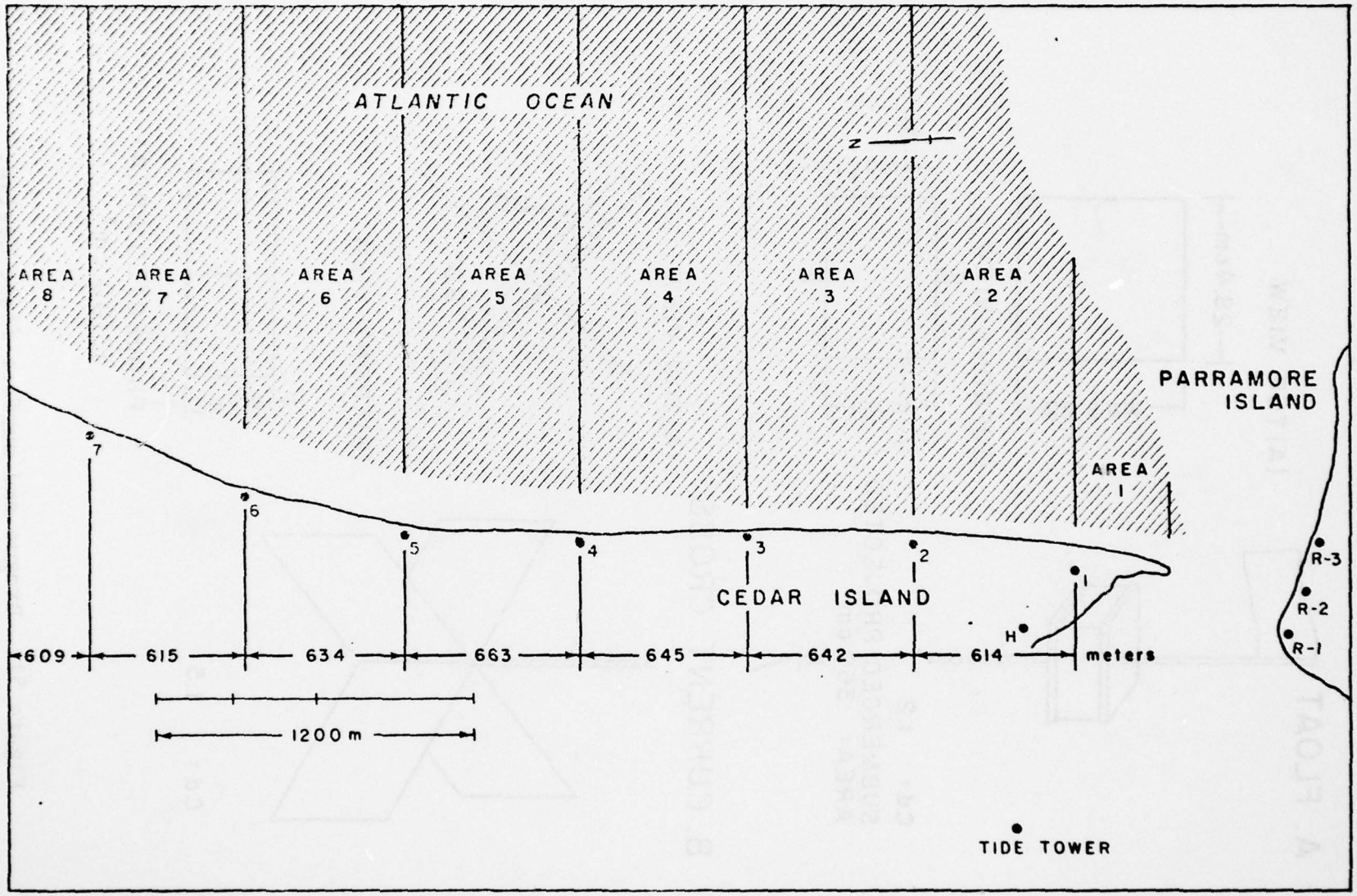

Figure 50. Ranging station on Cedar Island and nearshore subareas.

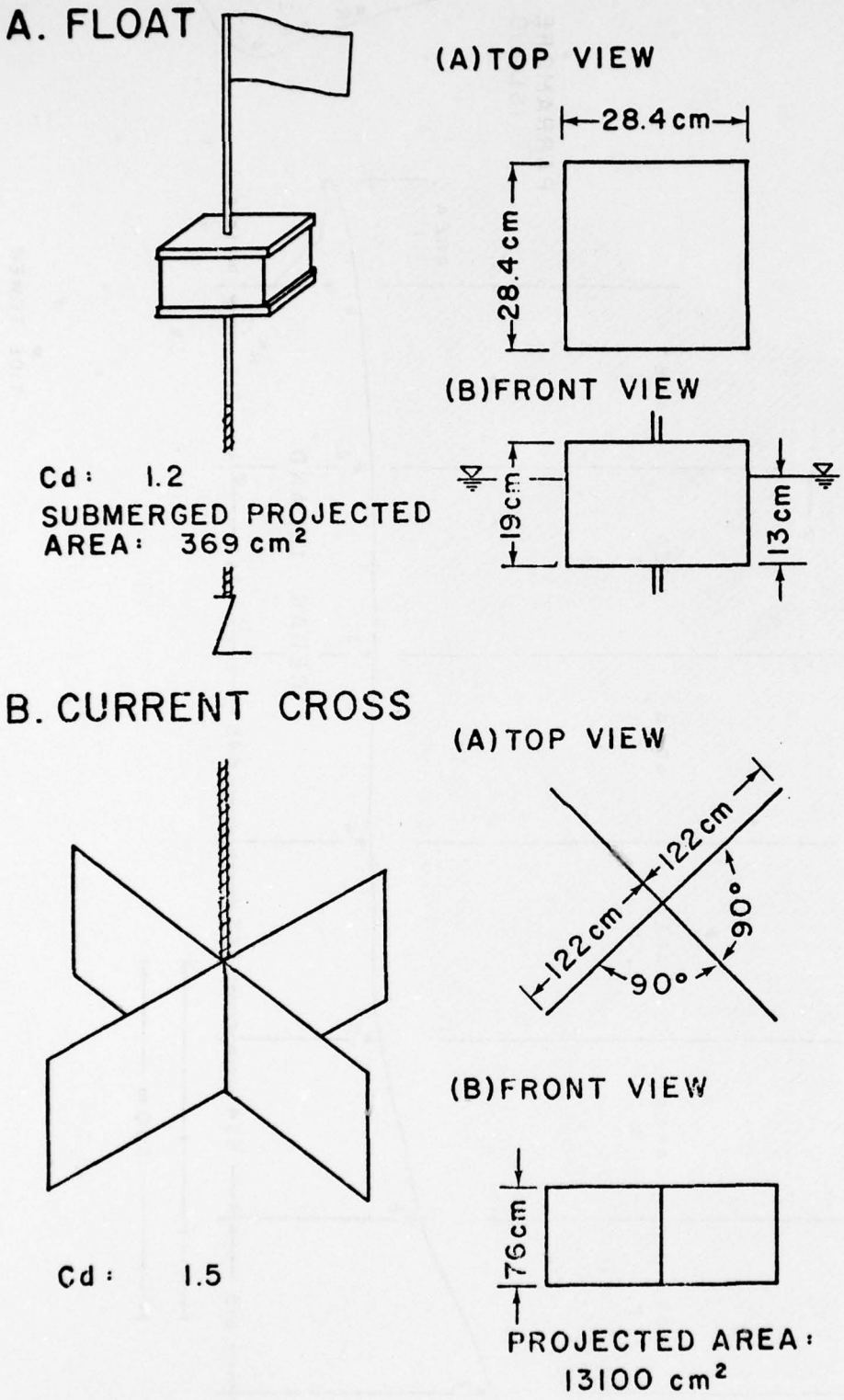

Figure 51. Drogue and surface float design.

of the tide, and at different positions in the study area. A total of 59 separate drogue tracks were run on eleven different days (six floods, five ebbs). The drogues were deployed at a depth below mid-water and above the bottom. This usually was two or three meters below water surface.

The observed drogue trajectories were corrected to remove the contribution that the surface float made to the motion of the system due to direct wind drag or wind induced motion of the surface layer. The correction technique is fully discussed in Appendix B. The drogue tracks and the descriptions of the field conditions during the observations are also presented in Appendix B. In order to organize the current data in a meaningful way the drogue velocity calculated from the segments of the trajectory were compared with the current speed in the inlet throat as recorded by the Savonius rotor current meter placed at a position of six tenths of the depth from the surface. Thus, the ratio of drogue current speed to the inlet current speed compensated for the tidal range variations. In addition, the use of the velocity ratio costs the analysis directly in terms of the phenomenon forcing the neashore currents.

Inspection of the corrected drogue trajectories (Figs. B3 thru B25 in Appendix B) shows that, during ebb flow conditions, the flow is directed away from the inlet and generally parallel to the beach, except close to areas 1 and 2 where the movement had a stronger seaward component. The data for the ebbing tidal phase in the inlet channel is shown in Figure 52. Only during the first two hours following the beginning of ebb currents in the inlet was there a noticeable influence of the inlet. After that time the currents along the southern end of Cedar Island were a small fraction, 0.1 to 0.2, of the inlet current. Moreover, the ratio is essentially constant along the length of the zone monitored.

Drogue tracks during flooding currents in the inlet ran parallel to the beach and entered the inlet. The summarization of the results shown in Figure 53 indicate the zone of influence of the inlet extends to area four, a distance of about 2,000 meters (about 3 times the inlet width) from the inlet channel. Furthermore, this zone of influence remained constant throughout the entire flood phase of the current in the inlet. The fact that the zone of influence remains constant suggests that the spatial accelerations are due to a topographically controlled flow convergence. To examine this aspect the coastwise perpendicular cross-sectional areas were computed from the mid-point of each subarea (Fig. 50) to the depth of 24 feet. The results are plotted in Figure 54 where the areas are expressed as a ratio of the individual area divided by the maximum area encountered

Figure 52. Mean velocity current ratio (corrected current velocity/velocity in inlet) vs. distance up Cedar Island (numbers refer to the mid-points between stations on Cedar Island approximately 630 meters apart), shown for six (I-VI) consecutive hours during ebb tide. Average velocity represented by ·, standard deviation by Δ.

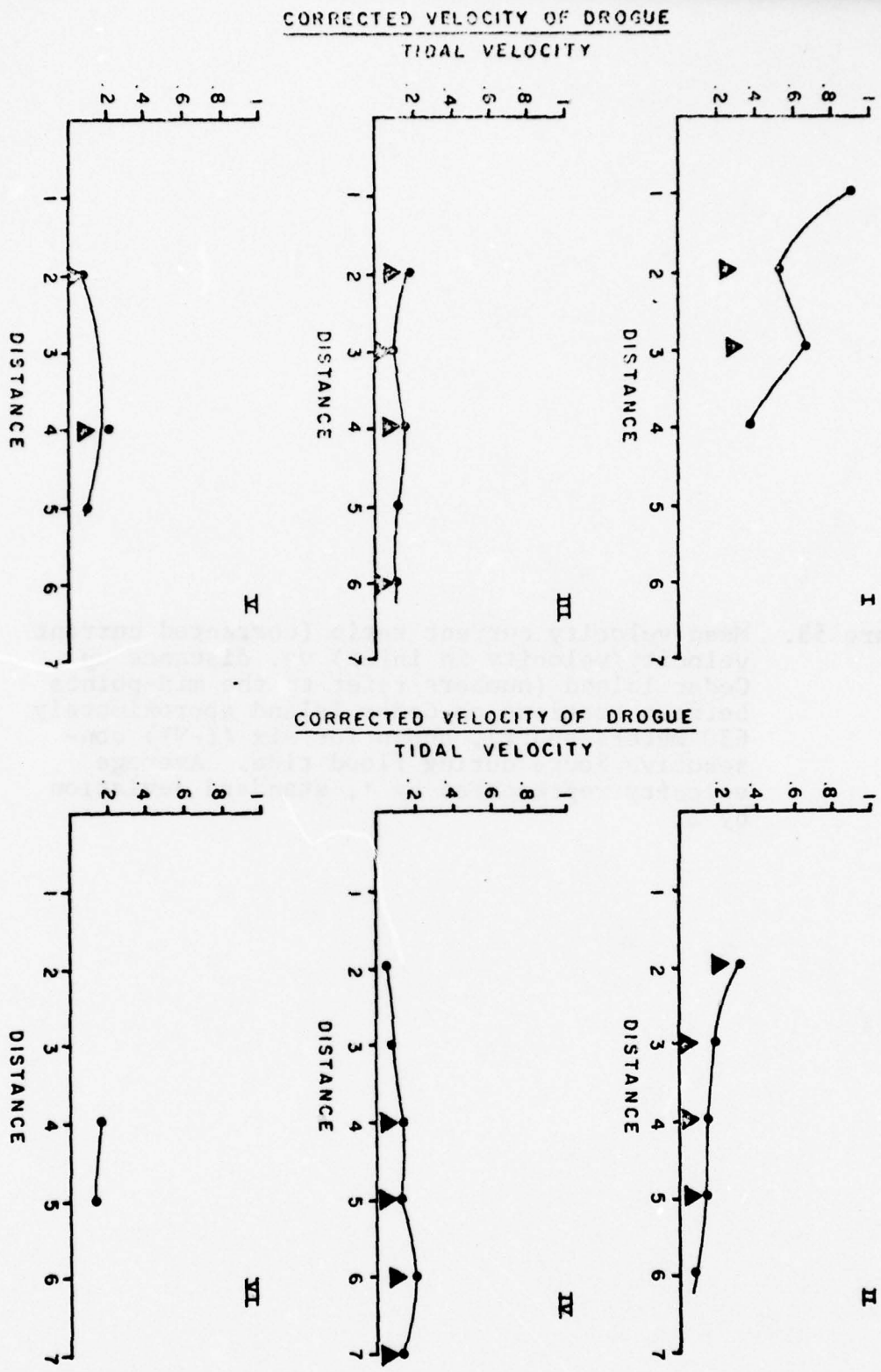
CORRECTED VELOCITY OF DROGUE
TIDAL VELOCITY
DISTANCE
I
II
III
IV
V
VI

Figure 53. Mean velocity current ratio (corrected current velocity/velocity in inlet) vs. distance up Cedar Island (numbers refer to the mid-points between stations on Cedar Island approximately 630 meters apart), shown for six (I-VI) consecutive hours during flood tide. Average velocity represented by •, standard deviation by Δ.

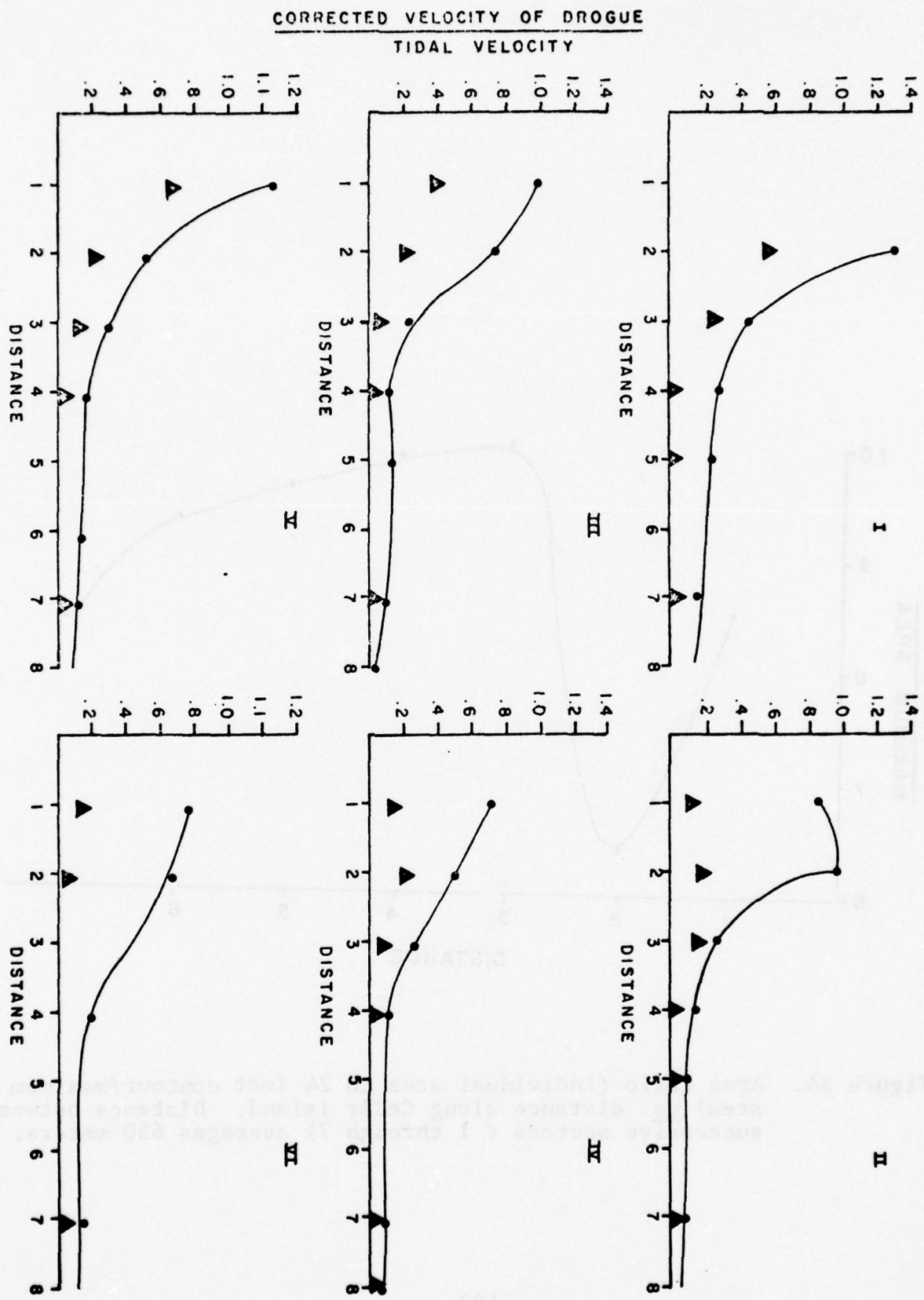
CORRECTED VELOCITY OF DROGUE
TIDAL VELOCITY
DISTANCE
I
II
III
IV
V
VI

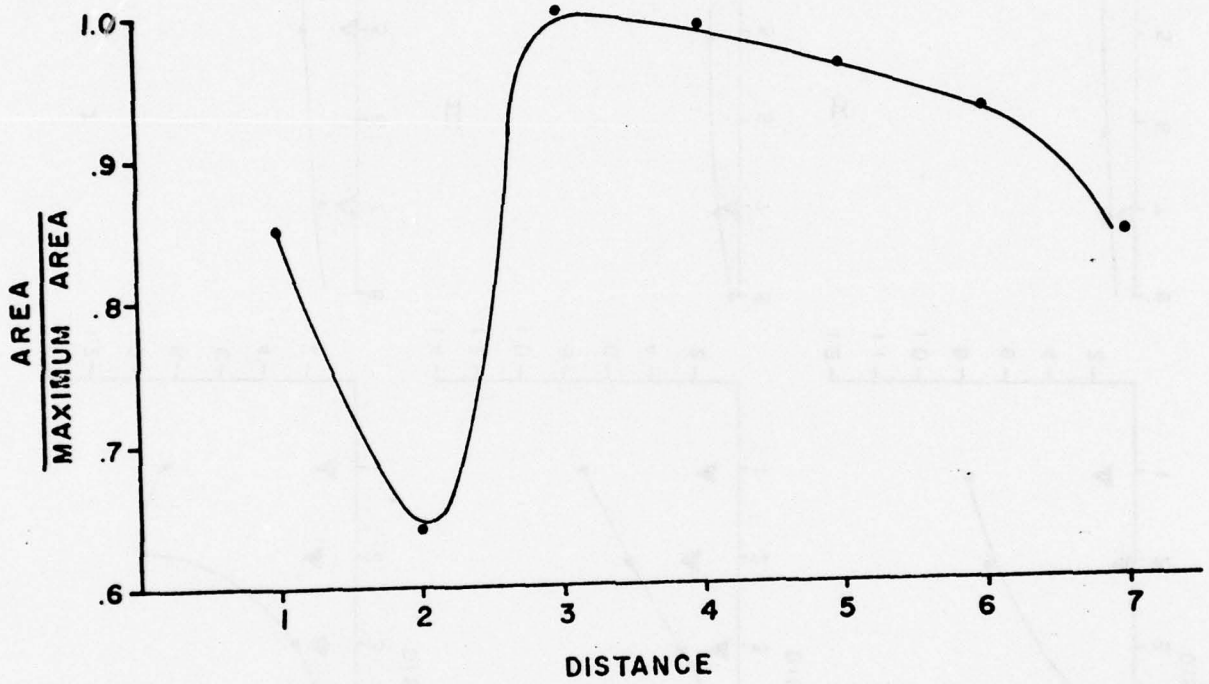

Figure 54. Area ratio (individual area to 24 foot contour/maximum area) vs. distance along Cedar Island. Distance between successive sectors (1 through 7) averages 630 meters.

(subarea 3) and plotted with respect to distance along Cedar Island. There is an abrupt decrease inflow south of the subarea 3 which corresponds with the zone of acceleration.

E. Response of the inlet channel cross-sectional area to short term variations in wave activity and tidal volumes and related matters

E1. Background discussion.

The early work of O'Brien (1931) and the more recent work by Jarrett (1976) indicate that a power function relationship exists between the cross-sectional area of the inlet channel and the tidal prism passing through the system. These relationships were generally derived from temporarily independent measurements of cross-sectional area, basin tidal range and bay area. The principal factor tending to reduce channel area is the introduction of sand from the adjacent longshore drift system. The tidal prism passing through the channel is determined by the storage characteristics of the embayment (area and slope), the ocean tide range and the impedance characteristics of the channel itself. The attainment of an equilibrium configuration may thus be considered (O'Brien, 1970) to represent a balance between the ratio of tidal power to scour the inlet and the wave power generating local longshore transport tending to close the channel. Since both of these factors vary through time it may be expected that an equilibrium area configuration will undergo modulations depending upon the relative strength of the wave and tidal power at a given time. Inasmuch as study of these short term modulations in an inlet channel had not been previously conducted such measurements were undertaken to learn more about the short-term response characteristics of an unmodified inlet channel.

E2. Methods.

In order to ascertain the changes in cross-sectional areas at different positions in the inlet channel range lines were established on the north shore of Parramore at intervals of about 200 meters (Fig. 46). Since the position of the inlet throat changed with time, three ranges (2, 22 and 22A) were established to accomodate the shifts in position. During operations the sounding boat progressed across the inlet on a range line while distances from the shore were recorded as horizontal angles, the base of which was a 400-meter baseline. The angle recorder would announce successive angles to the boat via voice actuated transcievers so that each "mark" could be annotated on the fathogram while progressing with the survey. The echo sounder, a Raytheon DE 719 Fathometer, was calibrated for each survey using a bar check, and all soundings were corrected to mean tide level. Repetitive surveys over the 10 range lines were conducted 46 times during the 13 month period of August, 1971 through September, 1972. Although the

goal was to obtain surveys on a weekly basis and following storms periodic equipment failure reduced the actual survey frequency. In addition there were times when severe wave conditions precluded completion of some of the seaward ranges. The precision of the survey technique was tested by running ten consecutive profiles within a one-hour time span at Range 22. The mean area was 4,596 m^2 with a standard deviation of 62 m^2.

Attempts to obtain local wave information using programmed time lapse photography on the uninhabited islands adjacent to inlet failed. Therefore, wave conditions were obtained from daily visual surf measurements (wave period and height) which were supplied by the Coastal Engineering Research Center, U.S. Army Corps of Engineers for a station on Assateague Island, some 45 km to the north.

In addition, some use was made of wave direction information taken by the U.S. Coast Guard at the Chesapeake Light station which is located southeast of the inlet some 35 km off the mouth of Chesapeake Bay.

E3. Cross-sectional area response.

Examination of Figure 46 shows that the inlet channel is straight and well defined with a shelf on the south side delineated by the 15 ft. contour. The shelf itself pinches out at the location of Range 7. In general, Range 1, just inside the inlet throat (Range 2, 22, 22A) has had the largest area and the smallest channel area is found at Ranges 7 and 8. As noted previously the sediment substrate on the south flank of the inlet is a rather firm cohesive material. The deeper parts of the bottom of the channel between Ranges 1 and 5 are a firm substrate with episodes of sand cover. The north flank of the channel is a sand wedge which has been deposited during the slow migration of the inlet channel to the south.

The results of the repetitive cross-sectional area measurements are shown in Figure 55 and in Table 16. Virtually all of the area modulations were the result of change in the volume of sand on the north side of the inlet channel. The 8 m contour on the steep south flank remained within $\pm$ 7 m of the mean position in 91% of the cases; these were not real shifts but instead represent the range of positioning errors on the steep slope. Variations of maximum depth at each range line was small; 83% of the maximum depths fell within $\pm$ 0.5 m of their means. Range 1 showed the greatest depth variation with a decrease of 2 m between mid-January and mid-February, 1972. The horizontal position of maximum depth for each range remained stable; for

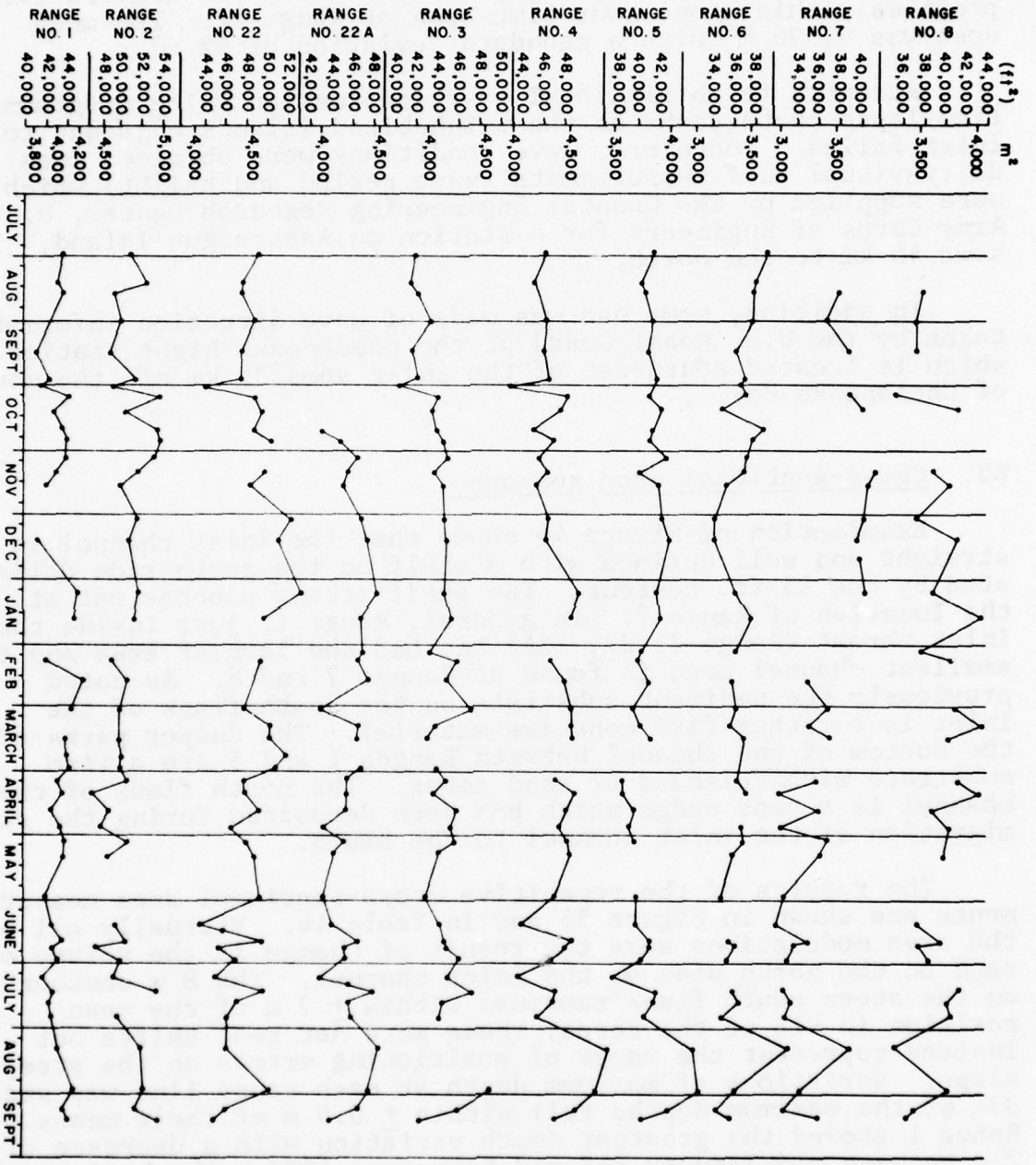

Figure 55. Cross-sectional area changes at Ranges 1 through 8, 1971-1972. Time ticks within months are 5th, 15th and 25th of month.

TABLE 16. CROSS-SECTIONAL AREAS AT RANGES (m^2)

Range	1	2	22	22A	3	4	5	6	7	8
Date										
7/30/71	4067	4755	4574	----	3903	4306	3866	3652	3618	----
8/13/71	4019	4887	4428	----	3864	4200	3760	3552	----	3570
8/18/71	4063	4609	4433	----	3932	4243	3972	3532	3546	3538
8/31/71	3954	4666	5433	----	4046	4306	3864	3533	3444	3493
9/15/71	3835	4578	4422	----	3872	4274	3820	3384	3636	3493
9/28/71	3944	4797	4421	----	3922	4339	3889	3465	----	----
10/1/71	3878	4592	4102	----	3767	3971	3620	3434	----	----
10/6/71	4121	5007	4531	----	4105	4484	3835	3469	3643	3299
10/13/71	3978	4707	4601	----	4055	4448	3934	3253	3753	3858
10/22/72	4058	4992	4534	4013	4092	4196	3857	3632	----	----
10/27/71	4103	5012	4683	4169	4153	4381	3828	3532	3660	----
11/4/71	4096	4955	----	4327	4191	4272	3984	3477	----	----
11/11/71	4001	4819	4641	4237	4077	4329	3741	3450	3861	3626
11/17/71	3927	4673	4511	4196	4145	4228	3914	3300	3802	3775
12/3/71	----	4813	4875	4361	4166	4331	3951	3198	3764	3487
12/13/71	3942	4744	4764	4410	4178	4311	4007	3190	3715	3850
1/7/72	4190	4822	4962	4503	4157	4610	3900	3568	3789	3636
1/19/72	4157	4791	4634	4355	4229	4540	3923	3518	----	4041
2/4/72	----	----	----	4373	4030	----	3772	3395	3453	3510
2/8/72	3923	4597	4607	4338	4277	4354	3736	----	----	3789
2/18/72	4238	4728	4535	4422	4183	4473	3833	3362	3299	----
3/2/72	4139	5661	4455	4006	4407	4536	3700	3392	3452	3838
3/10/72	----	----	4689	4336	4083	4549	3769	3352	3291	4071
3/16/72	4096	4740	4679	4322	4017	4553	3852	3469	3471	3766
3/24/72	4089	4668	4828	----	----	----	----	----	----	----
3/30/72	4113	4659	4738	4363	4102	----	----	----	----	----
4/5/72	4018	4721	4449	4235	4186	4409	3601	3403	3357	3862
4/11/72	4060	4405	4465	4072	4240	4576	3622	3482	3028	4041
4/19/72	3960	4569	4593	4233	4278	4497	3703	----	3373	3624
4/27/72	4041	4493	4333	4030	4232	4433	3661	3437	3045	3784
5/4/72	4076	4736	4500	4216	3259	4510	3715	3449	3454	----
5/10/72	4067	4560	4535	4123	4117	4526	3638	3359	3390	3719
5/30/72	3903	----	4584	4028	4001	4399	3725	3261	3072	----
6/12/72	3964	4616	4075	4104	4126	4108	3723	----	2991	3502
6/20/72	4063	4717	4623	4335	4167	4549	3851	3329	3285	3710
6/23/72	3968	4421	4223	4220	4191	4496	3852	3376	3161	3522
6/29/72	4016	4649	4360	4214	4296	4368	3770	3315	3094	3605
7/7/72	3893	4607	4188	3990	4192	4075	3518	----	----	----
7/14/72	3983	4995	4626	4473	4411	4428	3907	3356	3066	3875
7/19/72	3956	----	4394	4255	4157	4407	3886	3423	3136	3774
7/26/72	3973	4649	4301	4267	4125	4246	3805	3278	3093	3816
8/10/72	4123	4849	4294	4525	----	4875	4238	3871	3660	3317
8/30/72	4179	4885	4688	4438	4577	4771	4284	3391	3217	3773
9/8/72	4057	4700	4287	4338	4284	4591	4019	3230	3073	3482
9/13/72	4119	4891	4190	4089	3935	4404	3789	3361	3389	3401

all ranges and cases the position of maximum depth feel within ± 15 m of their means 83% of the time.

The results indicate that adjustments in inlet cross-section can take place very rapidly. A case of rapid response is illustrated by the surveys of 28 September, 1 October and 6 October, 1971. Between the first two dates Tropical Storm Ginger stagnated off the Virginia Coast during the waning of neap tides. The heavy northeast seas presumably resulted in large longshore sand transport and a consequent reduction in area throughout most of the channel. The throat (Range 22) was reduced in area by 7.2% between 28 September and 1 October. Then spring tides and residual storm surge resulted in very large tidal prisms which expanded the cross-sections beyond the pre-storm condition. The throat was expanded in area by 10.4% between 1 October and 6 October.

The largest average cross-sectional area change occurred at the throat and at Ranges 7 and 8 while the least response was evidenced at Range 1. The throat (22, 22A) and Range 7 and 8 also exhibited the highest percentage of large area changes ($>93\ m^2$). The coherence between ranges in the sense of the area changes (±) was generally high for large storms or large prisms. Examination of Figure 55 suggested that the ranges could be grouped in sets representing the throat (Ranges 2, 22, 22A), the seaward section just before the flair of the ebb tidal delta (Ranges 7, 8) and the center section (Ranges 3, 4, 5, 6). The averaged response for these sections is shown in Figure 56. During the period August, 1971 to mid-March 1972 there is very poor coherence between the throat and Ranges 7, 8; when the throat expanded the outer section generally closed. This was prior to the complete removal of the shoals flanking the channel on the north. After the reduction of the shoals there was generally high coherence between all three sections.

It is particularly interesting to note the behavior of Range 7 which exhibited a dramatic (17%) reduction in the area by February 1972 which persisted with modulations through September, 1972. This reduction occurred as a result of the formation of a lateral inflow induced delta deposit on the north which was time coincident with the diminuation of the large lateral shoal (Fig. 57). It is interesting to note that the other ranges did not reflect this dramatic reduction in area.

E4. Equilibrum cross-sectional area of Wachapreague Inlet channel.

The historical surveys of the inlet area (see Section III, A) indicate that the cross-sectional area of the inlet throat has

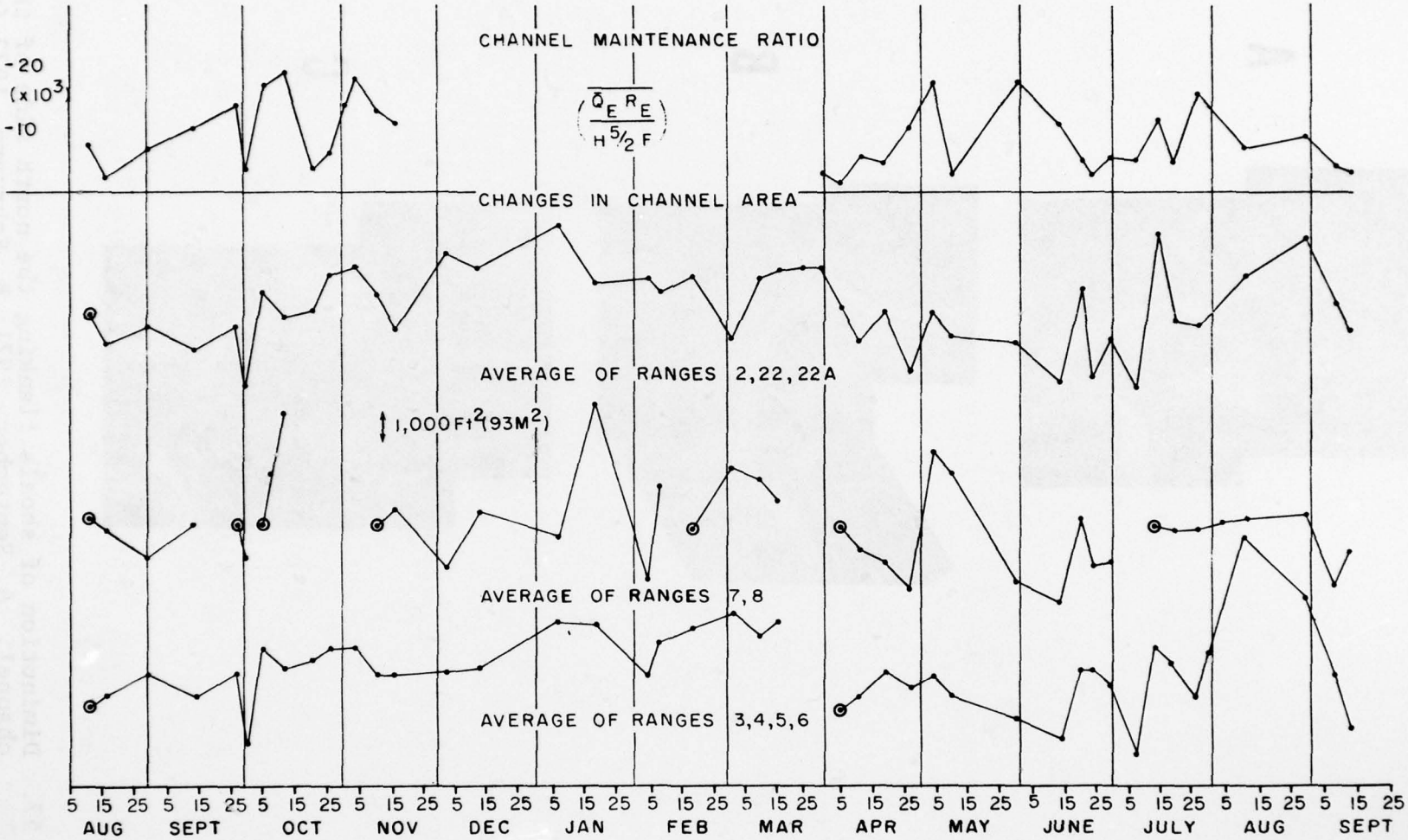

Figure 56. Comparison of channel maintenance ratio with changes in channel cross-sectional area. Circled points indicate starting position. Where gaps in data exist plots were restarted.

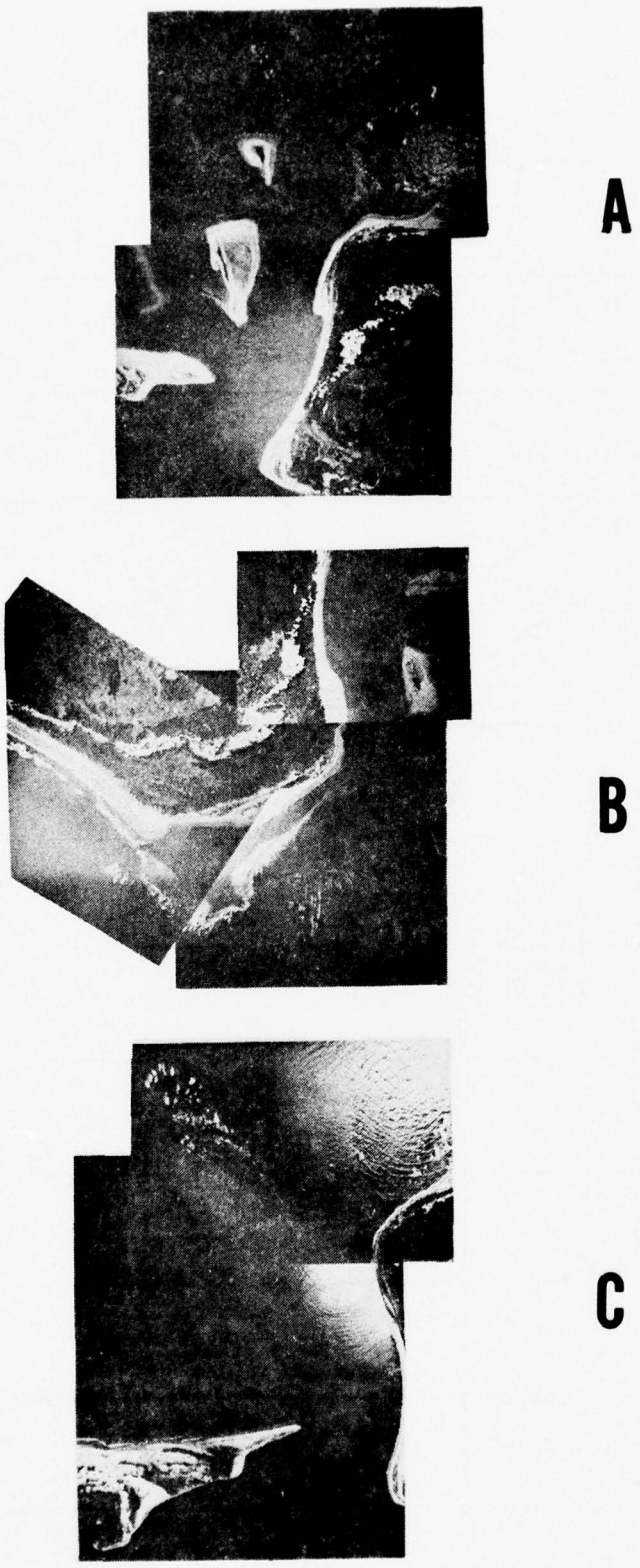

Figure 57. Diminution of shoals flanking the north side of the inlet channel. A, September, 1971; B, February, 1972 (photo inverted); C, September, 1972.

remained relatively stable since 1871 at about 4,200 m^2. Historical evidence further indicates that the interior marsh lagoon system configuration has changed very little since 1852, the data of the earliest reliable survey. The potential tidal prism of the system thus appears to have remained unchanged. It is of interest to ask whether the observed cross-sectional area of the inlet throat corresponds with that expected from the empirical relationship of O'Brien or the refinements by Jarrett (1976).

The average "throat" (transect 22A) area of the channel during the survey period was 45,850 ft^2 (4,260m^2). The spring tidal prism, deduced from the storage function is 3.245×10^9 ft^3 ($91.039 \times 10^6 m^3$). The results of the computations and the equations used are shown in Table 17. The comparisons indicate that the observed cross-sectional area is smaller than that expected from the empirical relationships. Although the observed ranges between 25% to 43% smaller than that expected the observed cross-sectional area falls within the 95% confidence limits of the relationships derived by Jarrett. Thus Wachapreague Inlet appears to follow the empirical relationship between tidal prism and throat cross-sectional area.

E5. Long term sediment transfer characteristics of the inlet.

The tidal characteristic of the system result in a duration difference between rising and falling tide phases such that the mean ebb discharge is expected to be somewhat greater than the flood. To qualitatively assess the potential significance of this the net transport tendency during the study was calculated. The sediment transport rate was assumed to be proportional to the cube of the mean discharge which was determined using the prism calculated from the storage function, Figure 44. The net sediment transport in the inlet channel for a given period is then given by:

$$\text{Net sediment transport} \quad \alpha \; \Sigma\left(\frac{P_F}{\Delta t_F}\right)^3 \Delta t_F - \Sigma\left(\frac{P_E}{\Delta t_E}\right)^3 \Delta t_E$$

where P_F and P_E are flood and ebb prism and Δt_F and Δt_E are flood and ebb durations. The cumulative transport for the year is shown in Figure 58 as is the average daily net transport within survey periods. Although there were periods of net inward transport the cumulative tendency over the long term is a net outward transport. This characteristic of the system offers an explanation for the absence of flood delta growth in recent times (120 years) and the maintenance of the highly developed ebb tidal delta system. This evidence and an examination of the morphology of the

Table 17. Observed and expected channel cross-sectional area.

Average area of Transect 2	51,152 ft² (4,752 m²)
Average area of Transect 22	48,536 ft² (4,509 m²)
Average area of Transect 22A, "Throat"	45,851 ft² (4,260 m²)

	Expected area	Observed area	$\frac{EXP-OBS}{EXP} \times 100$
For all U.S. inlets without jetties* $A = 1.04 \times 10^{-5} P^{1.03}$	64,492 ft² (5,992 m²)	45,851 ft²	28.9%
For Atlantic Coast inlets without jetties* $A = 5.37 \times 10^{-6} P^{1.07}$	79,935 ft² (7,426 m²)	45,851 ft²	42.6%
For all U.S. inlets with and without jetties* $A = 5.74 \times 10^{-5} P^{0.95}$	61,774 ft² (5,739 m²)	45,851 ft²	25.8%
All inlets without jetties (O'Brien, 1931) $A = 2.0 \times 10^{-5} P^{5}$	64,310 ft² (5,975 m²)	45,851 ft²	25.7%

*From Jarrett, 1976

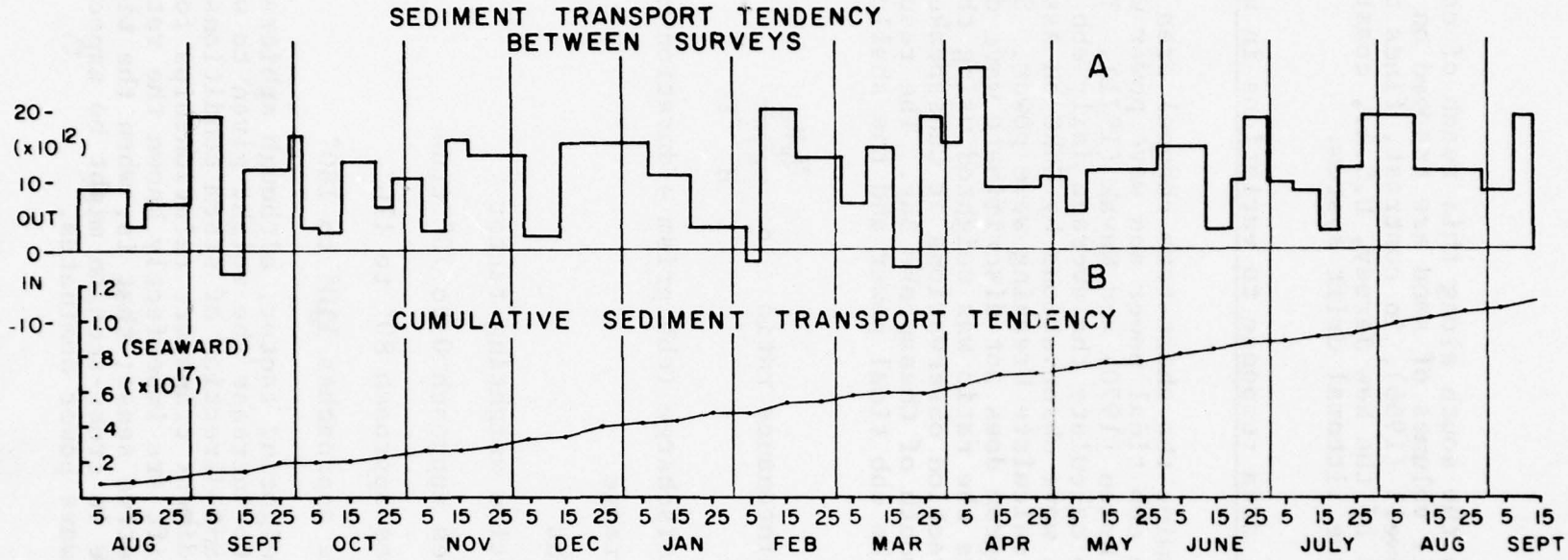

Figure 58. Net sediment transport tendency: A, average daily between survey dates of cross-sectional area. B, Cumulative tendency.

other deep inlets to the south along this reach of coast indicate that relatively small volumes of sand are trapped on the interior of the inlets. Caldwell (1966), in contrast, finds that the flood deltas of the inlets of the New Jersey, U.S.A., coast trap about 25% of the sand in the littoral drift system.

E6. Cross-sectional area response to variations in wave and tidal power.

In order to examine the short-term channel area response to these parameters the ebb tidal power and wave power were cast as a ratio following O'Brien (1970) and Nayak (1971). The storage function was used to calculate the average daily ebb tidal power and the daily visual wave observations by CERC on Assateague Island were used to calculate breaking wave power. Since the wave observation program does not discriminate wave direction for small wave angles the ratio was weighted using the U.S. Coast Guard wave direction observations at Chesapeake Light, some 35 km off the mouth of Chesapeake Bay. The resulting ratio is proportional to the ebb tidal power and the shallow water wave power.

$$\text{Channel maintenance ratio} \quad \alpha \quad \frac{\bar{Q}_E R_E}{H^{5/2} F}$$

where $\bar{Q}_E$ = mean ebb discharge (ebb prism ÷ duration of ebb)

R_E = ebb tide range

H = wave height

F = wave duration weighting factor

F = 3 waves approach 0 to 70° true

F = 2 waves approach 80° to 110°

F = 1 wave approaches 110° to 180°

The wave direction weighting factor, although arbitrary in its limit, was designed to increase the weight given to waves from the northeast, the dominant direction of storm conditions (Saville, 1954). Since the sediment transport relationships for the tidal flow and littoral drift are imperfectly known the ratio has meaning only in a qualitative sense; that is, when the tidal power dominates an increase in cross-section might be expected relative to those times when wave power dominates.

The comparison between the channel maintenance ratio, averaged over the sampling periods, and averaged channel response is shown in Figure 56. There is general qualitative agreement between the sense of area change in the throat section and the sense of the change in the maintenance ratio in 20 of 31 cases compared. The hiatus in the calculated values for the maintenance ratio between December through March is due to the absence of Assateague wave information. In those 19 cases where an area change greater than 93 m^2 occurred 14 agree with the sense of change in the ratio. However, it is of interest to note that the same ratio unweighted for wave direction agrees with the sense of area changes in 21 of the 31 cases and in 13 of the 19 cases where large ($>93\,m^2$) changes occurred. Thus essentially no improvements in the correlation resulted using the weighting scheme for wave direction Ww will return to this point.

It may be concluded that the ratio of ebb tidal power to wave power is a potentially useful parameter to characterize short-term inlet channel response. Since most of the dramatic area reduction occurred during wave activity from the northeast or east it is appealing to interpret the general correlation between the channel response and the maintenance ratio as indicating that channel closure is largely due to longshore drift from the north. However, there are several factors which indicate that the short-term modulations in cross-sectional area were due, to large degree, to a sand exchange between the channel and the ebb tidal delta complex. These elements of evidence are:

a.) The apparent insensitivity of the results to the direction of wave approach may be due to the pronounced wave refraction around the large ebb delta at this offset inlet (Hayes, et al., 1970; Goldsmith, et al., 1975). Examination of aerial photographs shows that during times when the nearshore wave direction is from the southeast the local refraction effects are strong enough to case the local wave approach on the north side of the inlet to be from the northeast. Thus the important aspect of the storm wave activity may simple be the agitation of the sand forming the lateral shoals and ebb delta such that entrainment by the flood tidal flows advects the material into the inlet. Particular cases during the survey period illustrate that southeast wave activity also can result in channel area reduction, particularly during low or moderate prisms and either an inward or low outward net sand transport conditions (14-19-26 July, 1972). In contrast, a case (26 July - 10 August 1972) with similar wave conditions and a somewhat larger prism but with a calculated strong net outward transport the channel widened dramatically

(ratio predicted decrease in area). Finally, it is noteworthy that Range 1 exhibited a depth decrease during mid-January to mid-February 1972, a time of sustained low net outward transport. These data suggest that the net sand transport characteristics during the given period also play a significant role in the modulation of channel area.

b.) Addition of the incremental sand volumes deposited and removed within the segment of the channel surveyed over the 13 month period total to a minimum of 2 X $10^6 m^3$. Considerations of what is known of longshore drift rates in the region preclude the conclusion that the sand deposited in the inlet is due solely to onput via longshore drift For example, the Corps of Engineers (1973) estimates that .46 X $10^6 m^3$/yr drifts to south along northern Assateague Island and that .3 X $10^6 m^3$/yr is trapped in the growth of Fishing Point at the southern terminus of Assateague. Consideration of the recession rates from 1852-1962 of the island chain between Wachapreague Inlet and Assateague Island indicate a sand volume loss of .33 X $10^6 m^3$/yr if the eroding marsh barrier islands are composed of 25% sand (probably an overestimate). Thus a reasonable estimate for maximum southerly drift to the inlet is .5 X $10^6 m^3$/yr. The results of computed wave refraction (Goldsmith, et al., 1975) and field observations indicate that wave refraction patterns allow only small volumes of northerly drift for waves from the southerly quadrants. Recognizing the considerable risk in comparing events over a one year period with averages based on decades, the estimate of drift versus the observed volumes deposited strongly suggests that a large fraction of the sand volume modulation in the inlet channel is due to adjustments between the channel and the ebb delta system.

c.) As previously mentioned (see III, A) approximately 1.5 X $10^6 m^3$ of sand was lost from the shoals flanking the north side of the channel in the course of the 13 month survey. Existing knowledge of the tidal flows near the inlet indicates that virtually all of this material must have been driven into the channel and subsequently flushed onto the ebb delta complex.

In summary it appears that the qualitative agreement between the channel response and the "maintenance ratio" reflects the

importance of wave activity on the ebb delta complex, regardless of wave directions, as well as generalized net southerly advection of sand along the coast on the littoral drift system.

III. SUMMARY DISCUSSION

The results of the present investigation, with the incorporation of the results of previous studies, permit a rather complete interpretation of the recent history of Wachapreague Inlet and a reasonable understanding of the contemporary response of the inlet resulting from the interaction of the basin tidal characteristics, the distribution of currents in and near the inlet, and the wave driven sediment transport. In addition, this study presents results which have applicability to the understanding of inlets in general, for example;

a.) Short term modulations in inlet channel area in response to fluctuations in tidal and wave power have been clearly documented.

b.) Evidence is presented which indicates that harmonics of the basin tide, due to either shallow water effects within the basin or to passage through the inlet entrance, can lead to asymmetries between the durations of rising and falling water stages (and to corresponding duration asymmetries in inlet currents). These duration differences can influence whether the inlet acts to bypass sand or to advect sand into the interior. In the case of Wachapreague Inlet the duration difference acts to inhibit advection into the inlet basin.

c.) Examination of the short term (days to months) fluctuations of sand input to the channel and flanking inlet morphology indicates that major transfers in sand volume occur between the morphological units in the inlet complex. Thus, modulations in the inlet channel area are not simply due to advection of sand from adjacent beaches.

d.) A method is presented which permits the approximation of the volume of water stored in the basin as a function of tide stage (storage function, App. A). The technique utilizes remote sensing by aircraft and it is particularly suited to basins with complex geometry and area-height relationships. Once the storage function is determined the tidal prism for any tide range can be calculated as can the mean discharge. In systems with small phase lags between water level extremes and slack water the storage function may be used to approximate the curves of instantaneous discharge in the inlet channel.

A. Summary of the History of Wachapreague Inlet

The work of other investigators suggests that the basin-inlet complex of the Wachapreague System formed in relation to a drainage formed on Pleistocene sediments (Fig. 4). With the recent transgression of the sea an extensive tidal flood delta system was formed by sand advected into the basin via an inlet, the ancestral Wachapreague Inlet. During and following the formation of the flood delta lagoon-tidal flat sedimentation progressed with ultimate formation of surficial marshes (starting about 1,500 yrs. B.P.) Radiocarbon dating of basal peat overlying the Pleistocene indicate that the lagoon had been in existence at least as long as 5,000 yrs. B.P.

The more recent history of the Wachapreague System was obtained by comparison of bathymetric surveys between 1852 and the present. The inlet channel has migrated to the south about 460 m (one inlet width) since 1852. During its slow migration a sand wedge has been deposited on the north flank of the inlet channel. The averaged annual sand deposition in the advancing wedge is about 73,000 m^3. The offset nature of the inlet has progressed since 1852 with the retreat of Cedar Island on the north and accretion to the northeastern face of Parramore Island situated on the southern side of the inlet. The accretion represents a storage of material on the south portion of the ebb delta. In the course of its migration the inlet has incised relatively firm cohesive lagoonal deposits which compose the southern side of the channel. At the deepest portions of the channel the exposed substrate sediments are very stiff clays and gravel horizons (Pleistocene?) which are abraded by the shells, gravels and sand shifting back and forth in the bedload driven by tidal currents.

Examination of the bathymetric surveys indicates that there has not been continuing storage of sand on the interior of the inlet, thus progressive growth of the flood delta system stopped sometime between about 1,500 yrs. B.P. and 1852. Moreover, comparison of the 1852 and 1962 planimetric maps indicates that the areal extent and configuration of the marsh lagoon system has changed very little during that period.

B. Summary of the Inlet Response to Tidal Hydraulics and Sediment Transport

The inlet admits the full semi-diurnal oceanic tide range so the full potential tidal prism of the basin is realized. As the tide elevation increases the feeder channels, tidal flats and extensive marshes are sequentially flooded. Analysis of tidal height records indicates that the durations of rising and falling

tide stages are unequal. The mean duration of rise is 0.45 hrs. longer than the duration of fall. The duration asymmetry is due to the generation of overtides. For a system with small phase lags such as Wachapreague the inlet currents may then also be expected to exhibit a duration asymmetry. This duration asymmetry was verified at Wachapreague Inlet wherein the ebb current duration is about 0.4 hrs. shorter than flood currents. Thus the average and peak ebb currents may be expected to be somewhat larger than those during flood currents. All other things being equal the ebb sediment transport might then be expected to be larger than that induced by flood currents. The tendency for a net seaward sand transport capacity is further augmented by a difference in flow channelization on the ebb versus flood currents. During the flood current phase approximately 10% of the incoming tidal prism passes over a shallow shelf on the south flank of the channel (see Fig. 47). However, during the ebb current phase only 4% of the outgoing prism passes over the shelf. This is due to flow channelization and, as a consequence, the ebb currents in the deeper part of the channel are enhanced. The combined influence of duration asymmetry and flow channelization lead to the inference that the inlet-basin hydraulics result in conditions which inhabit the advection of sand pass the throat into the interior parts of the system. The comparison of historical charts, as previously noted, indicates that there has not been additions to sand storage since 1852.

Given the totality of evidence presented in earlier chapters it is possible to formulate a qualitative model for sediment circulation within the inlet complex which is consistent with both the short-term channel response and the recent history of the inlet (Fig. 59). The system is driven by the combined influence of wave refraction, the regional tidal flow, and the flow distribution within the channel. The main element in the model is the inferred existence of a sediment flow loop on the north side of the inlet complex. The principal points of evidence to support the model are as follows:

1.) Wave refraction around the well developed ebb tidal delta tends to drive sand toward the inlet regardless of the direction of the incoming waves. Of particular importance is the fact that wave refraction effects tend to drive sand along the northern flank of the delta toward the inlet throat and along the exposed northern flank of the inlet channel through which appreciable lateral inflow occurs. Of course, during time of northeasterly wave approach the regional trend is for longshore transport of sand toward the inlet as well.

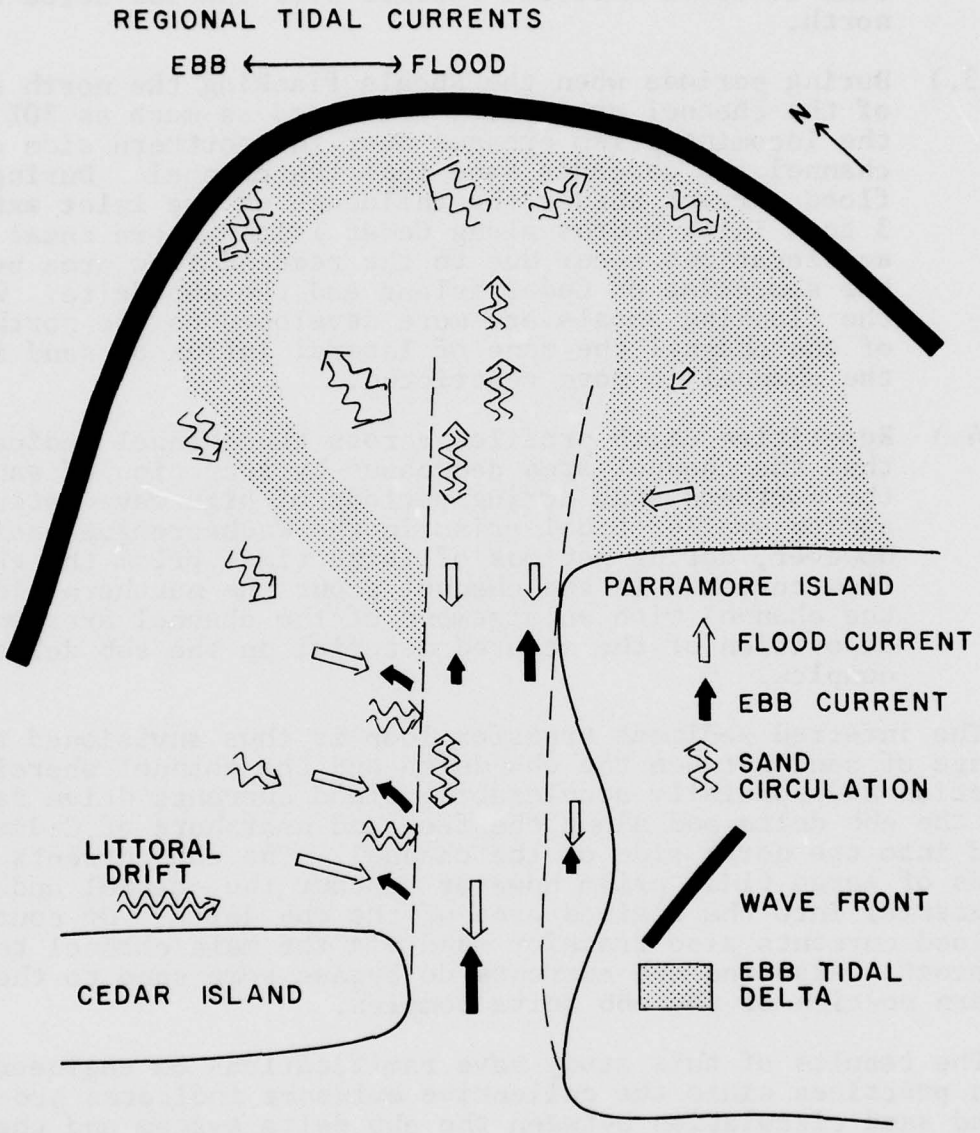

Figure 59. Model showing sand circulation loop between channel and ebb tidal delta and schematic of gross current flow characteristics within the channel.

2.) The regional tidal flow immediately offshore of the inlet is northerly during ebb flow in the channel which would tend to drive material carried over the ebb delta to the north.

3.) During periods when the shoals flanking the north side of the channel are poorly developed as much as 30% of the incoming prism crosses over the northern side of the channel and cascades sand into the channel. During flood current phases the influence of the inlet extends 3 to 4 inlet widths along Cedar Island where zonal accelerations occur due to the reduced flow area between the shoreline of Cedar Island and the ebb delta. When the flanking shoals are more developed on the north side of the channel the zone of lateral influx of sand into the channel is more restricted.

4.) Repetitive depth profiles across the channel indicate that the channel area decreases by accretion of sand on the northern side during periods of high wave intensity and/or smaller tidal prism in the Wachapreague basin. However, during periods of large tidal prism the ebb flow currents in the channel scour the northern side of the channel with enlargement of the channel area and deposition of the scoured material on the ebb delta complex.

The inferred sediment transfer loop is thus envisioned as an exchange of sand between the ebb delta and the channel wherein wave refraction and spatially accelerating flood currents drive sand along the ebb delta and along the face and nearshore of Cedar Island into the north side of the channel. The ebb currents during periods of large tidal prism however rescour the channel and drive the material into the flaired area of the ebb delta. Of course, the flood currents also transfer sand via the main channel toward the throat. Also the ebb currents do bypass some sand to the southern portion of the ebb delta complex.

The results of this study have ramifications on engineering design practices since the collective evidence indicates pronounced sand circulation between the ebb delta system and the channel. While these results should have general applicability to offset inlets they also probably apply to inlets in general. Thus, any engineering design should consider the local effects within the inlet complex as well as the littoral drift rates. For example, jetty-weir sand by-pass design considerations should include the question whether local sand circulation from the ebb delta will necessitate a larger impoundment basin or increased

dredging frequency. If such circulation does occur there may be a reduction in sand volumes on the ebb delta due to impoundment and mechanical by-passing.

This study and others investigating the Holocene evolution of the system indicate that during the Holocene transgression the open lagoon received a large volume of sand in the form of a well developed flood tidal delta. Subsequent deposition formed tidal flats and marshes. However, recent historical evidence and the examination of contemporary flow conditions indicates that the interior no longer receives significant sand input from the seaside. Thus, in the course of its evolution the inlet-lagoon system has changed from a condition where sand is advected into the basin to one where the tendency is to by-pass sand. This observation leads quite naturally to the question as to whether such an evolution is the normal sequence of events for inlet-lagoon systems. Clearly, if the system continued to advect sand to the interior the potential tidal prism would be reduced and the impedance of the inlet would be increased by the continuing deposition at the flood delta. These factors would reduce the stability of the inlet and perhaps lead to closure. It appears that a fruitful area for research would be the study of the evolution of inlet hydraulics for progressive stages of basin deposition.

REFERENCES

Boon, J.D., III, 1974, Sediment transport processes in a salt marsh drainage system, Unpublished Ph.D. dissertation, School of Marine Science, College of William and Mary, Williamsburg, Va.

Brown, E.I., 1928, Inlets on sandy coasts: Proc. Am. Soc. Civ. Eng., Vol. 54, No. 4, pp. 505-553.

Bruun, P., 1967, Tidal Inlets and Littoral Drift, University Book Co., Oslo, 220 pp.

Bruun, P. and Gerritsen, F., 1960, Stability of Tidal Inlets: North Holland Publ. Co., 130 pp.

Bruun, P., Gerritsen, F. and Bhakta, N.P., 1974, Evaluation of overall entrance stability of tidal entrances: Conf. Coas. Eng., 14th Proc., pp. 1566-1584.

Byrne, R.J. and Boon, J.D., III, 1973, An inexpensive fast response current speed indicator: Ches. Sci., Vol. 14, No. 3, pp. 217-219.

Caldwell, J.M., 1966, Coastal processes and beach erosion: Jour. Bus. Soc. Civ. Engr., Vol. 53, No. 2, pp. 142-157.

DeVries, D.A., 1970, Post-Miocene evolution of the barrier island-lagoon complex, southeastern Accomack County, Virginia: Unpublished manuscript.

Drake, C.L., 1969, Continental margins, In, The Earth's Crust and Upper Mantle, P.J. Hart, edition: Am. Geophysical Union, Washington, D.C., pp. 549-556.

Escoffier, F.F., 1940, The stability of tidal inlets: Shore and Beach, Vol. 8, No. 4, pp. 114-115.

Folk, R.L., and Ward, W.C., 1957, Brazo River bar: A study in the significance of grain size parameters: Jour. Sed. Pet., Vol. 27, pp. 394-416.

Goldsmith, V., Byrne, R.J., Sallenger, A.H., and Drucker, D.H., 1975, The influence of waves on the origin and development of the offset coastal inlets of the southern Delmarva Peninsula: In, Estuarine Research; Vol. II, Geology and Engineering (ed., L.E. Cronin), Academic Press, Inc., New York, pp. 183-201.

Goldsmith, V., Morris, W.D., Byrne, R.J., and Whitlock, C.H., 1974, Wave climate model of the mid-Atlantic shelf and shoreline: NASA SP-358 (also VIMS SRAMSOE No. 38), Nat. Aero and Space Adm., Washington, D.C., 145 pp.

Hack, J.T., 1957, Submerged river systems of Chesapeake Bay: Geol. Soc. Amer. Bull., Vol. 68, pp. 817-830.

Harrison, S., 1971, The sediments and sedimentary processes of the holocene tidal flat complex, Delmarva Peninsula, Virginia: Ph.D. Dissertation, The Johns Hopkins University, Baltimore, 167 pp.

Harrison, W.R., Malloy, R.J., Rusnak, G.A., and Terasmea, J., 1965, Late pleistocene uplift, Chesapeake Bay entrance: Jour. of Geol., Vol. 73, No. 2, pp. 201-229.

Hayes, M.O., Goldsmith, V., and Hobbs, C.H., 1970, Offset coastal inlets: Coas. Engr. Conf., 12th Proc., Vol. II, No. 75, pp. 1187-1200.

Ingram, C., 1975, Beach sands of the southern Delmarva peninsula, patterns and causes: M.S. Thesis, College of William and Mary, Williamsburg, Va., 89 pp.

Jarrett, J.T., 1976, Tidal prism-inlet area relationships: U.S. Army Engineers, Waterways Experiment Station, GITI Report 3, 55 p.

Kaye, C.A. and Barghoorn, E.S., 1964, Late quaternary sea level changes and crustal rise at Boston, Mass., with notes on autocompaction of peat: Geol. Soc. America Bull., Vol. 75, pp. 63-80.

Kemerer, T.F., 1972, Barrier island origin and migration near Wachapreague, Virginia: Master's Thesis, West Virginia University, Morgantown, 154 pp.

Keulegan, G.H., 1951, Third Progress Report on Tidal Flow in Entrances: Rept. No. 1146, National Bureau of Standards, Washington, D.C.

Keulegan, G.H., 1967, Tidal flow in entrances: Water level fluctuations of basins in communications with seas: U.S. Army, CE, Com. on Tidal Hyd., Tech. Bull. 14, Washington.

King, D.B., Jr., 1974, The dynamics of inlets and bags: Tech. Rept. No. 22, College of Engr., Univ. of Florida, Gainesville, 82 pp.

Kraft, J.C., 1971, Sedimentary facies patterns and geologic history of holocene marine transgression: Geol. Soc. America Bull., Vol. 82, pp. 2131-2158.

Leendertse, J.J., Alexander, R.C., and Liu, S.K., 1973, A three-dimensional model for estuaries and coastal seas; Vol. 1, Principals of computation: Rand Corp., Santa Monica, Ca., Rept. 1417--OWRR, 56 pp.

Lucke, J.B., 1934a, A Study of Barnegot Inlet: Shore and Beach, Vol 2, No. 2, pp. 45-94.

Lucke, J.B., 1934b, Tidal Inlets; A Theory of Evolution of Lagoon Deposits on Shoreline of Emergence: Jour. Geol., Vol. 42, pp. 561-584.

Monahan, E.C., Kaye, G.T. and Michelena, E.D., 1973, Drogue measurements of the circulation in Grand Traverse Bay, Lake Michigan: Dept. of Atmospheric and Oceanic Science, College of Engineering, Univ. of Mich. Tech. Report No. 35.

Morton, R.A. and Donaldson, A.C., 1973, Sediment distribution and evolution of tidal deltas along a tide dominated shoreline, Wachapreague, Va.: Sedimentary Geol., Vol. 10, pp. 285-299.

Murray, G.E., 1961, Geology of the Atlantic and Gulf coastal province of North America: New York, Harper and Bros., 692 pp.

Nayak, I.U., 1971, Tidal prism-area relationship in a model inlet: Tech. Rept. No. HEL-24-1, Univ. of Cal., Hyrdr. Engr. Lab., Berkeley, 72 pp.

Newman, W.S., and Munsart, 1967, Holocene geology of the Wachapreague Lagoon, Eastern Shore Peninsula, Virginia: Marine Geology, Vol. 6, pp. 81-105.

Newman, W S., and Rusnak, G.A., 1965, Holocene submergence of the Eastern Shore of Virginia: Science, Vol. 148, pp. 1461-1466.

O'Brien, M P., 1931, Estuary tidal prisms related to entrance areas: Jour. Civ. Engr., Vol. 1, No. 8, pp. 738-739.

O'Brien, M.P., 1969, Equilibrium flow areas of inlets on sandy coasts: Proc. Am. Soc. Civ. Eng., Jour. Waterways and Harbors Div., No. WWI, p. 43-52.

O'Brien, M.P. and Clark, R.R., 1973, Hydraulic constants of tidal entrances I: Data from tide tables, current tables and navigation charts: Tech. Rept. No. 21, College of Engr., Univ. of Florida, Gainesville, 59 pp.

O'Brien, M.P. and Dean, R.G., 1973, Hydraulics and Sedimentary Stability of coastal inlets: Conf. Coas. Engr., 13th Proc., pp. 761-780.

Oliveira, I.B. Mota, 1970, Natural flushing ability of tidal inlets: Conf. Coas. Engr., 12th Proc., p. 1827-1845.

Pattulo, J., Munk, W., Revelle R., and Strong, E., 1955, The seasonal oscillation in sea level: Jour. Mar. Res., Vol. 14, No. 1, pp. 88-156.

Saville T., Jr., 1954, North Atlantic coast wave statistics hindcast by Bretschneider-revised Sverdrup-Munk method: Beach Erosion Board, U.S. Army Corps of Engineers, Tech. Memo. 55.

Shepard, F.P., 1963, Thirty-five thousand years of sea levels: In, Essays in Marine Geology in Honor of K.O. Emery, U. Southern Col. Press, pp. 1-10.

Shureman, P., 1958, Manual of harmonic analysis and prediction of tides: U.S. Dept. Comm., Spec. Pub. No. 98, Washington, D.C., 315 pp.

Sinnott, A. and Tibbitts, G.C., 1961, Pleistocene terraces on the Eastern Shore Peninsula, Virginia: U.S. Geol. Survey, Prof. Paper No. 381, pp. D-248-D-250.

Sinnott, A. and Tibbitts, G.C., 1968, Groundwater resources of Accomack and Northampton Counties, Virginia: Mineral Resources Report No. 9, Div. Min. Res., Charlottesville, Virginia.

Taylor, P.T., Zietz, I. and Dennis, L.S., 1968. Geologic implications of aeromagnetic data for the eastern continental margin of U.S.: Geophysics, Vol. 33, No. 5, pp. 755-780.

Terhune, L.D.B., 1968, Free-floating current followers: Fisheries Research Board of Canada, Tech. Report No. 85.

Troskolanski, A.T., 1960, Hydrometry; Theory and Practice of Hydraulic Measurements, Pergoman Press, New York, 684 pp.

Woollard, G.P., 1958, Areas of tectonic activity in the United States as indicated by earthquake epicenters: Am. Geophys. Union Trans., Vol. 39, pp. 1135-1150.

APPENDIX A

DETERMINATION OF BASIN STORAGE VOLUMES VIA REMOTE SENSING

Approach. The central idea in the approach was to use the water surface itself as a contouring machine as the water surface rises over the variable topography during rising tide. This was achieved via sequential aerial photography using black and white infrared film to enhance the contrast between flooded and exposed surfaces. The following steps are involved:

1) Acquisition of sequential photography with overlap and sidelap suitable for mosaicing.

2) Observation of the changes in tidal elevation during the overflights.

3) Determination, from the sequential photography, of changes in flooded area as a function of tidal elevation.

4) Calculation of incremental water volumes stored in the basin as a function of tidal elevation. This is simply the product of incremental flooded area and the corresponding incremental change in tidal elevation.

Methods.

A. Mission Plan. The mission plan was to image the flooded surface of the study area at 30 minute intervals as the tide level rose from low to high water. During the overflights tidal elevations were monitored at eleven sites within the system and tidal discharge was measured at the two interior channels, The Swash and Teagles Ditch, which connect the Wachapreague marsh lagoon system with the adjacent systems serviced by the adjacent ocean inlets shown in Figure A1.

Mission W226, Flight 1, was accomplished on 28 June, 1973, utilizing the NASA-Wallops Station C54 aircraft equipped with two T-11 aerial mapping cameras using 152 mm lenses. The film was type 2425 Black and White infrared with a clear anti-vignetting and 89B filter combination. The flight was made in hazy weather with broken clouds. Visibility was from 5-7 miles. Nominal flight altitude was 9,500 ft. with a wind of 19 knots from 220°.

Twelve groups of three lines each were flown at approximately thirty minute intervals from 1300 to 1900 EDST. The orientation

of the lines made the photography generally suitable for mosaicing; however, four of the twelve groups could not be used due to one or more of a combination of excessive tip and tilt, crabbing or lack of sufficient overlap. The complete mission summary is available from NASA-Wallops Station, Chesapeake Bay Ecological Program Office.

The flight data was chosen so that the existing conditions represented a rising spring tide during daylight hours. A rising condition was specifically chosen so that the drained tidal flat faces would be as "dry" as possible.

B. Analysis of Data.

1.) Ground measurements. The positions of the tide elevation stations are shown in Figure A1 keyed to Table A1. Stations 5 and 6 are long-term recording tide gages for which tidal elevation data planes had been determined. The remainder were temporary tide staffs installed on the mission data. Inspection of Table A1 indicates a phase lag of up to 0.7 hr. and a range difference up to 0.4 ft. across the system. The most extreme comparison, that between Wachapreague Inlet and Wachapreague Dock, is shown in Figure A2 referred to long-term mean tide level which was assumed to be a level surface. Inspection indicates that a water slope of 0.5 to 0.6 ft. exists between the two positions during the central portion of the rising phase. This fact that the water surfaces slopes during the tide cycle necessitates the introduction of a correction factor since the tide gage at Wachapreague Dock will underestimate the volume of water in the system on the rising tide. Long-term comparisons between these two gages show an average range difference of 0.2 ft. and a phase lag of approximately 0.6 hr. for high and low water.

Discharge measurements at The Swash (#11 in Figure A1) and Teagles Ditch (#1 in Figure A1) indicated that tidal water enters the Wachapreague Inlet Basin system during the first part of rising tide and exits during the latter part. Measurements on 28 June 1973 give:

Swash	Teagles Ditch
Into system 69,000 m^3	Into system 400,000 m^3
Out of system 99,700 m^3	Out of system 548,000 m^3

This will be shown to be a negligible fraction of the total volume held in the system. Thus the effects of this "leakage" are ignored hereafter.

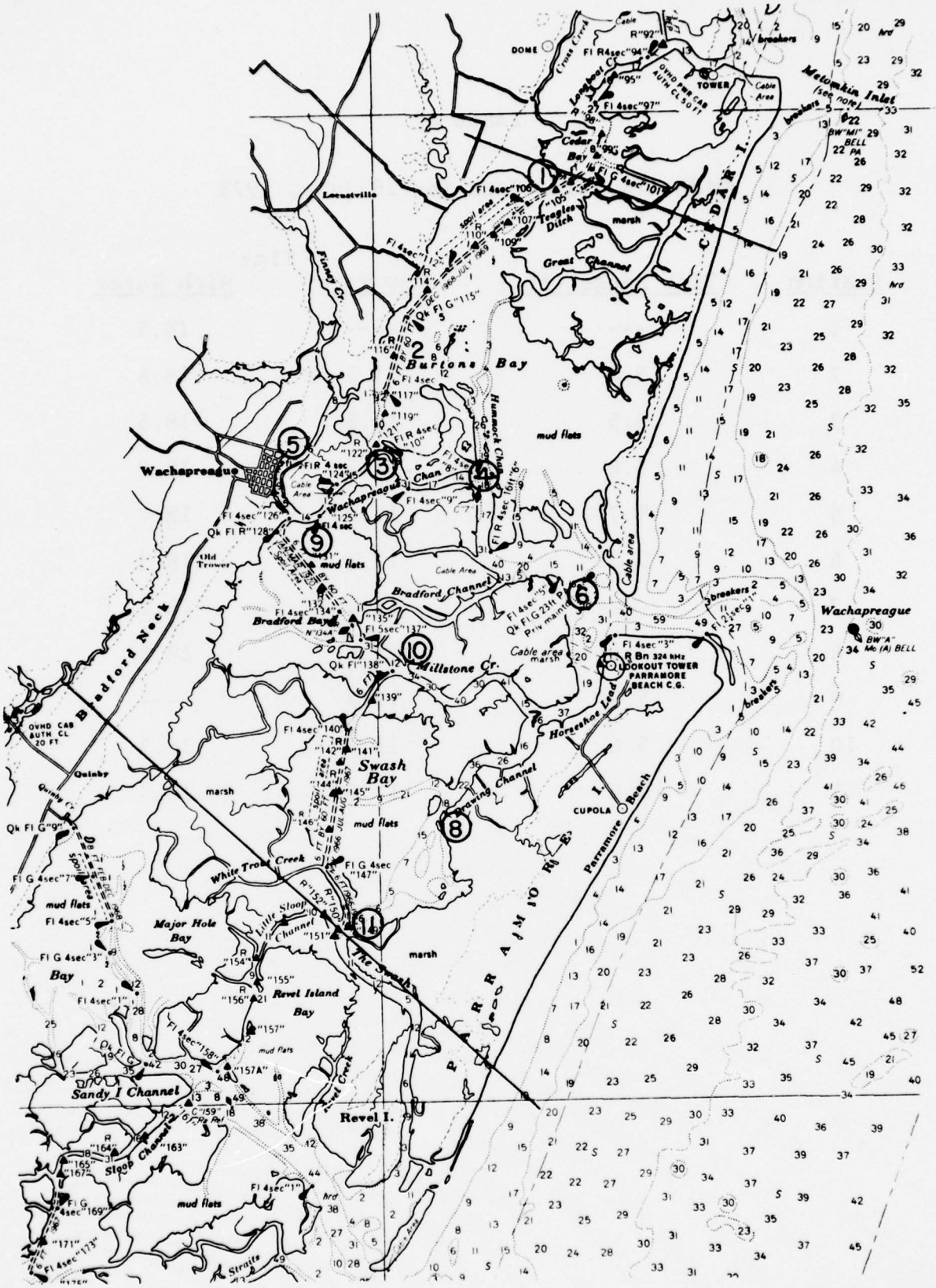

Figure A1. Location of tide staffs during overflights. Stations 1 and 6 are recording gages. Station 1 is Teagles Ditch and Station 11 is The Swash.

TABLE A1

Tide Elevation Data for 28 June, 1973

Station	Tide Range (ft.)	Time	
		Low Water	High Water
1	----	----	18.5
2	5.4	11.8 hr	18.4
3	5.5	11.8	18.5
4	5.4	11.3	18.2
5	5.7	12.0	18.7
6	5.3	11.3	18.3
7	----	11.4	18.2
8	5.6	11.6	18.5
9	5.7	11.7	----
10	5.6	11.0	18.3
11	5.6	12.0	18.5

2.) Imagery Analysis. Reproductions of the original transparencies were used in the analysis. Eight of the twelve flight groups were assembled into mosaics of the 28.9 square nautical mile ($86.65 \times 10^6 m^2$). The total area of each mosaic was determined using a polar planimeter.

The major absolute errors in the mosaicing procedure occur in aligning some sixteen frames having various edge distortions and in determining and cutting conjugate boundaries properly. These errors are indeterminate and are presumed random.

Determinations of the non-water covered areas in each mosaic were determined using the I^2S Digicol located at NASA-Langley Research Center, Hampton, Virginia. Water areas were determined by subtraction from total area. The instrument was adjusted so that exposed surface area could be coded as one color while the water covered surfaces and the masked areas registered an off-scale black. Absolute area calibrations were accomplished using masks of known area and plotting this with indicated percentage area. All mosaics were analyzed on the same day, a considerable savings in time over hand planimetry.

In order to specify film density boundaries associated with water boundaries, the water boundaries were visually identified with a sharp tipped pointer and the instrument settings were then adjusted to shift the boundaries to the proper position. This procedure was clear cut for tide levels below the marsh surface. At higher levels, marsh plants significantly decreased boundary contrast but sun glint assisted in boundary interpretation. For several runs analyzed more than once on different days total water areas varied as much as 5 percent which revealed a day to day bias in interpretation. These problems would likely be reduced if initial film exposure could be adjusted to give high contrast for very shallow depths. The exposures during the mission were, by error, adjusted to give maximum definition of water color differences and not maximum contrast between flooded and non-flooded surface. Contrast was heightened in reproduction of the transparencies. An example of the imagery is shown in Figure A2 for a conjugate area for low and high tide elevations.

Results: Analysis for flooded area and storage volume.

The times of the flight groups used in the analysis, relative to tidal stage are shown in Figure A3. Using this information and the water area determined from the sequential mosaics the relationship between flooded area and stage at the Wachapreague Town gage was constructed as shown in Figure A4. Observed area changes extended over the range in stage from 1.8 ft. to 7.2 ft.

Figure A2. Example of Black and White IR imagery for conjugate areas at high and low tide.

Figure A3. Tidal elevation curves at Wachapreague Inlet (Station 6) and Town of Wachapreague (Station 5) during overflight. Also shown is time of overflights (NASA Mission W226).

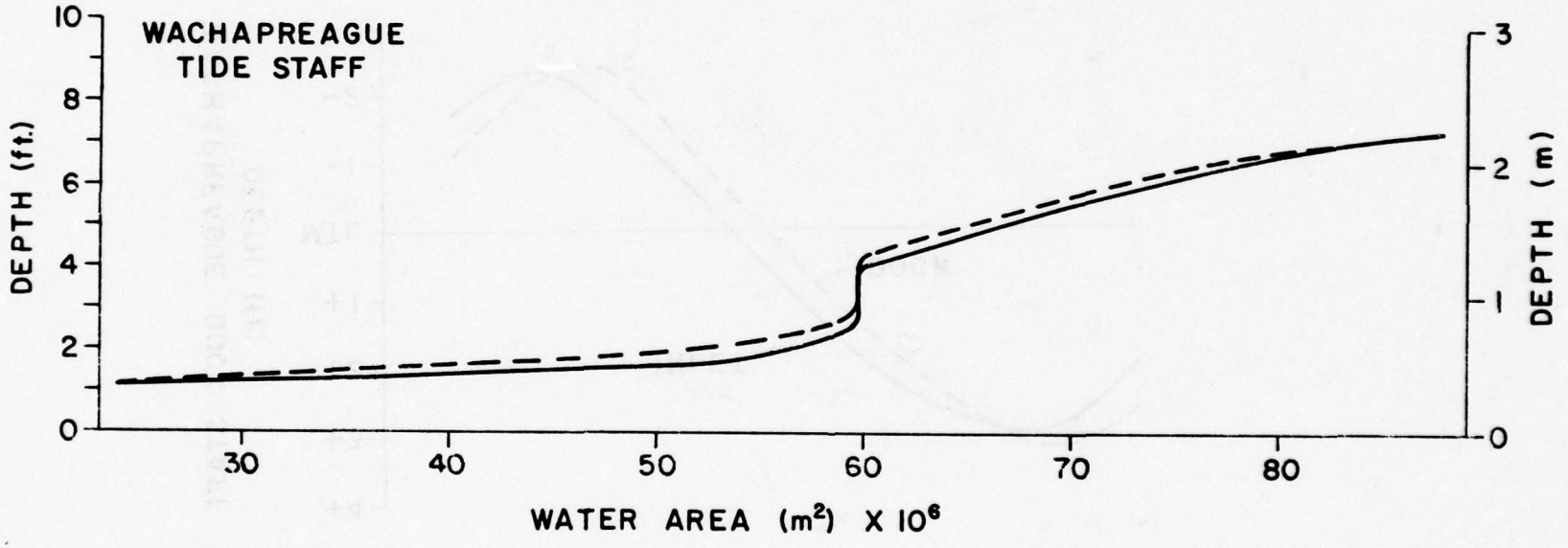

Figure A4. Area of flooded surface as a function of tidal stage at Wachapreague Dock. Solid line is raw data, dashed line is rectified to account for water slope.

at the Town gage. Since the water surface slopes up to as much as 0.6 ft. between the Wachapreague Dock and Inlet gages the flooded area measured is not the same as would be indicated if the surface was level across the area.

In order to make a first order correction it was assumed that at any particular tide stage the surface area flooded is equal to that at the stage $\frac{1}{2}\Delta Z$ (Fig. A3) lower. This shifts the curve to lower flooded area for a particular stage (dotted line, Figure A4). The segment of the curve between stages 2.5 and 4.3 indicates constant flooded area. This represents the near vertical banks of much of the major embayment and that area, 59.5 x $10^6 m^2$, represents the cut-off between areas of channels, flats, and bays and areas of marshes. This and other ancillary information are useful in extending the curve of flooded area versus stage to stages lower than the 1.8 ft. observed. Visual observations and measurements on the ground indicated about 0.5 ft. water depth in the bays at 1130 hrs. on the 28th of June. Thus, the cut-off for initiation of flooding in the bays was taken at 1.3 ft. on the Town gage. The first attempt utilized an estimated storage function based upon the areas of channels, marshes and bays and the artificial assumption that the bottom elevations of the bays and the marshes were uniform. The measured areas were:

Channel (major only)	8.087 x $10^6 m^2$
Bays	34.8 x $10^6 m^2$
Marsh (including drainage channels)	49.304 x $10^6 m^2$

The cut-off elevations were taken as 2.5 ft. and 5.5 ft., respectively for bays and marshes. The curve in Figure A4 indicates that the total channel area, including the drainage channel in the marshes and the bays totals to 59.5 x $10^6 m^2$. It is reasonable to assume that the area of bays is correct at 34.8 x $10^6 m^2$. Thus, the total channel area must be about 24 x $10^6 m^2$. This allows a statement of the component areas within the imaged area as:

Channels	24.0 x $10^6 m^2$
Bays	34.8 x $10^6 m^2$
Marsh	37.6 x $10^6 m^2$

Given the above, the curve in Figure A4 may be extended to the channel cut-off; 24 x $10^6 m^2$ at 1.3 ft. on the Town gage.

The cumulative volume of water stored in the marsh-bay-channel system was computed from the dotted curve in Figure A4

using incremental volume for every 0.5 ft. stage increase at the Town gage. The volumes are referred to 0 elevation of that gage which insures inclusion of all observed tides. The assumption was made in the calculations that the flooding for each incremental increase in stage occurred over a uniformly sloping bottom. The results are shown in Figure A5 as is the originally estimated storage using channel, bays and marshes as components with discreet cut-off elevations as previously discussed. The curve has been extended from 7.2 ft. to 10 ft. stage since visual observation indicated the entire system was flooded at stages beyond 7.2 ft. The shift to the left of the storage curve based on the imagery relative to that originally estimated is due to adoption of the 1.3 ft. stage as the cut-off between channel flooding and the initiation of bay flooding.

The storage relationships shown in Figure A5 are compared with tidal volumes measured at Wachapreague Inlet in Table A2. The observed values were determined by integration of instantaneous tidal discharge measured by current meter arrays at the inlet throat. Although accuracy of the directly measured prisms is not known, the measurements represent the best available estimates. Comparison of cycles 3 and 7 in Table A2 indicates an inconsistency in the values measured by integration of discharge; both cycles had the same maximum stage but the minimum stage of cycle 3 was 0.15 m less than cycle 7. In actuality cycle 3 must have had a larger prism than cycle 7 but the measurements indicate the converse. A similar inconsistency exists between cycles 5 and 6 although to a lesser degree. The data for measured prisms indicated the accuracy is no better than ± 10%.

Inspection of the percent differences between measured prisms and those deduced from the infrared imagery and the original estimated storage indicates that those calculated from the storage curve via imagery are in appreciably better agreement with the measured prisms. The average absolute differences are 9.7% (infrared imagery) and 14.3% (original estimate). It is also of interest to investigate how closely the time history of instantaneous discharge at the inlet may be approximated by application of the storage curves as referenced to the tide gage at the Town of Wachapreague. To test this question the field monitor of discharge on 13 and 14 September 1972 (cycles 4 through 7 in Table A2) were used. Using tidal elevations at the Town gage at a Δt of 30 mins, the incremental water volumes were then calculated from the storage curves and then converted to average discharge for that time increment. The results are shown in Figures A6 and A7. The originally estimated storage failed to approximate the measured instantaneous discharge when the marshes started to flood. This was due to the assumption of constant marsh elevation. Clearly the storage based upon

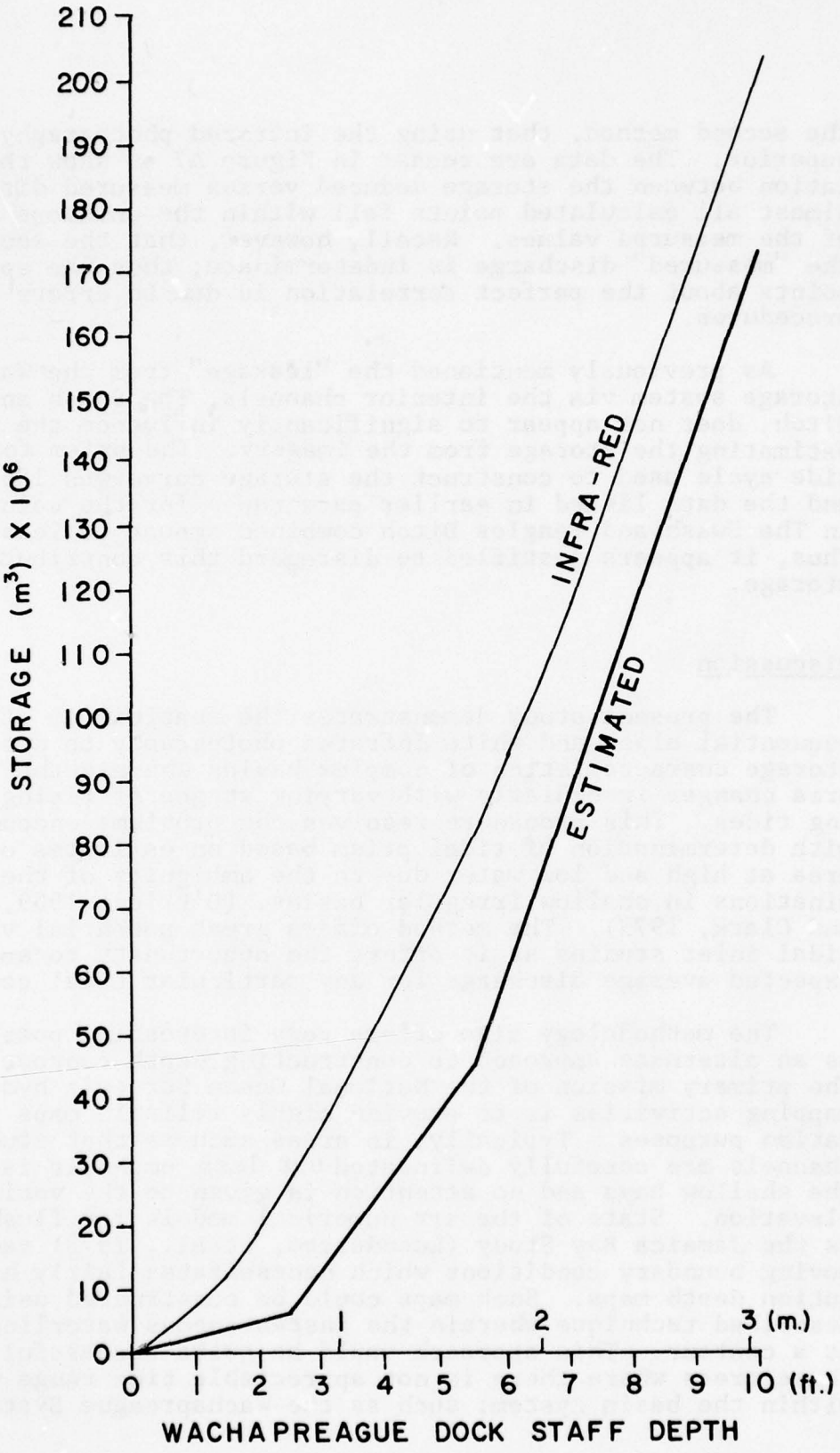

Figure A5. Storage function for Wachapreague Inlet basin as determined by infra-red imagery and as originally determined by estimates from topographic maps.

the second method, that using the infrared photography is far superior. The data are recast in Figure A7 to show the correlation between the storage deduced versus measured discharge. Almost all calculated points fall within the envelope of ± 20% of the measured values. Recall, however, that the accuracy of the "measured" discharge is indeterminate; thus the spread of points about the perfect correlation is due to errors in both procedures.

As previously mentioned the "leakage" from the Wachapreague storage system via the interior channels, The Swash and Teagles Ditch, does not appear to significantly influence the error in estimating the storage from the imagery. The prism for the tide cycle used to construct the storage curve was $106.5 \times 10^6 m^3$ and the data listed in earlier paragraphs for the volume passage in The Swash and Teagles Ditch combined amount to less than 1%. Thus, it appears justified to disregard this contribution of the storage.

Discussion

The present study demonstrates the feasibility of utilizing sequential black and white infrared photography to determine the storage characteristics of complex basins wherein the flooded area changes irregularly with varying stages of rising and falling tides. This procedure resolves the problems encountered with determination of tidal prism based on estimates of basin area at high and low water due to the ambiguity of these determinations in shallow irregular basins, (O'Brien, 1969, O'Brien and Clark, 1973). The method offers great potential value in tidal inlet studies as it offers the opportunity to specify the expected average discharge for any particular tidal condition.

The methodology also offers very interesting possibilities as an alternate approach to constructing depth contour maps. The primary mission of the National Ocean Survey's hydrographic mapping activities is to provide highly reliable maps for navigation purposes. Typically, in areas such as that studied channels are carefully delineated but less emphasis is given to the shallow bays and no attention is given to the variable marsh elevation. State of the art numerical models for flushing such as the Jamaica Bay Study (Leendertse, et al., 1973) require moving boundary conditions which necessitates fairly high resolution depth maps. Such maps could be constructed using the described technique wherein the instantaneous waterline acts as a contour. This approach would be quite successful in those areas where there is not appreciable tide range variation within the basin system; such as the Wachapreague System.

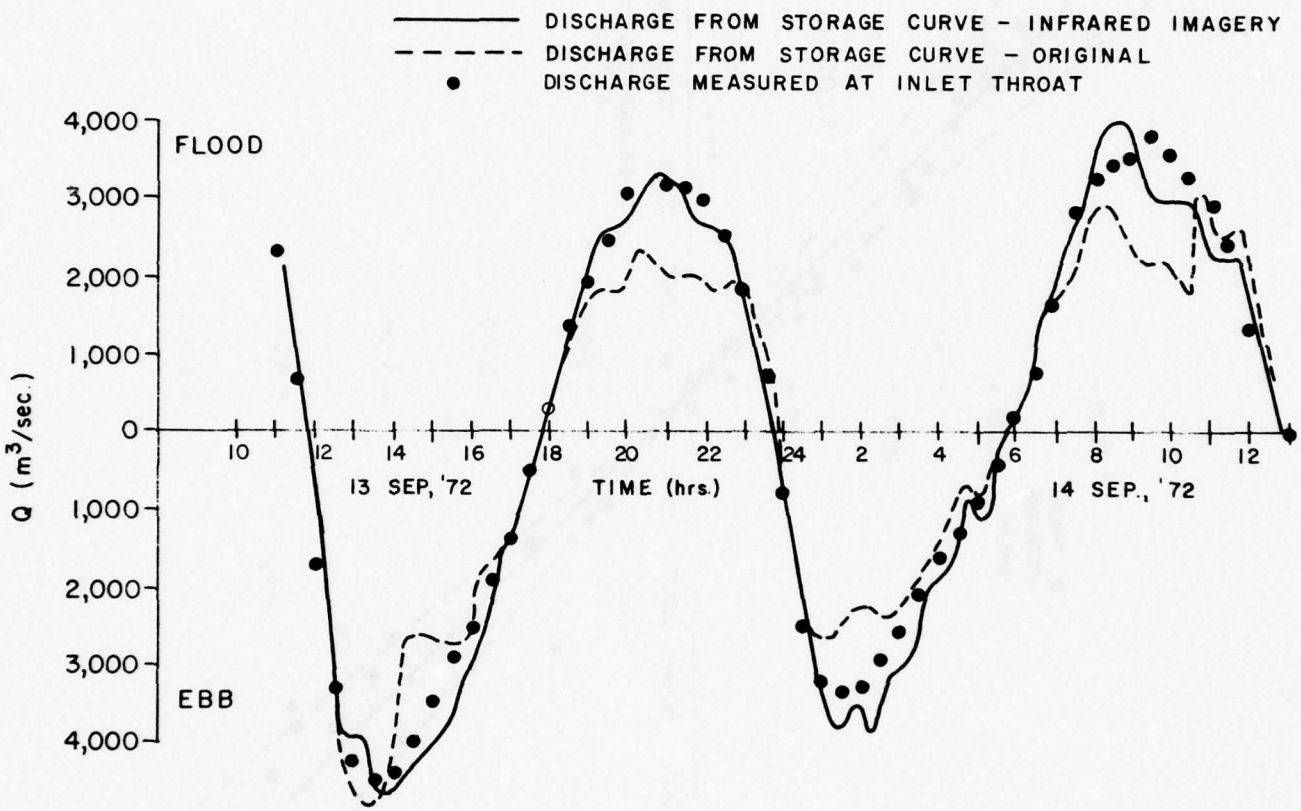

Figure A6. Comparison of measured discharge at the inlet throat with that calculated from the derived storage functions (Figure A5).

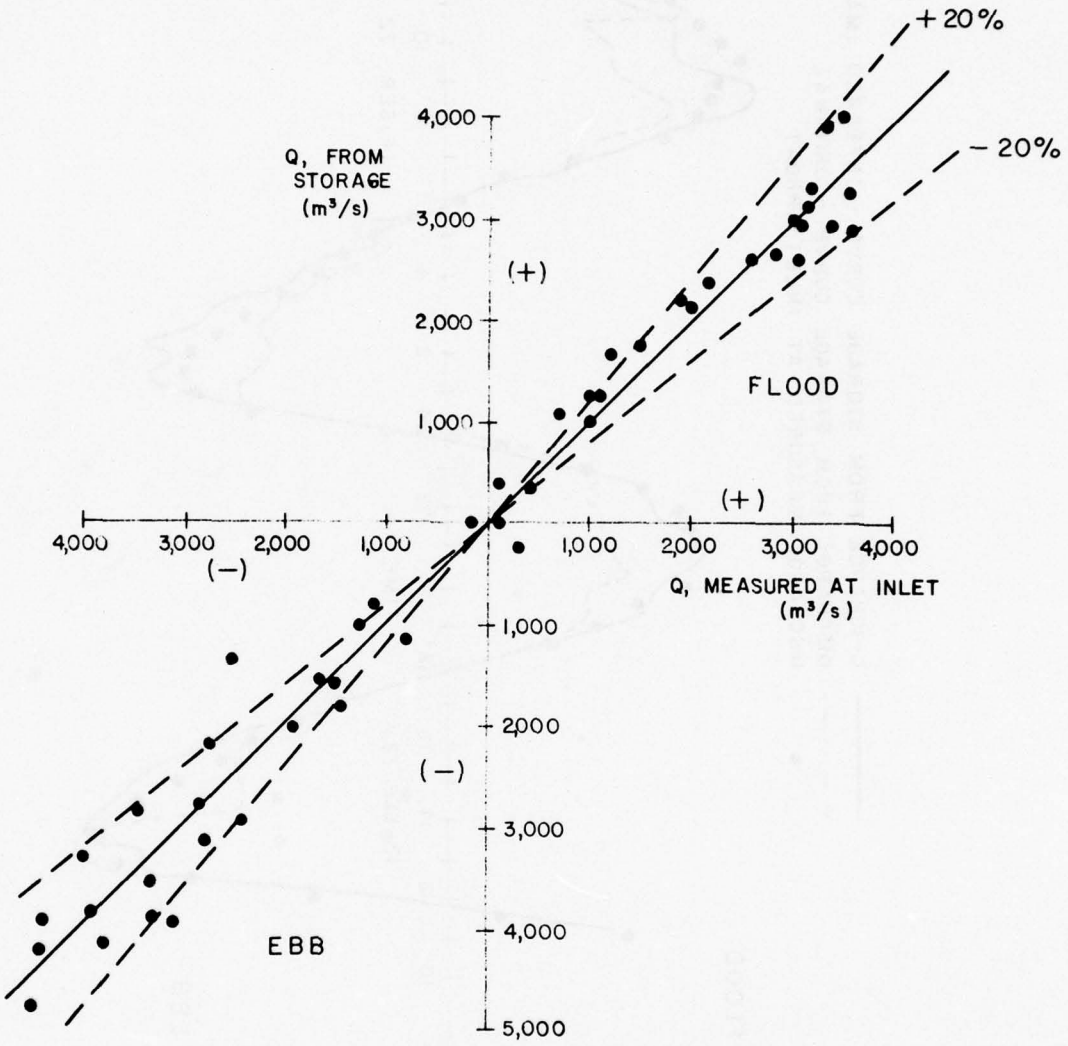

Figure A7. Correlation between instantaneous measured discharge and that calculated from the storage function derived from using sequential infrared imagery.

Finally, it should be noted that the technique offers a possible method to study tidal range variations in those basins with large range and phase differences within the system. Existing methods involve the installation of a large number of tide gages and a data base over a period of one month or longer. The tidal datum plane is then established and mean range and phase differences determined. In those areas where such detailed surveys cannot be conducted the method discussed herein would supply very useful data. It is also likely that application of the method would be useful in planning tide gage locations for a detailed survey. In such applications the stage variations as a function of time would be measured using stereo photogrammetric techniques.

APPENDIX B

METHOD FOR DROGUE TRAJECTORY CORRECTION AND DATA ANALYSIS

Drogue Trajectory Calculation.

Drogue design and technology date back to the voyage of the Challenger (1885) where drogues were used, then as now, in the study of currents at the selected drogue depth. More recently, thought has been given to errors inherent in the commonly used drogue float system. Terhune (1968) pointed out the importance of maximizing the area of the drogue with respect to the float in order to minimize the drag effect the float has on the drogue. The surface effect of the float becomes a greater problem as the shear stress between the surface float and the drogue increases. This can happen when high winds cause the depth of the effected surface layer to increase. Terhune applied the equation of fluid drag $F = \frac{1}{2}C_d A \rho V^2$ (where F is the drag force, C_d the drag coefficient, A the cross sectional area, ρ mass density of fluid, and V the velocity) to compute the worst possible effect of the float on the drogue. This technique could be utilized to estimate the magnitude of the probable error if the shear stress in the system were known.

Monahan, et al. (1973) proceeded one step further by actually subtracting the error caused by the shear of the float from the drogue. Assuming steady state conditions, this treatment corrects for the effect of the float and gives a more accurate picture of the current velocities along the original drogue track.

Like Terhune, Monahan's treatment begins with the equation of fluid drag; the actual drag forces on Monahan's drogue float system were measured during tow tank experiments so computation of the drag force was not necessary. The drag coefficient became apparent once the drag force was measured experimentally and the velocity noted. A log-log plot of the drag force and velocity measurements for the drogue float system is shown in Figure B1. Using this relationship the error in the current measurement could be calculated provided one knew the magnitude of the surface current and, ultimately a value determined for the current velocity at the depth of the drogue. Monahan's original treatment of this correction method was restricted to the colinear case of both drogue and surface float moving in the same direction but at different velocities. Vector addition and subtraction were utilized to adapt this technique to the two dimensional case encountered in the field.

The fundamental argument for this system lies in the fact that the forces on the surface float and on the drogue are the

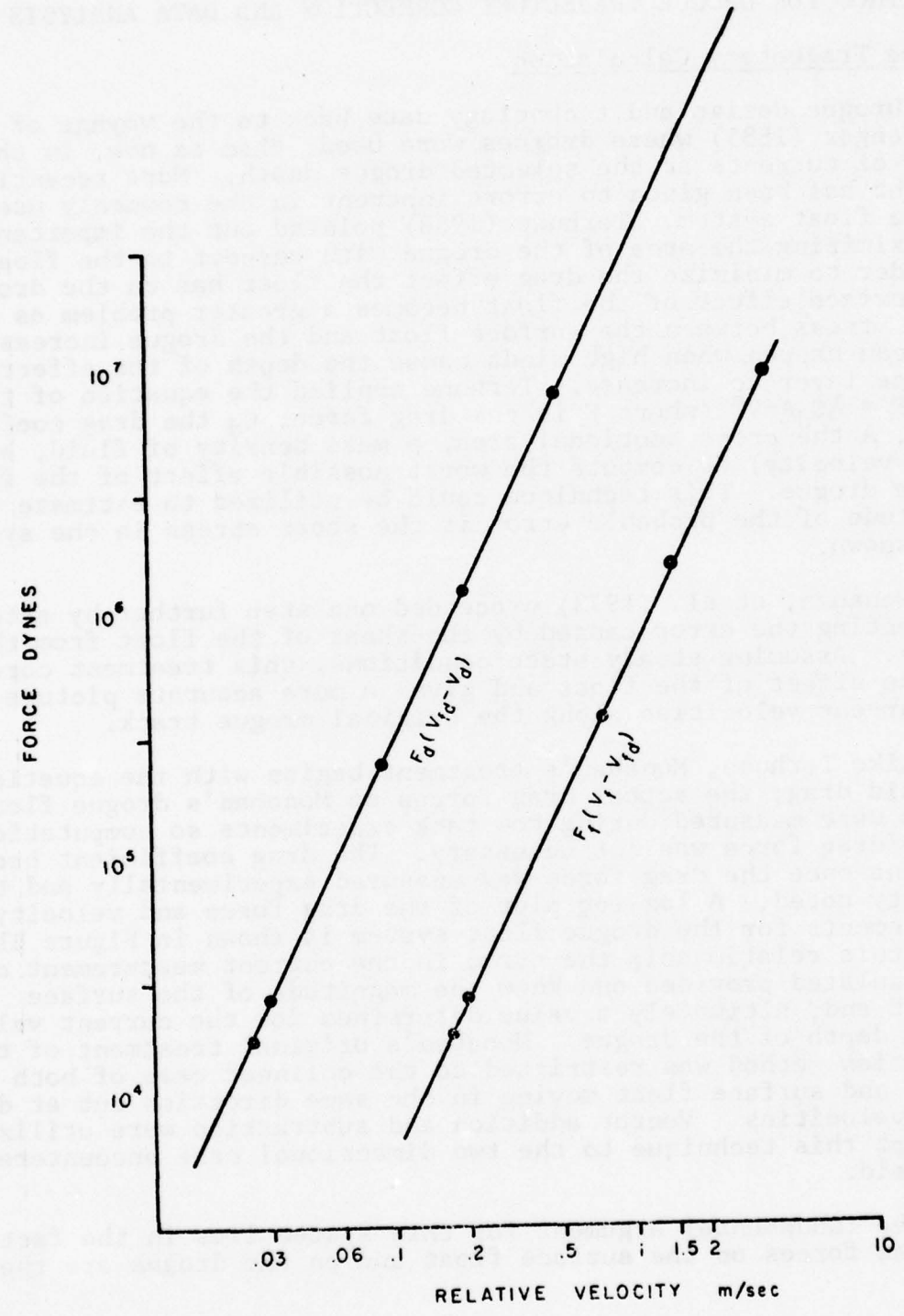

Figure B1. Log-log plot of drag force vs. relative velocity for drogue (F_d) and float (F_f).

same. Thus each point on the float curve (F_f) corresponds to a point on the drogue curve (F_d) along the same horizontal line. This procedure consists of vector subtration of the velocity of the drogue float system (obtained by monitoring such a system) from the velocity of the surface current (V_f) (obtained by monitoring a surface float with no drogue attached). This gives a relative velocity for the surface current with respect to the drogue float system. The value of the drag force on the float can then be obtained by going to the graph at this particular relative velocity and finding the force on the float corresponding to that velocity $F_f(V_f-V_{fd})$. Moving horizontally along the graph (the force on the float and the force on the drogue are equal) to the curve for the drogue $F_d(V_{fd}-V_d)$ and then down vertically to the velocity scale one can obtain the velocity of the drogue through the water at its depth of deployment. The final step consists of vectorially subtracting this velocity (speed of drogue through the water) from the velocity of the drogue float system and arriving at the corrected current velocity at the respective drogue depth. A sample of the above calculation is shown graphically in Figure B2.

This method of correction, with some modifications, was utilized during the study. As tow tank facilities were not available, graphs were plotted assuming a constant drag ratio (a valid assumption for flat plates at high Reynolds numbers, such as those encountered during the study). Arbitrary velocities which might occur during a drogue run were selected and the projected area of the drogue and float calculated. This led to the computation of the drag forces on the float and the drogue as plotted in Figure B1.

The computer program for the calculation of corrected drogue velocities is given in Table B1.

Analysis of observed drogue trajectories. The ambient environment conditions on the days of the drogue deployment are given in Table B2. The raw and corrected drogue velocities are presented in Table B3 and the graphic presentation of the trajectories are showing in Figures B3 through B25.

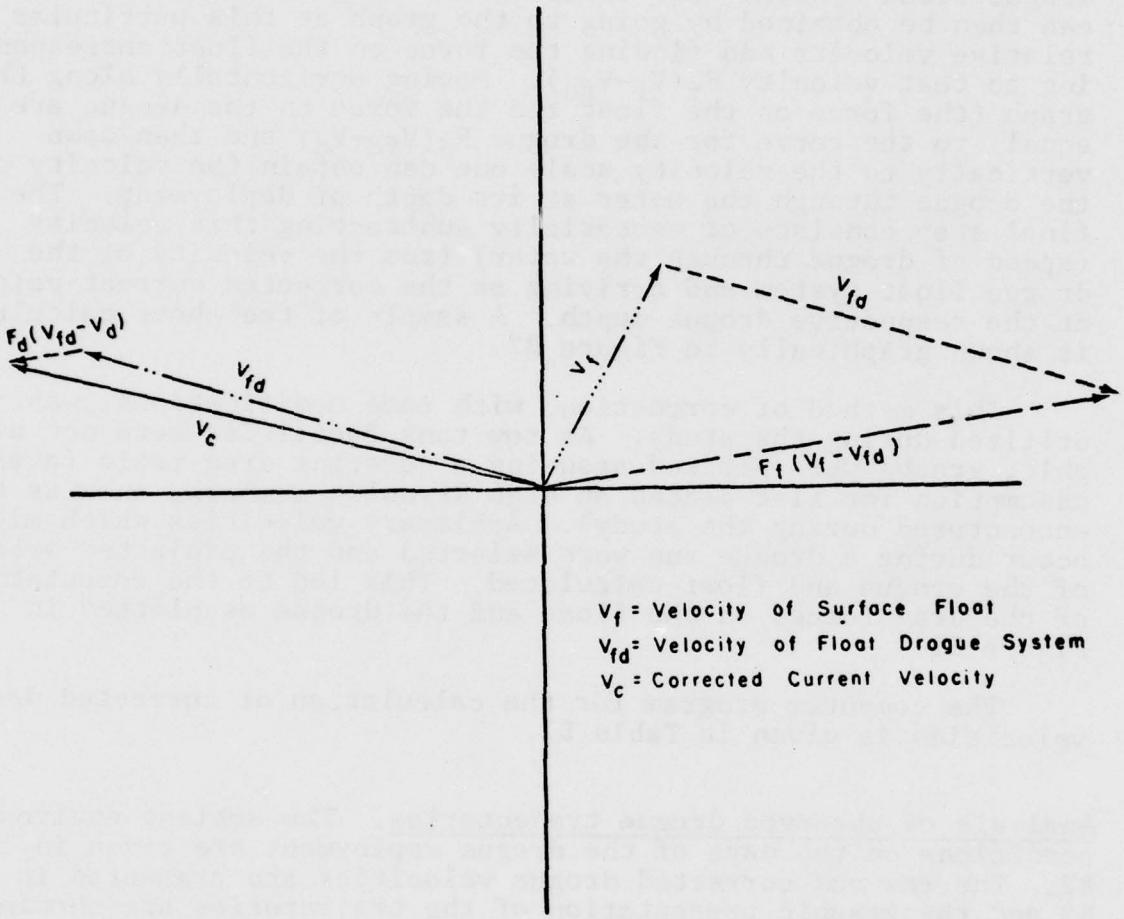

Figure B2. Sample vector calculation of drogue correction method.

TABLE B1

PROGRAM FOR CORRECTING DROGUE VELOCITIES

```
      DIMENSION TITLE (20)
      DO 38 N=1,500
      READ(5,10) A,B,VFD,VF,TV,IT
   10 FORMAT (F6.2,5X,F7.2,3X,F6.3,4X,F6.3,2X,F5.2,3X,I4)
      IF (A.LE.400.) GO TO 950
      READ(5,11) TITLE
   11 FORMAT(20A4)
      WRITE(6,12) TITLE
   12 FORMAT(20A4)
      GO TO 38
C     CONVERT ANGLES TO RADIANS
  950 CONTINUE
      RADA=A*3.14159/180.0
      RALB=B*3.14159/180.0
      VFLX=VFD*COS(RADA)
      VFLY=VFD*SIN(RADA)
      VFX=VF*COS(RALB)
      VFY=VF*SIN(RALB)
      VFRX=VFX-VFLX
      VFRY=VFY-VFLY
      VFR=SQRT((ABS(VFRX))**2+(ABS(VFRY))**2)
      RTAN=VFRY/VFRX
      C=VFRY/VF
      S=VFRX/VF
      IF(C.GT.0.0)GO TO 15
      IF(C.LT.0.0)GO TO 21
      ANGLE=(3.14159 +ATAN(RTAN))
      GO TO 33
   21 ANGLE=(6.2831+ATAN(RTAN))
      GO TO 33
   15 IF (S.GT.0.0)GO TO 27
      ANGLE=(3.14159+ATAN(RTAN))
      GO TO 33
   27 ANGLE=ATAN(RTAN)
      GO TO 33
C      ROTATE ANGLE BY 180 DEGREES
   33 BANGLE=ANGLE +3.14159
      VFR=VFR*100
      TF=221.5*(VFR)**2
      VD=SQRT(TF/5640.)
      VD=VD*0.71
      VRX=VD*COS(BANGLE)
      VRY=VD*SIN(BANGLE)
      VWX=VRX+VFLX
      VWY=VRY+VFLY
      VW=SQRT((ABS(VWX))**2+(ABS(VWY))**2)
      ANGLE=(BANGLE*180.)/3.14159
      AVLIN=VWY/VWX
      AVLIN=ATAN(AVLIN)
```

```
      VL=WV/TV
      IF(VWX.LT.C.C) GO TO 50
      IF(VWY.GT.C.C)GO TO 52
      WVDIR=6.28318 +WVDIR
      GO TO 61
   50 IF(VWY.LT.C.C) GO TO 51
      WVDIR=3.14159+WVDIR
      GO TO 61
   51 WVDIR=WVDIR+3.14159

LEVEL  21                    MAIN                    DATE = 74157          08/14/10

      GO TO 61
   52 WVDIR=WVDIR
      GO TO 61
   61 WVDIR=(WVDIR*180.)/3.14159
      GO TO 37
   37 WRITE(6,38)II,A,VEL,B,VF,TV,WV,WVDIR
   38 CONTINUE
   36 FORMAT(5X14,4X,F6.2,4X,F5.3,6X,F6.2,4X,F5.3,4X,F6.3,6X
     1F6.3,4X,F7.2)
      STOP
      END
```

TABLE B2

AMBIENT ENVIRONMENTAL CONDITIONS

DROGUE EXPERIMENTS

Flood Currents at the Inlet

Date (1973)	Time of Low Water EST	Time of High Water EST	High and Low Tide Elevations (meters)	Wind Velocity (m/sec.) direction	Wave Height (meters) direction
May 10	8:00 am	14:40 pm	0.9; 2.0	1.7N	1.2E
May 11	9:00 am	16:00 pm	0.84; 2.0	4.5-6.5W	0.6E
May 22	5:30 am	11:30 am	0.96; 1.74	2.5SW	0.4E
June 5	5:00 am	11:30 am	0.63; 1.86	2.1-4.5WSW	0.1-0.2SW
June 7	6:50 am	13:00 pm	0.63; 1.90	6.5-8.8 SSW	0.3-0.6SW
June 21	5:30 am	11:30 pm	0.96; 1.00	0.0-2.5SW	0.1SW

Ebb Currents at the Inlet

May 4	9:00 am	14:40 pm	1.01; 0.66	2.1N	0.6E
May 21	11:00 am	16:30 pm	1.86; 1.0	6.5-8.8NW	0.3NE
June 4	10:40 am	16:20 pm	1.96; 0.54	4.5-6.5SW	0.15SW
June 13	6:20 am	12:20 pm	1.62; 0.72	4.5-6.5SW	0.15SW
June 14	7:20 am	12:30 pm	1.80; 0.93	2.1-4.5N	0.15NE

Figures B3 through B25. Drogue trajectories. Solid line is observed drogue track. Dotted line is trajectory corrected for influence of wind on drogue-float system.

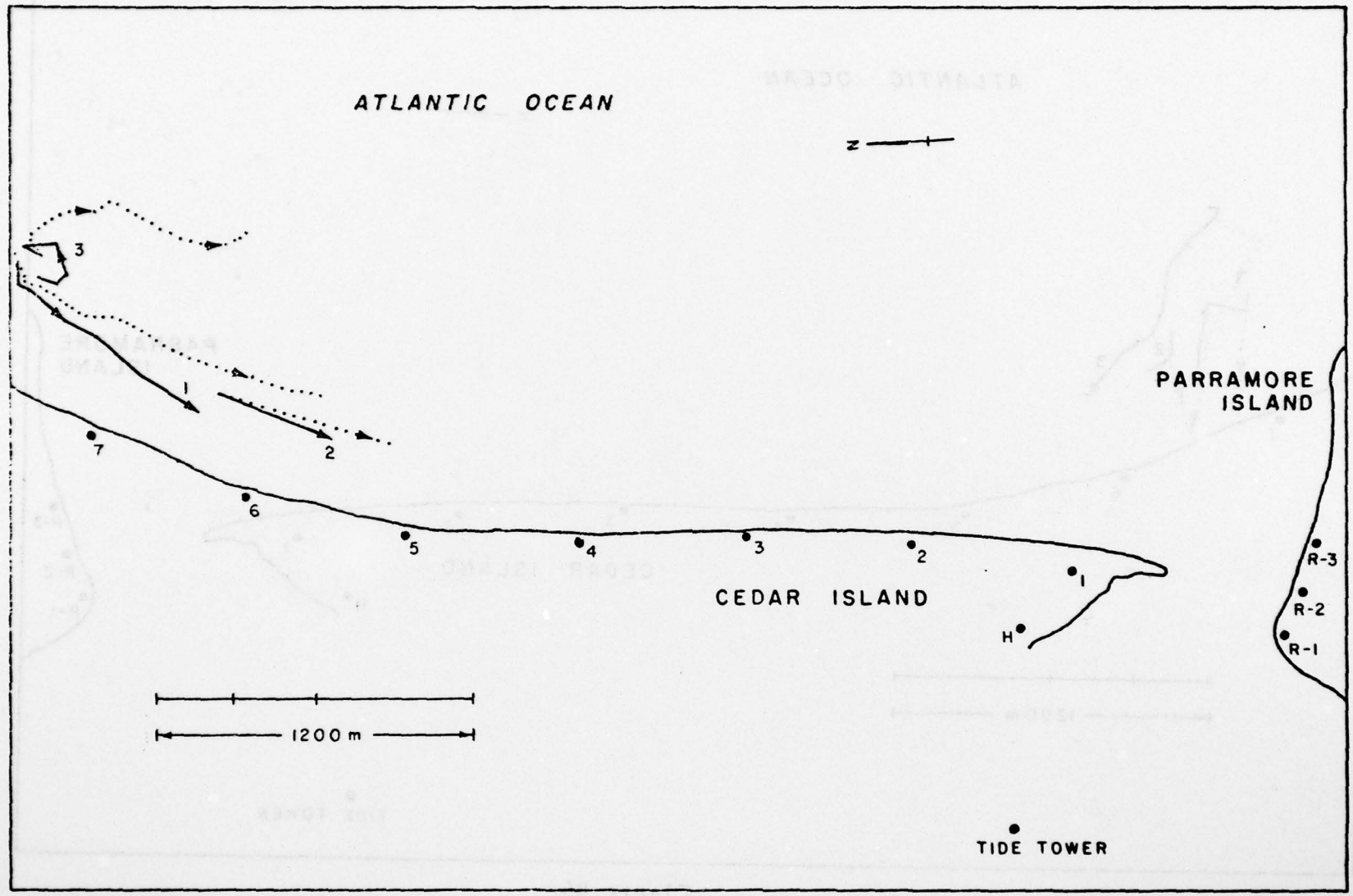

May 10, Flood

Figure B3

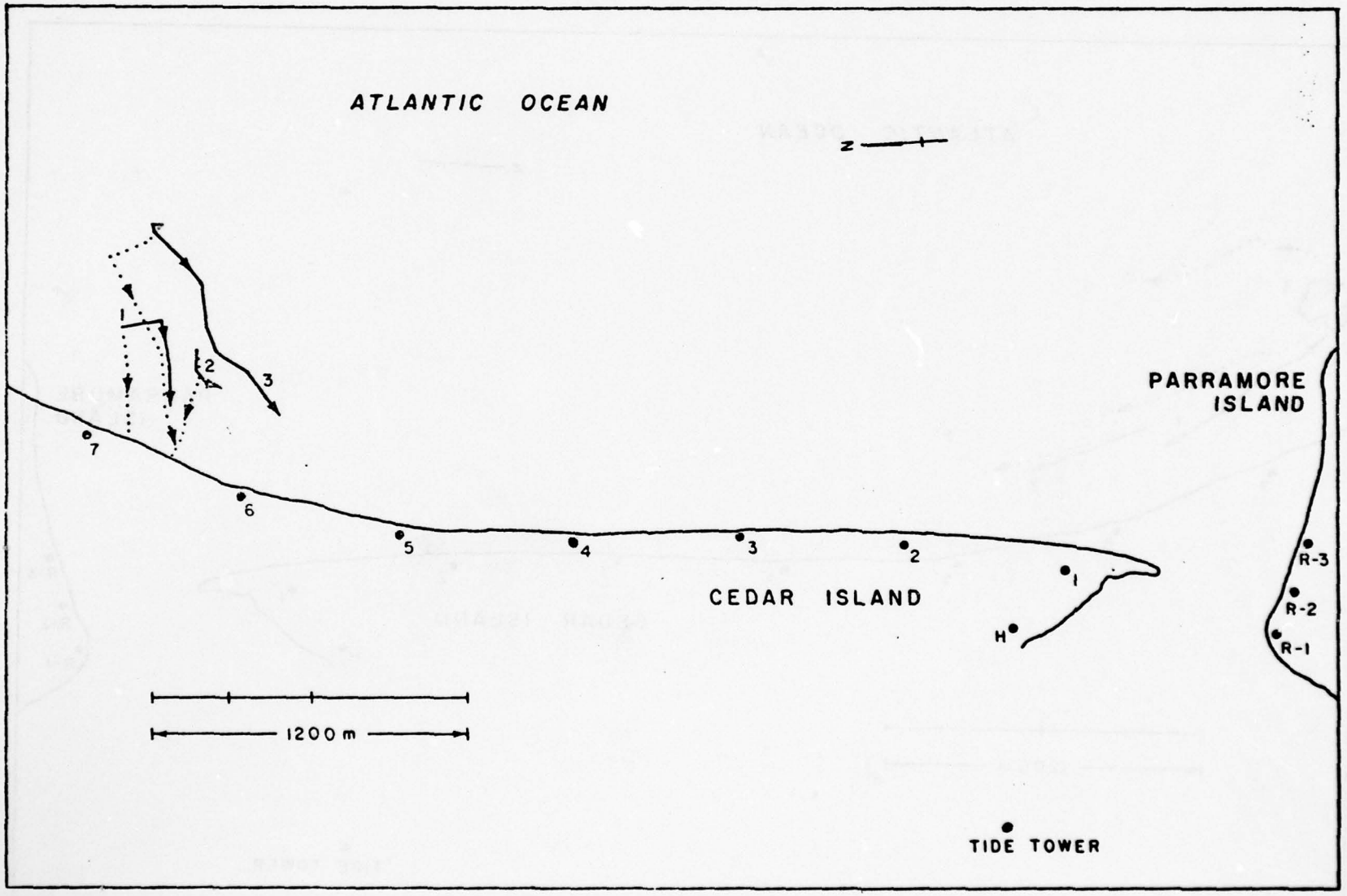

May 11, Flood

Figure B4

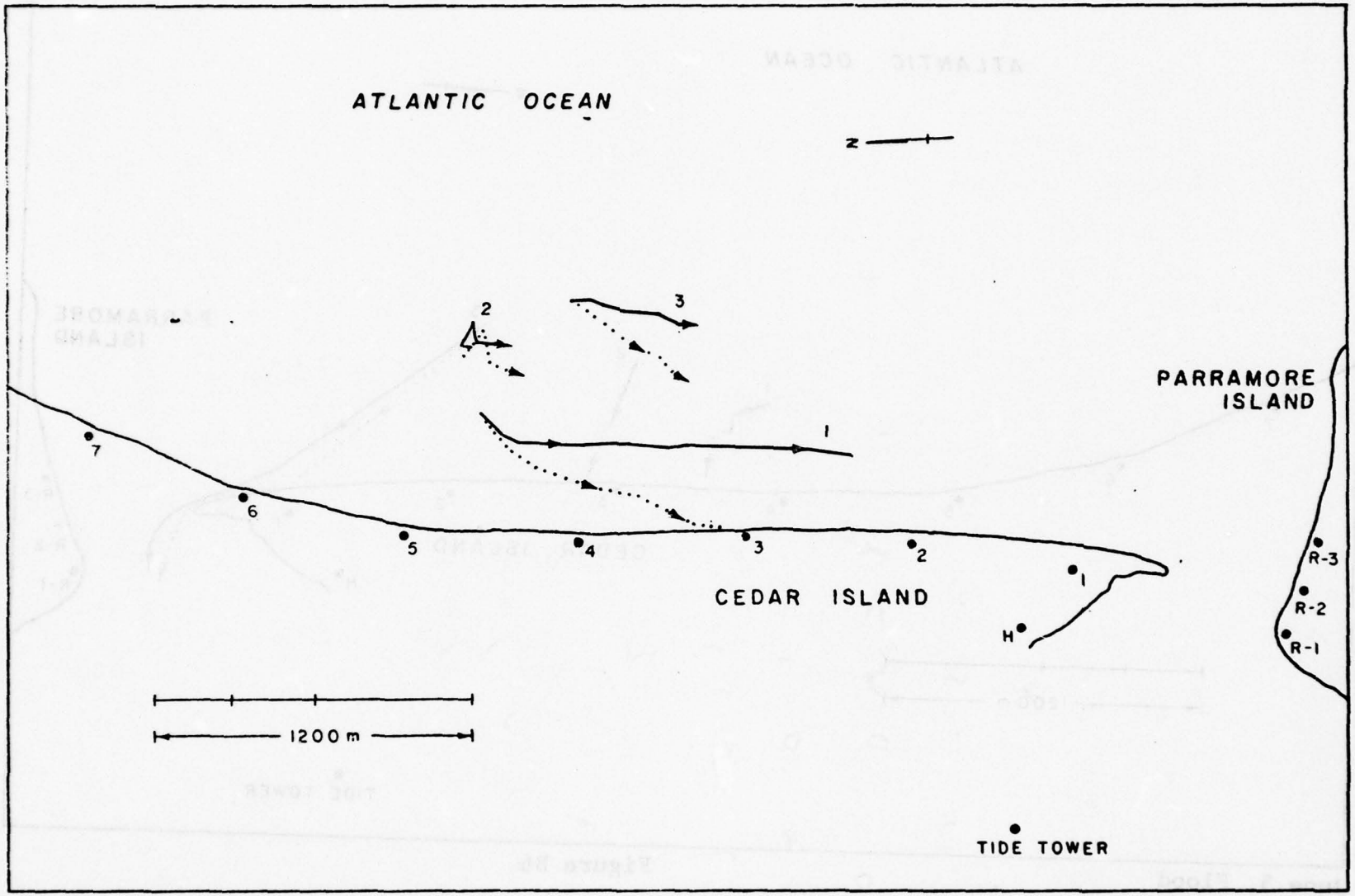

May 22, Flood

Figure B5

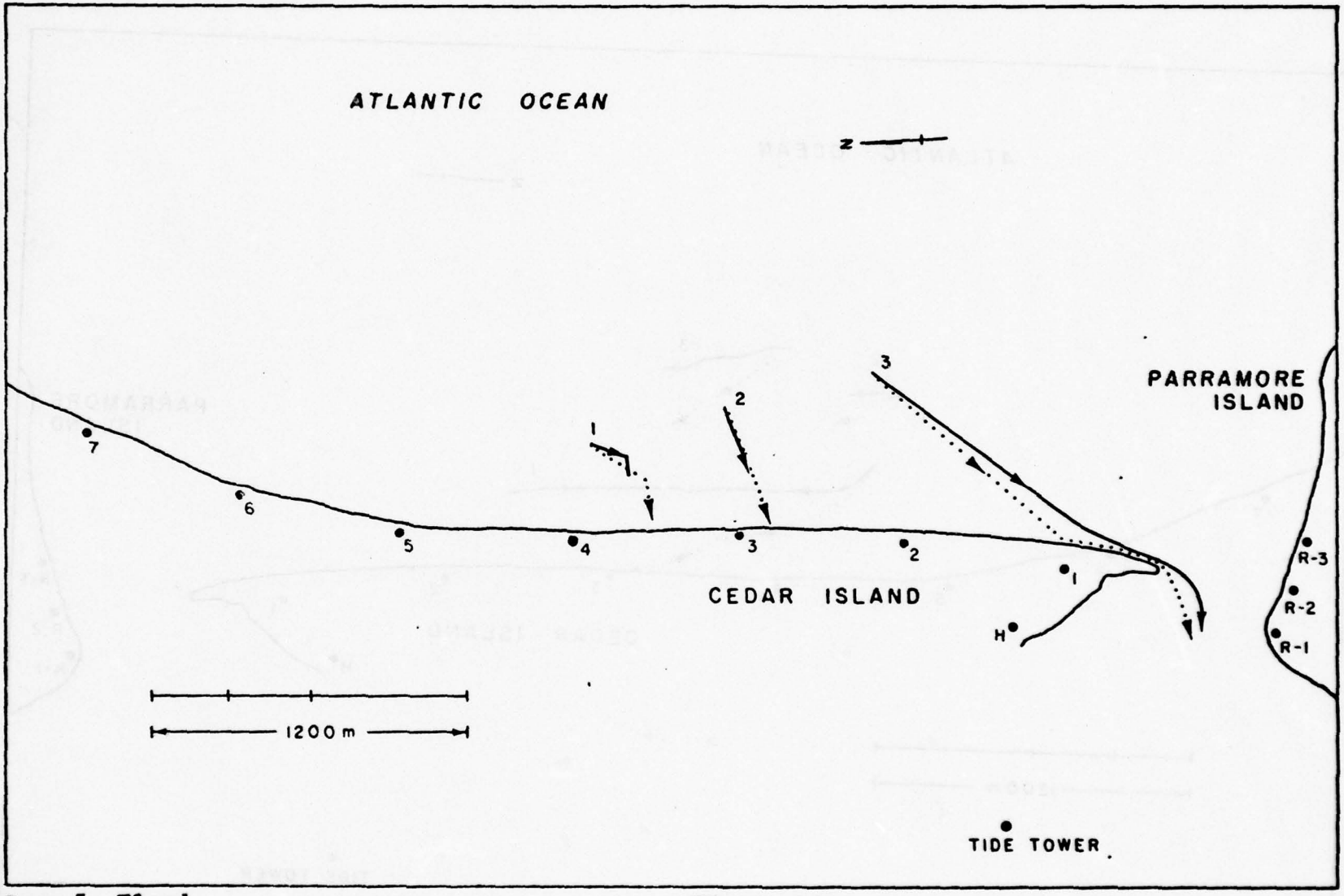

June 5, Flood

Figure B6

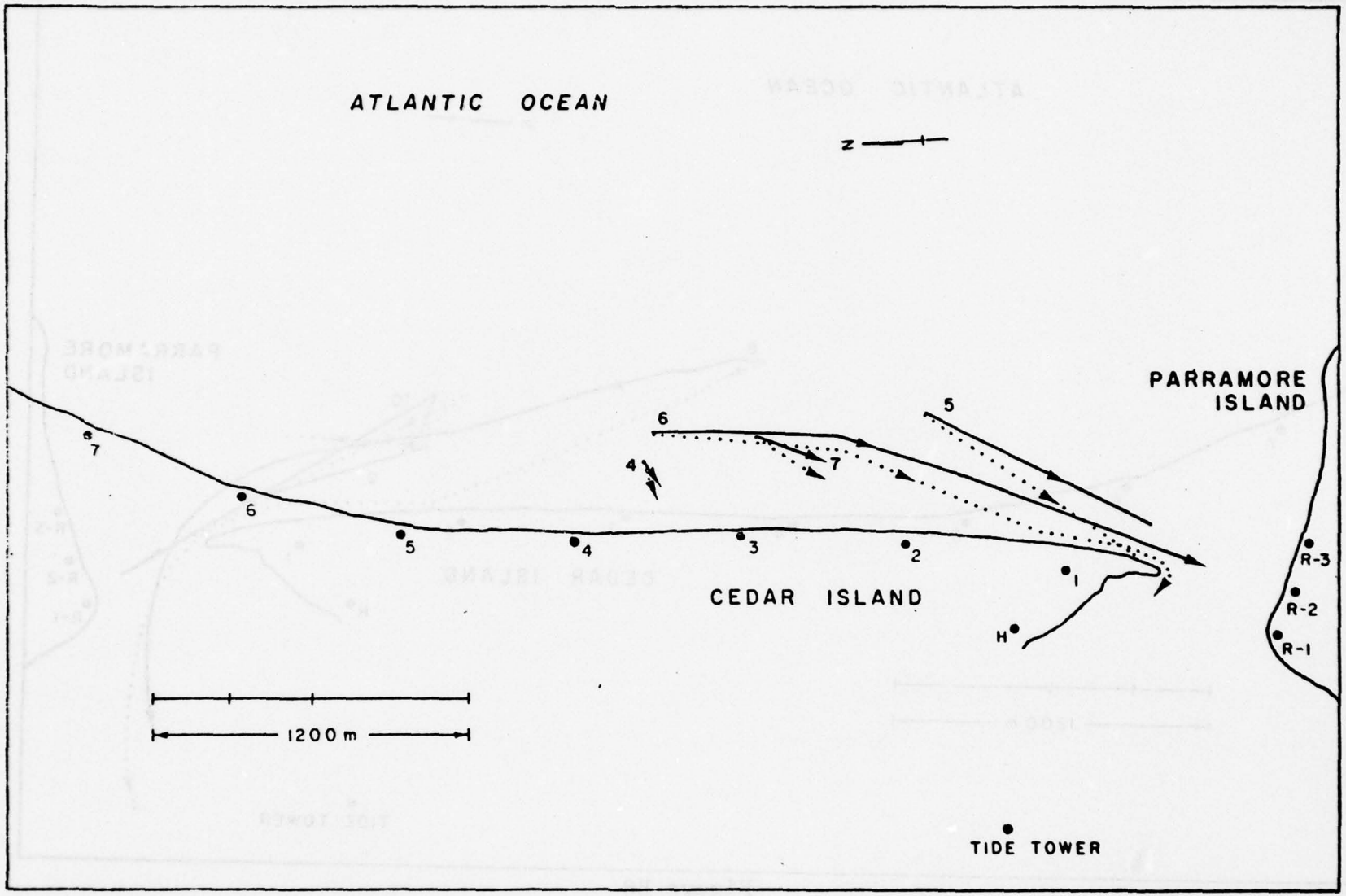

June 5, Flood

Figure B7

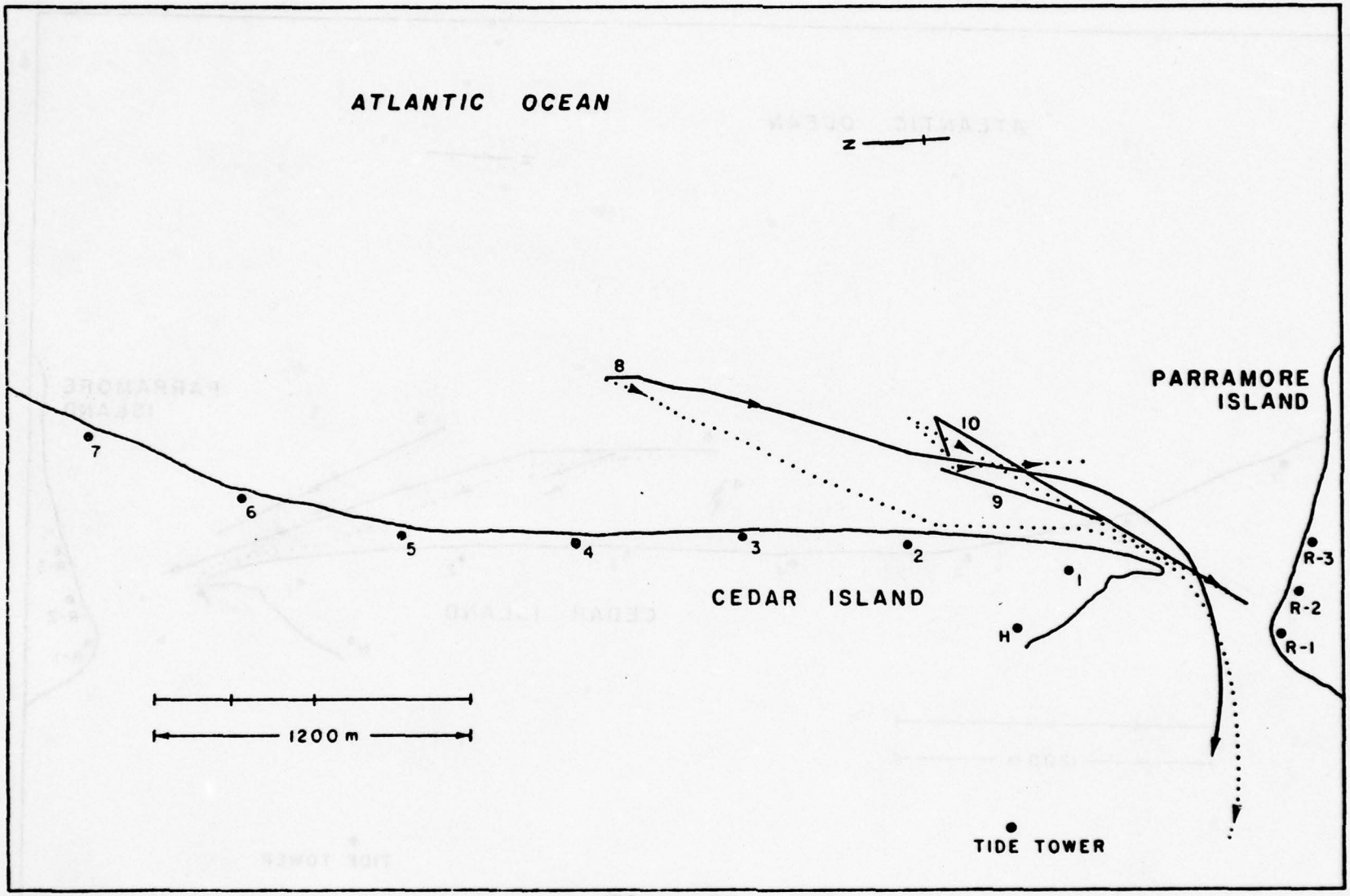

June 5, Flood

Figure B8

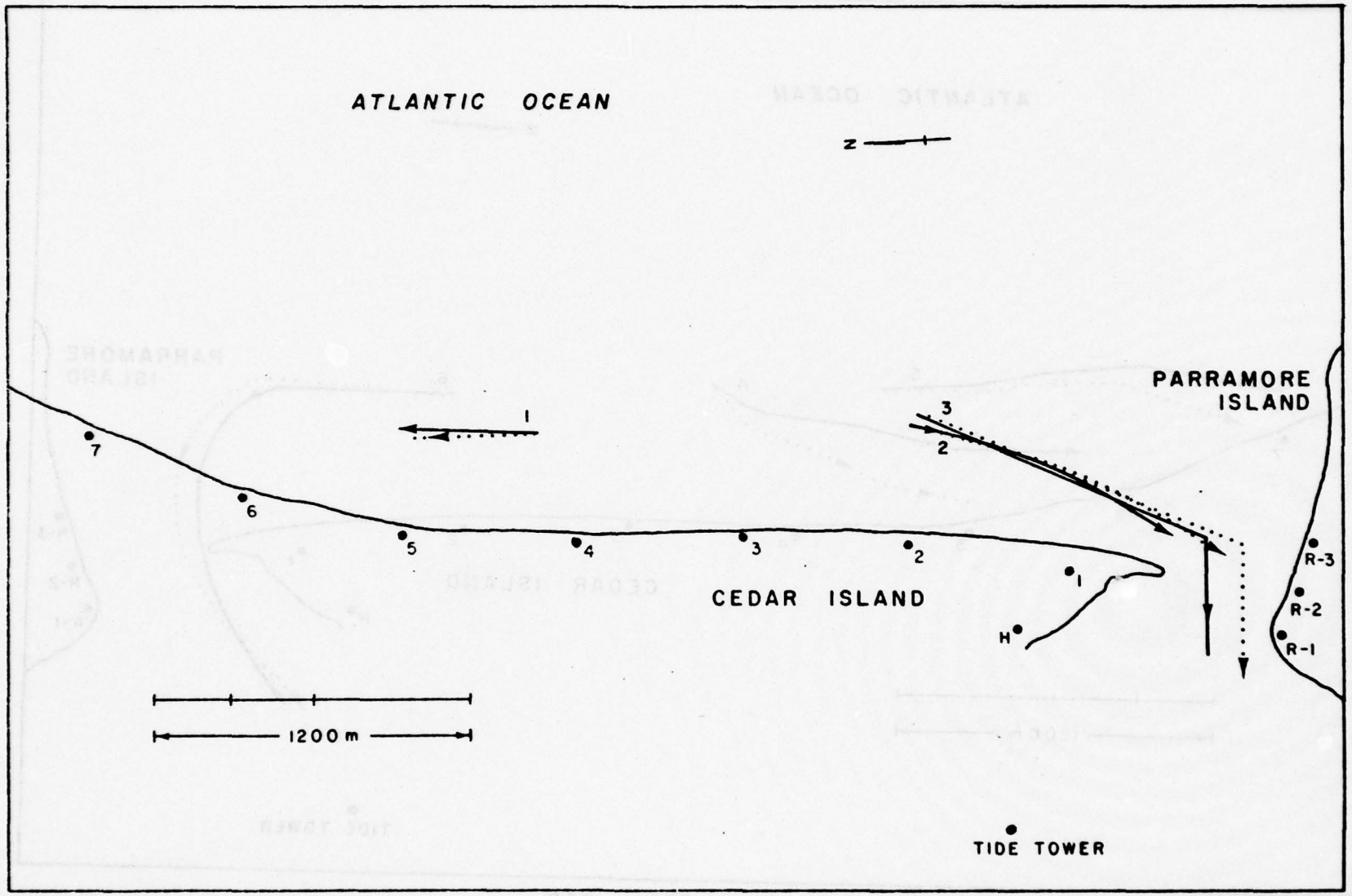

June 7, Flood

Figure B9

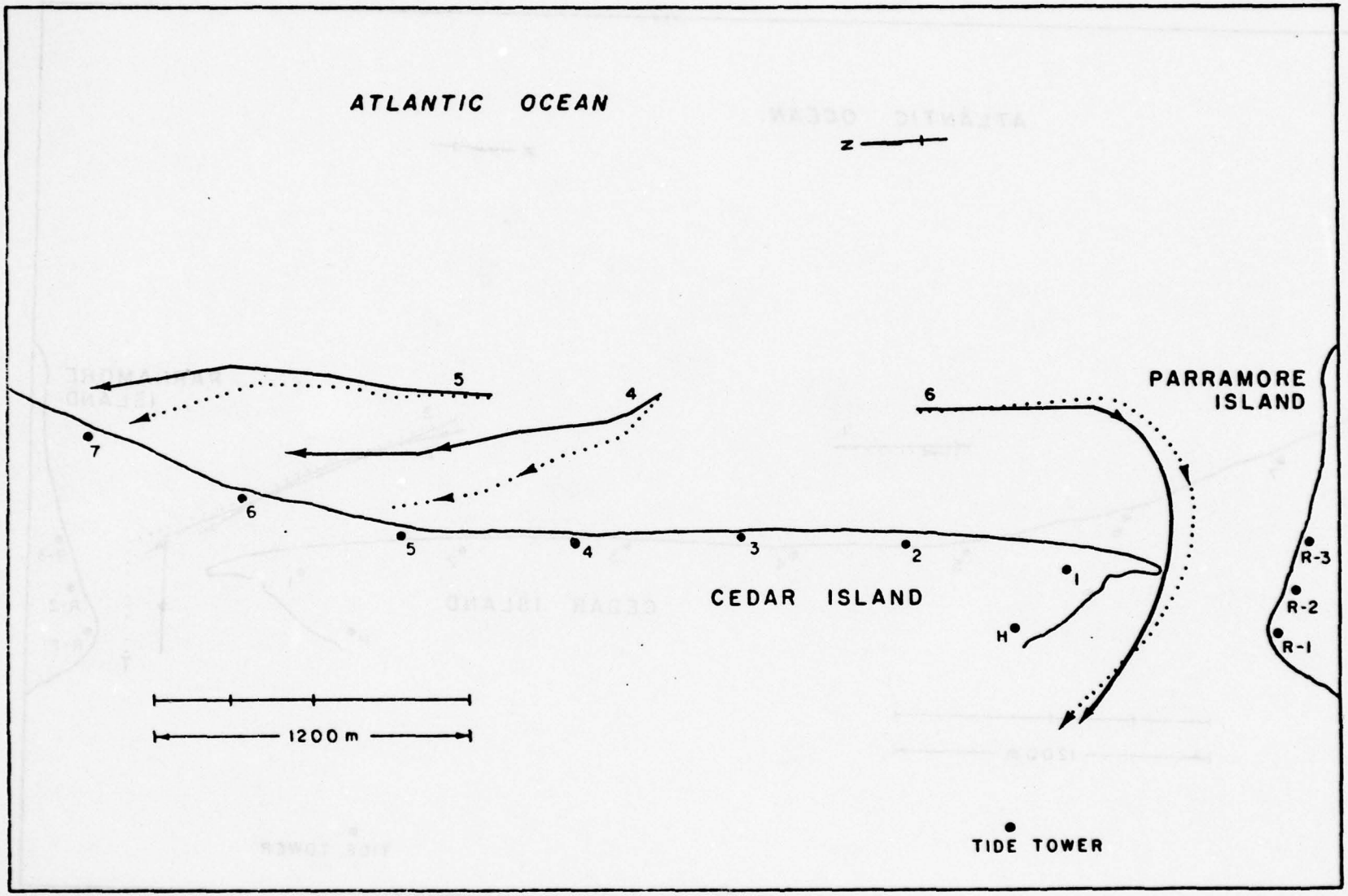

June 7, Flood

Figure B10

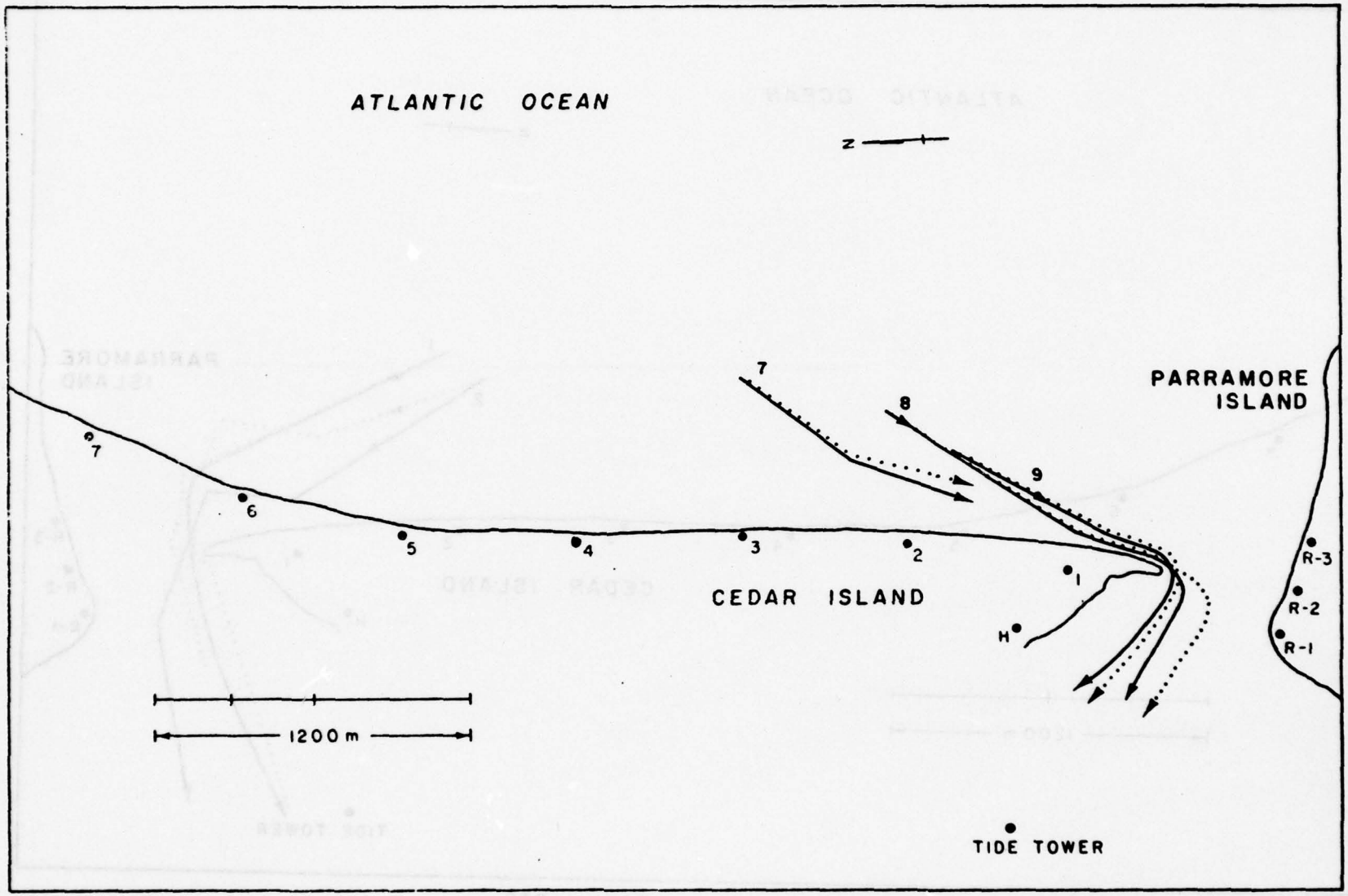

June 7, Flood

Figure B11

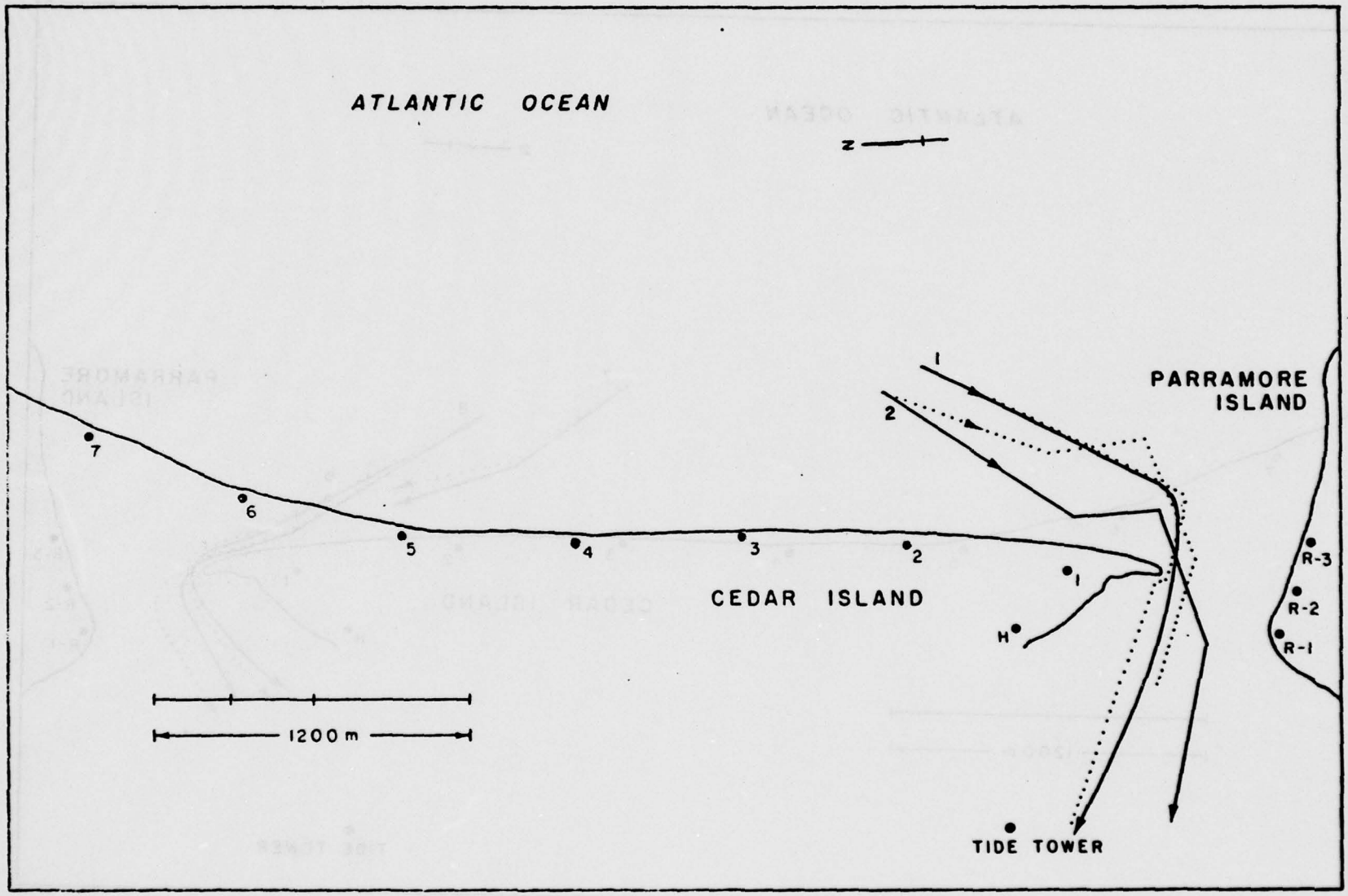

June 21, Flood

Figure B12

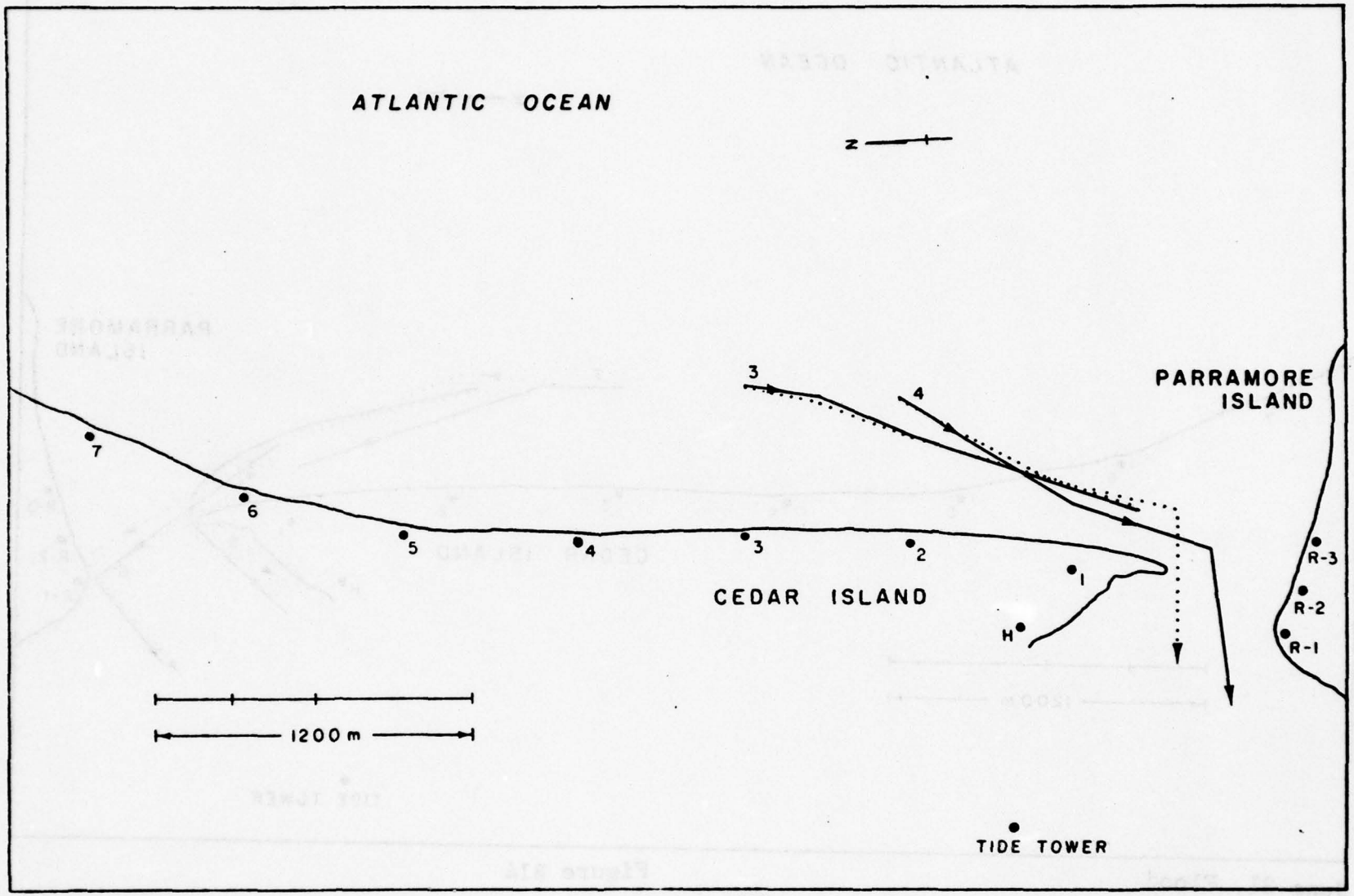

June 21, Flood

Figure B13

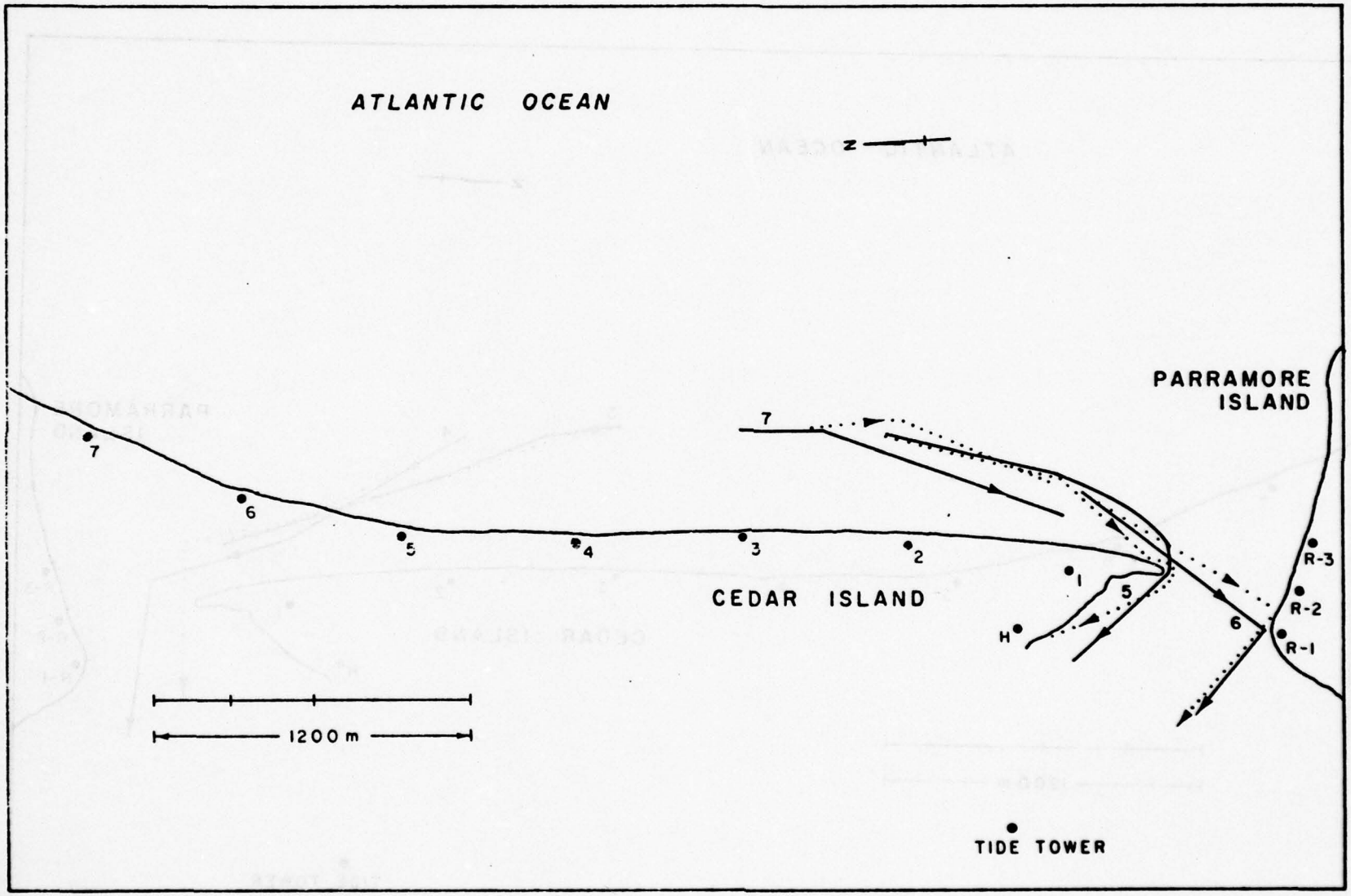

June 21, Flood

Figure B14

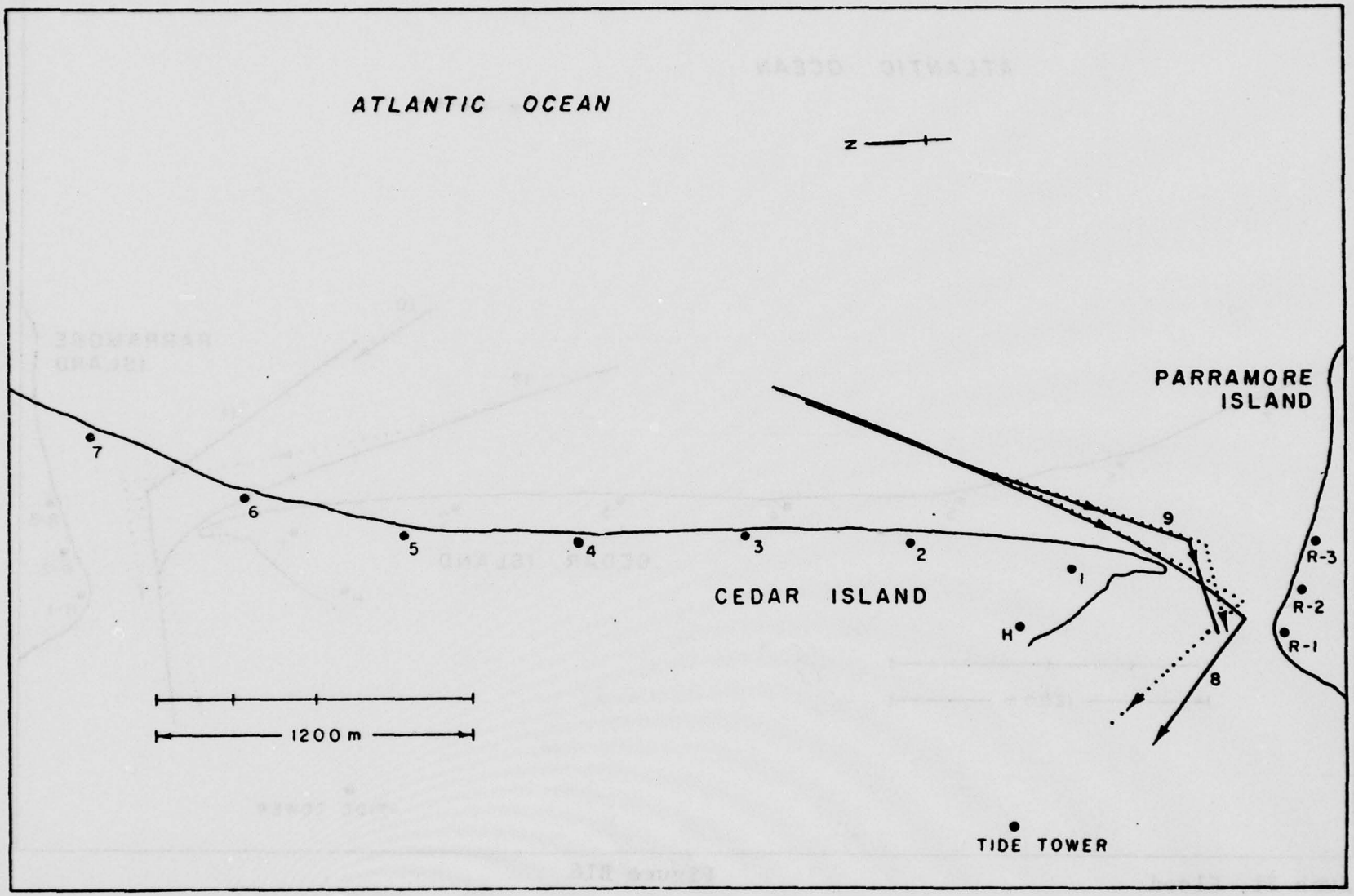

June 21, Flood

Figure B15

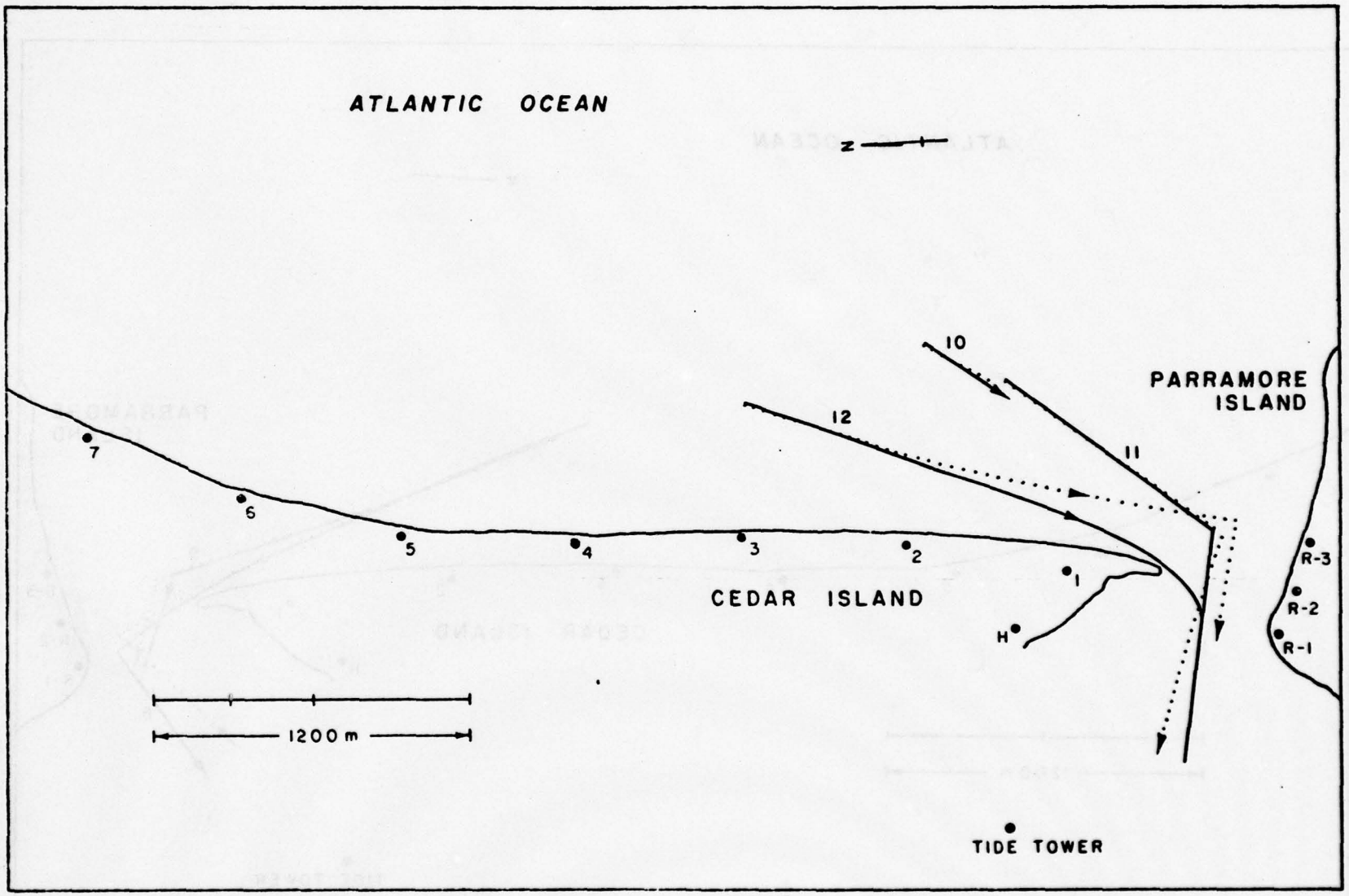

June 21, Flood

Figure B16

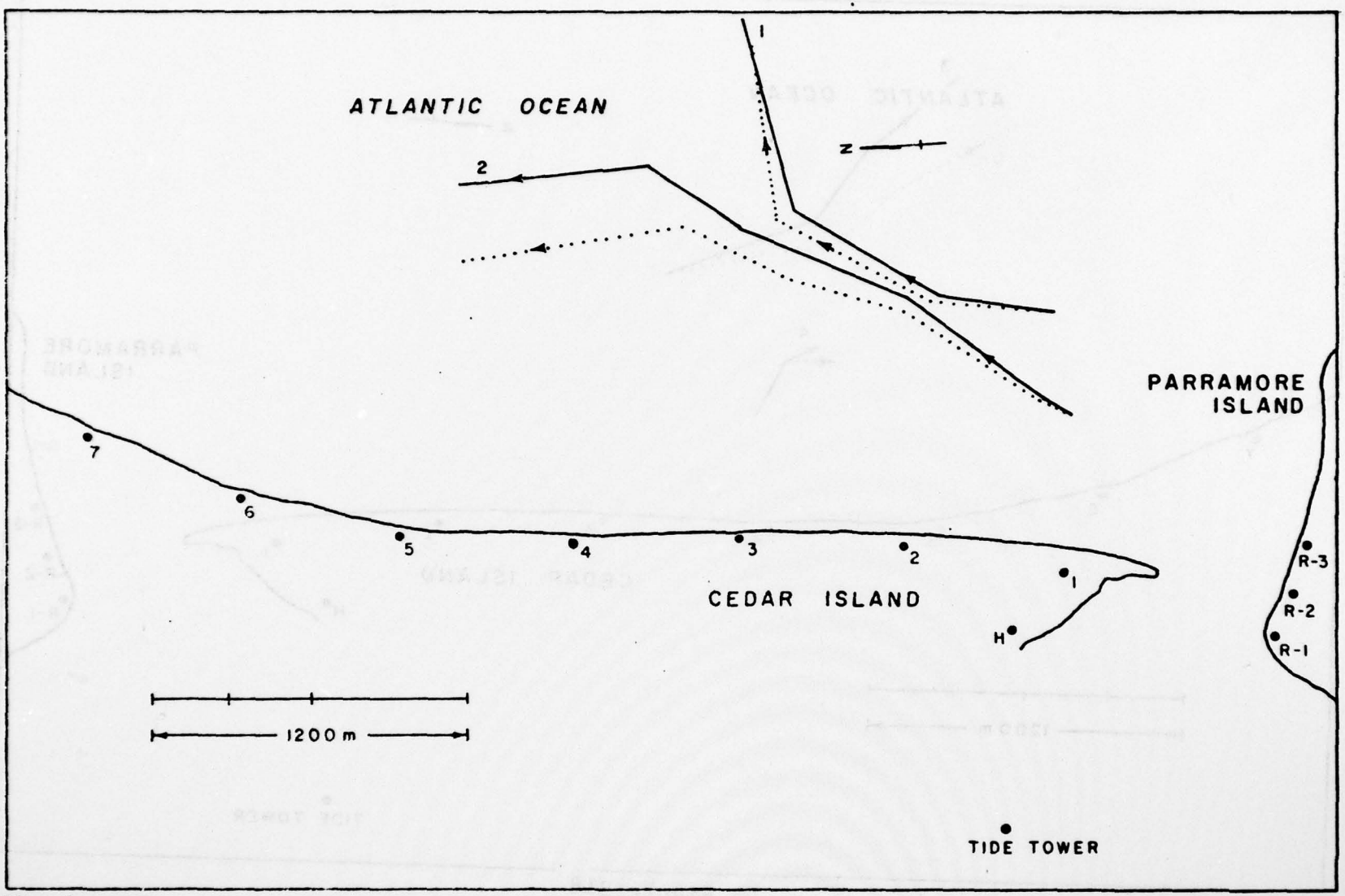

May 4, Ebb

Figure B17

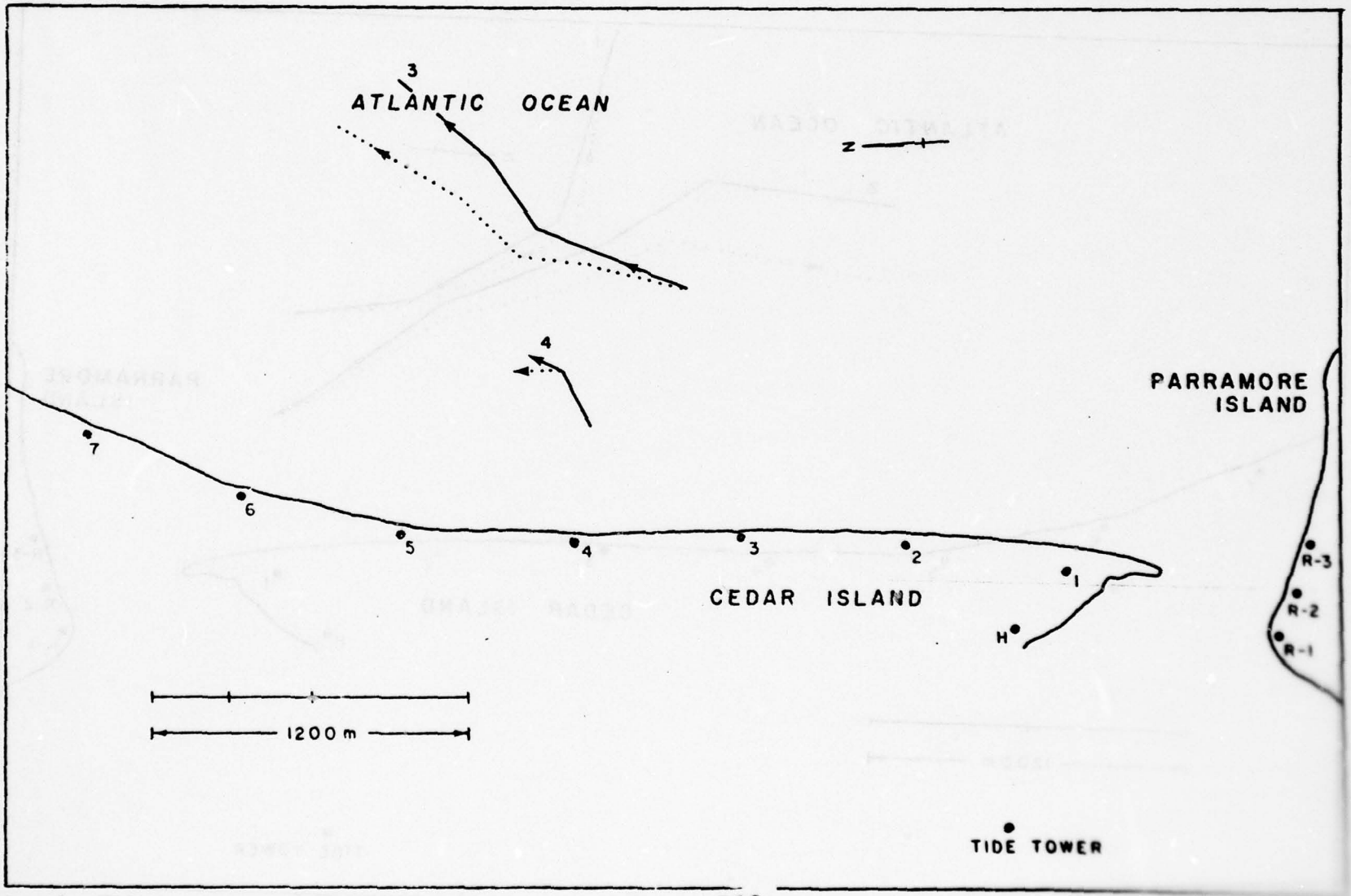

May 4, Ebb

Figure B18

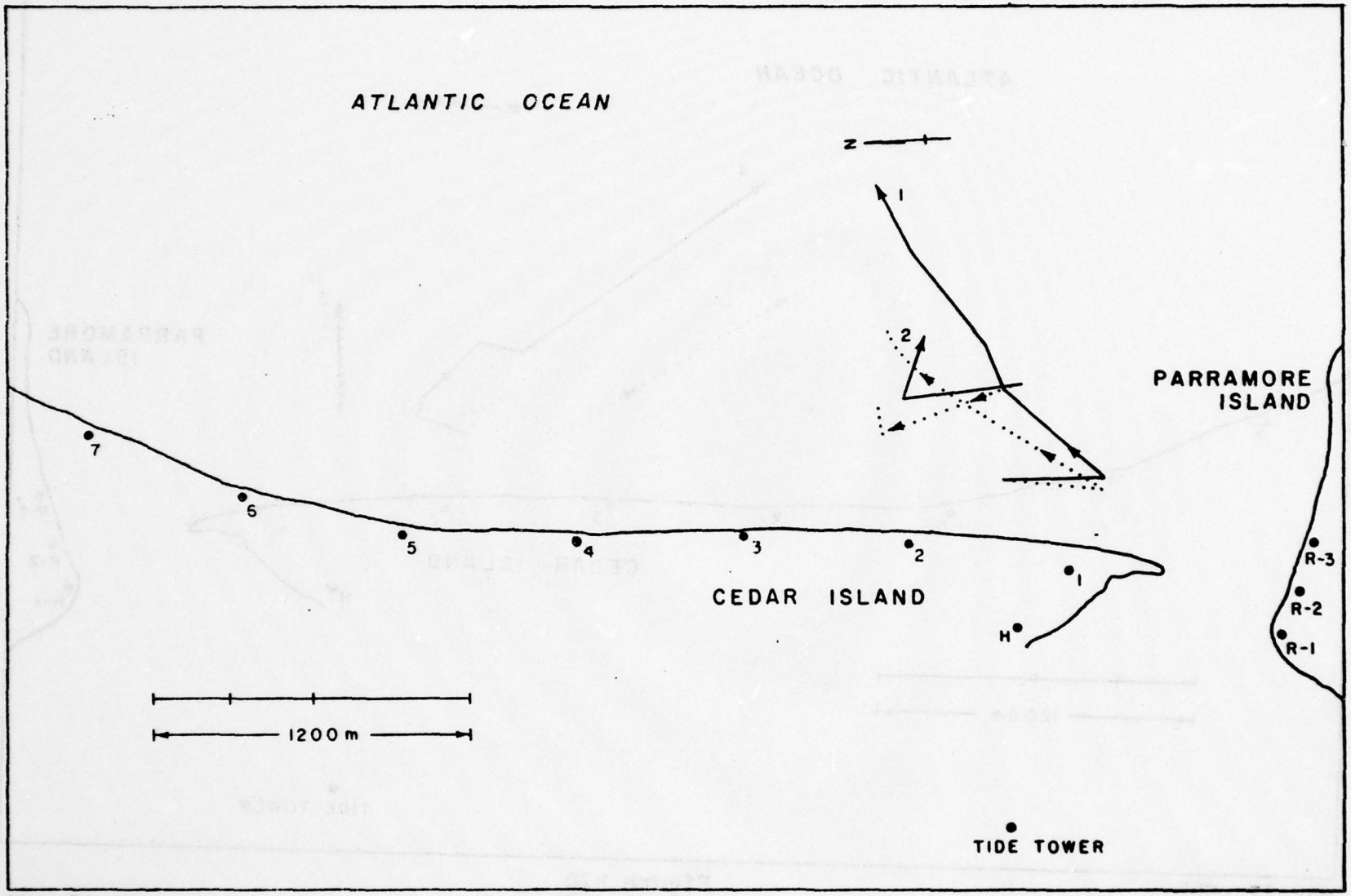

May 21, Ebb

Figure B19

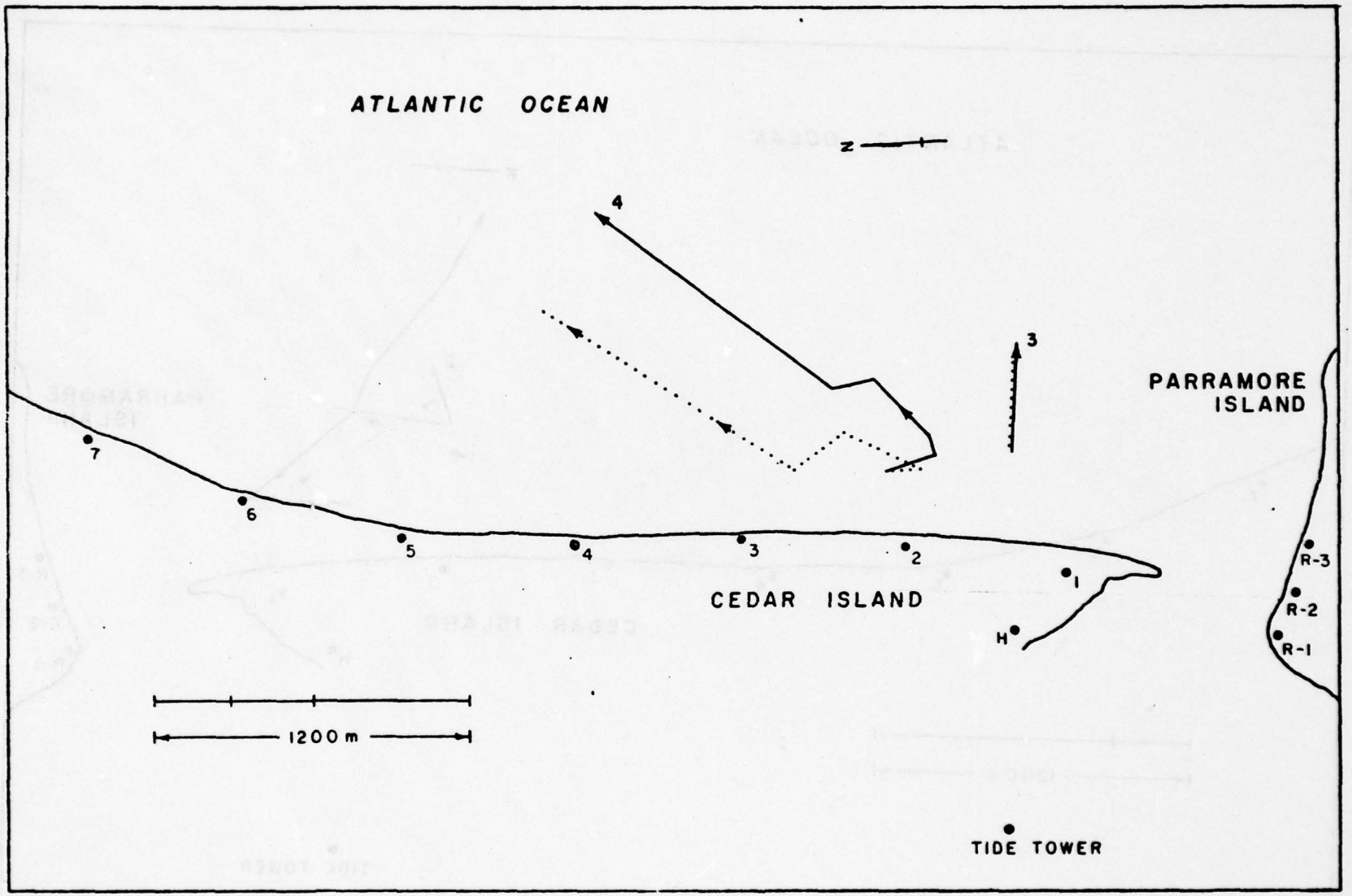

May 21, Ebb

Figure B20

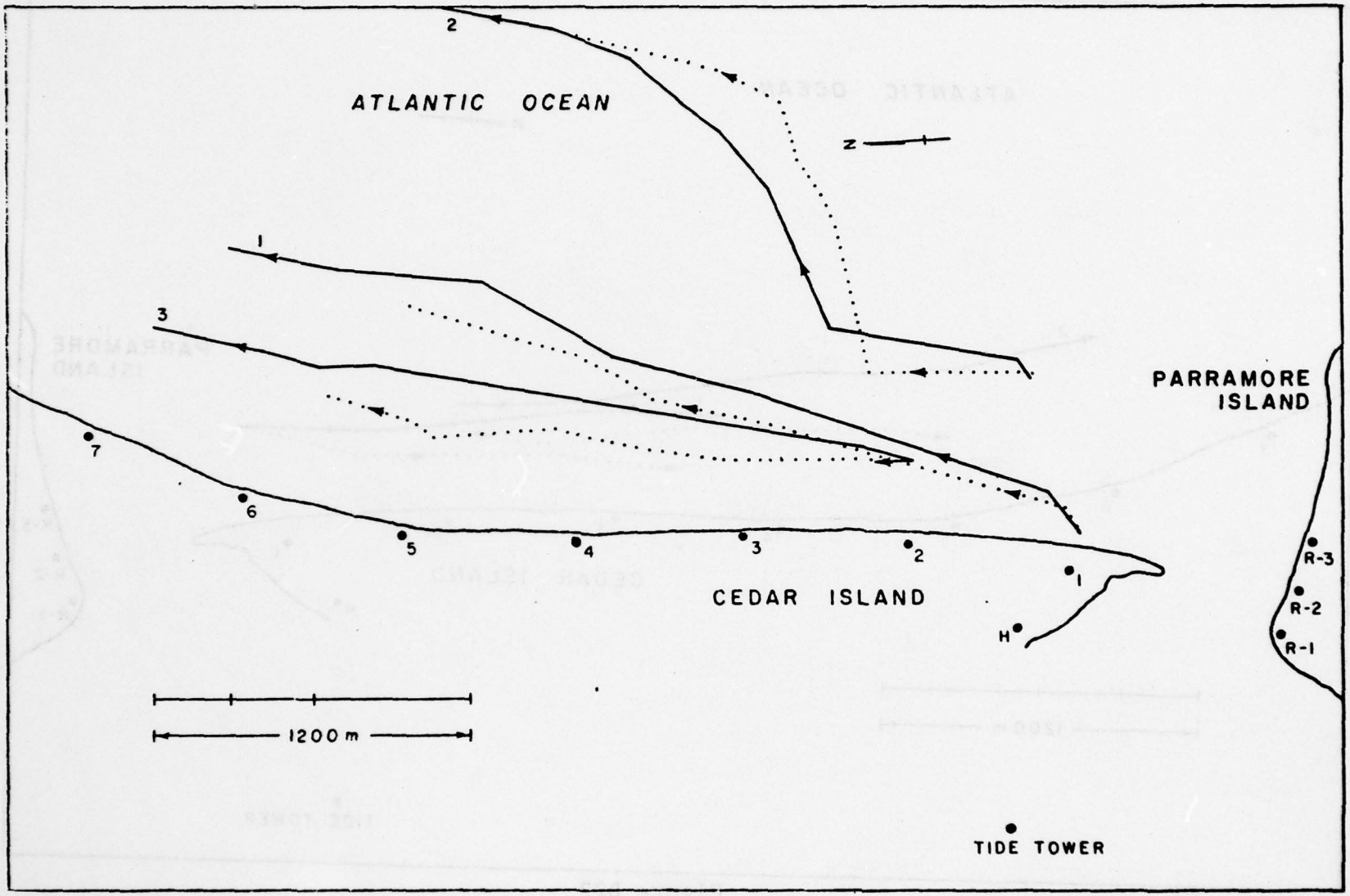

June 4, Ebb

Figure B21

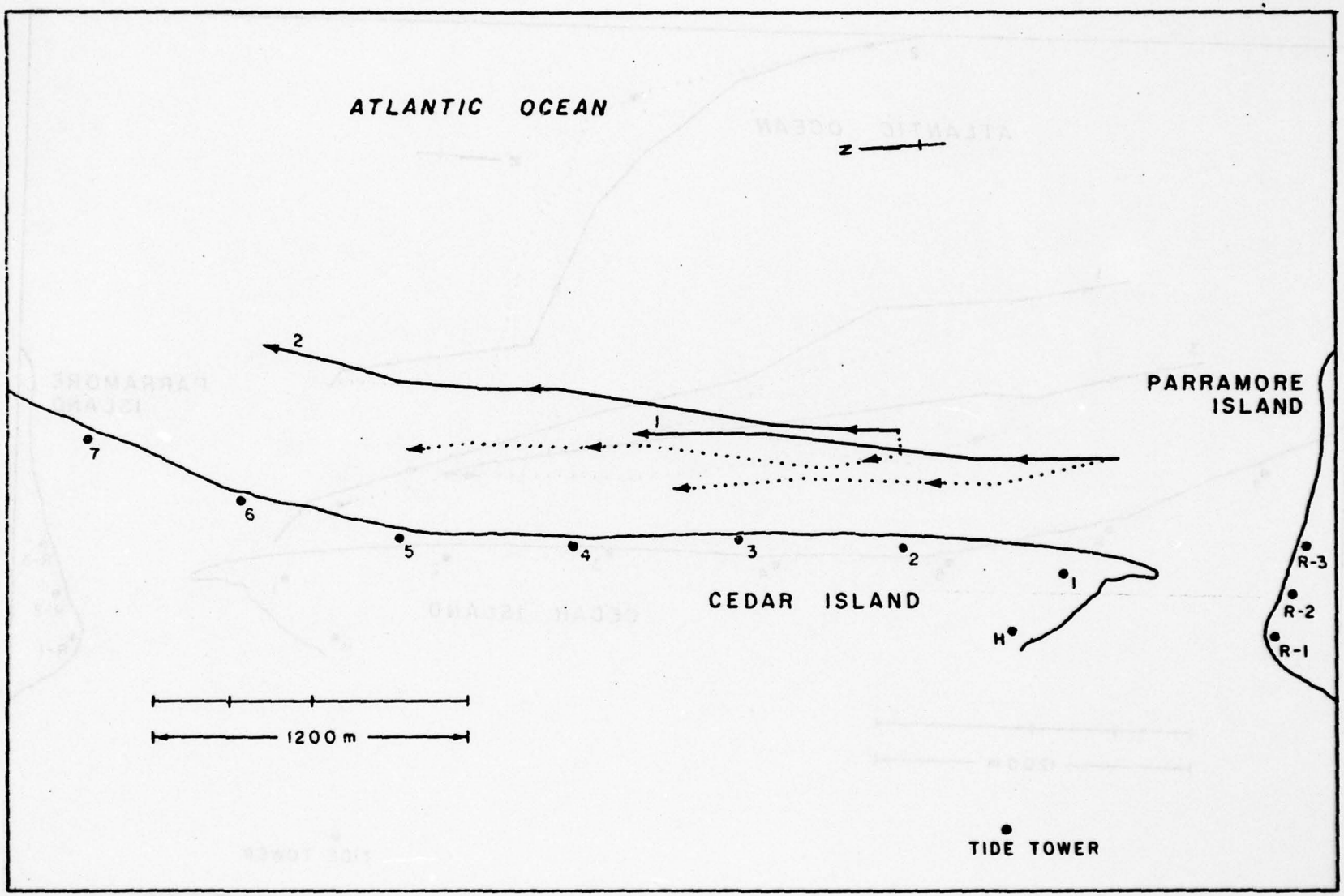

June 13, Ebb

Figure B22

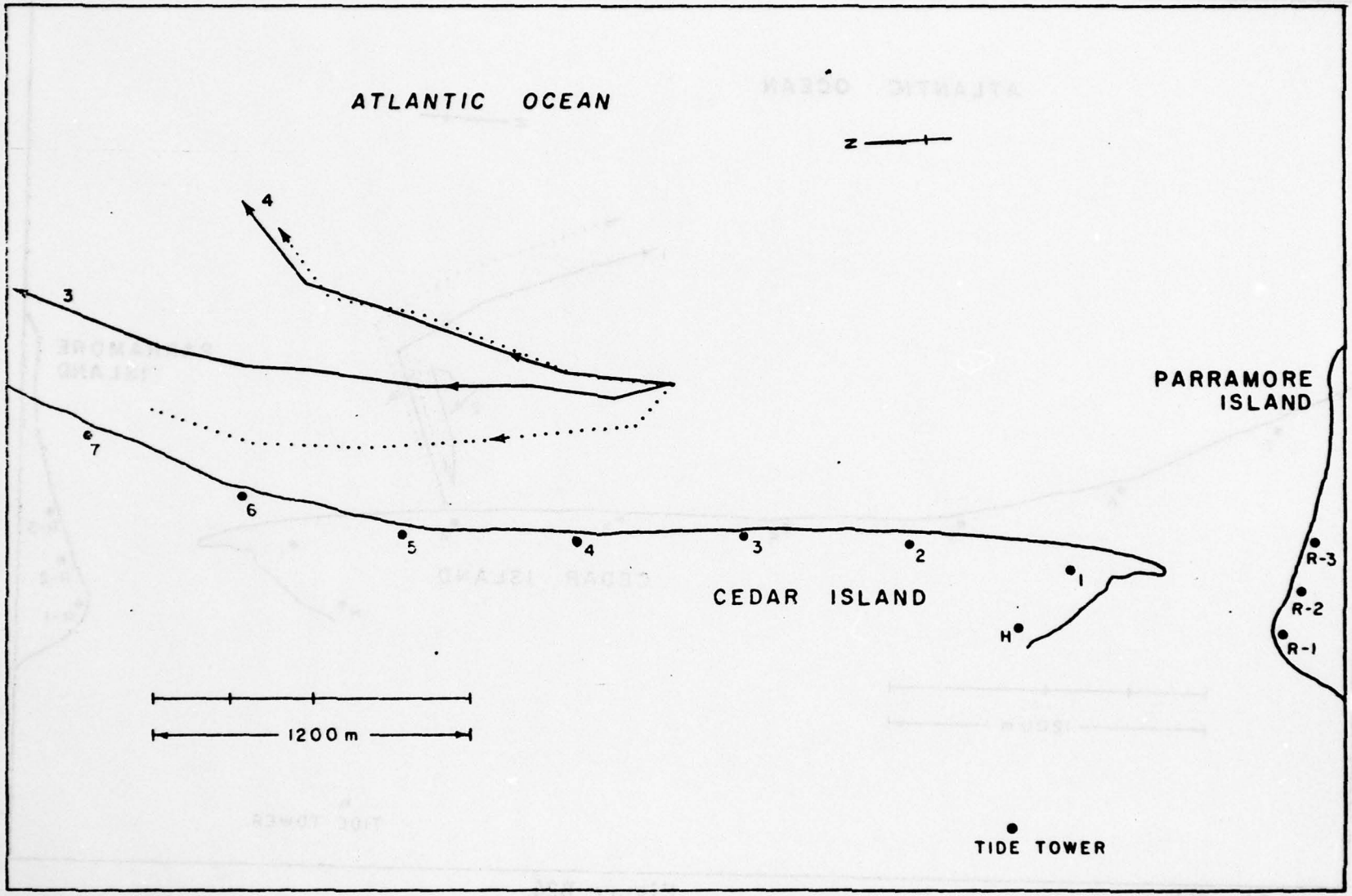

June 13, Ebb

Figure B23

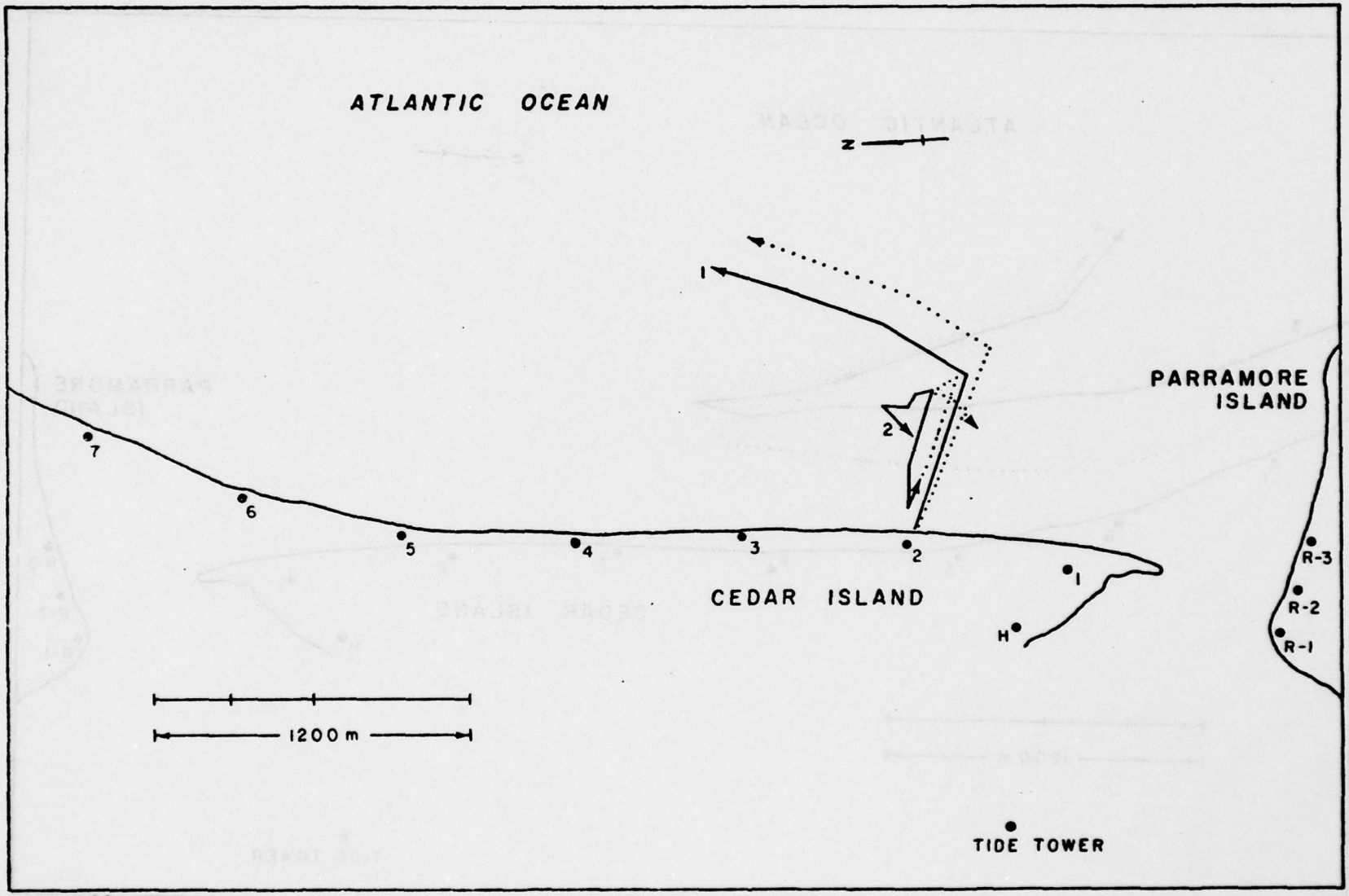

June 14, Ebb

Figure B24

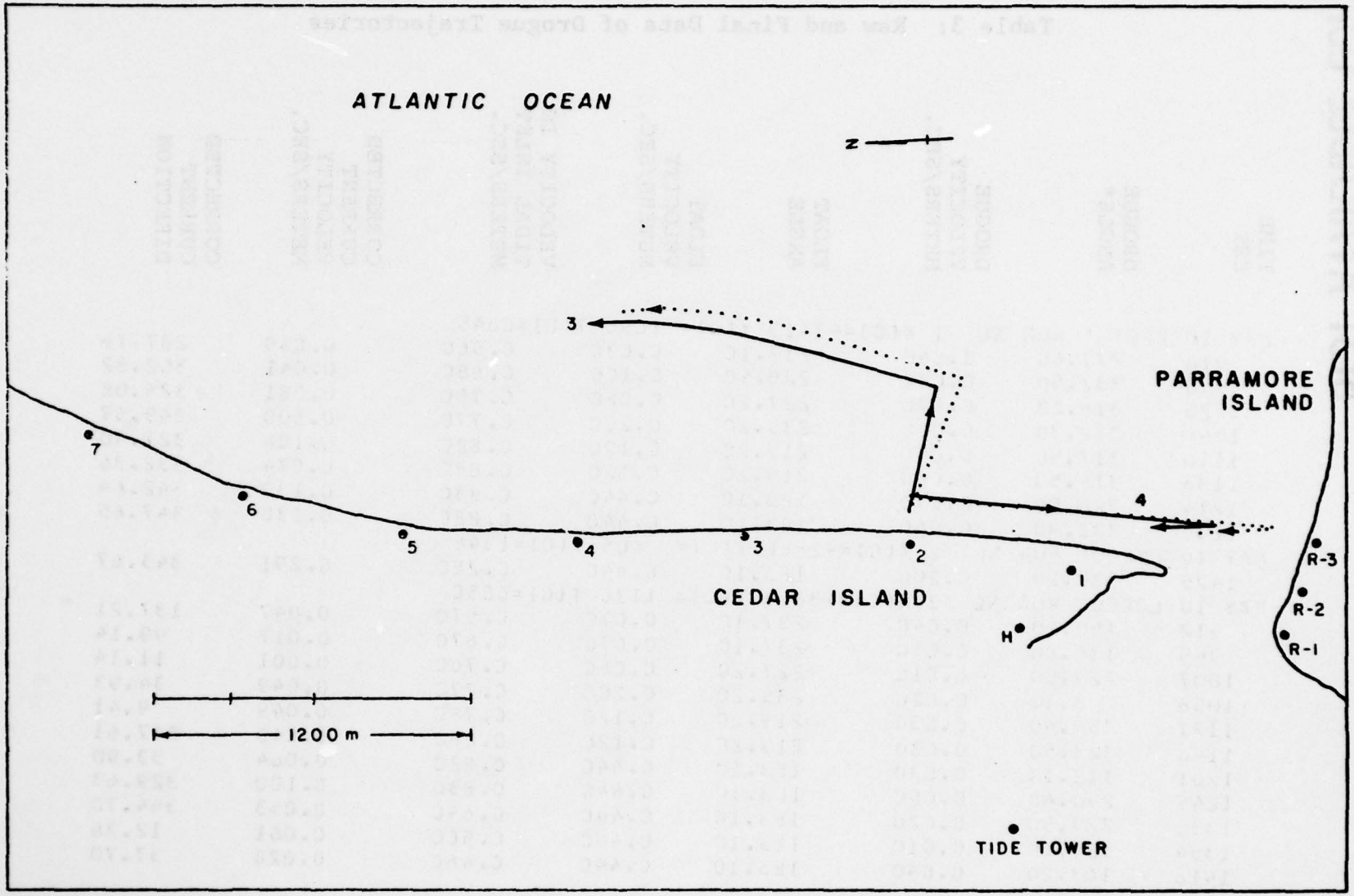

June 14, Ebb

Figure C25

Table 3: Raw and Final Data of Drogue Trajectories

TIME EST	DROGUE ANGLE*	DROGUE VELOCITY METERS/SEC.	FLOAT ANGLE	FLOAT VELOCITY METERS/SEC.	VELOCITY IN TIDAL INLET METERS/SEC.	CORRECTED CURRENT VELOCITY METERS/SEC.	CORRECTED CURRENT DIRECTION
MAY 10 DROGUE RUN NO 1 X(C)=-3413 Y(C)= 1090 T(C)=0845							
916	277.60	C.C4C	237.1C	C.C7C	C.56C	C.C39	287.76
940	332.50	C.C3C	225.5C	C.1CC	C.68C	C.C41	352.82
1020	316.60	C.C7C	227.2C	C.CFC	C.76C	C.C81	325.08
1048	332.30	C.CFC	235.2C	C.2CC	C.77C	C.100	349.57
1116	317.90	C.C9C	219.2C	C.12C	C.82C	C.1C8	327.40
1133	318.50	C.C6C	219.2C	C.12C	C.88C	C.C74	332.36
1214	326.00	C.C7C	183.1C	C.44C	C.83C	C.139	342.64
1235	332.90	C.C6C	183.1C	C.44C	C.88C	C.130	347.65
MAY 10 DROGUE RUN NO 2 X(C)=-2668 Y(C)= 605 T(C)=1348							
1425	328.20	C.2CC	183.1C	C.44C	C.28C	C.291	343.67
MAY 10 DROGUE RUN NO 3 X(C)=-2323 Y(C)= 1136 T(C)=C85C							
912	150.20	C.C4C	237.1C	C.C7C	C.57C	C.047	137.21
945	136.80	C.C1C	237.1C	C.C7C	C.67C	C.017	99.14
1007	229.00	C.C1C	227.2C	C.C8C	C.76C	C.001	11.14
1058	8.10	C.C2C	235.2C	C.2CC	C.77C	C.C49	34.93
1121	354.40	C.C3C	219.2C	C.12C	C.78C	C.049	9.41
1140	323.50	C.C3C	219.2C	C.12C	C.88C	C.C43	347.61
1201	112.10	C.C3C	183.1C	C.44C	C.82C	C.064	33.90
1245	290.40	C.C5C	183.1C	C.44C	C.83C	C.100	329.63
1330	229.50	C.C2C	183.1C	C.44C	C.69C	C.053	344.70
1354	125.00	C.C1C	183.1C	C.44C	C.5CC	C.061	12.36
1416	163.20	C.C4C	183.1C	C.44C	C.46C	C.028	37.70

MAY 11 DROGUE RUN NO 1 X(C)=-2953 Y(C)= 776 T(C)=0937

1010	9.40	C.C80	73.70	C.3CC	C.5CC	0.083	340.20
1037	283.60	C.C50	10.60	C.61C	C.71C	0.108	222.77
1105	278.90	C.C60	79.50	C.24C	C.77C	0.103	270.59
1143	272.40	C.C60	94.40	C.23C	C.83C	0.103	273.07

MAY 11 DROGUE RUN NO 2 X(C)=-2660 Y(C)= 696 T(C)=1152

1218	269.20	C.C50	99.70	C.17C	C.83C	0.083	271.19
1250	303.10	C.C30	43.50	C.39C	C.86C	0.073	251.47
1316	346.70	C.C30	43.50	C.39C	C.78C	0.049	260.00

MAY 11 DROGUE RUN NO 3 X(C)=-2806 Y(C)= 1160 T(C)=0943

1007	164.20	C.C20	73.70	C.3CC	C.41C	0.057	231.59
1032	282.70	C.C20	10.60	C.61C	C.64C	0.093	204.84
1107	317.60	C.C70	74.50	C.24C	C.77C	0.102	299.26
1136	306.50	C.C70	94.40	C.23C	C.83C	C.111	297.02
1220	273.00	C.C60	95.70	C.17C	C.85C	0.094	277.38
1249	293.90	C.C40	95.40	C.17C	C.82C	0.071	287.33
1313	281.10	C.C2C	43.50	C.39C	C.81C	0.073	239.15
1352	223.30	C.C6C	43.90	C.39C	C.7CC	0.078	282.80
1416	208.60	C.C50	21.00	C.38C	C.54C	0.068	255.17
1506	206.70	C.C4C	26.20	C.34C	C.35C	0.061	253.80

MAY 22 DROGUE RUN NO 1 X(C)=-1600 Y(C)= 475 T(C)=0540

607	313.90	C.C20	127.50	C.15C	C.15C	0.045	310.74
626	315.90	C.C50	132.50	C.12C	C.35C	0.075	315.09
655	333.00	C.C50	105.30	C.12C	C.49C	0.071	322.18
719	355.40	C.C70	91.00	C.13C	C.54C	0.085	342.16
745	358.70	C.C70	74.00	C.17C	C.53C	0.078	340.29
812	6.90	C.C80	83.20	C.17C	C.55C	0.089	350.84
831	353.60	C.C70	76.80	C.18C	C.57C	0.082	334.49
858	354.90	C.C70	77.10	C.2CC	C.55C	0.082	333.66
917	8.30	C.C80	77.10	C.2CC	C.5CC	0.086	349.30
937	359.80	C.C9C	62.10	C.19C	C.46C	0.094	344.19
1007	356.10	C.11C	49.30	C.22C	C.44C	0.110	342.21
1027	358.80	C.12C	42.50	C.21C	C.39C	0.117	348.11
1046	352.70	C.14C	42.50	C.21C	C.33C	0.143	343.00

MAY 22 DROGUE RUN NO 2 X(C)=-1635 Y(C)= 727 T(C)=0545

610	181.00	C.C30	127.50	C.15C	C.15C	0.028	221.54
631	63.30	C.C9C	132.50	C.12C	C.34C	0.087	52.19
656	266.50	C.C9C	105.30	C.12C	C.39C	0.075	283.17
725	357.00	C.C7C	91.00	C.13C	C.54C	0.085	341.79

MAY 22 DRCCUE RUN NC 3 X(C)=-1270 Y(C)= 900 T(C)=0816

900	2.20	0.050	83.20	0.170	0.570	0.059	337.01
920	340.20	0.050	76.80	0.180	0.500	0.066	316.34
941	345.00	0.060	77.10	0.200	0.480	0.076	321.86
1012	355.20	0.070	62.10	0.190	0.440	0.074	334.50
1032	335.20	0.070	49.30	0.220	0.350	0.078	311.27
1052	12.90	0.050	42.50	0.210	0.230	0.034	345.61

JUNE 5 DRCCUE RUN NC 1 X(C)=-1173 Y(C)= 361 T(C)=0515

602	340.70	0.051	116.80	0.200	0.280	0.083	326.81
636	279.20	0.032	111.10	0.180	0.500	0.063	284.23

JUNE 5 DRCCUE RUN NC 2 X(C)=- 600 Y(C)= 505 T(C)=0525

600	292.00	0.038	118.80	0.200	0.270	0.074	294.77
636	287.80	0.030	111.10	0.180	0.500	0.061	289.25
712	295.10	0.030	96.90	0.170	0.570	0.059	287.38

JUNE 5 DRCCUE RUN NC 3 X(C)=- 130 Y(C)= 640 T(C)=0835

907	322.80	0.500	350.10	0.610	0.910	0.495	317.94
924	323.20	0.560	325.10	0.430	0.830	0.580	322.99

JUNE 5 DRCCUE RUN NC 4 X(C)=- 983 Y(C)= 300 T(C)=0643

718	298.30	0.032	96.90	0.170	0.810	0.061	289.57

JUNE 5 DRCCUE RUN NC 5 X(C)= 55 Y(C)= 485 T(C)=0951

1031	333.00	0.390	13.30	0.530	0.570	0.391	325.45

JUNE 5 DRCCUE RUN NC 6 X(C)=- 950 Y(C)= 410 T(C)=0722

753	1.40	0.120	61.90	0.120	0.750	0.130	354.49
831	357.70	0.200	19.60	0.180	0.830	0.205	354.89
914	342.00	0.190	350.10	0.610	0.850	0.129	336.25
930	339.40	0.490	350.10	0.610	0.780	0.474	337.35
942	338.20	0.650	12.90	0.550	0.730	0.681	334.25

JUNE 5 DROGUE RUN NO 7 X(C)=- 570 Y(C)= 403 T(O)=0716

759	339.50	C.097	61.90	C.150	C.770	0.111	327.90

JUNE 5 DROGUE RUN NO 8 X(C)=-1117 Y(C)= 624 T(O)=0520

504	0.0	C.043	118.30	C.200	C.280	0.069	337.65
645	344.20	C.056	111.10	C.180	C.500	C.083	329.21
705	353.00	C.065	61.90	C.150	C.560	C.092	339.83
756	343.30	C.120	61.90	C.150	C.700	C.135	333.93
823	341.10	C.230	19.60	C.180	C.820	0.244	337.15
910	350.60	C.210	325.50	C.430	C.840	0.185	359.09
983	297.50	C.700	325.50	C.430	C.780	0.748	296.26

JUNE 5 DROGUE RUN NO 9 X(C)= 114 Y(C)= 270 T(C)=1010

1037	341.10	C.360	301.50	1.250	C.530	0.327	2.54

JUNE 5 DROGUE RUN NO 10 X(C)= 140 Y(C)= 321 T(C)=0934

993	101.10	C.130	13.30	C.530	C.670	0.175	134.98
1005	328.00	1.880	301.50	1.250	C.580	1.996	330.40

JUNE 7 DROGUE RUN NO 1 X(C)=-1430 Y(C)= 411 T(C)=1145

1226	178.20	C.195	160.30	C.300	C.630	0.182	182.55

JUNE 7 DROGUE RUN NO 2 X(C)=- 31 Y(C)= 445 T(C)=0728

755	344.20	C.320	165.20	C.120	C.420	0.386	344.25
825	332.20	C.310	165.20	C.120	C.470	0.374	332.82

JUNE 7 DROGUE RUN NO 3 X(C)= 5 Y(C)= 490 T(C)=0934

1007	337.10	C.600	306.60	C.180	C.790	0.667	338.28
1015	271.80	C.910	312.00	C.210	C.820	1.023	270.66

JUNE 7 DROGUE RUN NO 4 X(C)=- 920 Y(C)= 558 T(C)=0735

809	214.50	C.058	165.20	C.120	C.340	0.057	228.43
837	202.90	C.068	157.30	C.220	C.500	0.060	226.04
917	187.30	C.079	174.00	C.320	C.560	0.046	201.32
936	185.70	C.119	160.30	C.300	C.710	0.098	197.03
1026	192.20	C.130	160.30	C.300	C.800	0.114	204.25
1137	179.50	C.104	160.30	C.300	C.800	0.079	190.35

JUNE 7 DROGUE RUN NO 5 X(C)=-1545 Y(C)= 555 T(O)=0740

815	175.80	C.110	165.20	C.120	C.400	0.109	177.54
841	174.70	C.088	157.30	C.220	C.540	0.070	182.75
913	167.80	C.130	157.30	C.220	C.580	0.117	170.74
941	174.60	C.195	160.30	C.300	C.710	0.181	178.12
1030	189.40	C.176	160.30	C.300	C.840	0.165	197.04

JUNE 7 DROGUE RUN NO 6 X(C)= 26 Y(C)= 493 T(C)=1126

1152	0.50	C.420	322.20	C.31C	C.78C	0.447	4.19
1216	268.40	C.750	323.90	C.70C	C.6CC	0.808	262.25

JUNE 7 DROGUE RUN NO 7 X(C)=- 625 Y(C)= 62C T(C)=1043

1130	323.10	C.180	312.CC	C.21C	C.82C	C.176	325.07
1214	341.20	C.180	322.2C	C.31C	C.64C	0.164	346.50

JUNE 7 DROGUE RUN NO 8 X(C)=- 84 Y(C)= 495 T(C)=1022

1050	328.00	C.490	312.CC	C.21C	C.87C	C.533	328.93
1107	324.10	C.490	322.2C	C.31C	C.83C	0.517	324.27
1114	239.70	C.89C	322.2C	C.31C	C.81C	1.018	237.11

JUNE 7 DROGUE RUN NO 9 X(C)= 161 Y(C)= 353 T(C)=C83C

849	331.70	C.52C	306.8C	C.18C	C.55C	C.574	332.84
926	267.40	C.27C	306.8C	C.18C	C.61C	0.290	264.03

JUNE 21 DROGUE RUN NO 1 X(C) 51 Y(C)= 67C T(C)=C815

857	333.60	C.400	335.CC	C.19C	C.7CC	C.431	333.51
913	255.40	1.39C	297.9C	1.12C	C.68C	1.478	251.43

JUNE 21 DROGUE RUN NO 2 X(C)=- 85 Y(C)= 57C T(C)=C717

746	328.50	C.450	301.7C	1.31C	C.61C	0.349	340.14
759	5.10	C.490	335.9C	C.35C	C.75C	0.518	7.93
810	287.40	C.81C	270.CC	1.41C	C.74C	C.735	294.88
832	259.30	C.50C	270.CC	1.41C	C.7CC	C.369	253.20

JUNE 21 DROGUE RUN NO 3 X(C)=- 615 Y(C)= 58C T(C)=C652

719	350.10	C.17C	356.CC	C.32C	C.54C	0.148	348.19
744	338.70	C.23C	335.9C	C.35C	C.6CC	C.212	339.39
820	342.20	C.42C	335.9C	C.35C	C.72C	0.431	342.96

JUNE 21 DROGUE RUN NO 4 X(C) - 55 Y(C)= 546 T(C)=1CC6

1036	328.90	C.42C	326.7C	C.82C	C.54C	C.362	331.68
1058	341.90	C.41C	320.7C	C.82C	C.4CC	C.360	349.00
1115	277.80	C.56C	320.7C	C.82C	C.2CC	0.560	269.21

JUNE 21 DROGUE RUN NO 5 X(C)=- 94 Y(C)= 40C T(C)=C556

624	346.50	C.39C	353.3C	C.33C	C.23C	0.399	345.66
653	311.70	C.42C	295.CC	C.72C	C.39C	0.381	316.37
712	232.60	C.38C	295.CC	C.72C	C.54C	0.399	218.72

JUNE 21 DROGUE RUN NO 6 X(C)= 626 Y(C)= 18C T(C)=C724

746	323.80	C.92C	301.7C	1.31C	C.6CC	0.879	328.62
750	227.10	C.69C	301.70	1.31C	C.75C	0.765	212.78

JUNE 21	LRCCUE RUN NC 7 X(C)=-		633 Y(C)=	416 T(C)=C6C3			
630	0.50	C.18C	358.3C	C.33C	C.25C	0.158	2.75
700	341.50	C.22C	295.CC	C.72C	C.42C	0.195	5.15
724	338.80	C.39C	356.CC	C.32C	C.53C	C.403	336.78
JUNE 21	LRCCUE RUN NC 8 X(C) -		392 Y(C)=	526 T(C)=C92C			
955	334.30	C.27C	335.CC	C.19C	C.68C	0.282	338.63
1030	330.70	C.6CC	320.7C	C.82C	C.5CC	0.569	332.85
1047	234.70	C.56C	320.7C	C.82C	C.48C	0.647	223.78
JUNE 21	LRCCUE RUN NC 9 X(C)=-		511 Y(C)=	585 T(C)=C838			
924	337.00	C.25C	335.CC	C.19C	C.68C	0.259	337.22
952	340.80	C.5CC	338.4C	C.44C	C.68C	0.578	341.07
1000	288.10	C.74C	297.9C	1.12C	C.62C	0.686	285.71
JUNE 21	LRCCUE RUN NC 10 X(C)		65 Y(C)=	776 T(C)=C936			
956	326.1C	C.27C	320.7C	C.82C	C.68C	0.188	329.62
JUNE 21	LRCCUE RUN NC 11 X(C)		365 Y(C)=	631 T(C)=1C14			
1028	322.8C	1.14C	320.7C	C.82C	C.55C	1.188	323.02
1052	253.2C	C.56C	320.7C	C.82C	C.48C	C.587	253.03
JUNE 21	LRCCUE RUN NC 12 X(C)=-		6CC Y(C)=	545 T(C)=C756			
617	340.1C	C.2CC	335.9C	C.35C	C.74C	0.178	341.34
641	340.8C	C.26C	335.9C	C.35C	C.71C	C.247	341.84
916	330.4C	C.6CC	270.CC	1.41C	C.7CC	0.614	347.82
926	262.9C	C.74C	270.CC	1.41C	C.71C	0.642	260.57

MAY 4	LRCCUE RUN NC 1 X(C)=		506 Y(C)=	861 T(C)=C924			
944	171.2C	C.36C	136.CC	C.27C	-C.62C	0.381	174.65
1006	149.2C	C.42C	132.7C	C.37C	-1.13C	0.499	151.01
1028	104.9C	C.25C	123.2C	C.45C	-1.37C	0.224	99.49
1100	103.2C	C.22C	123.2C	C.45C	-1.44C	0.191	96.26
MAY 4	LRCCUE RUN NC 2 X(C)=		570 Y(C)=	472 T(C)=C914			
930	149.60	C.18C	136.60	C.27C	-C.58C	0.168	152.71
947	144.50	C.25C	136.60	C.27C	-C.8CC	0.247	145.90
1012	143.50	C.24C	132.7C	C.37C	-1.2CC	0.222	146.19
1037	156.70	C.3CC	123.2C	C.45C	-1.42C	0.291	164.05
1113	145.30	C.19C	75.2C	C.21C	-1.39C	0.210	153.41
1142	185.2C	C.41C	75.2C	C.21C	-1.34C	0.483	188.71

AD-A049 161 VIRGINIA INST OF MARINE SCIENCE GLOUCESTER POINT F/G 8/6
RECENT HISTORY AND RESPONSE CHARACTERISTICS OF WACHAPREAGUE INL--ETC(U).
MAY 77 R J BYRNE, J T DEALTERIS, J P SOVICH N00014-71-C-0334

UNCLASSIFIED NL

3 OF 3
AD
A049161

END
DATE
FILMED
2-78
DDC

MAY 4 DROGUE RUN NO 3 X(C)=- 876 Y(C)= 96C T(0)=112C							
1155	158.20	0.180	75.20	C.21C	-1.3CC	0.206	166.94
1219	156.70	C.160	113.30	C.4CC	-1.2CC	0.146	173.05
1243	123.90	C.220	45.40	C.4CC	-1.C5C	C.248	137.60
1315	133.00	C.230	65.20	C.32C	-C.76C	0.254	148.37
MAY 4 DROGUE RUN NO 4 X(C)=-1244 Y(C)= 445 T(0)=1203							
1231	116.50	C.130	113.30	C.4CC	-1.18C	0.090	118.64
1252	155.90	C.C9C	45.40	C.4CC	-C.83C	0.137	180.18
MAY 21 DROGUE RUN NO 1 X(C)= 336 Y(C)= 224 T(0)=1015							
1038	2.20	C.270	30.70	C.46C	C.14C	C.252	354.70
1100	130.40	C.3CC	68.10	C.35C	-C.1CC	0.331	146.98
1142	110.90	C.C8C	93.CC	C.5CC	-C.27C	0.031	158.97
1213	127.70	C.25C	110.30	C.99C	-C.68C	0.145	139.37
1240	116.60	C.16C	116.30	C.99C	-1.CCC	0.036	117.85
MAY 21 DROGUE RUN NO 2 X(C)= 4CC Y(C)= 585 T(0)=125C							
1322	187.10	C.23C	85.50	C.43C	-1.C2C	0.285	199.92
1343	71.60	C.21C	60.30	1.19C	-C.84C	0.075	99.29
MAY 21 DROGUE RUN NO 3 X(C)= 371 Y(C)= 365 T(0)=C54C							
1518	60.00	C.200	85.50	C.43C	-1.CCC	C.166	88.97
MAY 21 DROGUE RUN NO 4 X(C)=- 110 Y(C)= 282 T(0)=102C							
1045	17.90	C.13C	30.70	C.46C	C.1CC	C.C84	7.38
1115	103.80	C.C4C	68.10	C.35C	-C.C7C	C.031	187.46
1140	134.30	C.2CC	93.CC	C.5CC	-C.27C	0.181	150.19
1210	192.CC	C.14C	93.CC	C.5CC	-C.57C	0.188	215.20
1232	143.80	C.85C	110.30	C.99C	-C.91C	0.849	148.43

JUNE 4 DROGUE RUN NO 1 X(0)= 636 Y(0)= 60 T(0)=1017

1044	128.40	0.120	135.60	0.420	0.030	0.076	123.16
1130	161.70	0.410	149.70	0.540	-0.350	0.394	164.94
1216	166.10	0.200	161.30	0.430	-0.800	0.166	167.96
1256	149.50	0.120	154.10	0.370	-0.990	0.083	146.42
1329	158.30	0.130	161.10	0.400	-1.000	0.090	156.43
1405	171.10	0.140	179.80	0.400	-0.960	0.102	166.01
1442	169.70	0.100	176.00	0.380	-0.820	0.059	161.72
1523	170.30	0.090	177.10	0.320	-0.660	0.056	164.50
1558	162.30	0.120	174.30	0.440	-0.610	0.073	163.81

JUNE 4 DROGUE RUN NO 2 X(0)= 451 Y(0)= 636 T(0)=1023

1046	128.10	0.060	135.60	0.420	0.110	0.011	76.82
1235	170.60	0.240	149.70	0.540	-0.350	0.206	180.41
1215	114.70	0.240	161.30	0.430	-0.890	0.236	103.27
1254	150.20	0.120	154.10	0.370	-0.980	0.090	115.77
1323	143.20	0.100	161.10	0.400	-1.020	0.061	125.56
1409	139.20	0.090	179.80	0.400	-0.960	0.070	105.26
1437	159.20	0.190	178.00	0.380	-0.810	0.166	152.84
1535	170.20	0.190	178.00	0.380	-0.620	0.162	167.47

JUNE 4 DROGUE RUN NO 3 X(0)= 10 Y(0)= 323 T(0)=1029

1050	165.00	0.150	135.60	0.420	0.010	0.122	179.72
1127	171.50	0.260	149.70	0.540	-0.320	0.229	180.35
1205	170.20	0.210	161.30	0.430	-0.770	0.178	173.41
1242	164.40	0.160	161.30	0.430	-0.980	0.120	166.07
1331	176.70	0.150	161.10	0.400	-1.020	0.116	184.70
1403	182.10	0.100	179.80	0.400	-0.950	0.055	184.60
1445	164.20	0.090	178.00	0.380	-0.820	0.050	148.46
1522	169.00	0.110	177.10	0.320	-0.670	0.079	164.11
1545	166.70	0.120	177.10	0.320	-0.520	0.091	161.25

JUNE 13	CRCCUT RUN NC	1 X(C)=	746 Y(C)=	324 T(C)=C625			
659	180.80	C.240	146.6C	C.53C	-C.24C	0.215	192.79
737	173.10	C.36C	146.6C	C.53C	-C.83C	0.345	179.00
825	169.10	C.18C	166.3C	C.34C	-1.32C	0.158	184.51
JUNE 13	CRCCUT RUN NC	2 X(C)=-	74 Y(C)=	434 T(C)=C557			
631	183.20	C.C54	146.6C	C.53C	C.11C	0.047	275.22
703	175.20	C.2CC	146.6C	C.53C	-C.25C	0.165	188.55
745	171.40	C.18C	166.3C	C.34C	-C.82C	0.156	173.06
838	171.3C	C.13C	169.3C	C.32C	-1.33C	C.1C2	172.24
905	179.1C	C.15C	169.3C	C.32C	-1.43C	0.125	182.83
1003	175.10	C.C89	171.5C	C.25C	-1.3CC	0.065	177.17
1037	182.6C	C.1CC	136.CC	C.32C	-C.87C	0.075	179.18
1157	166.1C	C.C85	133.CC	C.27C	-C.65C	0.068	185.19
JUNE 13	CRCCUT RUN NC	3 X(C)=-	933 Y(C)=	588 T(C)=C6C5			
635	183.0C	C.13C	146.6C	C.53C	C.26C	C.111	224.27
709	171.2C	C.15C	146.6C	C.53C	-C.27C	0.106	189.45
747	166.2C	C.1C0	166.3C	C.34C	-C.83C	0.158	184.64
837	171.3C	C.15C	136.CC	C.32C	-1.38C	0.137	183.78
912	176.6C	C.11C	171.5C	C.25C	-1.37C	C.C89	178.74
953	166.4C	C.14C	156.2C	C.42C	-1.23C	0.102	176.31
1042	153.3C	C.12C	156.2C	C.42C	-C.86C	0.C76	165.88
1115	156.2C	C.12C	156.2C	C.27C	-C.54C	0.C98	158.68
JUNE 13	CRCCUT RUN NC	4 X(C)=-	959 Y(C)=	596 T(C)=C924			
902	173.7C	C.21C	169.3C	C.32C	-1.41C	0.194	174.79
957	160.5C	C.2CC	171.5C	C.25C	-1.24C	0.193	158.38
1032	151.9C	C.17C	136.CC	C.32C	-C.95C	0.154	169.73
1120	127.2C	C.13C	133.CC	C.27C	-C.6CC	0.109	125.06

JUNE 14 DROGUE RUN NO 1 X(C)=			10 Y(C)=	30 T(C)=0722			
759	72.20	0.290	164.20	0.180	-0.330	0.349	68.44
828	149.60	0.220	156.50	0.320	-0.560	0.205	147.99
907	161.10	0.160	170.00	0.190	-0.870	0.156	159.48
945	163.70	0.120	172.80	0.120	-0.960	0.120	162.34
JUNE 14 DROGUE RUN NO 2 X(C)=			30 Y(C)=	145 T(C)=0913			
945	69.50	0.081	172.80	0.120	-0.950	0.093	77.42
1025	72.60	0.120	172.80	0.120	-0.820	0.142	65.45
1093	197.20	0.039	172.50	0.140	-0.600	0.027	215.98
1135	248.10	0.026	184.30	0.130	-0.440	0.025	280.48
1225	177.00	0.035	184.40	0.130	-0.240	0.021	174.07
1305	314.40	0.075	184.30	0.130	0.100	0.100	322.98
JUNE 14 DROGUE RUN NO 3 X(C)=			35 Y(C)=	128 T(C)=0804			
881	70.10	0.300	156.50	0.320	-0.600	0.339	70.12
907	166.30	0.200	170.00	0.190	-0.350	0.202	164.64
950	166.20	0.130	172.80	0.120	-0.960	0.132	165.30
1027	172.60	0.087	172.80	0.120	-0.820	0.082	172.56
1059	175.50	0.091	172.50	0.140	-0.600	0.084	176.25
1144	184.10	0.074	184.30	0.130	-0.440	0.066	184.04
JUNE 14 DROGUE RUN NO 4 X(C)=			35 Y(C)=	188 T(C)=1230			
1256	354.90	0.750	184.30	0.130	0.130	0.882	355.11
1311	182.60	0.280	184.30	0.130	0.220	0.302	182.49

* Drogue angle measured from a line drawn between Cedar Island stations two and four. This line tends 2° east of north and represents 0°--0". Coordinate system originates at station 2 (x = 0, y = 0).

SECURITY CLASSIFICATION OF THIS PAGE (When Data Entered)

REPORT DOCUMENTATION PAGE

READ INSTRUCTIONS BEFORE COMPLETING FORM

1. REPORT NUMBER	2. GOVT ACCESSION NO. / 3. RECIPIENT'S CATALOG NUMBER
4. TITLE (and Subtitle) Recent History and Response Characteristics of Wachapreague Inlet, Virginia	5. TYPE OF REPORT & PERIOD COVERED: FINAL 4/71 - 12/74
	6. PERFORMING ORG. REPORT NUMBER
7. AUTHOR(s) Robert J. Byrne, Joseph T. DeAlteris, Jerome P. Sovich	8. CONTRACT OR GRANT NUMBER(s): ONR N00014-71-C-0334 new
9. PERFORMING ORGANIZATION NAME AND ADDRESS: Virginia Institute of Marine Science, Gloucester Point, Virginia 23062	10. PROGRAM ELEMENT, PROJECT, TASK AREA & WORK UNIT NUMBERS: Geography Programs Task 388-103
11. CONTROLLING OFFICE NAME AND ADDRESS: Office of Naval Research, Geography Programs, Arlington, Virginia 22217	12. REPORT DATE: May, 1977
	13. NUMBER OF PAGES: 183 p.
14. MONITORING AGENCY NAME & ADDRESS(if different from Controlling Office)	15. SECURITY CLASS. (of this report): Unclassified
	15a. DECLASSIFICATION/DOWNGRADING SCHEDULE

16. DISTRIBUTION STATEMENT (of this Report)

17. DISTRIBUTION STATEMENT (of the abstract entered in Block 20, if different from Report)

18. SUPPLEMENTARY NOTES

19. KEY WORDS (Continue on reverse side if necessary and identify by block number)

Tidal inlets
Nearshore currents
Hydraulics
Equilibrium channels

20. ABSTRACT (Continue on reverse side if necessary and identify by block number)

Wachapreague Inlet, a large downdrift offset inlet in the barrier island complex of the mid-Atlantic coast (Delmarva peninsula), was studied during the period 1971-1974. The inlet channel width is about 500 m and the throat cross-sectional is about 4,500 m². The inlet channel is about 3 km in length, approximately one-half of which is within the well-developed horseshoe shaped ebb delta complex. The maximum channel depth

DD FORM 1 JAN 73 1473 EDITION OF 1 NOV 65 IS OBSOLETE

Unclassified

SECURITY CLASSIFICATION OF THIS PAGE (When Data Entered)

is 20 m which occurs at the throat. Elements of the study included: (1) the inlet morphometric history (120 years), (2) assessment of surficial and sub-bottom sediments within the inlet complex, (3) determination of the distribution of tidal flows within the inlet channel, (4) determination of the zone of influence of inlet hydraulic currents along the face of the updrift barrier island and (5) the determination of the response of the channel cross-sectional area to short-term variations in wave activity and tidal prisms.

Weekly and post-storm cross-sectional area surveys over 10 range lines along the inlet channel length documented pronounced area modulations in area which showed a qualitative agreement with the sense of change in the ratio of ebb tidal power to incident wave power. The large sediment volume modulations observed during the surveys ($> 2 \times 10^6 m^3$) and other observations of sediment volume modulation on the flanking shoals suggests that the area modulations observed in the channel were due, for the most part, to sand transfers between the ebb delta complex and the channel. An internally consistent qualitative model for such a sediment flow loop which incorporates the influence of wave refraction, the regional tidal flow, and asymmetric flow, distribution within the channel accounts for the interchange.

Comparisons between stratigraphic evidence collected by others and the recent morphological changes of the inlet complex indicates that while the basin acted as a sink during the Holocene transgression, the inlet now acts in a bypassing mode. This condition is at least partially explained by existing hydraulic conditions wherein the duration of ebbing currents is shorter than flooding currents. Thus, on the average, the mean ebb currents are stronger than the flood currents.

DISTRIBUTION LIST

OFFICE OF NAVAL RESEARCH 2 COPIES
GEOGRAPHY PROGRAMS
CODE 462
ARLINGTON, VIRGINIA 22217

DEFENSE DOCUMENTATION CENTER 12 COPIES
CAMERON STATION
ALEXANDRIA, VIRGINIA 22314

DIRECTOR, NAVAL RESEARCH LAB 6 COPIES
ATTENTION TECHNICAL INFORMATION OFFICER
WASHINGTON, D. C. 20375

DIRECTOR
OFFICE OF NAVAL RESEARCH BRANCH OFFICE
1030 EAST GREEN STREET
PASADENA, CALIFORNIA 91101

DIRECTOR
OFFICE OF NAVAL RESEARCH BRANCH OFFICE
219 SOUTH DEARBORN STREET
CHICAGO, ILLINOIS 60604

DIRECTOR
OFFICE OF NAVAL RESEARCH BRANCH OFFICE
495 SUMMER STREET
BOSTON, MASSACHUSETTS 02210

COMMANDING OFFICER
OFFICE OF NAVAL RESEARCH BRANCH OFFICE
BOX 39
FPO NEW YORK 09510

CHIEF OF NAVAL RESEARCH
ASST. FOR MARINE CORPS MATTERS
CODE 100M
OFFICE OF NAVAL RESEARCH
WASHINGTON, D. C. 22217

CHIEF OF NAVAL RESEARCH
OCEAN SCIENCE AND TECHNOLOGY GROUP
CODE 480
OFFICE OF NAVAL RESEARCH
WASHINGTON, D. C. 22217

OFFICE OF NAVAL RESEARCH
OPERATIONAL APPLICATIONS DIVISION
CODE 200
ARLINGTON, VIRGINIA 22217

OFFICE OF NAVAL RESEARCH
SCIENTIFIC LIAISON OFFICER
SCRIPPS INSTITUTION OF OCEANOGRAPHY
LA JOLLA, CALIFORNIA 92038

DIRECTOR, NAVAL RESEARCH LABORATORY
ATTN LIBRARY, CODE 2628
WASHINGTON, D. C. 20375

COMMANDER
NAVAL OCEANOGRAPHIC OFFICE
ATTN. LIBRARY CODE 1600
WASHINGTON, D. C. 20374

NAVAL OCEANOGRAPHIC OFFICE
CODE 3001
WASHINGTON, D. C. 20374

CHIEF OF NAVAL OPERATIONS
OP 987P1
DEPARTMENT OF THE NAVY
WASHINGTON, D. C. 20350

OCEANOGRAPHER OF THE NAVY
HOFFMAN II BUILDING
200 STOVALL STREET
ALEXANDRIA, VIRGINIA 22322

NAVAL ACADEMY LIBRARY
U. S. NAVAL ACADEMY
ANNAPOLIS, MARYLAND 21402

COMMANDING OFFICER
NAVAL COASTAL SYSTEMS LABORATORY
PANAMA CITY, FLORIDA 32401

LIBRARIAN
NAVAL INTELLIGENCE
SUPPORT CENTER
4301 SUITLAND ROAD
WASHINGTON, D. C. 20390

COMMANDING OFFICER
NAVAL CIVIL ENGINEERING LABORATORY
PORT HUENEME, CALIFORNIA 93041

OFFICER IN CHARGE
ENVIRONMENTAL PREDICTION
RESEARCH FACILITY
NAVAL POST GRADUATE SCHOOL
MONTEREY, CALIFORNIA 93940

DR. WARREN C. THOMPSON
DEPT OF METEOROLOGY & OCEANOGRAPHY
U.S. NAVAL POST GRAD. SCHOOL
MONTEREY, CALIFORNIA 93940

DIRECTOR
AMPHIBIOUS WARFARE BOARD
U.S. ATLANTIC FLEET
NAVAL AMPHIBIOUS BASE
NORFOLK, LITTLE CREEK, VIRGINIA 23521

Distribution List, Cont'd.

COMMANDER, AMPHIBIOUS FORCE
U. S. PACIFIC FLEET
FORCE METEOROLOGIST
COMPHIBPAC CODE 25 5
SAN DIEGO, CALIFORNIA 92155

COMMANDING GENERAL
MARINE CORPS DEVELOPMENT AND
EDUCATIONAL COMMAND
QUANTICO, VIRGINIA 22134

DR. A. L. SLAFKOSKY
SCIENTIFIC ADVISOR
COMMANDANT OF THE MARINE CORPS (CODE AX)
WASHINGTON, D. C. 20380

DEFENSE INTELLIGENCE AGENCY
DIAAP-10A
WASHINGTON, D. C. 20301

DIRECTOR
COASTAL ENGINEERING RESEARCH CENTER
U.S. ARMY CORPS OF ENGINEERS
KINGMAN BUILDING
FORT BELVOIR, VIRGINIA 22060

CHIEF, WAVE DYNAMICS DIVISION
USAE-WES
P. O. BOX 631
VICKSBURG, MISSISSIPPI 39180

COMMANDANT
U.S. COAST GUARD
ATTN# GECV/61
WASHINGTON, D. C. 20591

OFFICE OF RESEARCH AND DEVELOPMENT
RDS/62
U.S. COAST GUARD
WASHINGTON, D.C. 20591

NATIONAL OCEANOGRAPHIC DATA
CENTER RD764
ENVIRONMENTAL DATA SERVICES
NOAA
WASHINGTON, D. C. 20235

CENTRAL INTELLIGENCE AGENCY
ATTENTION OCR/DD-PUBLICATIONS
WASHINGTON, D. C. 20505

DR. DONALD SWIFT
MARINE GEOLOGY AND GEOPHYSICS LABORATORY
AOML - NOAA
15 RICKENBACKER CAUSEWAY
MIAMI, FLORIDA 33149

MINISTERIALDIREKTOR DR. F. WEVER
RUE/FO
BUNDESMINISTERIUM DER VERTEIDIGUNG
HARDTHOEHE
D-5300 BONN, WEST GERMANY

OBERREGIERUNGSRAT DR. JAEGER
RUE/FO
BUNDESMINISTERIUM DER VERTEIDIGUNG
HARDTHOEHE
D-5300 BONN, WEST GERMANY

MR. TAGE STRARUP
DEFENCE RESEARCH ESTABLISHMENT
OSTERBROGADES KASERNE
DK-2100 KOBENHAVN O. DENMARK

PROF. DR. RER.NAT. H.G. GIERLOFF-EMDEN
INSTITUT F. GEOGRAPHIE
UNIVERSITAET MUENCHEN
LUISENSTRASSE 37/III
D-800 MUENCHEN 2, WEST GERMANY

PROF. DR. EUGEN SEIBOLD
GEOL.-PALAEONTOLOG. INSTITUT
UNIVERSITAET KIEL
OLSHAUSENSTRASSE 40-60
D-2300 KIEL, WEST GERMANY

DR. R. KOESTER
GEOL.-PALAEONTOLOG. INSTITUT
UNIVERSITAET KIEL
OLSHAUSENSTRASSE 40-60
D-2300 KIEL

PROF. DR. FUEHRBOETER
LEHRSTUHL F. HYDROMECHANIK U.
KUESTENWASSERBAU
TECHNISCHE HOCHSCHULE BRAUNSCHWEIG
BEETHOVENSTRASSE 51A
D-3300 BRAUNSCHWEIG, WEST GERMANY

PROF. DR. WALTER HANSEN
DIREKTOR D. INSTITUTS F. MEERESKUNDE
UNIVERSITAET HAMBURG
HEIMHUDERSTRASSE 71
D-2000 HAMBURG 13, WEST GERMANY

PROF. DR. KLAUS HASSELMANN
INSTITUT F. GEOPHYSIK
UNIVERSITAET HAMBURG
SCHLUETERSTRASSE 22
D-2000 HAMBURG 13, WEST GERMANY

Distribution List, Cont'd.

PROF. DR. NILS JERLOV
INSTITUTE FOR PHYSICAL OCEANOGRAPHY
KOBENHAVNS UNIVERSITET
HARALDSGADE 6
DK-2200 KOBENHAVN, DENMARK

DR. J. B. MATTHEWS
COASTAL OCEANOGRAPHY GROUP
BEDFORD INSTITUTE OF OCEANOGRAPHY
DARTMOUTH, NOVA SCOTIA
CANADA

IR. H. J. SCHOEMAKER
WATERLOOPKUNDIG LABORATORIUM TE DELFT
61 RAAM, DELFT
NETHERLANDS

IR. M. W. VAN RATENBERG
PHYSISCH LABORATORIUM TNO
OUDE WAALSDORPER WEG 63, DEN HAAG
NETHERLANDS

MR. H. G. TURNATURE
ITT AVIONICS
9140 OLD ANNAPOLIS ROAD
COLUMBIA, MARYLAND 21043

COASTAL STUDIES INSTITUTE
LOUISIANA STATE UNIVERSITY
BATON ROUGE, LOUISIANA 70803

DR. BERNARD LE MEHAUTE
TETRA TECH, INC.
630 NORTH ROSEMEAD BOULEVARD
PASADENA, CALIFORNIA 91107

DR. RICHARD A. DAVIS, JR.
DEPARTMENT OF GEOLOGY
UNIVERSITY OF SOUTH FLORIDA
TAMPA, FLORIDA 33620

DR. WILLIAM T. FOX
DEPARTMENT OF GEOLOGY
WILLIAMS COLLEGE
WILLIAMSTOWN, MASSACHUSETTS 01267

DR. WILLIAM S. GAITHER
DEAN, COLLEGE OF MARINE STUDIES
ROBINSON HALL
UNIVERSITY OF DELAWARE
NEWARK, DELAWARE 19711

DR. JOHN T. KUO
HENRY KRUMB SCHOOL OF MINES
SEELEY W. MUDD BUILDING
COLUMBIA UNIVERSITY
NEW YORK, NEW YORK 10027

DR. EDWARD B. THORNTON
DEPARTMENT OF OCEANOGRAPHY
NAVAL POSTGRADUATE SCHOOL
MONTEREY, CALIFORNIA 93940

PROF. C. A. M. KING
DEPARTMENT OF GEOGRAPHY
UNIVERSITY OF NOTTINGHAM
NOTTINGHAM, ENGLAND

DR. DOUGLAS L. INMAN
SCRIPPS INSTITUTE OF OCEANOGRAPHY
LA JOLLA, CALIFORNIA 92037

DR. DONN S. GORSLINE
DEPARTMENT OF GEOLOGY
UNIVERSITY OF SOUTHERN CALIFORNIA
LOS ANGELES, CALIFORNIA 90007

DR. WILLIAM W. WOOD
DEPARTMENT OF GEOSCIENCES
PURDUE UNIVERSITY
LAFAYETTE, INDIANA 47907

DR. ALAN W. NIEDORODA
DIRECTOR, COASTAL RESEARCH CENTER
UNIVERSITY OF MASSACHUSETTS
AMHERST, MASSACHUSETTS 01002

DR. BENNO M. BRENNINKMEYER, S. J.
DEPT. OF GEOLOGY AND GEOPHYSICS
BOSTON COLLEGE
CHESTNUT HILL, MASSACHUSETTS 02167

DR. OMAR SHEMDIN
JPL-CALTECH
MAIL STOP 183-501
4800 OAK GROVE DRIVE
PASADENA, CALIFORNIA 91103

DR. LESTER A. GERHARDT
RENNSSELAER POLYTECHNIC INSTITUTE
TROY, NEW YORK 12181

DR. FRED THOMSON
ENVIRONMENTAL RESEARCH INSTITUTE
P.O. BOX 618
ANN ARBOR, MICHIGAN 48107

Distribution List, Cont'd.

DR. J.A. DRACUP
ENVIRONMENTAL DYNAMICS, INC.
1609 WESTWOOD BOULEVARD, SUITE 202
LOS ANGELES, CALIFORNIA 90024

DR. THOMAS K. PEUCKER
SIMON FRASER UNIVERSITY
DEPARTMENT OF GEOGRAPHY
BURNABY 2, B.C., CANADA

DR. BRUCE HAYDEN
DEPARTMENT OF ENVIRONMENTAL SCIENCES